ANNUAL REVIEW

INSTITUTE FOR MOLECULAR SCIENCE

1988

ANNUAL REVIEW

INSTITUTE FOR MOLECULAR SCIENCE

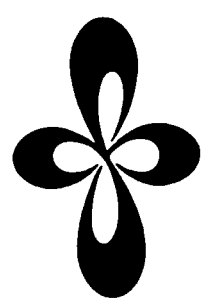

1988

Published by
Institute for Molecular Science
Okazaki National Research Institutes
Myodaiji, Okazaki 444, Japan
Phone 0564-54-1111
Telex 4537-475 KOKKEN J

IMS 1988

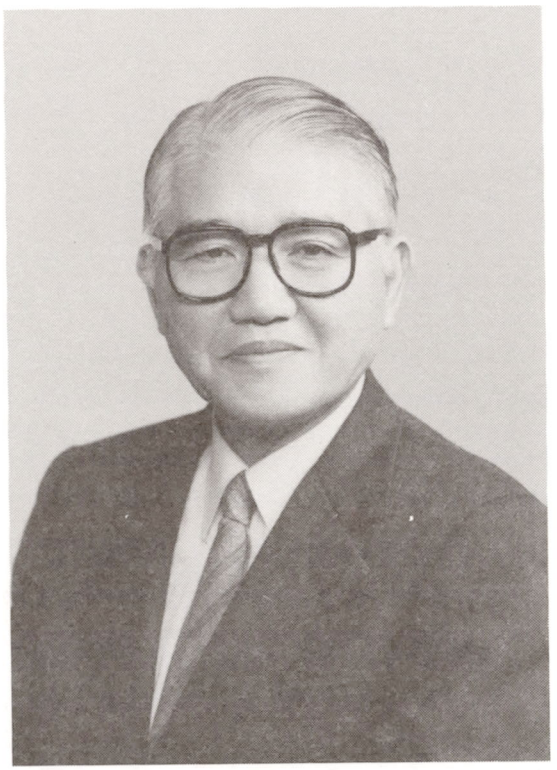

The mission of our Institute is twofold: to carry out good research, and to participate in and to promote joint studies among molecular scientists from all over Japan and from abroad. During the past year (1987–88) all our research groups have contributed much to achieve these goals. The accumulated results of these efforts are briefly presented in this issue of Annual Review 1988. It is worth nothing that, the IMS serving as the key institution for international collaborative programs in the field of molecular science has made further progress since 1987.

In this ever advancing technological world, it is very important for us to cope with the improvement of new instruments and equipment, and with the demand for higher rate of operation of existing research facilities. In particular, to meet with the recent accelerated progress in low temperature chemistry research, a new and more powerful helium compressor has been installed at the Low-Temperature Center. The supply capacity is expected to be about five times larger than before.

Further, we have had a very lively and through discussion among the in-house and adjunct staff members about the future plan of the Institute. A new plan has been completed and approved by the IMS Council.

In order to maintain the activity of an institute, circulation of its research and technical staff is essential. During the present fiscal year many of our researchers and technical associates including two associate professors have been promoted to positions in other universities and institutions. We have hired Dr. Kyuya Yakushi, formerly an associate professor of the Faculty of Science, the University of Tokyo, to fill the position of Professor of Solid State Chemistry Laboratory. Dr. Kazuhiro Nakasuji, formerly associate professor of Faculty of Science, Osaka University, is promoted to Professor of Applied Material Science I Laboratory. Prof. Hitoshi Ohtaki of the Tokyo Institute of Technology was appointed to Professor of Complex Catalysis Laboratory, Coordination Chemistry Laboratories. Prof. Eiichi Kimura of Hiroshima University and Associate Professor Ryuichi Ikeda of Nagoya University were appointed to Professor and Associate Professor of the Complex Synthesis Laboratory for a two year term.

Prof. M. Eigen who served as foreign member of the IMS Council retired from the position. We would like to express our sincere thanks to Prof. Eigen for his contribution. Prof. H.A. Staab, President of Max-Planck Foundation, is invited as a successor of Prof. Eigen to membership of IMS Council. We have already received valuable advice from Prof. Staab, to whom we are thankful.

September, 1988

H. Inokuchi

Hiroo INOKUCHI

OBITUARY

Professor Hideo Akamatu

1910–1988

Professor Hideo Akamatu, the founding Director-General of IMS, died on the 8th of January 1988 at the age of 77. Although he retired in 1981 he remained, as a Councillor and Emeritus Professor of IMS, a continuous source of advice and encouragement to all of us.

Professor Akamatu was born in Nagasaki in 1910 and studied at the University of Tokyo from 1932 to 1935. He started his research on colloid and surface chemistry as a post-graduate student of Prof. S. Sameshima. He studied the rheological problems of the oiliness of liquids and its relation to friction, adsorption at the solid-liquid interface, multiple built-up films, and analysis of thixotropy phenomena. In 1942 he was promoted to Associate Professor. During World War II, he started his new work on carbons.

He studied the structural changes occurring in cokes and carbon blacks in the graphitization process. He observed microcrystallite alignment and subsequent crystal growth by X-ray analysis and also examined the diamagnetic susceptibility and electrical conductivity in these processes. He further became interested in studying large condensed aromatic molecules such as violanthrone, in analogy with the single layer of carbon black. He found with his young coworker, H. Inokuchi, now a successor as Director-General of IMS, that many condensed aromatic hydrocarbons did in fact exhibit electrical conductivity. In 1951 he was appointed as professor of chemistry at the University of Tokyo. In 1954 he discovered with his coworkers that aromatic molecules with halogen molecules in the lattice become highly conducting. This finding provoked many researchers to work on charge transfer solids, including ion radical salts. The studies on the well-known TCNQ salts, and the wide variety of other salts which give metal like conductivity and superconductivity, derive from the observations of Professor Akamatu.

Professor Akamatu and his co-workers made electron spin resonance spectroscopy, low-temperature polarized absorption spectroscopy, and structural and theoretical studies of charge transfer solids. These studies led to the present understanding of the molecular and electronic structures of these solids. For these achievements, he received the Chemical Society Award in 1958 and the Japan Academy Prize in 1965.

Many of us look back with admiration on those years after the War, when Professor Akamatu, with rudimentary equipment, developed his idea of the electrical conductivity of organic materials. He wrote in his book "Shiten" ("View Point"). *The study of chemistry is for me nothing but the process of developing my personal "intuitive view of matter" (Busshitsu-Kan); this is done by work in the laboratory. It is more than my pleasure if my personal intuitive view becomes common knowledge to others.* He often advised his students to sharpen their own *Busshitsu-kan*.

In 1971 he retired from the University of Tokyo and joined Yokohama National University, where he served as Dean of the Faculty of Engineering in 1974–1975. In 1975 he was appointed as the first Director-General of the Institute for Molecular Science and contributed greatly to the successful foundation of this Institute. During his six year term of office, he established the fundamental direction of the institute and contributed to the creation of an atmosphere conductive to the pursuit of basic science. In collaboration with other leaders in molecular science he introduced many new principles in operating a scientific institution, which included an open system for personnel selection and planning of collaborative works, foreign councillorship and so on.

He was known for his service to the scientific communities both domestically and internationally. He served as a member of the Science Council of Japan for many years and as president of the Chemical Society of Japan. He organized the Symposium on Carbon in Tokyo in 1964 and the IUPAC Congress in Tokyo in 1981. He was an enthusiast for the use of renewable energy resources and acted as chairman of the Hydrogen Energy Society. In 1981 he was invested with the Second Order of Merit with the Cordon of the Rising Sun.

Professor Akamatu will be remembered with affection as a warm hearted friend to all who knew and worked with him. He was a man of diverse interests which were reflected in his private and professional lives. He was an outstanding poet of Tanka (the 31 syllable Japanese poem). This discipline was reflected in his scientific communications; his writings and talks were always concise and essential. His clear and deep thinking in science was perhaps much related to his artists mind.

K. Yoshihara

CONTENTS

ORGANIZATION AND STAFF

Organization

The Institute for Molecular Science comprises seventeen research laboratories – each staffed by a professor, and associate professor, two research associates and a few technical associates –, two research laboratories with foreign visiting professors, and six research facilities. The laboratories are grouped into five departments and one facility for coordination chemistry:

Department of Theoretical Studies	Theoretical Studies I
	Theoretical Studies II
	Theoretical Studies III[1)]
Department of Molecular Structure	Molecular Structure I
	Molecular Structure II[1)]
	Molecular Dynamics
Department of Electronic Structure	Excited State Chemistry
	Excited State Dynamics
	Electronic Structure[1)]
	Molecular Energy Conversion[2)]
Department of Molecular Assemblies	Solid State Chemistry
	Photochemistry
	Molecular Assemblies Dynamics
	Molecular Assemblies[1)]
	Synchrotron Radiation Research[2)]
Department of Applied Molecular Science	Applied Molecular Science I
	Applied Molecular Science II[1)]
Coordination Chemistry Laboratories	Synthetic Coordination Chemistry
	Complex Catalysis
	Coordination Bond[1)]

Research facilities are:	Computer Center
	Low-Temperature Center
	Instrument Center
	Chemical Materials Center
	Equipment Development Center
	Ultraviolet Synchrotron Orbital Radiation (UVSOR) Facility.

1) Professors and associate professors are adjunct professors from universities.

2) Research Laboratories with foreign visiting professors.

Scientific Staff

Hiroo INOKUCHI	**Professor, Director-General**

Department of Theoretical Studies

Theoretical Studies I

Keiji MOROKUMA	Professor
Iwao OHMINE	Associate Professor
Koichi YAMASHITA	Research Associate
Masaki SASAI	Research Associate
Satoshi YABUSHITA	Technical Associate (–March '88)[1]
Mutsumi AOYAGI	Technical Associate
Osamu KITAO	Technical Associate (April '88–)
Andrea DORIGO	Postdoctoral Fellow (February '88–)
Yuriko AOKI	Graduate Student from Hiroshima Univ.* (–March '88)
Keiichiro SAMESHIMA	Graduate Student from Hoshi College of Pharm.* (April '88–)
Kyoichi SAWABE	Graduate Student from Univ. of Tokyo* (April '88–)
Hiroo FUKUNAGA	Visiting Research Fellow from Fuji Photo Film Co. (April '88–)
Hiroshi KAWAMURA	Visiting Research Fellow from Sumitomo Chemical Co. (April '88–)
Tadahiro OZAWA	Visiting Research Fellow from Kao Corp.

Theoretical Studies II

Hiroki NAKAMURA	Professor
Keiichiro NASU	Associate Professor
Masahiro IWAI	Research Associate
Hidemitsu HAYASHI	Research Associate
Akihiko OHSAKI	Technical Associate
Jun-ichi TAKIMOTO	Technical Associate
Masato NAKAMURA	IMS Fellow (–March '88)
Yoshiyuki USAMI	Graduate Student from Keio Univ.* (–March '88)

Theoretical Studies III

Akira YANASE	Adjunct Professor from Univ. of Osaka Pref. (–March '88)
Akira IMAMURA	Adjunct Professor from Hiroshima Univ. (April '88–)
Yuichi FUJIMURA	Adjunct Associate Professor from Tohoku Univ. (–March '88)
Kazuo KITAHARA	Adjunct Associate Professor from Tokyo Inst. of Tech. (April '88–)
Nobuaki KOGA	Research Associate
Kiyohiko SOMEDA	Research Associate (January '88–)

Department of Molecular Structure

Molecular Structure I

Eizi HIROTA	Professor
Norio MORITA	Associate Professor
Chikashi YAMADA	Research Associate
Hideto KANAMORI	Technical Associate (–March '88) Research Associate (April '88–June '88)[2]

Toshifumi SUZUKI	Research Associate (October '87–)
Keiichi SATO	Technical Associate (–March '88)
Toshinori SUZUKI	Technical Associate (July '88–)
Masatoshi KAJITA	IMS Research Fellow (–August '88)[3)]
Haruhiko ITO	JSPS Post-doctoral Fellow (April '88–)
Masaharu FUJITAKE	Graduate Student from Hiroshima Univ.*

Molecular Structure II

Akifumi UENO	Adjunct Professor from Toyohashi Univ. of Tech.
Takayoshi KOBAYASHI	Adjunct Associate Professor from Univ. of Tokyo (–March '88)
Yasuki ENDO	Adjunct Associate Professor from Univ. of Tokyo (April '88–)
Kentarou KAWAGUCHI	Research Associate
Takashi OGURA	Research Associate

Molecular Dynamics

Teizo KITAGAWA	Professor
Yasuo UDAGAWA	Associate Professor
Keiji KAMOGAWA	Research Associate
Kazuyuki TOHJI	Research Associate
Takanori MIZUSHIMA	Technical Associate
Shin'ichiro SATO	Technical Associate (April '88–)
Ryuichi MORIMO	Visiting Scientist from Miyakonojo National College of Technology (April '88–)
Shoji KAMINAKA	Graduate Student from Osaka Univ.*
Masashi NAKAGAWA	Graduate Student from Univ. of Tokyo*
Tsuyoshi EGAWA	Graduate Student from Tokyo Metropolitan Univ.* (April '88–)
Takeshi MIKI	Graduate Student from Toyohashi Univ. of Tech.*
Naoyuki TAKAHASHI	Graduate Student from Toyohashi Univ. of Tech.*

Department of Electronic Structure

Excited State Chemistry

Keitaro YOSHIHARA	Professor
Tadayoshi SAKATA	Associate Professor
Hrvoje PETEK	Research Associate
Kazuhito HASHIMOTO	Research Associate
Tohru KOBAYASHI	Technical Associate
Masahiro HIRAMOTO	Technical Associate (–June '88)
Masashi AZUMA	Technical Associate (November '87–)
Stephen R. MEECH	Visiting Scientist (October '87–)
Limin ZHANG	Visiting Scientist (October '87–)
Robert PANSU	Visiting Scientist (July '88–)
Hanhein WANG	Visiting Scientist (November '87–April '88)
Bu Yong LEE	Visiting Scientist (June '88–August '88)
Yoshihisa FUJIWARA	Graduate Student from Kanazawa Univ.* (April '87–March '88)
Masanori KOSHIOKA	Graduate Student from Kyoto Inst. of Tech. (October '87–)
Andrew K. CAMPEN	Graduate Student from Univ. of Southampton (April '87–October '87)

Hidetomo NODA	Graduate Student from Nagoya Inst. of Tech.* (October '87–September '88)

Excited State Dynamics

Ichiro HANAZAKI	Professor
Nobuyuki NISHI	Associate Professor
Masao TAKAYANAGI	Research Associate
Hisanori SHINOHARA	Research Associate (–August '88)[4]
Minoru SUMITANI	Research Associate (October '87–)
Teruhiko NISHIYA	Technical Associate
Kazunori YAMAMOTO	Technical Associate
Hiroshi OHOYAMA	IMS Fellow (April '87–)
Fuminori MISAIZU	Graduate Student from the Univ. of Tokyo* (April '88–)

Electronic Structure

Koichi ITO	Adjunct Professor form Osaka City Univ. (April '88–)
Haruo ABE	Adjunct Associate Professor from Inst. of Phys. and Chem. Res. (April '87–)
Ryoichi NAKAGAKI	Research Associate
Hiromi OKAMOTO	Research Associate

Molecular Energy Conversion

Graham BLACK	Visiting Professor from SRI International (April '87–May '88)
Hans TOFTLUND	Visiting Associate Professor from Odense Univ., Denmark (June '87–March '88)
Vlastimil FIDLER	Visiting Associate Professor from Charlus Univ., Czechoslovakia (September '88–)

Department of Molecular Assemblies

Solid State Chemistry

Kyuya YAKUSHI	Professor (May '88–)
Inosuke KOYANO	Associate Professor
Takashi IMAMURA	Research Associate
Shinzo SUZUKI	Technical Associate
Kenichi IMAEDA	Technical Associate
Hitoshi FUJIMOTO	Toyota Rikagaku Kenkyusho Postdoctoral Fellow (April '88–)
Hiromichi YAMAMOTO	Visiting Research Fellow (April '86–March '88)
Takashi IMAJO	IMS Fellow (April '87–)
Hideo YAMAKADO	Graduate Student from the Univ. of Tokyo* (September '88–)

Photochemistry

Katsumi KIMURA	Professor
Kosuke SHOBATAKE	Associate Professor

Kiyohiko TABAYASHI	Research Associate
Katsuhiko OKUYAMA	Research Associate
Atsunari HIRAYA	Technical Associate (–June '88)
Nobuo HAYASAKA	Visiting Research Fellow from Toshiba Corp. (–March '88)
Kohji KAMIYA	JSPS Post-doctoral Fellow (April '88–)
Takato HIRAYAMA	IMS Fellow (December '87–)
Haruhiko OHASHI	Graduate Student from Toyohashi Univ. of Technology (April '88–)

Molecular Assemblies Dynamics

Yusei MARUYAMA	Professor
Masatoshi SATO	Associate Professor
Tamotsu INABE	Research Associate
Masashige ONODA	Research Associate
Masafumi SERA	Research Associate
Hajime HOSHI	Technical Associate
Shin-ichi SHAMOTO	Technical Associate
Toshifumi TERUI	Graduate Student from Muroran Inst. of Technology (November '87–)
Kenji FUKUDA	Graduate Student from Hokkaido Univ. (October '87–)
Yoichiro KAWAI	Visiting Research Fellow from TOYOTA Motor Co., Ltd. (April '87–)
Shinji KONDOH	Visiting Research Fellow from Asahi Glass Co., Ltd. (June '87–)
Yoshiyasu ANDO	Visiting Research Fellow from Nippon Soken, INC. (November '87–)
Chikako NAKANO	Visiting Research Fellow (September '87–)
Hiromichi YAMAMOTO	Visiting Research Fellow (April '88–)

Molecular Assemblies

Koji KAYA	Adjunct Professor from Keio Univ. (April '87–)
Ichimin SHIROTANI	Adjunct Associate Professor from Muroran Inst. of Technology (April '87–)
Takehiko MORI	Research Associate
Shin-ichi NAGAOKA	Research Associate

Synchrotron Radiation Research

Peter G. WOLYNES	Visiting Professor from Univ. of Illinois, U.S.A. (June '87–January '88)

Department of Applied Molecular Science

Applied Molecular Science I

Kazuhiro NAKASUJI	Professor (September '88–)
Kiyoshi ISOBE	Associate Professor
Koshiro TORIUMI	Research Associate
Yoshiki OZAWA	Research Associate (December '87–)

Yoshihito HAYASHI	Technical Associate (December '87–)
Keisuke UMAKOSHI	IMS Fellow (April '88–)
Masahiro EBIHARA	JPSJ Post-doctoral Fellow (April '88–September '88)

Applied Molecular Science II

Kazuhiro MARUYAMA	Adjunct Professor from Kyoto Univ. (April '87–)
Hiroharu SUZUKI	Adjunct Professor from Tokyo Inst. of Tech. (July '87–)
Hiroki OSHIO	Research Associate

Coordination Chemistry Laboratories

Eiji HIROTA	Director (–May '88)
Hitoshi OHTAKI	Director (June '88–)

Synthetic Coordination Chemistry

Eiichi KIMURA	Professor (April '88–)
Ryuichi IKEDA	Associate Professor (April '88–)
Mitsuhiko SHIONOYA	Research Associate (April '88–)
Hideki MASUDA	Research Associate (April '88–)
Hiromasa KUROSAKI	Graduate Student form Hiroshima Univ. (April '88–)
Yukari YOSHIYAMA	Graduate Student form Hiroshima Univ. (April '88–)
Yoshihiko KOTAKE	Graduate Student form Hiroshima Univ. (April '88–)
Yasuhisa KUROKI	Graduate Student form Hiroshima Univ. (April '88–)
Atsushi ISHIKAWA	Graduate Student form Nagoya Univ. (April '88–)
Yutaka TAI	Graduate Student form Nagoya Univ. (April '88–)

Complex Catalysis

Hitoshi OHTAKI	Professor (April '88–)
Toshikatsu YOSHIDA	Adjunct Professor from Univ. Osaka Pref. (April '88–)
Reiko KURODA	Adjunct Associate Professor from Univ. of Tokyo (April '88–)
Kiyohiko NAKAJIMA	Research Associate
Dominique N. LUNEAU	JSPS Post-Doctoral Fellow (January '88–)
Nobuhiro FUKUSHIMA	Graduate Student from Tokyo Inst. of Tech. (April '88–)
Masahumi MIZUNO	Graduate Student from Nagoya Univ. (April '88–)

Coordination Bond

Akira UEHARA	Adjunct Professor from Kanazawa Univ. (April '88–)
Hisashi ŌKAWA	Adjunct Associate Professor from Kyushu Univ. (April '88–)

Research Facilities

Computer Center

Keiji MOROKUMA	Director
Hiroshi KASHIWAGI	Associate Professor
Umpei NAGASHIMA	Research Associate
Shigeyoshi YAMAMOTO	Technical Associate

Instrument Center

Ichiro HANAZAKI	Director
Iwao YAMAZAKI	Associate Professor (–March '88)[5]
Kiyokazu FUKE	Associate Professor (November '88–)
Keisaku KIMURA	Research Associate
Naoto TAMAI	Research Associate (–October '88)[6]
Naoki SATO	Visiting Research Fellow from Kao Corp. (April '87–)

Chemical Materials Center

Keitaro YOSHIHARA	Director
Hidemasa TAKAYA	Associate Professor (–March '88)[7]
Kazushi MASHIMA	Research Associate (–May '88)[8]
Tetsuo OHTA	Technical Associate

Low-Temperature Center

Yusei MARUYAMA	Director
Kunio AWAGA	Research Associate

Equipment Development Center

Teizo KITAGAWA	Director
Tadaoki MITANI	Associate Professor
Yoshihiro TAKAGI	Research Associate
Hiroshi OKAMOTO	Research Associate

Ultraviolet Synchrotron Orbital Radiation Facility

Katsumi KIMURA	Director
Makoto WATANABE	Associate Professor
Toshio KASUGA	Associate Professor
Shun-ichi NAOÉ	Adjunct Associate Professor from Kanazawa Univ. (April '87–)
Hiroto YONEHARA	Research Associate
Kazutoshi FUKUI	Research Associate
Atsunari HIRAYA	Research Associate

Technical Staff

Akira UCHIDA	Technical Division Head
Keiichi HAYASAKA	Technical Section Chief
Kusuo SAKAI	Technical Section Chief
Satoshi INA	Computer Center (Unit Chief)
Fumio NISHIMOTO	Computer Center
Fumitsuna TESHIMA	Computer Center
Takaya YAMANAKA	Instrument Center
Shunji BANDOW	Instrument Center
Kiyonori KATO	Low-Temperature Center (Unit Chief)
Shuji NAKANE	Low-Temperature Center

Taeko MAEDA	Chemical Materials Center
Kazuo HAYAKAWA	Equipment Development Center (Unit Subchief)
Hisashi YOSHIDA	Equipment Development Center
Masashi NAGATA	Equipment Development Center
Kouichi UCHIYAMA	Equipment Development Center
Toshio HORIGOME	Equipment Development Center (Unit Subchief)
Norio OKADA	Equipment Development Center
Mitsukazu SUZUI	Equipment Development Center
Nobuo MIZUTANI	Equipment Development Center
Shinji KATO	Equipment Development Center
Osamu MATSUDO	UVSOR Facility (Unit Chief)
Toshio KINOSHITA	UVSOR Facility
Masami HASUMOTO	UVSOR Facility
Jun-ichiro YAMAZAKI	UVSOR Facility
Eiken NAKAMURA	UVSOR Facility

* Carries out graduate research at IMS on the Cooperative Education Programs of IMS with graduate schools.
1) Present Address: Dept. of Chemistry, Hiroshima Univ., 1-1-89, Higashi-Senda, Naka-ku, Hiroshima 730
2) Present Address: College of Arts and Sciences, Univ. of Tokyo, 3-8-1, Komaba, Meguro-ku, Tokyo 153
3) Present Address: Dept. of Phys., Faculty of Science, Univ. of Tokyo, 7-3-1, Hongo, Bunkyo-ku, Tokyo 113
4) Present Address: Chem. Dept. of Resources, Mie Univ., Tsu 514
5), 6) Present Address: Dept. of Chemical Process Engineering, Faculty of Engineering, Hokkaido Univ., Sapporo 060
7), 8) Present Address: Dept. of Industrial Chemistry, Faculty of Engineering, Kyoto Univ., Sakyo-ku, Kyoto 606

Foreign Visiting Staff

Ping Wang	Inst. Chem., Acad. Sin., China	Oct. 1986–Nov. 1988
Ye Wen	Inst. Chem., Acad. Sin., China	Feb. 1987–Aug. 1988
Anthony J. Dann	Univ. of Nottingham, UK	May 1987–May 1989
Hasuck Kim	Seoul Natl. Univ., Korea	Jul.–Sep. 1987
		Jan.–Feb. 1988
Dongho Kim	Korea Adv. Inst. Sci. Tech., Korea	Jul.–Sep. 1987
		Jan.–Mar. 1988
		Jun.–Jul. 1988
Marshal D. Newton	Brookhaven Natl. Lab., USA	Nov. 1987–Mar. 1988
Seung C. Park	Kangweon Natl. Univ., Korea	Dec. 1987–Feb. 1988
Zbignew R. Grabowski	Inst. Phys. Chem., Pol. Acad. Sci., Poland	Dec. 1987–Mar. 1988
Martin A. Bennett	Australian Natl, Univ., Australia	Feb.–May 1988
Lin He	General Inst. for Non-Ferrous Metals, China	Apr.–Sep. 1988
Yoon S. Kong	Chonbuk Natl. Univ., Korea	Jun. 1988–
Cuiji Zhang	Inst. Chem., Acad. Sin., China	Jul.–Nov. 1988
Michael R. Fahy	Univ. of Nottingham, UK	Jul. 1988–Jul. 1989

COUNCIL

Hiroo INOKUCHI **Director-General**

Councillors

Chairman	Kenichi FUKUI	President, Institute for Fundamental Chemistry
Vice-Chairman	Hiroaki BABA	Professor, The Research Institute of Applied Electricity, Hokkaido University
	Eiichi FUJITA	President, Osaka University of Pharmaceutical Sciences
	Sachio HAYAKAWA	President, Nagoya University
	Ryuichi HIRANO	Professor Emeritus, The University of Tokyo
	Namio HONDA	President, Toyohashi University of Technology
	Sho ITO	Professor, Tokushima Bunri University
	Kouzou KUCHITU	Professor, Nagaoka University of Technology
	Michio KURATA	Professor Emeritus, The University of Kyoto
	Masatoshi MORITA	Chief Executive Officer, Toyota Central Research & Development Laboratories, INC
	Haruo NISHIHARA	President, Waseda University
	Minoru ODA	President, Institute of Physical and Chemical Research
	Yoshihiko SAITO	Professor, Keio University
	Kenji TAMARU	Professor, The Science University of Tokyo
	Ikuzou TANAKA	President, Tokyo Institute of Technology
	Yutaka TOYOZAWA	Professor, Chuo University
	Manfred EIGEN	Head of Department, Max-Planck Institute of Physical Chemistry and Professor, Technical University of Gottingen (–December '86)
	Robert G. PARR	Professor, University of Northcarolina (August '86–)
	Heinz A. STABB	President, Max-Planck Society for The Advancement of Science, F.R.G. (January '88–)

The Council is the advisory board for the Director-General. Two of the councillors are selected among distinguished foreign scientists.

Distinguished Research Consultants

Kenichi FUKUI	President, Kyoto Institute of Technology; Professor Emeritus, Kyoto University
Masao KOTANI	Professor Emeritus, The University of Tokyo
Yonezo MORINO	Professor Emeritus, The University of Tokyo; Director and Supreme Consultant, Sagami Chemical Research Center
Saburo NAGAKURA	President, The Graduate University for Advanced Studies

Administration Bureau

Kiyoshi INOUE	Director-General, Administration Bureau (–March '88)
Shousuke WAKISAKA	Director-General, Administration Bureau (April '88–)
Yukio OHMURA	Director, General Affairs Department
Hozumi KISHIYAMA	Director, Finance and Facilities Department (–October '87)
Jitsuo SUZUKI	Director, Finacne and Facilities Department (November '87–)
Hideo ISHIKAWA	Head, General Affairs Division (–October '87)
Nobuaki SHIMIZU	Head, General Affairs Division (November '87–)
Junsaku NAGATA	Head, Personnel Division
Minoru AKIMOTO	Head, Research Cooperation and International Affairs Division
Takashi TAKIGAWA	Head, Budget Division
Kaoru KATO	Head, Accounts Division
Michitaro MATUI	Head, Construction Division
Motokazu FURUYA	Head, Equipment Division

BUILDINGS AND CAMPUS

The IMS campus covering 62,343 m^2 is located on a low hill in the middle of Okazaki City. The inequality in the surface of the hill and growing trees are preserved as much as possible, and low-storied buildings are adopted for conservation of the environment. The buildings of IMS are separated according to their functions as shown in the map. The Research Office Building and all Research Facilities except for the Computer Center are linked organically to the Main Laboratory Building by corridors. Computer Center, Library, and Administration Buildings are situated between IMS and the neighboring National Institute for Basic Biology and National Institute for Physiological Sciences, because the latter two facilities are common to these three institutes.

The lodging facility of IMS called Yamate Lodge, located within 10 min walk, has sleeping accommodations for 19 guests and two families. Since June 1, 1981 a new lodging facility called Mishima Lodge has been opened. Mishima Lodge, located within four minutes' walk east of IMS can accommodate 68 guests and ten families. Scientists who visit IMS as well as the two other institutes can make use of these facilities. Foreign visiting scientists can also live at these lodgings with their families during their stays.

The Institute for molecular Science

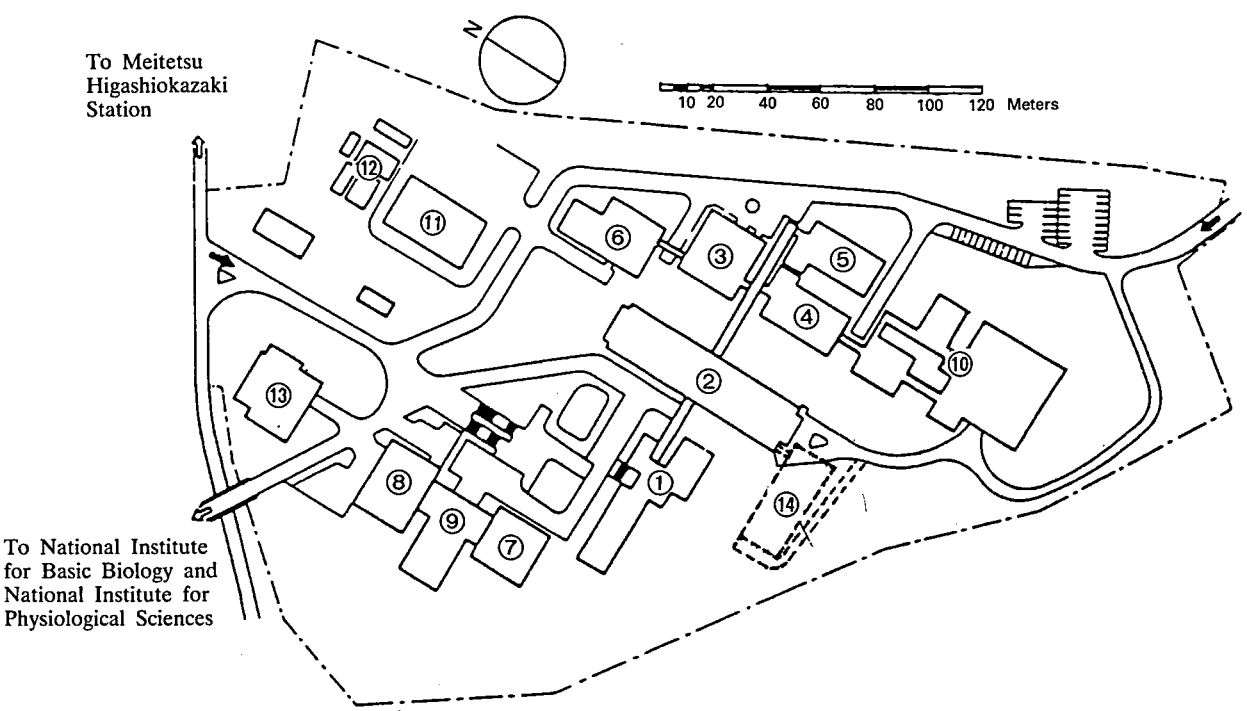

1. Research Office Building
2. Main Laboratory Building
3. Equipment Development Center
4. Instrument Center
5. Chemical Materials Center
6. Low-Temperature Center
7. Computer Center
8. Library
9. Central Administration
10. UVSOR Facility
11. Power Station
12. Waste-Water Disposition Facilities
13. Faculty Club
14. South Laboratory Building (under construction)

Okazaki (population 280,000) is 260 km southwest of Tokyo, and can be reached by train in about 3 hours from Tokyo via New Tokaido Line (Shinkansen) and Meitetsu Line.
The nearest large city is Nagoya, about 40 km west of Okazaki

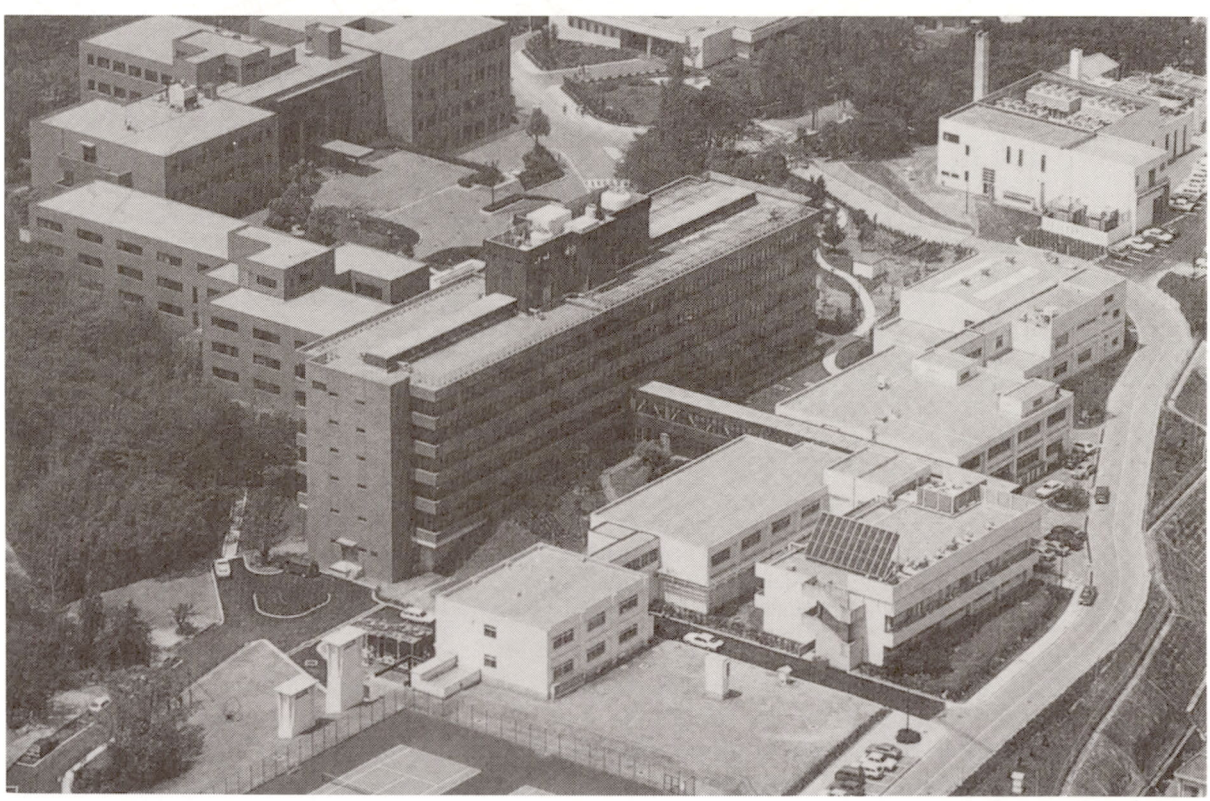

RESEARCH ACTIVITIES I
Department of Theoretical Studies

I–A Potential Energy Surfaces and Dynamics of Elementary Chemical Reactions

The theoretical study of potential energy surfaces and dynamics for elementary chemical reactions, with the emphasis of those involving more than one potential energy surface, remains to be one of the central themes of research of the Morokuma group. Though Dr. Satoshi Yabushita who were with our group since October 1986 left IMS in April 1988 for a permanent job at the Hiroshima University, we hope to continue collaboration with him in connection with his new code incorporating spin-orbit interaction in a large scale CI calculation.

I-A-1 A Theoretical Study of Transition State Spectroscopy: Laser Dressed Potential Energy Surface and Surface Hopping Trajectory Calculations on K + NaCl and Na + KCl

Koichi YAMASHITA and Keiji MOROKUMA

Spectroscopy during the chemical reactions, K + NaCl and its reverse, has been studied by surface hopping trajectory calculations. Laser-absorption and emission processes are modeled as the nonadiabatic transitions between the laser-dressed ground and excited state potential energy surfaces, which are constructed from our ab initio potential energy and transition dipole functions.[1] The theoretical Na-D emission spectrum as a function of laser wavelength agrees qualitatively with the experiment by Maguire et al.[2] The emission spectrum is found to be very different from the absorption spectrum, because only a small portion of excited trajectories reach the Na* product due to the endothermicity of the excited state reaction. Therefore the emission spectrum reflects only the excited state dynamics but not the transition state spectroscopy. We also predicted the absorption and emission spectra for the reverse reaction and found that this emission spectrum may reflect to a large extent the transition state spectroscopy.

References

1) K. Yamashita and K. Morokuma, *J. Phys. Chem.* **92**, 3109 (1988).
2) T.C. Maguire, P.R. Brooks, R.F. Curl, J.H. Spence and S.J. Ulvick, *J. Chem. Phys.* **85**, 844 (1986).

I-A-2 Ab Initio Potential Energy Surfaces of Charge-Transfer Reactions: $F^+ + CO \rightarrow F + CO^+$

Koichi YAMASHITA, Keiji MOROKUMA, Yasushi SHIRAISHI* and Isao KUSUNOKI* *(*Tohoku Univ.)*

The ab initio potential energy surfaces of the charge-transfer reaction $F^+ + CO \rightarrow F + CO^+$, studied experimentally by Kusunoki and Ishikawa,[1] are calculated by the MRSD-CI method using the DZP basis set. Twelve low-lying $^3A'$ and $^3A''$ states, originated from the initial $F^+(^3P) + CO(X^1\Sigma^+)$, the final $F(^2P) + CO^+(A^2\Pi)$ and the ground state $F(^2P) + CO^+(X^2\Sigma^+)$, are investigated for full three dimensional interactions between the F atom and the CO molecule. Based on the potential energy surface characteristics and the nonadiabatic coupling between the initial and final states, the mechanism of charge transfer are discussed; i.e. where the charge transfer occurs and which electronic states are involved. A simple theoretical model which emphasizes an importance of the nonadiabatic coupling along the CO vibrational coordinate is introduced to interpret the vibrational excitation of the product $CO^+(A)$.

Reference

1) I. Kusunoki and T. Ishikawa, *J. Chem. Phys.* **82**, 4991 (1985).

I-A-3 Potential Energy Surfaces for ClCN Photodissociation Reaction

Satoshi YABUSHITA, Shi-jun ZHENG *(Hebei Teachers' College and IMS)*, **and Keiji MOROKUMA**

Ab initio MCSCF calculations are performed to understand the mechanism of the fragment rotation in the photodissociation of ClCN molecule in the lowest absorption band. Using the standard DZP basis set and the $(3\sigma,3\pi_x,3\pi_y)^{12}$ CAS, we have found that the lowest siglet excited state is $^1\Pi$ ($\pi\rightarrow\sigma^*$), in conflict with Waite et al., whose assignment was $^1\Sigma^-(\pi\rightarrow\pi^*)$ in the X-α method. A simple correlation diagram and our actual calculations showed that the $^1\Pi$ state correlates directly to the product of $CN(^2\Sigma^+)$ and $Cl(^2P)$, while the $^1\Sigma^-$ state correlates adiabatically to the $CN(^2\Pi)$ channel via an avoided crossing. We have also found that both components ($^1A'$ and $^1A''$) of the $^1\Pi$ surface are unstable to the molecular bending (Renner-Teller effect), in consistent with the experimentally observed fragment rotation. These results suggest that at least these two components of the $^1\Pi$ surface must be included in the dynamics calculations.

I-A-4 An Implementation of Spin-Orbit Direct CI Method Based on the Spin-Dependent UGA.

Satoshi YABUSHITA and Keiji MOROKUMA

In recent years, there has been increasing interest in the inclusion of relativistic effects for molecules containing heavy atoms. One of the most practical yet reliable methods is to use relativistically derived effective core potentials. Based on the spin-dependent UGA,[1] we have extended and reorganized the COLUMBUS direct CI program package[2] to carry out large scale spin-orbit (SO) CI calculations in which one-electron spin-orbit Hamiltonian is treated explicitly as a part of the total Hamiltonian in the L-S coupling scheme. The formulae of the necessary SO coupling coefficients, originally derived by Drake and Schlesinger,[3] were further simplified for the actual coding. We use the "real spherical" form of spin functions for an even number electron system to facilitate the symmetry adaptation and to make the CI matrix elements completely real. For an odd number electron system, we devise the program to compute only one component of a Kramers pair. The CI program was fully vectorized on the Hitachi S820 supercomputer.

References

1) M.D. Gould and G.S. Chandler, *Int. J. Quant. Chem.*, **26**, 441 (1984).
2) H. Lischka, R. Shepard, F.B. Brown and I. Shavitt, *ibid.*, **15S**, 91 (1981).
3) G.W.F. Drake and M. Schlesinger, *Phys. Rev.*, **A15**, 1990 (1977).

I-A-5 Potential Energy Surfaces for Rotational Excitation of CH_3 Product in Photodissociation of CH_3I

Satoshi YABUSHITA and Keiji MOROKUMA

[*Chem. Phys. Lett.*, in press]

Potential energy surfaces of low-lying excited states of CH_3I have been calculated for symmetric (C_{3v}) and bent(C_s) dissociation using the ab initio CI method with the effective spin-orbit Hamiltonian. A small but significant bending torque arises for the A′ surfaces near the $3E\text{-}2A_1$ conical interesection, which can be the origin of CH_3 rotational excitation observed in CH_3I photodissociation.

I-A-6 Potential Energy Surface Characteristics and Mode-Selective Reactivity

Koichi YAMASHITA and Keiji MOROKUMA

Vibrational enhancement of the following reactions are

$$HCl(v) + C_2H_2(v') \rightarrow C_2H_3Cl \qquad (R1)$$
$$NH_3^+(v) + H_2(v') \rightarrow NH_4^+ + H \qquad (R2)$$

investigated by ab initio calculations. The structures of the reactants, the transition states, and the products are optimized and the intrinsic reaction coordinates (IRC) connecting them are traced by the analytical gradient method at the 6-31G*/RHF (for R1) and MP2 (Moller-Plesset) (for R2) levels. The vibrational frequency analyses along IRC are carried out to obtain the curvature of IRC and the coupling elements among the

vibrational modes perpendicular to IRC. In R1 the curvature has a maximum at the reactant side due to the coupling between IRC and the mode which relates to the HCl stretching mode at the reactant. On the other hand, in R2, the curvature has a maximum at around the transition state and another on the product side. The main components of the curvature are the modes which correlate respectively to the H_2 stretching mode and NH_3 umbrella mode at the reactant. We discuss how much these reactions are vibrationally adiabatic by comparing the location of transition state and the location of large reaction coordinate curvature. The results suggest two different cases where the vibrational enhancement might be expected.

I–B Theoretical Studies on Mechanisms of Organic Reactions

Dr. Andrea Dorigo, a PhD from UCLA under Ken Houk, joined our group in February 1988 as a Postdoctoral Fellow and has been involved actively in theoretical studies of various aspects of stereoselectivity in organic reactions. We have also had a pleasant collaboration with Professors Borden and Skancke on some electrocyclic reactions.

I-B-1 Theoretical studies of Nucleophilic Additions of Organocopper Reagents to Acrolein. Rationalization of the Differences in Regioselectivity in the Reactions of Methylcopper and Methyllithium.

Andrea E. DORIGO and Keiji MOROKUMA

[*J. Am. Chem. Soc.*, in press]

Ab initio molecular orbital studies of the addition of methyllithium and methylcopper to acrolein have been performed. Transition states for addition to the carbonyl group (which gives the alcohol as the final product), to the carbon – carbon double bond, and across the π system (both of which lead to formation of the saturated ketone) have been located. Calculations at the HF/3-21G (with full geometry optimization), HF/6-31G*, and MP2/6-31G* levels indicate that reaction of methyllithium with the carbonyl group is preferred to conjugate addition to the double bond, in agreement with experimental data. In the computations of all species containing copper, an effective core potential was used in place of the inner-shell electrons. Calculations at the HF/3-21G-ECP(SZ) and -ECP(DZ) levels were performed with full geometry optimization, and single-point energy calculations were carried out at the HF/6-31G*-ECP(DZ) and, in selected cases, MP2/6-31G*-ECP(DZ) levels. All calculations indicate that 1,4-addition across the π system *via* a six-membered transition state is greatly favored over 1,2-addition. 1,4-addition *via* a four-membered transition state is calculated to be slightly disfavored with respect to 1,2-addition to the carbonyl group.

I-B-2 Stereoselectivity of the Nucleophilic Addition of Organometallic Reagents to α,β-Unsaturated Chiral Carbonyl Compounds. Theoretical Model Studies of Steric and Electronic Effects.

Andrea E. DORIGO and Keiji MOROKUMA

Ab initio molecular orbital studies have been conducted on the addition of methyllithium to the C=C bond of *E* and *Z*-crotonaldehyde (both for the *s-trans* and for the *s-cis* conformation). In the reaction with *E*-β-ethyl acrolein, the most stable conformation in the transition state has the methyl group *anti* to the nucleophile, with the *inside* position being preferred to the *outside* position. In contrast, calculations suggest that the *outside* position is favored over the *inside* position in the reaction with *Z*-β-ethyl acrolein. These calculations suggest that *E*- and *Z*-α,β-unsaturated carbonyl compounds should give, respectively, Felkin-Anh-type and anti-Felkin-Anh-type stereoselectivity. The effect of an alkoxy substituent has also been investigated, by using the hydroxy group as a model, in the reaction of *E*-β-hydroxymethyl acrolein. The con-

formational preference exhibited by the hydroxy group is found to be dictated by electronic, rather than steric, considerations. The two sets of calculations lead to the conclusion that when both an alkyl and a hydroxy group are present, the favored transition state has the alkyl group *anti* and the alkoxy group *inside* with respect to the incoming nucleophile. These results are in full agreement with recently published experimental data.

I-B-3 Chair and Boat Transition States for the Cope Rearrangement. A CASSCF Study

Keiji MOROKUMA, Weston T. BORDEN *(Univ. of Washington and IMS)*, **and David A. HROVAT** *(Univ. of Washington)*

[*J. Am. Chem. Soc.*, **110**, 4474 (1988)]

Complete active space SCF (CASSCF) calculations have been performed on the Cope rearrangement with an MCSCF wavefunction, consisting of all the configurations which arise from the occupancy of 6 orbitals by 6 electrons. Both chair (C_{2h}) and boat (C_{2v}) geometries were optimized, using the 3-21G basis set; and each was characterized as a transition state by a full vibrational analysis. The bond lengths, R, between the two allylic fragments in the optimized chair (R = 2.09Å) and boat (R = 2.32Å) geometries are considerably longer than those (R < 1.67Å) predicted by semiempirical calculations. The computed CASSCF differences in the entropies and enthalpies between the two transition states are both smaller than those obtained by experiment. A possible explanation of this discrepancy is proposed.

I-B-4 A Theoretical Study of the Thermal Degenerate Rearrangement in Methylenecyclobutane

Per N. SKANCKE *(Univ. of Tromsö and IMS)*, **Nobuaki KOGA, and Keiji MOROKUMA**

[*J. Am. Chem. Soc.*, in press]

Ab initio molecular orbital calculations, using 3-21G through 6-31G* basis sets and including electron correlation through CASSCF and MP4 have been applied in a study of the thermal degenerate rearrangement of methylenecyclobutane (**1**). Our calculations indicate that the process goes through an intermediate stabilized by π-electron delocalization in the allylic moiety. The intermediate nearly has C_s symmetry, with very low barrier to rotation of the migrating CH_2 group. The transition state between (**1**) and the intermediate is found to have a CCCC dihedral angle of 67° and one CH_2 group perpendicular to the CCH_2 group within the allylic moiety. The CASSCF calculations with the UHF-based zero point energy correction give a barrier height of 49 kcal/mol. Estimates of the barrier height by UMPn calculations were found to be uncertain due to extensive spin contamination in the UHF wave function of the TS. Exploratory calculations on the conversion of spiropentane to methylenecyclobutane suggest that the process is initiated by a peripheral bond fission in spiropetane.

I-B-5 Theoretical Study of Hydroboration of Norbornene Derivative

Nobuaki KOGA, Tadahiro OZAWA *(Kao Corp. and IMS)*, **and Keiji MOROKUMA**

The hydroboration of tricyclo[6.2.1.$0^{2,7}$]undec-2(7)-ene (**1**), the norbornene derivative gives exclusively exo tricyclo[6.2.1.$0^{2,7}$]undecan-3-ol (**5a**), suggesting the isomerization from the alkyl borane (**3**) of the direct hydroboration product corresponding to tricyclo-[6.2.1.$0^{2,7}$]undecan-2-ol (**3a**) to the alkyl borane (**5**) corresponding to **5a**. In order to clarify factors which makes **5** more favorable, we have carried out the ab initio RHF MO calculations on the reactions: **1**+BH_3 → **1**...BH_3 complex (**2**) → TS1 → **3** → TS2 → tricyclo[6.2.1.$0^{2,7}$]undec-2(3)-ene...BH_3 complex (**4**) → TS3 → **5**. The basis functions used are 3-21G for the reaction center and STO-3G for the remaining fragment. The energetics (in kcal/mol) obtained are −4, 10, −19, 12, −9, 8, and −20 for **2**, TS1, **3**, TS2, **4**, TS3, and **5**, respectively, relative to **1**+BH_3. The energy difference between **3** and **5** are less than 1 kcal/mol and thus the preference of **5a** may not be interpreted based on the potential energy profile. It has been experimentally found that the two norbornene derivatives add to one BH_3. **5** would be more favorable in such a hindered compound.

I–C Structure and Reactions of Transition Metal Complexes

In the last several years organometallic chemistry has been one of the most active fields of our theoretical studies. With a heavy use of the supercomputer at the Computer Center, we have been able to extend our study into several general and important reactions of transition metal complexes, including intermolecular C-H bond activation by a Rh complex and olefin insertion by a Ti complex. We have also enjoyed a continued and fruitful collaboration with Professor Sakaki of Kumamoto University.

I-C-1 Intermolecular CH Bond Activation and Alkane Complex Intermediate. An Ab Initio MO Study

Nobuaki KOGA and Keiji MOROKUMA

Intermolecular CH bond activation is currently drawing a considerable attention and several examples are known in which oxidative addition of a CH bond to a coordinatively unsaturated complex realizes the CH activation. In order to investigate the potential energy surface of the CH bond activation, we have studied the oxidative addition of CH_4 to coordinatively unsaturated $RhCl(PH_3)_2$ with an ab initio MO method under the effective core potential approximation.

$$CH_4 + RhCl(PH_3)_2 \rightarrow HRhCl(PH_3)_2(CH_3)$$

We have found the methane complex, $CH_4 \ldots RhCl(PH_3)_2$ in which two CH bonds of the CH_4 interact with the Rh atom. The energies of the stationary points relative to the isolated reactants are −17 kcal/mol for the CH_4 complex, −14 kcal/mol for the transition state, and −24 kcal/mol for the product at the MP4 level. The small activation energy of 3 kcal/mol suggests that oxidative addition to a coordinatively unsaturated complex is extremely easy. Since the transition state is lower than the isolated reactants in energy, the Rh fragment can migrate from one CH bond to another intramolecularly.

I-C-2 Potential Energy Surface of Olefin Hydrogenation by Wilkinson Catalyst $RhCl(PR_3)_2$. Comparison between Trans and Cis Biphosphine Intermediates

Nobuaki KOGA and Keiji MOROKUMA

In our previous study,[1] we have studied with the ab initio MO method the model catalytic cycle of the Halpern mechanism for olefin hydrogenation by the Wilkinson catalyst by using ethylene and PH_3 as olefin and PR_3. Since the intermediates in this mechanism have been considered to have trans biphosphine ligands, we have calculated the potential energy profile of the cycle with the trans biphosphine Rh intermediates. Recently, however, Brown et al. have suggested the possibility that the cis biphosphine Rh intermediates may be involved and proposed the new mechanism in which the cis biphosphine intermediates are involved.[2] Therefore, we calculated with the ab initio MO method the potential energy profile of the Brown mechanism in order to compare it with the Halpern mechanism. We have found that the profile of the former is quite different from that of the latter. For instance, while in the Halpern mechanism the ethylene insertion is endothermic by 16 kcal/mol, that is exothermic by 6 kcal/mol in the Brown mechanism. The isomerization from trans-diphosphine dihydride complex to cis-diphosphine dihydride complex, the key step in the Brown mechanism, was found to be difficult.

References

1) C. Daniel, N. Koga, J Han, X.Y. Fu, and K. Morokuma, *J. Am. Chem. Soc.* **110**, 3773 (1988).
2) J.M. Brown, P.L. Evans, and A.R. Lucy, *J. Chem. Soc. Perkin Trans. II* 1589 (1987).

I-C-3 Ab Initio MO Study of Olefin Insertion: $CH_3TiCl_2^+ + C_2H_4 \rightarrow C_3H_7TiCl_2^+$

Nobuaki KOGA, Hiroshi KAWAMURA *(Sumitomo Chemical Co. and IMS)*, **and Keiji MOROKUMA**

In order to understand the polymerization of olefin

by Ziegler-Natta catalysts, we have performed all electron ab initio MO calculations of the ethylene insertion reaction into Ti-CH_3 bond. Different from usual olefin complexes in which the two M-C bond lengths are similar, the ethylene coordinates to $CH_3TiCl_2^+$ in an unsymmetrical way; one M-C bond is much shorter than the other. Therefore, two structures of the ethylene complex were found. Their energies are close to each other and the barrier for the isomerization between them is quite low, showing that the slide of the ethylene ligand within the coordination sphere is easy. This may be one of the reasons for the low activation energy: 12 kcal/mol at the RHF level and 7 kcal/mol at the MP2 level. The effect of the substituents on the energetics has been discussed.

I-C-4 Electronic Structure and Enhanced Reactivity of Carbon Dioxide Coordinated with Rhodium (I) Complex. An Ab Initio MO Study

Shigeyoshi SAKAKI*, Tetsuro AIZAWA*, Nobuaki KOGA, Keiji MOROKUMA, and Katsutoshi OHKUBO* *(*Kumamoto Univ.)*

[*Inorg. Chem.*, in press]

An ab-initio MO study has been carried out on $RhCl(AsH_3)_4(CO_2)$ and its isolobal complex, $(NH_3)(CO_2)$. Although $RhCl(AsH_3)_4(CO_2)$ has a pseudo-octahedral structure with a $4d^8$ electron configuration, a singlet state is calculated to be the most stable. This result agrees well with the experimentally reported diamagnetism. The reactivity of carbon dioxide for electrophilic attack is predicted to be much more enhanced in $RhCl(AsH_3)_4(CO_2)$ than in $(NH_3)(CO_2)$, which is rationalized in relation with the coordinate bonding nature of carbon dioxide.

I-D Theoretical studies of Molecular Electronic Properties

In collaboration with two research graduate students, Ms. Aoki and Mr. Sameshima, we have been able to participate in development of MO methods for polymer-molecule interaction and to extend our previous study on the intramolecular electron-transfer reaction.

I-D-1 Stereoelectronic Effects in Intramolecular Long-Distance Electron Transfer and Triplet Energy Transfer in Organic Compound. An Ab Initio MO Study

Nobuaki KOGA, Keiichiro SAMESHIMA *(Hoshi College of Pharm. and IMS)* **and Keiji MOROKUMA**

As an extention of our previous studies,[1] we have performed ab initio MO calculations with the STO-3G and 4-31G basis sets on radical anion and cation and triplet state of trans-1, 4-divinylcyclohexane, the model of experimentally studied organic compounds, to evaluate the trans annular interaction matrix element, $V_{a,b}$, for electron transfer (ET), hole transfer (HT), and triplet energy transfer (TT). The matrix element was calculated as the function of torsional angles of vinyl groups. It was found that the matrix element is highly dependent on the vinyl torsional angle. The matrix element for TT is much smaller than that for ET and HT, since TT is a two electron process while ET and TT are one electron processes.

Reference

1) K. Ohta, G.L. Closs, K. Morokuma, and N.J. Green, *J. Am. Chem. Soc.*, **108**, 1319 (1986).

I-D-2 Self-Consistent-Field Iterative Transfer Perturbation Method and its Application to the Interaction between a Polymer and a Small Molecule

Yuriko AOKI*, Akira IMAMURA* *(*Hiroshima Univ. and IMS)*, **and Keiji MOROKUMA**

[*J. Chem. Phys.* **89**, 1147 (1988)]

An iterative transfer perturbation method is proposed to treat the interaction between a polymer and a small molecule at the level of the ab initio method. The validity of our method is examined by applying it to a simple model system and comparing the results with those from the conventional tight-binding SCF crystal orbital method. The interaction energies and charge distributions obtained are in excellent agreement between the two methods. The present perturbational approach is promising for application to the more complicated interaction between a polymer and impurities.

I-D-3 Self-Consistent-Field Variational Approach to the Interaction between a Polymer and a Small Molecule

Yuriko AOKI*, Akira IMAMURA* *(*Hiroshima Univ. and IMS)*, **Keiji MOROKUMA**

[*Theor. Chim. Acta*, in press]

A variational SCF treatment based on a perturbational concept is developed and applied to the interaction between trans-polyacetylene and a small molecule. The validity of the present method is examined by comparing the results with those from the conventional tight-binding SCF crystal method. The interaction energies and charge distributions obtained are in good agreement between the two methods. This result suggests that the present variational approach is promising for application to complicated interactions between a polymer and impurities.

I-D-4 An ESR Study on Solvated Electrons in Water and Alcohols: Difference in the g Factor and Related Analysis of the Electronic State by MO Calculation

Hirotsugu SHIRAISHI*, Kenkichi ISHIGURE* *(*Univ. of Tokyo)*, **and Keiji MOROKUMA**

[*J. Chem. Phys.* **88**, 4637 (1988)]

An induction-detecting ESR spectrometer system, capable of μs time resolution, has been set up, and measurements were made on the radiolytically produced solvated electrons in water, methanol, ethanol, and mixtures of water and these alcohols. The spectrum of the solvated electron was a singlet in all these solvents. The g factor of the hydrated electron was measured to be 2.00047 ± 0.00007 at 22°C in reasonable agreement with the reported data. While this value is significantly smaller than the free electron g factor, the corresponding g factors in methanol and in ethanol, respectively 2.00205 ± 0.00007 and 2.00197 ± 0.00007 at 22°C, were found much closer to it. In both methanol-water and ethanol-water mixtures the g factor of the solvated electron varied approximately in proportion to the mole fraction. The g shift of the hydrated electron was interpreted as arising from spin density in the proximity of oxygen nuclei of water molecules. *Ab initio* MO calculations were performed for an anionic cluster of water and that of methanol, assuming a cavity-like structure. The result showed that while in a water cluster the spin population on oxygen $2p$ atomic orbitals was in fact significant, the corresponding orbital spin population was smaller in a methanol cluster especially with a dipole-oriented model. The difference was considered to be related to increased diffuseness of the half-occupied orbital in the latter cluster.

I-E Chemical Reaction Dynamics in Gas and Liquid Phases

To understand the chemical reactions in gas and liquid phases, we need to know not only the electronic and dynamic properties of reacting molecules, but also the nature of reactant and solvent molecular interactions such as solvation mechanism. We have made the following three studies for this purpose; (i) Nonadiabatic coupling between the excited and ground states of molecule, (ii) the energy dissipation mechanism of the excited molecules in liquid phases, (iii) the structure of the solvent and solute interactions (hydration structure) and (iv) liquid dynamics.

I-E-1 Large Local Energy Fluctuations in Water; (II) Cooperative Motions and Fluctuations

Iwao OHMINE, H. TANAKA *(Kyoto Univ.)* **and Peter G. WOLYNES** *(Illinois Univ. and IMS)*

[*J. Chem. Phys.*, in press]

Large local energy fluctuations in liquid water and their physical origin are investigated by using classical Molecular Dynamics (MD) calculation and quenching techniques. Performing a trajectory calculation of 100 picosecond, it is found that large rotational motions of individual water molecules, which are always associated with potential energy destabilizaition of 10–20kcal/mole, occure once in about 10 picoseconds. The stabilization and destabilization of the individual water molecules are induced by cooperative motions. In order to analyze these cooperative motions in the liquid water, the water structures are quenched to their local minima (called the inherent structures). Comparing the inherent structures successively visited by the system, it is found that collective motions of about 10–40 molecules localized in space occur in unstable regions. The potential energy fluctuation of individual molecule can reach up to 15kcal/mole even in the inherent structures. The strong potential energy correlation among neighbouring molecules indicates these cooperative motions cause the "flip-flop" type energy exchanges; as a molecule is stabilized, another is to be unstabilized and vice versa. A flip-flop motion does not involve a (large) energy barrier but causes large energy fluctuations of the individual molecules.

I-E-2 Transition State Analysis for Water Fluctuation Dynamics

Hideki TANAKA *(Kyoto Univ.)* **and Iwao OHMINE**

In the previous study, we have analysed the quenched structures (local minimum energy structures) of liquid water, successively visited by the system. We have found that the collective motions involving 20–40 water molecules, which as localized in space, are the main cause for the water fundamental structure changes. In the present work, we try to determine the transition states of these collective motions, the corresponding reaction coordinates, and the normal mode changes along the reaction coordinates. The physical origin for the large energy fluctuations of the individual water molecules is investigated by analyzing molecular dynamics along the reaction coordinates. The mode coupling along the large displacement of normal modes are examined. The similar analysis is also made for liquid Ar, in collaboration with Dr. Y.S. Kong.

I-E-3 Onset Behavior of the Vibrational Energy Relaxation Processes in Liquid Phases

Osamu KITAO and Iwao OHMINE

The optically activated molecules are followed by vibrational motions with large geometrical transformations. In order to investigate the relaxation processes of such large vibrational motions, we perform the MD calculation with an oscillator in Ar as a model system. We find that there exists an onset of the vibrational energy decay process. As shown in Figure 1, the energy decay rate sharply rises at the point where the amplitude of the oscillator becomes R=1.5 Å (the average amplitude of the ground state oscillator is 1.1 Å).

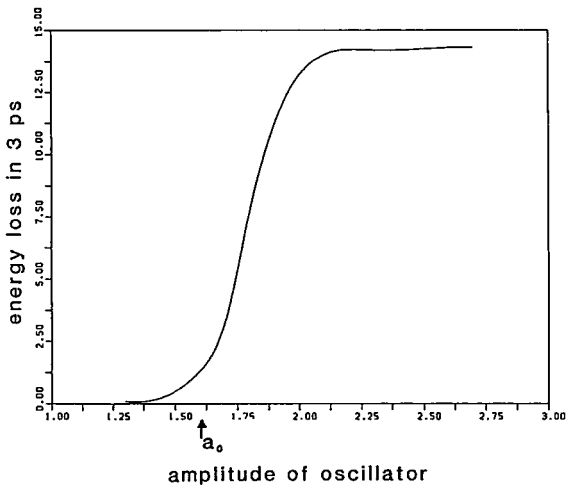

Figure 1. The vibrational energy decay of the oscillator (after 3 picoseconds) v.s. the initial amplitude of the excited oscillator.

I-E-4 A Theoretical Study of the Potential Energy Surface for the Charge Transfer Reaction $N^+ + CO \rightarrow N + CO^+$

Mutsumi AOYAGI

The mechanism of the charge transfer reaction $N^+ + CO \rightarrow N + CO^+$ is studied theoretically. The potential energy surface of this reaction is constructed by using ab initio multi-configuration (MC) SCF and multi-reference (MR) configuration interaction (CI) calculations. We found that the avoided crossing between $1^3\Sigma$ and $2^3\Sigma$ states exists when N^+ ion approaches linearly to CO from the O-side; $[N-OC]^+$. Relatively week coupling was observed in the other collinear approach $[N-CO]^+$. This difference in the coupling strength is explained by a simple MO picture. The potential energy surface calculated for bent geometries indicated that the transition from the $2^3A''$ state (corresponds to $1^3\Pi$ state in collinear, not $2^3\Sigma$ state) to the $1^3A''$ state ($1^3\Sigma$) might be also significant.

I-F Theoretical Studies of Chemical Reaction Dynamics

On the basis of the physical idea that mechanism of vibrational transition in atom-diatom chemical reaction is quite different from that of rotational transition, we treat them separately. As for vibrational transition, the sudden and adiabatic approximations reformulated in terms of the hyperspherical coordinates are applied to various reaction systems. A new theory (called IOS-DW approximation) was formulated, on the other hand, for the rotational transitions and proved to be quite useful.

I-F-1 Chemical-Reaction-Theoretical Approach to the Muon-Transfer Process

Akihiko OHSAKI, Hiroki NAKAMURA and Michael BAER *(Soreq Nuclear Research Center and IMS)*

[*Phys. Rev. A*, **38**, 2798 (1988)]

In view of the fact that the mass of the muon is only one-ninth of the mass of the proton, we propose to use a chemical-reaction-theoretical approach to investigate muon (μ^-) transfer between two nucleons such as d (deuteron), t (triton), and p (proton). In this paper we apply the recently proposed new implementation of the adiabatic approximation (with respect to hindered rotation) to the process $d\mu + t \rightarrow d + t\mu$. Cross sections are calculated at collision energies $E \cong 5 \sim 100$eV and are found to be in good agreement with the recent accurate quantum-mechanical calculations at $E \lesssim 10$eV. This indicates the usefulness of the present approximation.

I-F-2 Theory of Rotational Transition in Atom-Diatom Chemical Reaction

Masato NAKAMURA and Hiroki NAKAMURA

Rotational transition in atom-diatom chemical reaction is theoretically studied. A new approximate theory (which we call IOS-DW approximation) is proposed on the basis of the physical idea that rotational transition in reaction is induced by the following two different

mechanisms: rotationally inelastic scattering in both initial and final arrangement channels, and coordinate transformation in the region of potential ridge. This theory gives a compact expression for the state-to-state transition probability. Introducing the additional physically reasonable assumptions that reaction (particle rearrangement) takes place in a spatially localized region and that rotational degree of freedom does not strongly participate in reaction dynamics, we have succeeded in reducing this expression into a simpler analytical form which can explicitly give overall rotational state distribution in reaction. Numerical application was made to the H + H_2 reaction and demonstrated the effectiveness of the formula for its simplicity.

I-F-3 On the Evaluation of Cross Section and Rate Constant of Atom-Diatom Chemical Reaction in the Sudden and Adiabatic Approximations

Akihiko OHSAKI, Hiroki NAKAMURA and Seung C. PARK *(Kangweon National University and IMS)*

[*Comp. Phys. Commun.*, in press]

Usefulness of the constant centrifugal potential approximation is explicitly demonstrated. This method is treated in both the sudden (RIOS) and the adiabatic (reduced dimensionality) approximations by the direct numerical applications to the reaction systems Cl + H_2, Cl + HBr and O + HCl. Formulation of these two approximations in terms of the hyperspherical coordinates reported before is employed. This constant centrifugal potential approximation saves a lot of cpu time, because the orbital angular momentum ℓ necessary to obtain converged cross sections can easily be more than 100 and what we have to evaluate in this apporoximation is only the $\ell=0$ reaction probability as a function of collision energy. Brief discussion is also made concerning the choice of the position where the constant centrifugal potential is evaluated.

I-F-4 Quantum Mechanical Studies of Atom-Diatom Chemical Reactions in the Sudden and Adiabatic Approximations

Akihiko OHSAKI, Seung C. PARK *(Kangweon National University and IMS)* **and Hiroki NAKAMURA**

The sudden and adiabatic approximations reformulated in terms of the collinear-type hyperspherical coordinates are employed to study various atom-diatom reaction systems. A particular attention is paid to the clarification of the reaction mechanisms. Especially the effects of potential energy surface topography, and masses and internal energies of reactants on the reaction dynamics are investigated. Importance of the potential ridge is clearly demonstrated.

I–G Dynamic Processes of Electronically Highly Excited States of Simple Molecules

An ultimate purpose of this study is to understand the mechanisms of various dynamic processes of higher-(super-) excited states of molecules.

I-G-1 Theoretical Study of Associative Ionization of Hydrogen Atoms

Hidekazu TAKAGI *(Kitasato Univ.)* **and Hiroki NAKAMURA**

[*J. Chem. Phys.* **88**, 4552 (1988)]

Associative ionization of hydrogen atoms at low collision energies (~0.8–1.5eV),

$$H^*(2s) + H \rightarrow H_2^+(v^+) + e$$

is studied by using the multi-channel quantum defect theory. This process proceeds through the two-electron excited autoionizing state $^1\Sigma_g(2p\sigma_u)^2$. Vibrationally excited Rydberg states play a role of intermediate state and give a very rich resonance structure. The final vibrational states considered are $v^+=0$, 1, 2 and $v^+=1$ was found to give a dominant contribution.

I-G-2 Autoionization Mechanism of NO Molecule: Calculation of Quantum Defect and Theoretical Analysis of REMPI Experiment

Keiji NAKASHIMA *(Kyushu Univ. and IMS)*, **Hiroki NAKAMURA, Yohji ACHIBA** *(Tokyo Metropolitan Univ. and IMS)*, **and Katsumi KIMURA**

Quantum defects of $\ell\lambda$-Rydberg states (ℓ=s, p, d, $\lambda=\sigma$, π, δ) of NO were calculated by SCF and CI methods at various internuclear distances. Employing the multichannel quantum defect theory (MQDT), the recently observed REMPI photoelectron spectra were analyzed with use of the calculated quantum defects. Analysis was made particularly to the autoionization of vibrationally excited Rydberg states of the δ-symmetry. It is concluded that the autoionization is dominated by the two-step electronic mechanism in which dissociative superexcited state plays a role of intermeidiate state. Potential curve and electronic coupling strength of the relevant dissociative state were determined from this analysis. This provides us with a useful information to investigate various dynamic processes involving these superexcited states. Importance of dissociative superexcited state is again confirmed.

I–H Theory for High-T_c Superconductivity

To clarify the physical and chemical natures of the Cu-O type ceramic high-temperature superconductors, we theoretically study macroscopic and microscopic electronic structures of this material. The main purpose of this study is to clarify the origin of pairing attraction in this type material.

I-H-1 Ab Initio MO Calculations of Effective Exchange Integrals between Transition-Metal Ions via Oxygen Dianios: Nature of the Copper-Oxygen Bonds and Superconductivity

Kizashi YAMAGUCHI*, Yoichi TAKAHARA*, Takayuki FUENO* *(*Osaka Univ.)* **and Keiichiro NASU**

[*Jpn. J. Appl. Phys.* **26**, L1362 (1987)]

The superexchange interaction between transition-metal ions via oxygen dianion was investigated by the ab initio molecular orbital (MO) method. It is found that the magnitude of the effective exchange integral (J_{ab}) for the CuOCu unit is far larger than those of the NiONi, CrOCr and FeOFe units. Implications of this result are discussed in relation to the high T_c superconductivity for Ba-La-Cu-O and R-Ba-Cu-O (R=Y, etc.).

I-H-2 Ab Initio MO Studies on the Correlation and Spin Correlation Effects for Copper-Oxygen and Copper-Halogen Bonds in High-T_c Copper Oxide Superconductors

Kizashi YAMAGUCHI*, Yoichi TAKAHARA*, Takayuki FUENO* *(*Osaka Univ.)* **and Keiichiro NASU**

[*Jpn. J. Appl. Phys.* **26**, L2037 (1987)]

The correlation and spin correlation effects for $Cu^{+2}XCu^{+2}$ ($X=F^{-1}$, Cl^{-1} and O^{-2}) were investigated by the ab initio molecular orbital (MO) method. It is found that these effects are particularly strong for $Cu^{+2}F^{-1}Cu^{+2}$, while they are rather weak for $Cu^{+2}O^{-2}Cu^{+2}$. Implications of the ab initio MO results are discussed in relation to the high-T_c superconductivity for La-Ba-Cu-O and R-Ba-Cu-O (R=Y, etc.). The working hypotheses derived are applied to the molecular design of organic superconductors.

I-H-3 Ab Initio MO Studies of the Hole Delocalization in Copper Oxides and Related Species: Necessity of the Extended Hubbard Model

Kizashi YAMAGUCHI*, Yoichi TAKAHARA*, Takayuki FUENO* *(*Osaka Univ.)* **and Keiichiro NASU**

[*Jpn. J. Appl. Phys.* **27**, L509 (1988)]

The positive holes for copper oxides and isoelectronic species were investigated by the ab initio molecular orbital (MO) method. It is found that the hole is delocalized over the oxide clusters because of the strong $3d_\sigma$-$2p_\sigma$ hybridization, and that the spin polarization of the closed-shell pairs is remarkable, indicating an important role of the spin fluctuation for high-T_c superconductivity. The extended Hubbard model is necessary for theoretical studies of the hole delocalizations in copper oxides.

I-H-4 Ab Initio Molecular Orbital Calculations of Effective Exchange Integrals for Transition Metal Oxides and Halides: Strong Superexchange Interactions and High T_c Superconductivity

Kizashi YAMAGUCHI*, Yoichi TAKAHARA*, Takayuki FUENO* *(*Osaka Univ.)* **and Keiichiro NASU**

[*Physica* **C153–155**, 1213 (1988)]

Ab initio unrestricted Hartree-Fock (UHF) calculations involving the correlation corrections by the Mϕller-Plesset (MP) perturbation method are carried out for K_2NiF_4-type transition-metal halides and related copper oxides. The magnitude of effective exchange integrals (J_{ab}) obtained by the spin-projected UHF MP method is found to be particularly large for copper oxides, in agreement with recent experiments. Implications of these results are discussed in relation to spin-mediated theories for the mechanism of high-T_c superconductivity of copper oxides.

I-H-5 Superconductivities of a Quasi Two-Dimensional Peierls-Hubbard Model

Keiichiro NASU

[*Physica* **C153–155**, 231 (1988)]

As a model for Cu-O type high-T_c ceramics, we study a quasi two-dimensional Peierls-Hubbard model. The aim of this study is twofold. The first is to clarify whether the high-T_c's such as 100K can really be possible when the electron-phonon (e-p) coupling alone exists. The second is to clarify the effects of charge and spin fluctuations. For this sake, we have derived a new theory which can cover the whole region of the e-p coupling strength, from the weak (BCS) limit to the strong (bipolaronic) limit. T_c is found to become maximum at the intermediate region between these two limits, and the breathing mode of the ceramics is shown to be able to give a high-T_c of about 100K. In the next, the Hubbard-type correlation is taken into account, and the double excitation of magnons as well as the charge transfer excitations are shown to enhance this phonon-mediated s-wave pairing.

I–I Nonlinear Lattice Relaxation of Charge-Transfer Exciton in Halogen-Bridged Mixed Valence Metal Complexes

To clarify the nonlinear lattice relaxation process of the photo-generated charge transfer exciton in halogen-bridged mixed valence metal complexes, we study ground and excited states of a quasi one-dimensional Peierls-Hubbard model with half-filled electrons.

I-I-1 Nonlinear Lattice Relaxation of Photo-Generated Charge-Transfer Excitation in Halogen-Bridged Mixed-Valence Metal Complexes I, — Soliton and Self-Trapped Exciton —

Akiomi MISHIMA *(Kanazawa Inst. of Tech.)* **and Keiichiro NASU**

[*Phys. Rev. B*, in press]

The ground and excited states of a one-dimensional extended Peierls-Hubbard model with half-filled electrons are studied so as to clarify the lattice relaxation paths of photo-generated charge-transfer excitations in halogen-bridged mixed-valence metal complexes. The adiabatic potential energy surfaces that describe the nonlinear relaxation from the Franck-Condon state to

the solitonic states as well as to the self-trapped state of exciton (STE) are calculated within the mean-field theory for electrons. It is shown that the lowest excited state is a pair of doubly-charged spinless solitons, and it gives a photo-induced absorption band with an energy of about a half of the gap. It is also shown that the STE is separated from this soliton pair by only a small barrier, in agreement with the recent experiments on the unusual short decay time of this state.

I-I-2 Nonlinear Lattice Relaxation of Photo-Generated Charge-Transfer Excitation in Halogen-Bridged Mixed-Valence Metal Complexes II, —Polaron Channel—

Akiomi MISHIMA *(Kanazawa Inst. of Tech.)* **and Keiichiro NASU**

[*Phys. Rev. B*, in press]

The one-dimensional extended Peierls-Hubbard model with half-filled electrons is studied in order to clarify the lattice relaxation path of the photo-generated charge-transfer excitation in halogen-bridged mixed-valence metal complexes. The ground and excited states are calculated within the mean-field theory for electrons and the adiabatic approximation for phonons. It is concluded that the main origin of the experimentally observed photo-induced absorption is a distant pair of the hole-polaron and the electron-polaron. This distant pair is created not from the ground state of the self-trapped exciton (STE) but from the excited states of the STE through their auto-dissociation. This is consistent with the experiment on the excitation energy dependency of the photo-induced absorption yield.

I–J Electronic Structure of the Polymers

I-J-1 A Through Space/Bond Interaction Analysis of the Shape of the Band Structure of Polyacetylene

Yuriko AOKI *(Hiroshima Univ.)*, **Akira IMAMURA** *(Hiroshima Univ. and IMS)*, **and Takae SASAKI** *(Hiroshima Univ.)*

[*Bull. Chem. Soc. Jpn.*, **61**, 1063 (1988)]

The band structure of all-trans-polyacetylene is examined by using through space/bond interaction analysis. It is found that the cross-term in the perturbation expansion between two kinds of interactions governs the band shape near the gap. One kind is the interaction within the backbone, and the other is that between the backbone and the side chain. The relationship between the band structure and the symmetry of the interacting orbitals is also discussed.

I-J-2 A Theoretical Study on the Ionized State of Polymers with Localized Molecular Orbital Method

Akira IMAMURA *(Hiroshima Univ. and IMS)*, **Ye KEHONG** *(Hiroshima Univ.)*, **and Masahiro TAKETOSHI** *(Hiroshima Univ.)*

A Localized molecular orbital method for the investigation of ionized state of polymers is presented. It is based on the crystal orbital method. By performing a super cell method and Edmiston-Ruedenberg's LMO method, the Bloch function was transformed into nearly completely localized Wannier function. Furthermore, calculations of configuration interactions were carried out to obtain more reasonable results. The present method was applied to polyacetylene, polyethylene and polypropylene. Ionization potentials of these polymers were calculated and compared with experimental and other theoretical results. All the calculations were performed using CNDO/S approximation.

I–K Non-Equilibrium Statistical Processes in Condensed Matter

We study the effect of dynamical fluctuations on the relaxation phenomena in the frame of non-equilibrium statistical mechanics. We cover, at present, three fields; 1) spin relaxation of muon in solids, 2) kinetics of phase transition by coupled map lattice method, and 3) electron transport and recombination in a weakly ionized plasma.

I-K-1 Spin Depolarization of a Quantum Particle on a Linear Chain with Alternating Larmor Frequencies

Klaus W. KEHR *(Kernforschungsanlage Jülich, West Germany)* **and Kazuo KITAHARA** *(Tokyo Inst. of Tech. and IMS)*

[*J. Phys. Soc. Jpn* **57**, 2819 (1988)]

The spin depolarization of a particle on a linear chain with alternating Larmor frequencies is considered. The particle is initially prepared at one site with polarized spin. A crossover from initially classical behavior to an asympototic polarizaion is found, as a consequence of quantum-mechanical tunneling. The influence of dynamic fluctuations on the spin depolarization is studied in the frame of the Haken-Strobl model.

I-K-2 Phase Separation Dynamics and External Force Field

Kazuo KITAHARA *(Tokyo Inst. of Tech., Univ. of Illinois, USA and IMS)*, **Yoshitugu OONO** *(Univ. of Illinois, USA)* **and David JASNOW** *(Univ. of Pittsburgh, USA)*

[*Modern Physics Letters* **B2**, 765 (1988)]

If spinodal decomposition is modeled by the Cahn-Hilliard (-Cook) equation, the effect of a uniform external force such as gravitation does not appear in the bulk phase kinetics. In contrast, in the Kawasaki exchange modeling of the local dynamics of binary alloys, this effect directly modifies the bulk phase kinetics. We resolve this paradox through the cell-dynamical-system modeling of the Kawasaki exchange dynamics. Its continuum version has turned out to be a modified Cahn-Hilliard equation already proposed by Langer *et al.* about ten years ago. We demonstrate some examples in which the correction to the Cahn-Hilliard equation is significant.

I-K-3 Gas Kinetic Approach for Electron Mobility in Dense Media

Kazuyo KANEKO *(Tokyo Inst. of Tech.)*, **Yoshiyuki USAMI** *(Tokyo Inst. of Tech. and IMS)* **and Kazuo KITAHARA** *(Tokyo Inst. of Tech. and IMS)*

[*J. Chem. Phys.* in press]

The motion of electrons in nonpolar dense media is studied in the framework of gas kinetic transport theory. The observed external electric field dependence of electron mobility is explained by means of the solution of Boltzmann-type transport equation. Numerical calculations of the mobility, mean energy, and energy distribution function of electrons in liquid Ar and in liquid CH_4 are presented and a good agreement with experimental data is obtained. Also the cases of gaseous Ar is studied.

RESEARCH ACTIVITIES II
Department of Molecular Structure

II–A High Resolution Spectroscopy of Transient Molecules and Ions

During the course of chemical reactions many transient molecules and ions appear as intermediates. Because of their high reactivities, i.e. their short lifetimes, these transient species have remained to be explored and some of them have even escaped detection. Many of these molecules have open-shell electronic structure, which characterizes them as free radicals. Unpaired electrons in a molecule cause splittings in high resolution spectra of such species through fine and hyperfine interactions, and, when properly analyzed, these splittings provide us with information on the electronic properties of the molecule which is not obtainable for molecules without unpaired electrons. High resolution spectroscopy not only provides molecular constants of transient molecules at very high precision, but also allows us to unambiguously identify chemical species occuring in reaction systems and to unravel the details of reaction mechanisms, in particular, when it is combined with some time-resolved detection methods. The present project will also be of some significance in related fields such as astrophysics and environmental sciences, and even in semiconductor fabrication.

II-A-1 Infrared Diode Laser Spectroscopy of Lithium Hydride

Chikashi YAMADA and Eizi HIROTA

[*J. Chem. Phys.*, **88**, 6702 (1988)]

The fundamental and hot bands of the vibration-rotation transitions of ^{6}LiH, ^{7}LiH, ^{6}LiD, and ^{7}LiD were observed by infrared diode laser spectroscopy at Dopple-limited resolution. Lithium hydride molecules were produced by the reaction of the Li vapor with hydrogen at elevated temperatures. Some 40 transitions were observed and, after combined with submillimeter-wave spectra reported by G. M. Plummer et. al. [*J. Chem. Phys.*, **81**, 4893 (1984)], were analyzed to yield Dunham-type constants with accuracies more than an order of magnitude higher than those published in the literature. It was clearly demonstrated that the Born-Oppenheimer approximation did not hold, and some parameters representing the breakdown were evaluated. The Born-Oppenheimer internuclear distance r_e^{BO} was derived to be 1.594 914 26(59)Å, where a new value of Planck's constant recommended by CODATA was employed. The relative intensity of absorption lines was measured to determine the ratio of the permanent dipole moment to its first derivative with respect to the internuclear distance: $\mu_e/[(\partial \mu/\partial r)_e r_e]=1.743(86)$. The pressure broadening parameter $\Delta\nu_p/P$ was determined to be 6.40(22) MHz/Torr by measuring the linewidth dependence on the pressure of hydrogen, which was about four times larger than the value for the dipole-quadrupole interaction estimated by Kiefer and Bushkovitch's theory.

II-A-2 Infrared Diode Laser Spectroscopy of the Deuterium Bifluoride Anion

Kentarou KAWAGUCHI and Eizi HIROTA

We have previously reported a band at 1848.699 and at 1397.236 cm^{-1} for FHF^- and FDF^-, respectively, and assigned it to the ν_3 band.[1] However, we subsequently extended the measurement on FHF^- to 1300 cm^{-1} region and detected the ν_3 as well as ν_2 bands.[2] This result required the 1849 cm^{-1} band to be reassigned to $\nu_1 + \nu_3$. The spectrum of FDF^- was then reexamined, and we found the ν_3 and ν_2 bands in 930 cm^{-1} region, which were in strong Coriolis interaction with each other. By assuming the transition moment of the ν_2 band to be about one fifth of that of the ν_3 band, we could explain the observed intensities of the two bands. It was then found that neither of the upper and

lower states of the 1397 cm^{-1} band previously reported coincided with the ground state, and this band was thus reassigned to $2\nu_1 + \nu_3 \leftarrow \nu_1$. The $\nu_1 + \nu_3$ band was observed at 1469 cm^{-1}. Molecular constants derived from the observed spectra are listed in Table I. The equilibrium rotational constant was calculated to be 0.342 119(31) cm^{-1}, which was in good agreement with that of FHF^-, 0.342 069(21) cm^{-1}.

Table I. Molecular Constants of FDF^- (cm^{-1})[a]

State	B	$D \times 10^6$	η[b]	$\Delta\nu_0$
G.S.	0.335 787(13)	0.4240(18)		
ν_2	0.337 106(15)	0.4447(98)	0.591 532(18)	928.7303(17)
ν_3	0.322 944(14)	0.4565(69)		934.1933(7)
$\nu_1 + \nu_3$	0.319 687(43)		0.470 4(49)	1469.1852(8)
$\nu_1 + \nu_2$	[0.3346]	[0.464]		1509.55(53)

a. Values in parentheses denote three standard deviations and apply to the last digits of the constants. Values in square brackets are assumed.
b. Coriolis interaction constant.

References

1) K. Kawaguchi and E. Hirota, *J. Chem. Phys.*, **84**, 2953 (1986).
2) K. Kawaguchi and E. Hirota, *J. Chem. Phys.*, **87**, 6838 (1987).

II-A-3 Photochemical Processes of Acetylene at 193 nm. Kinetics of the CCH Radical

Hideto KANAMORI and Eizi HIROTA

The photolysis process of acetylene at 193 nm was examined through time-resolved observation of the infrared spectra of the CCH radical, which was thought to be one of the most important intermediate species in the process. In the case of pure acetylene, CCH radicals were not prepared initially. The time profile of a line at 1849 cm^{-1}, which was ascribed to a U species, possibly hot CCH, was analyzed using $d[U]/dt = k_1 [C_2H_2][X] - k_2[C_2H_2][U]$, where X was identified as excited acetylene, yielding $k_1 = 1.1\times10^{-10}$ and $k_2 = 6.6\times10^{-11}$ cm^3 $molecule^{-1}s^{-1}$. It should be noted that the formation of U is also proportional to $[C_2H_2]$. Addition of buffer gas primarily increases both k_1 and k_2; the effect is in the following order $H_2 \gg Ar > He > C_2H_2$. This effect is mainly ascribed to opening a second channel which relaxes U to the ground vibronic state. For H_2, the modified k_1 (k_1') and the relaxation rate constant k_2' were nearly identical, both being 1.9×10^{-11} cm^3 $molecule^{-1}s^{-1}$. Further careful examination of the time profile of the ν_3 band P(6) line indicated that the signal changed from absorption to emission and then returned to absorption again. This behavior is ascribed to competition between the ν_2 ladder and rotational relaxations.

II-A-4 Microwave Spectroscopic Detection of Dichlorosilylene $SiCl_2$ in the Ground Vibrational State

Mitsutoshi TANIMOTO *(Sagami Chem. Res. Center and Shizuoka Univ.)*, **Harutoshi TAKEO** *(Nat. Chem. Lab. Ind.)*, **Chi MATSUMURA** *(Nat. Chem. Lab. Ind.)*, **Masaharu FUJITAKE, and Eizi HIROTA**

Dichlorosilylene $SiCl_2$ has been characterized through its microwave spectrum. The molecule was generated by the thermal reaction between silicon powder and tetrachlorosilane at about 1000°C. The rotational constants and the centrifugal distortion constants were determined for the three isotopic species $Si^{35}Cl_2$, $Si^{35}Cl^{37}Cl$, and $Si^{37}Cl_2$, as shown in Table I. The nuclear quadrupole coupling constants were determined from the hyperfine splitting observed for several transitions with high K_a values.

Table I. Molecular Constants of Dichlorosilylene[a]

Constant	$Si^{35}Cl_2$	$Si^{35}Cl^{37}Cl$	$Si^{37}Cl_2$
A/MHz	14 781.0820(56)	14 667.3053(67)	14 552.097(34)
B/MHz	2 822.4122(17)	2 745.5121(15)	2 670.0649(79)
C/MHz	2 366.4822(16)	2 309.3659(15)	2 252.9943(93)
Δ_J/kHz	1.332 36(41)	1.266 88(35)	1.204 1(16)
Δ_{JK}/kHz	−14.878 3(35)	−14.438 0(34)	−14.015 9(64)
Δ_K/kHz	139.196(36)	136.812(41)	134.57(16)
δ_J/kHz	0.328 382(48)	0.307 504(42)	0.287 97(10)
δ_K/kHz	3.906 8(48)	3.755 7(39)	3.597(31)
Φ_J/Hz	0.001 030(33)	0.000 958(27)	0.000 873(93)
Φ_{JK}/Hz	0.016 21(51)	0.015 34(41)	0.013 1(23)
Φ_{KJ}/Hz	−0.702(10)	−0.676 8(95)	−0.642(18)
Φ_K/Hz	4.787(82)	4.581(88)	4.53(22)
ϕ_J/Hz	0.000 505 0(58)	0.000 460 2(47)	0.000 429(12)
ϕ_{JK}/Hz	0.001 81(54)	0.001 71(41)	0.000 4(36)
ϕ_K/Hz	0.581(17)	0.560(41)	0.482(99)

a. Values in parentheses denote three standard deviations and apply to the last digits of the constants.

II-A-5 Microwave Spectroscopy of Dichlorosilylene in Excited Vibrational States

Masaharu FUJITAKE and Eizi HIROTA

If the rotational spectra of a bent YXY molecule are observed for all the three fundamental vibrational states, we can determine the equilibrium structure and all the six third-order anharmonic potential constants. We aimed at carrying out such measurements for $SiCl_2$. Table I lists the rotational constants of $Si^{35}Cl_2$ and $Si^{35}Cl^{37}Cl$ in the $v_2=1$ and $v_2=2$ states. As shown there, the rotational constants change almost linearly with the v_2 bending vibration quantum number (within 2%), precluding the possibility of the $v_2=2$ state being in Fermi resonance with the $v_1=1$ state through the ϕ_{122} anharmonic term. On the other hand, the two stretching vibrations v_1 and v_3 are quite close in frequency and interact each other by Coriolis coupling. The inertia defects in the $v_2=1$ and ground states yield the Coriolis coupling constant ζ_{13}^c to be 0.61. Rotational spectra in these two states were analyzed by explicitly taking into account the Coriolis interaction between them. Preliminary molecular parameters are listed in Table I. It is interesting to note that the two states are separated by only 5.40 cm^{-1}.

Table I. Molecular Constants of $SiCl_2$ in Excited Vibrational States (MHz)

Species		*A*	*B*	*C*
$Si^{35}Cl_2$	(v_2-GS)	(125.83)	(−3.993)	(−5.150)
	v_2	14 906.91	2 818.419	2 361.332
	($2v_2$-v_2)	(128.12)	(−4.053)	(−5.239)
	$2v_2$	15 035.03	2 814.366	2 356.093
$Si^{35}Cl^{37}Cl$	(v_2-GS)	(122.97)	(−3.837)	(−4.949)
	v_2	14 790.28	2 741.675	2 304.417
	($2v_2$-v_2)	(125.05)	(−3.791)	(−4.906)
	$2v_2$	14 915.33	2 737.884	2 299.511

$Si^{35}Cl_2$	v_1	v_3
A	14 817.54	14 669.76
B	2 810.39	2 819.25
C	[2 358.18][a]	2 360.70
D	2 823.3	
F	−17.0	
E_1-E_3	161 900.(5.4004 cm^{-1})	

a. Fixed to a value calculated from the inertia defect.

II-A-6 Detection of the NaO Radical by Microwave Spectroscopy

Chikashi YAMADA, Masaharu FUJITAKE, and Eizi HIROTA

The rotational spectrum of the NaO radical in the four lowest vibrational states was observed in millimeter- and submillimeter-wave region. The NaO radical was generated by the reaction of the sodium vapor with N_2O directly in a high-temperature absorption cell. Analysis of the observed spectra yielded the rotational and centrifugal distortion constants, Λ-type doubling constants, spin-orbit interaction constants, and hyperfine interaction constants in the four vibrational states, as listed in Table I. The NaO radical is clearly shown to have the $^2\Pi_i$ ground electronic state with an anomalously large Λ-type doubling constant and very small hyperfine interaction constants. These results are consistent with the presence of a low-lying $^2\Sigma$ excited electronic state and with the Na-O bond being almost completely ionic.

Table I. Molecular Constants of NaO (MHz)[a]

Constant	v=0	v=1	v=2	v=3
$A\times10^{-6}$	−3.2123(59)	−3.1244(66)	−2.9633(63)	−2.5365(94)
A_D	0.06(18)	1.65(21)	5.13(21)	18.20(42)
B	12662.6762(12)	12528.7569(13)	12396.2916(13)	12265.5884(18)
D	0.0377829(91)	0.0375731(93)	0.0373657(91)	0.03716(12)
$H\times10^8$	4.7(21)	5.1(21)	8.7(21)	6.1(25)
p	2650.112(72)	2832.044(87)	3101.905(87)	3586.71(11)
p_D	−0.27323(29)	−0.30611(34)	−0.36353(34)	−0.49656(53)
$p_H\times10^5$	1.516(89)	1.749(94)	2.537(96)	4.68(12)
q	18.687(27)	19.742(29)	21.195(29)	23.240(30)
$q_D\times10^3$	−1.052(69)	−1.192(70)	−1.511(68)	−2.131(57)
a	8.121(92)	8.26(24)	8.66(24)	8.52(54)
b	−52.4(33)	−48.1(58)	−57.0(56)	−42.7(113)
c	3.9(31)	−0.1(50)	6.7(49)	−6.5(95)
d	7.03(21)	6.61(49)	6.20(50)	5.1(11)
eqQ_1	−6.81(21)	−7.33(51)	−6.85(47)	−6.25(78)

a. Values in parentheses denote one standard deviation and apply to the last digits of the constants.

II-A-7 Microwave Spectroscopy of a High-Temperature Radical LiO

Chikashi YAMADA, Masaharu FUJITAKE, and Eizi HIROTA

Freund et al.[1] observed the radio frequency spectrum of $^7Li^{16}O$ generated in beam by heating Li_2O to 1800 K and derived the spin-orbit interaction and hyperfine coupling constants in the v=0 and v=1 states. We have been investigating this molecule as a most typical example of high-temperature molecules. It is also the first member of the alkali monoxides, on which we are carrying out a systematic study using microwave and infrared laser spectroscopy.[2] We generated LiO by the reaction of Li heated to 700°C with N_2O directly induced in a stainless steel cell. The pressure in the cell was about 100 mTorr. The transitions of J=1.5-0.5 up to 5.5-4.5 were observed for the v=0 and v=1 states. Figure 1 shows an example of the observed spectra, J=1.5-0.5 f transition of $^7Li^{16}O$ in $^2\Pi_{1/2}$. The observed line frequencies were analyzed by the least-squares method. The data of Freund et al.[1] were included in the fit, but their result on the $^2\Pi_{1/2}$ state could not be reproduced and was thus discarded. Table I summarizes molecular parameters thus obtained. The equilibrium bond length was calculated to be r_e= 1.688 207(18)Å with one standard deviation in parentheses. The harmonic frequency ω_e was estimated using $\omega_e=(4B_e^3/D_e)^{1/2}$ to be 803.0(13) cm^{-1}. The observed Λ-doubling constant was employed in the relation $p=4AB/\Delta E$ to estimate the $^2\Sigma$-$^2\Pi$ energy separation ΔE to be 2460 cm^{-1}. The observed hyperfine constants are consistent with nearly 100% ionic character of the bond.

Table I. Molecular Constants of LiO (MHz)[a]

Constant	v=0	v=1
A	−3 213 808(31)	−3 177 956(63)
B	36 091.445(13)	35 554.814(22)
D	0.327 431(44)	0.318 8(21)
H	0.000 405(44)	0.000 251(74)
L	−0.000 005 73(47)	−0.000 004 37(80)
p	6 274.43(11)	6 967.21(26)
p_D	−0.425 8(83)	−0.655(16)
q	−51.751(22)	−57.505(75)
q_D	0.002 0(12)	0.003 1(25)
a	8.163(45)	8.061(81)
b	−21.57(53)	−22.3(15)
c	13.27(58)	13.8(16)
d	4.009(56)	4.05(14)
eQq	0.493(76)	0.67(27)

a. Values in parentheses denote standard deviation and apply to the last digits of the constants.

References

1) S.M. Freund, E. Herbst, R.P. Mariella, Jr., and W. Klemperer, *J.Chem. Phys.*, **56**, 1467 (1972)
2) II-A-6 and II-A-8.

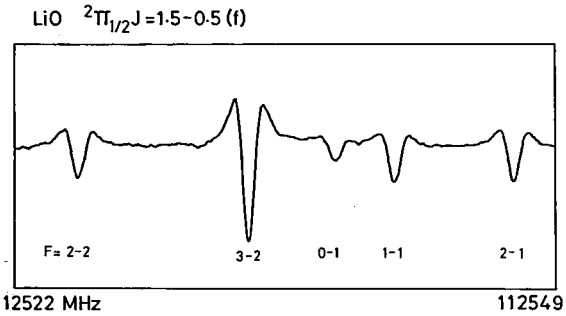

Figure 1. J=1.5-0.5 f of $^7Li^{16}O$ in $^2\Pi_{1/2}$ v=0.

II-A-8 Microwave Spectroscopy of the KO Radical

Chikashi YAMADA, Masaharu FUJITAKE, Eizi HIROTA, Satoshi YAMAMOTO *(Nagoya Univ.)*, **and Shuji SAITO** *(Nagoya Univ.)*

As an extension of a study on LiO[1] and NaO[2] by microwave spectroscopy, the KO radical was investigated. This molecule is particularly interesting among alkali monoxides, because the lowest $^2\Sigma$ state becomes lower as one proceeds from LiO to CsO and is expected to overtake the lowest $^2\Pi$ state around KO.[3] We have generated KO by the reaction of K heated to 150~190°C with N_2O, as in the cases of LiO and NaO. The rotational transitions in both the $^2\Pi$ and $^2\Sigma$ states were observed. It was found that the interaction between the $^2\Pi$ and $^2\Sigma$ states were necessary to be explicitly included in analyzing the observed spectra. The $^2\Sigma$ v=0 state is likely to be located just below the $^2\Pi_{1/2}$ v=1 state.

References

1) II-A-7.
2) II-A-6.
3) J.N. Allison and W.A. Goddard III, *J. Chem. Phys.*, **77**, 4259 (1982); J.N. Allison, R.J. Cave, and W.A. Goddard III, *J. Phys. Chem.*, **88**, 1262 (1984); S.R. Langhoff, C.W. Bauschlicher, Jr., and H.P. Partridge, *J. Chem. Phys.*, **84**, 4474 (1986).

II-A-9 Photofragmentation Dynamics of CH_3I at 248 nm

Hideto KANAMORI, Stephen R. LEONE *(JILA, Univ. Colorado, and IMS)*, **and Eizi HIROTA**

A number of studies have been carried out on the photolysis of CH_3I at 248 or 266 nm. Most of these studies agree in that the channel leading to I in $^2P_{1/2}$ is dominant (about 70%) and the CH_3 radical has a vibrational population peaking at $v_2=2$[1]. We have examined this process at 248 nm by monitoring the CH_3 radical v_2 and associated hot bands by infrared diode laser kinetic spectroscopy. An example of the observed time-resolved spectra is shown in Figure 1. The absorption signal has a parabolic shape, as expected from the process being directly dissociative. No preference was observed for the CH_3 radical distribution along a particular azimuthal angle of the excimer laser beam. At an initial stage the signal is broadened by a large Doppler effect which corresponds to the $^2P_{1/2}$ channel. All the signals of v=1-0 up to 4-3 were observed essentially as absorptions and the vibrational population was found to be largest at v=0 and to decrease monotonically with v_2. This population is at sharp variance with most of the previous results. However, Lee and his coworkers[2] have recently repeated the TOF measurements with much improved resolution and have obtained the vibrational distribution in qualitative agreement with the present result. We also found that the rotational temperature was about 700 K. We could not detect any signals of CH_3 generated by the other channel leading to I in $^2P_{3/2}$.

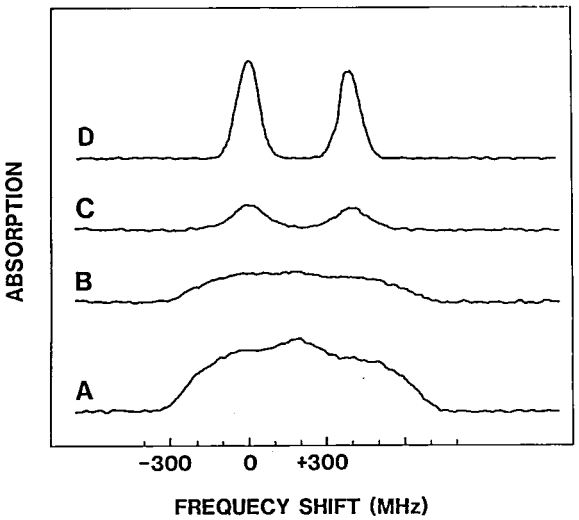

Figure 1. Time-resolved observation of the $v_2=1$-0 R(5,3) line of CH_3 generated by the photolysis of CH_3I at 248 nm. The delay time is 0, 1, 3, and 13 μs for traces A, B, C, and D, respectively, whereas the gate width is fixed to 1 μs.

References

1) For example, M.D. Barry and P.A. Gorry, *Mol. Phys.*, **52** 461 (1984).
2) Y.T. Lee, private communication.

II-A-10 Microwave Spectrum, Molecular Structure, and Force Field of HBO

Yoshiyuki KAWASHIMA *(Kanagawa Inst. Tech.)*, **Yasuki ENDO, and Eizi HIROTA**

The HBO molecule was generated as a transient intermediate in the reaction of diborane with oxygen induced by a dc discharge. The $J=3 \leftarrow 2$ transition was observed for $H^{10}BO$ and was combined with the spectra already reported[1] to derive the rotational, centrifugal distortion, and nuclear quadrupole coupling constants for this species. The rotational and centrifugal distortion constants were determined also for $D^{11}BO$, $D^{10}BO$, $H^{11}B^{18}O$, and $H^{10}B^{18}O$. The measurement was extended to rotational transitions of $H^{11}BO$ and $H^{10}BO$ in the v_1, v_2, $2v_2$, and v_3 states and to those of $D^{11}BO$ and $D^{10}BO$ in the v_2, $2v_2$, and v_3 states. The vibrational frequencies and the rotational, vibration-rotation, ℓ-type doubling, and centrifugal distortion constants thus determined for the six isotopic species were simultaneously analyzed to derive the equilibrium molecular structure and the harmonic and third-order anharmonic potential constants of the HBO molecule. The equilibrium bond lengths thus obtained are r_e(H-B)=1.166 67(41)Å and r_e(B-O)=1.200 68(10)Å, and the substituted, average, and effective structures were also

calculated for ocmparison.

Reference

1) Y. Kawashima, Y. Endo, K. Kawaguchi, and E. Hirota, *Chem. Phys. Lett.*, **135**, 441 (1987)

II-A-11 Microwave Spectroscopy of Chlorofluorosilylene

Masaharu FUJITAKE and Eizi HIROTA

Both difluorosilylene[1] and dichlorosilylene[2] have been investigated in detail by microwave spectroscopy. It may be interesting to study a mixed halide FSiCl. To generate this species, the precursor SiF_nCl_{4-n} (n=1 ~ 3) was made by passing $SiCl_4$ over SbF_3 at room temperature and then reacted with Si heated to about 1000°C. In addition to those of SiF_2 and $SiCl_2$, the rotational lines of new species were observed in the region 340 to 357 GHz and were assigned to FSiCl. Both b-type and a-type transitions were recorded, the former being stronger than the latter. Least-squares analysis gave molecular parameters listed in Table I. The structure parameters (r_0) were calculated from the observed rotational constants and were compared with those of SiF_2 and $SiCl_2$.

Table I. Molecular Constants of Chlorofluorosilylene

Constant[a]	$FSi^{35}Cl$	$FSi^{37}Cl$
A/MHz	23 772.153(48)	23 711.553(25)
B/MHz	4 525.886(14)	4 396.925(37)
C/MHz	3 795.041(15)	3 702.445(29)
Δ_J/kHz	2.886(9)	2.720(11)
Δ_{JK}/kHz	−18.475(16)	−17.19(17)
Δ_K/kHz	277.1(7)	—
δ_J/kHz	0.680(4)	0.629(4)
δ_K/kHz	13.17(5)	13.20(27)

	$SiF_2(r_e)$[1]	$SiCl_2(r_e)$[2]	$FSiCl(r_0)$
r(Si-F)/Å	1.5901	—	1.602
r(Si-Cl)/Å	—	2.065	2.060
θ(XSiY)/°	100.767	101.55	101.25

a. Values in parentheses denote three standard deviations and apply to the last digits of the constants.

References

1) V.M. Rao, R.F. Curl, Jr., P.L. Timms, and J.L. Margrave, *J. Chem. Phys.*, **43**, 2557 (1965); V.M. Rao and R. F. Curl, Jr., *J. Chem. Phys.*, **45**, 2032 (1966); H. Shoji, T. Tanaka, and E Hirota, *J. Mol. Spectrosc.*, **47**, 268 (1973)
2) II-A-4 and II-A-5.

II-A-12 Infrared Diode Laser Kinetic Spectroscopy of the CCD Radical ν_3 Band

Hideto KANAMORI and Eizi HIROTA

[*J. Chem. Phys.*, **88**, 6699 (1988)]

Infrared diode laser kinetic spectroscopy was applied to the photodecomposition of the deuterated acetylene at 193 nm to observe the ν_3 (C=C stretching) band of the CCD radical. The band origin which was derived from the observed spectrum is 1743.1785(3) cm^{-1}, in agreement with the result of a previous matrix study. As in the case of CCH, the spin-rotation interaction constant was found to change by as much as 31% upon ν_3 excitation, presumably because of the interaction with the lowest excited electronic state. Many lines with lifetimes shorter than those of the ν_3 band were observed, but remained to be assigned.

II-A-13 Infrared Diode Laser Spectroscopy of the CCD Radical $\nu_2+\nu_3$ Band

Hideto KANAMORI and Eizi HIROTA

In order to clarify the vibronic interaction between the $\tilde{X}^2\Sigma^+$ and $\tilde{A}^2\Pi$ states of the ethynyl radical, we have extended the observation to CCD. The ν_3 band is described in II-A-12. The precursor C_2D_2 was synthesized by $CaC_2 + D_2O$ and was mixed with H_2 of various pressures. The mixture with the total pressure of about 3 Torr was photolyzed by an ArF laser of the output of 90 mJ/pulse with the repetition rate of 20 Hz. The absorption signal observed showed that CCD was not prepared initially in the ground vibronic state; the rising of the signal was dependent on the pressure of H_2. We have observed 48 Q branch and 22 P/R branch lines for a $^2\Pi$-$^2\Sigma$ type band and have assigned them to $\nu_2+\nu_3$. This band was about one third as strong as the ν_3 band. Least-squares analysis yielded molecular parameters shown in Table I. We have attempted to observe the $\nu_2+\nu_3-\nu_2$ band to determine the ν_2

frequency, but without success. On the other hand, we observed a number of strong lines with fast rise and ascribed them to the 3513 cm^{-1} ← ν_3 band.

Table I. Molecular Constants of the CCD $\nu_2+\nu_3$ Band (cm^{-1})[a]

B	1.189 099 7(42)	p	0.000 364(76)
D	0.000 002 704(13)	q	0.010 741 9(44)
γ	−0.001 773(25)	q_D	−0.000 000 129(14)
A	−0.805 1(11)	ν_0	1962.336 56(25)

a. Ground-state parameters were fixed to the microwave values reported in M. Bogey, C. Demuynck, and J.L. Destombes, *Astron. Astrophys.*, **144**, L15 (1985). Values in parentheses denote standard deviation and apply to the last digits of the constants.

II-A-14 Infrared Diode Laser Kinetic Spectroscopy of the Vinyl Radical

Hideto KANAMORI, Yasuki ENDO, and Eizi HIROTA

Although the vinyl radical is an important intermediate in many chemical reactions, little has been known about it. Hunziker et al.[1] observed absorption spectra of vinyl in the visible and assigned them to $\tilde{A}^2A''-\tilde{X}^2A'$. Shepherd and Graham[2] reported the infrared spectrum of vinyl prepared in low temperature matrices. They reported that the ν_7 band, i.e. the CH_2 out-of-plane bend, was particularly strong. We have applied infrared diode laser kinetic spectroscopy to vinyl chloride and vinyl bromide to observe the ν_7 band of vinyl in the gas phase. Both the precursors were found to absorb 193 nm light strongly. Although they also absorbed in the infrared around 900 cm^{-1}, we succeeded to observe transient signals common to the two precursors. The signals lasted for about 200 μs when the precursors were diluted with H_2 to the total pressure of 1 Torr. The observed lines were assigned to two bands, which showed 1:3 statistical weight, alternative to each other, i.e. 1:3 for one band and 3:1 for the other. These observations were ascribed to a double-minimum potential for the C-H in-plane rocking, although the observed bands were the CH_2 out-of-plane wagging. Preliminary rotational constants and band origins are listed in Table I. It is interesting to note that the identical spectra were observed when acetylene of 10 Torr was employed as a precursor.

Table I. Preliminary Rotational Constants of C_2H_3 (cm^{-1})[a]

Constant	Symmetric ν_7=1	Symmetric G.S.	Antisymmetric ν_7=1	Antisymmetric G.S.
A	7.855 09(50)	7.913 30(23)	7.801 63(38)	7.904 19(27)
B	1.077 354(51)	1.083 035(56)	1.077 277(55)	1.083 116(49)
C	0.951 552(53)	0.948 825(57)	0.951 334(47)	0.948 500(57)
ν_0	895.163 06(75)		895.217 12(83)	

a. Values in parentheses denote one standard deviation and apply to the last digits of the constants.

References

1) H.E. Hunziker, H. Kneppe, A.D. McLean, P. Siegbahn, and H.R. Wendt, *Can. J. Chem.*, **61**, 993 (1983).
2) R.A. Shepherd and W.R.M. Graham, 42nd Symposium on Molecular Spectroscopy, Columbus, Ohio, 1987, Paper TD1.

II-A-15 Vibronic Bands of the CCH Radical Observed by Infrared Diode Laser Kinetic Spectroscopy

Hideto KANAMORI and Eizi HIROTA

[*J. Chem. Phys.*, in press]

Five infrared bands of the CCH radical were observed by diode laser kinetic spectroscopy. Two Π-Π type bands were assigned to hot bands from the (01^10) state in $\tilde{X}^2\Sigma^+$, namely to $\nu_2+\nu_3-\nu_2$ and $7\nu_2-\nu_2$. The latter band was found to share the upper state with a Π-Σ type band, of which the lower state was the ground vibronic state. Two other Π-Σ type bands corresponded to transitions from the ν_3 state in $\tilde{X}^2\Sigma^+$ to two vibronic Π states. Simultaneous analysis of all the observed bands yielded molecular parameters with high precision including the ν_2 fundamental frequency, which was determined to be 371.6034(3) cm^{-1}. The parity of each rovibronic level was determined unambiguously because $\Pi-\Sigma^+$ transitions were observed, allowing us to choose the signs of K-type doubling constants p and q uniquely.

II-A-16 Infrared Diode Laser Kinetic Spectroscopy of the ν_3 Band of C_3

Keiji MATSUMURA *(Seinan Gakuin Univ.)*, **Hideto KANAMORI, Kentarou KAWAGUCHI, and Eizi HIROTA**

[*J. Chem. Phys.*, in press]

Infrared diode laser kinetic spectroscopy was applied to reaction intermediates generated by the photolysis of diacetylene and allene at 193 nm. A strong band was observed around 2040 cm^{-1} and was assigned to the ν_3 band of C_3. The observed spectrum was analyzed by using an energy level expression for a linear molecule; higher-order centrifugal distortion terms were necessary to be included in the least-squares fit. The band origin was determined to be 2040.0198(8) cm^{-1}. The rotational and centrifugal distortion constants obtained suggest the presence of a potential barrier at the linear configuration in both the ground and ν_3 states.

II-A-17 Generation of the SiH Radical by the 193 nm Photolysis of Phenylsilane Investigated by Infrared Diode Laser Kinetic Spectroscopy

Koichi SUGAWARA *(Nat. Chem. Lab. Ind.)*, **Hideto KANAMORI, and Eizi HIROTA**

The present study was initiated to examine what species were generated by photolyzing phenylsilane ($PhSiH_3$) at 193 nm and to clarify the decomposition process by tracing the time profile of the signals of transient species. Because good laser diodes were available only around 2000 cm^{-1}, the observation was limited to the $R_1(9.5)f$ transition of SiH at 2094.320 cm^{-1}. Figure 1a shows the time profile of the line obtained from a mixture of 1.8 mTorr of $PhSiH_3$ and 390 mTorr of Ar. The initial rise was completed within 1μs, followed by a slow increase lasting for about 40 μs, and then the signal decayed exponentially. The slow rise at the intermediate stage was also found to be exponential, as also shown in Figure 1a. The decay rate was found to be proportional to the pressure of $PhSiH_3$ with the rate constant $(2.5\pm0.3)\times10^{-10}$ cm^3 $molecule^{-1}s^{-1}$, as shown in Figure 1b, but to be independent of the Ar pressure. In contrast, the slow rise rate was proportional to the Ar pressure with the rate constant $(1.1\pm0.2)\times10^{-11}$ cm^3 $molecule^{-1}s^{-1}$, as shown in Figure 1c, but not to be influenced by $PhSiH_3$. The signal strength extrapolated to $t=0$ was proportional to the pressure of $PhSiH_3$, but was independent of the Ar pressure. We conclude that the slow rise is due to rotational relaxation by collision with Ar and the decay is primarily ascribed to reaction with $PhSiH_3$. The SiH radical seems to be generated from $PhSiH_3$ by a unimolecular process.

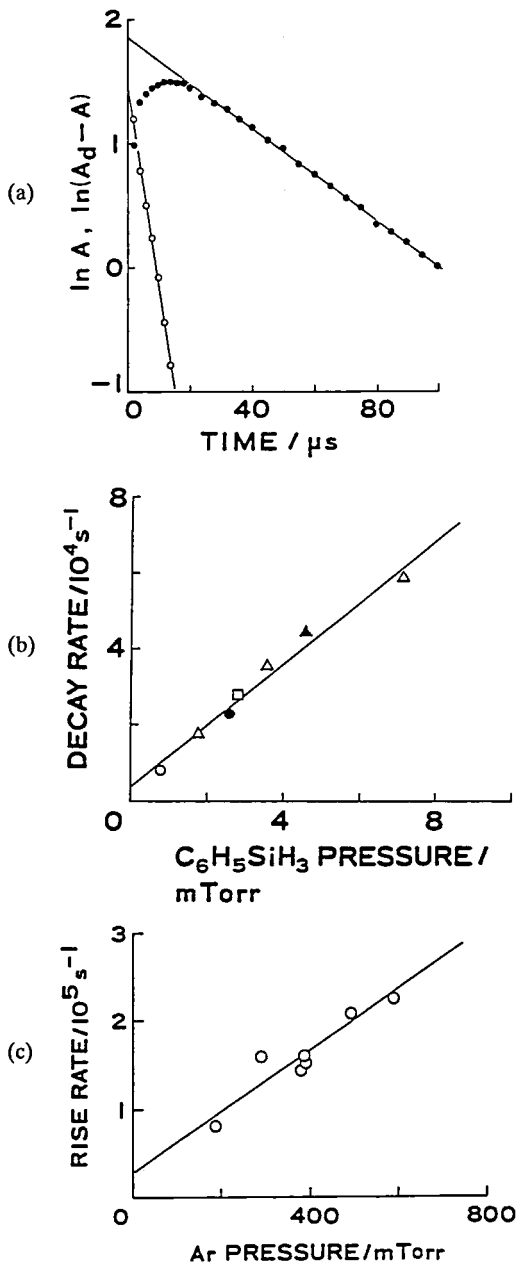

Figure 1. (a) Time profile of the $R_1(9.5)f$ transition of SiH generated by the 193 nm photolysis of a 1.8 mTorr phenylsilane and 309 mTorr Ar mixture. Closed circles denote the observed time profile, while open circles represent the differences between the time profile extrapolated for the time between 0 and 30 μs and the observed data. (b) decay rate dependence on the phenylsilane pressure, and (c) slow rise rate dependence on the Ar pressure.

II-A-18 Measurements of SiH($X^2\Pi$, v=0) Radicals in Ar/SiH_4 Plasma Using an Infrared Diode Laser

Kozo KATO *(Nagoya Univ.)*, **Naoshi ITABASHI** *(Nagoya Univ.)*, **Nobuki NISHIWAKI** *(Nagoya Univ.)*, **Toshio GOTO** *(Nagoya Univ.)*, **Chikashi YAMADA, and Eizi HIROTA**

In order to understand the formation mechanism of amorphous silicon (a-Si:H) thin film by plasma chemical vapor deposition (PCVD) of silane, the vibration-rotation signals of SiH in a modulated DC discharge were investigated using infrared diode laser kinetic spectroscopy.

The discharge cell employed consisted of a 117 cm long, 10 cm inner diameter stainless-steel tube acting as a hollow cathode and of two 1.5 mm diameter tungsten pin anodes. The laser beam passed 40 times through the cell. The discharge current was half-rectified wave of 680 Hz with the peak current of 700 mA and the peak voltage was 0.7 kV. An Ar/SiH_4 mixture of 0.35/0.17 Torr was flowed through the cell with the speed of 150 sccm. An example of the observed time profile is shown in Figure 1. The Einstein A coefficient was calculated to be 143.0 s^{-1} by transferring a B2-CISD ab initio calculated transition dipole moment.[1] The absorption coefficients measured for eleven rotational transitions yielded the rotational temperature to be 400 K. The number of SiH radicals in the present condition was determined to be 3.2×10^{10} cm^{-3}.

Reference

1) W.D. Allen and H.F. Schaefer III, *Chem. Phys.*, **108**, 243 (1986).

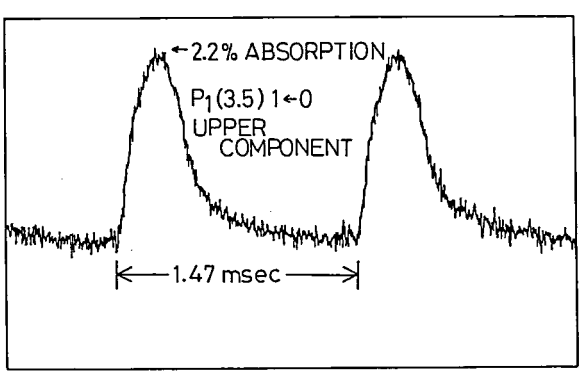

Figure 1. Time profile of the $P_1(3.5)$ transition of SiH.

II-A-19 Measurement of the SiH_3 Radical Density in Silane Plasma Using an Infrared Diode Laser Absorption Method

Naoshi ITABASHI *(Nagoya Univ.)*, **Kozo KATO** *(Nagoya Univ.)*, **Nobuki NISHIWAKI** *(Nagoya Univ.)*, **Toshio GOTO** *(Nagoya Univ.)*, **Chikashi YAMADA, and Eizi HIROTA**

[*Jpn. J. Appl. Phys.*, in press]

The SiH_3 radical is an important precursor in amorphous silicon thin film formation, but its density in silane discharge plasma has not been measured. In the present study, we have developed a method for measuring the SiH_3 radical density using infrared diode laser absorption spectroscopy and have determined the SiH_3 density in a pulsed SiH_4/H_2 plasma.

The absorption cell used was identical to that reported in II-A-18. The discharge current consisted of the pulse 0.45 ms in duration with the peak of 1A and the repetition rate of 35 Hz. The precursor was a mixture of SiH_4/H_2 with 0.2/1.8 Torr pressures and was flowed through the cell with a rate of 60 sccm. An example of the observed spectrum is shown in Figure 1(a), which may be compared with that in a previous study using Zeeman modulation.[1] Figure 1(b) shows the time profile of the R(4,0) $v_2=1^- \leftarrow 0^+$ lower spin doublet component line. By assuming an ab initio calculated transition dipole moment,[2] the SiH_3 density in the $\tilde{X}^2A_1$ state was estimated to be $(8\pm2)\times10^{11}$ cm^{-3}.

References

1) C. Yamada and E. Hirota, *Phys. Rev. Lett.*, **56**, 923 (1986).
2) W.D. Allen and H.F. Schaefer III, *Chem. Phys.*, **108**, 243 (1986).

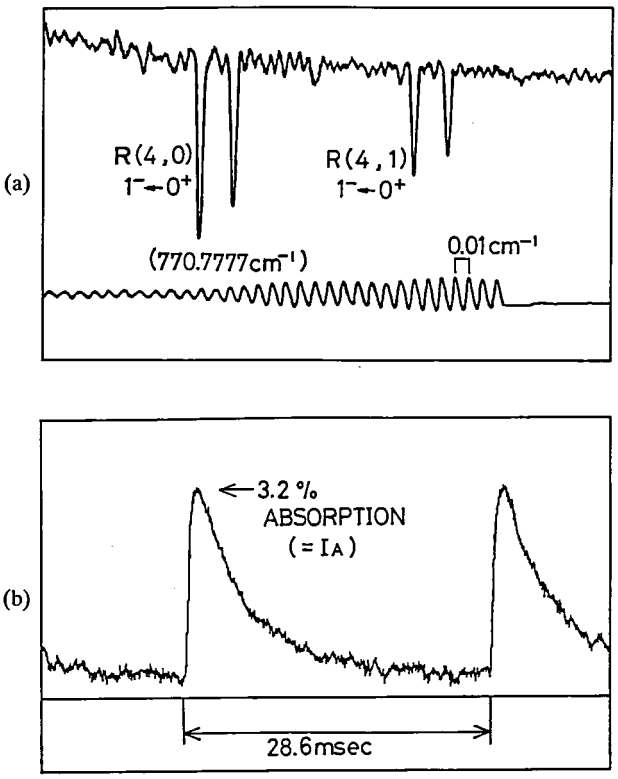

Figure 1. (a) R(4,0) and R(4,1) transitions of $\nu_2=1^- \leftarrow 0^+$ of SiH_3 recorded by discharge modulation, (b) time profile of the R(4.0) $\upsilon_2=1^- \leftarrow 0^+$ lower spin component.

II-A-20 Infrared Diode Laser Kinetic Spectroscopy of the SiH_2 Molecule

Chikashi YAMADA, Hideto KANAMORI, Eizi HIROTA, Naoshi ITABASHI *(Nagoya Univ.)*, **Kozo KATO** *(Nagoya Univ.)*, **Nobuki NISHIWAKI** *(Nagoya Univ.)*, **and Toshio GOTO** *(Nagoya Univ.)*.

The silylene molecule SiH_2 may also play an important role in amorphous silicon thin film formation by silane discharge plasma. Although the spectrum of SiH_2 in the visible has been known for long time, no gas-phase infrared spectra of SiH_2 have been identified. We thus started the present study to detect and assign the vibration-rotaion spectra of SiH_2 using infrared diode laser kinetic spectroscopy. Because silane absorbs strongly in regions where we expect to observe SiH_2 spectral lines, we employed phenylsilane as a precursor. When it was decomposed by an excimer laser at 193 nm, we observed a number of transient absorption lines around 2000 cm^{-1}. Most of them are probably ascribed to the ν_3 band, but possible interactions of the ν_3 state with the ν_1 and $2\nu_2$ states have made it difficult to assign the observed lines. We then turned to 10-μm region where we expect to detect the ν_2, i.e. bending band. We have observed about 40 lines and have assigned most of them. Table I lists preliminary rotational constants thus obtained.

Table I. Rotational Constants and Band Origin of the ν_2 Band of SiH_2 (cm^{-1})[a]

Constant	G.S.	$\nu_2=1$
A	8.098 48(21)	8.368 68(12)
B	7.023 44(16)	7.150 27(17)
C	3.702 510(69)	3.646 196(64)
ν_0	998.624 11(44)	

a. Values in parentheses denote one standard deviation and apply to the last digits of the constants.

II-A-21 Infrared Diode Laser Kinetic Spectroscopy of the Photodissociation of Cl_2SO

Eberhard TIEMANN *(Univ. Hannover)*, **Hideto KANAMORI, and Eizi HIROTA**

Thionyl chloride was photolyzed by a KrF laser at 248 nm and the fragments were detected by time-resolved infrared diode laser spectroscopy. The Cl fine-structure transition showed a pronounced time dependence; at an initial stage, the signal consisted of a broad emission and a sharp absorption at the center, as shown in Figure 1. The two features were interpreted in terms of the two channels: I. $Cl_2SO+h\nu$(248 nm) → $Cl(^2P_{1/2}$ with large translational energy)+ClSO and II. $Cl_2SO+h\nu$ (248 nm) → $2Cl(^2P_{3/2}$ with small translational energy)+SO. Namely, the broad emission feature corresponds to Cl in $^2P_{1/2}$ generated by I, whereas II produces the sharp absorption signal of Cl in the $^2P_{3/2}$ ground state. The available energy is 20000 and 2700 cm^{-1} for I and II, respectively. We attempted to detect ClSO without success. This failure is probably ascribed to quite a large amount of energy being allocated to ClSO. For SO only the three lowest bands v=1-0, 2-1, and 3-2 in the $X^3\Sigma^-$ were observed in absorption; all lines did not show any appreciable broadening. These observations are all consistent with SO being primarily prepared by II. It can also be produced by III. $Cl_2SO+h\nu$(248 nm) → Cl_2 (in high vibrational

states)+SO.

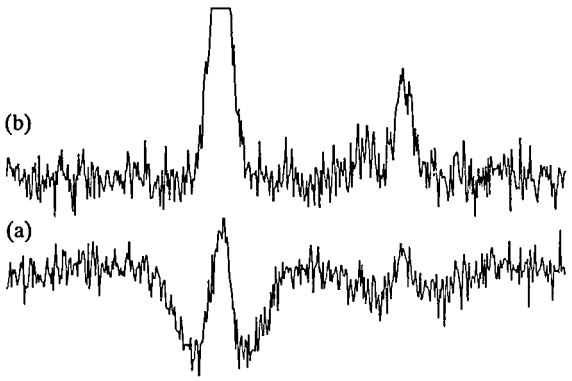

Figure 1. Two fine structure transitions of Cl generated by the 248 nm photolysis of Cl_2SO: no delay for trace (a) and 10 μs delay for trace (b), both observed with a gate width of 1 μs.

II-A-22 Infrared Diode Laser Kinetic Spectroscopy of Fragments from the Photodissociation of SCl_2 and S_2Cl_2

Eberhard TIEMANN *(Univ. Hannover)*, **Hideto KANAMORI, and Eizi HIROTA**

Two molecules SCl_2 and S_2Cl_2 were photodissociated by a KrF excimer laser at 248 nm. The relative yield of Cl in the $^2P_{1/2}$ excited state was determined to be ϕ=0.17(2) and 0.22(5), respectively, for S_2Cl_2 and SCl_2, both values being considerably smaller than the statistical distribution ϕ=0.33. The second fragment, the SCl radical, was detected in its ground electronic state; both the v=1 ← 0 and 2 ← 1 bands were observed for $^{32}S^{35}Cl$, in addition to the v=1 ← 0 band for $^{32}S^{37}Cl$. These data are being employed to improve molecular parameters reported previously.[1)]

Reference

1) C. Yamada, J.E. Butler, K. Kawaguchi, H. Kanamori, and E. Hirota, *J. Mol. Spectrosc.*, **116**, 108 (1986).

II-A-23 Infrared Diode Laser Spectroscopy of the $HCCCNH^+$ ν_3 Band

Kentarou KAWAGUCHI, Masatoshi KAJITA, Keiichi TANAKA *(Kyushu Univ.)*, **and Eizi HIROTA**

The protonated cyanoacetylene cation ν_3 band was observed by infrared diode laser spectroscopy. The ion was produced by 4.3 kHz hollow cathode discharge with the current of 200 mA peak-to-level in a cyanoacetylene and hydrogen mixture with the partial pressures of 20 and 500 mTorr, respectively. The observation was carried out at room temperature, and the signal was detected by discharge modulation. Some 33 transitions were detected and were analyzed by the least-squares method with ground-state parameters being fixed to the values of Lee and Amano.[1)] Molecular constants thus derived for the ν_3 state are listed in Table I, together with the ground-state values assumed. The present study confirmed the rotational assignment of ref.1 to be correct.

Table I. Molecular Constants of $HCCCNH^+$ in the ν_3 State[a]

Constant	ν_3=1	Ground State[b]
B/MHz	4310.530(40)	4328.892(71)
D/kHz	0.697(32)	0.445(23)
H/Hz	0.0680(68)	
ν_0/cm^{-1}	2315.1425(4)	

a. Values in parentheses denote three standard deviations and apply to the last digits of the constants.
b. Reference 1.

Reference

1) S.K. Lee and T. Amano, *Astrophys. J.*, **323**, L145 (1987)

II-A-24 Observation of Chlorine Atomic Transitions by Infrared Diode Laser Spectroscopy

Masatoshi KAJITA, Kentarou KAWAGUCHI, and Eizi HIROTA

In the course of studying transient species, atomic lines were often observed. Those lines that were confirmed to be due to atomic chlorine are reported below. The precursors employed include $CHCl_3$, CF_2Cl_2, and $POCl_3$ with the partial pressure of 3 to 4 mTorr diluted with 3 Torr of He. Discharge modulation at 4.3 kHz was employed with the peak-to-peak current of 200 mA. A 1.2-m long cell was used in single path. Table I lists only strong lines among the observed; 10 and 12 lines were detected in 1300 and 2500 cm^{-1} regions, respectively. Some of them showed hyperfine splittings, and it will be interesting to compare them

with theoretical predictions for the hyperfine structure in excited states. Only a few of the observed lines were identified based on the published energy levels.

Table I. Infrared Transitions of the Atomic Chlorine

ν_{obs}/cm^{-1}	Relative intensity	Assignment	ν_{calc}/cm^{-1}
1342.0725	25		1342.08
1346.5201	21		
1351.167	4 broad	$^3P_1$ 6f'-5f'	1351.171
1354.68	7		
1359.9268			
1360.0779			
1366.6595	4		
1366.8355	4	$^3P_2$ 6f-5f	
1367.1949	15		
1367.6619	5	$^3P_1$ 6f'-5f'?	1367.49
2500.04	38		
2500.25	58		
2505.433		$6s^4P_{5/2}$-$5p^4D°_{9/2}$	2505.46
2507.06			
2515.47	100		
2515.63	35		
2516.88	28	5f'[3,4,2]-4f'[3,4.2]	2516.885
2523.55	50	$4p^2P_{3/2}$-$4p^4P_{5/2}$	2523.55
2524.30	50		
2526.89	40		
2526.915	35		
2526.933	30		
2526.946	22		
2535.22	42		
2535.26	32		

II-B Development of New Instruments and New Experimental Methods for High Resolution Spectroscopy

The scope of a research is limited by the techniques and the capabilities of instruments available to a researcher. This is particularly true for spectroscopic investigations of simple molecules, free radicals, and ions, which are main research themes this Department is interested in. The high precision with which we determine molecular parameters often unravels new features of molecular structure which have previously escaped experimental observation. The diversity of molecular systems which we can detect and analyze is often limited by the sensitivity of the spectrometer employed. It is thus imperative for us to steadily improve our research facilities and to develop equipments of radically new conceptual design. The rewards of these efforts will include not only the detailed knowledge of the molecules under investigation, but also contributions to related fields. Various technical problems need to be solved to attain these goals. In this respect the collaboration of the Equipment Development Center is indispensable. New instruments developed in this program promise to open new research area in the field of molecular science.

II-B-1 Molecular Beam Apparatus for Infrared Diode Laser Absorption Spectroscopy

Masatoshi KAJITA and Eizi HIROTA

Molecular beam is an ideal medium for studying transient species of large size. For samples contained in a cell, the Doppler broadening limits the size of molecules to be studied; the vibration-rotation spectral lines of benzene, for example, are often not completely resolved. The lifetime of transient molecules is in most cases governed by intermolecular collisions. One of the most serious disadvantages of molecular beam spectroscopy would be inherent low sensitivity, although rotational cooling remedies this drawback to some extent. We have designed and set up an apparatus of pulsed beam, which was incorporated with an excimer laser for photolysis and with an infrared diode laser for monitoring fragments. The pumping system consisted of a 10 inch diffusion pump followed by a mechanical booster pump and a rotary pump. We have tested the performance by observing vibration-rotation transitions of SO generated by the 193 nm photolysis of SO_2. Although the infrared beam crossed the molecular beam ejected from a nozzle of 0.5 mmϕ only once, we could observe the absorption signal.

II–C High Resolution Spectroscopy of Molecules of Fundamental Importance

The need for high quality spectroscopic data has recently been increasing, especially for molecules of fundamental importance. Perhaps such spectroscopic data have been accumulated in the past because of interest in precise molecular structure determination. However, research activities in other related fields such as reaction kinetics, environmental sciences, plasma chemistry and physics, astronomy, and semiconductor technology have recently been advanced such that precise spectroscopic data are indispensable as a means of monitoring molecules. Spectroscopic data which are available at present are not necessarily good enough and must often be replaced by new data that meet necessary requirements. Such spectroscopic data on chemically stable molecules of fundamental importance will be presented in this section.

II-C-1 The Microwave Spectra of *cis*-Cyclobutane-1,2-d_2 and Cyclobutane-1,1,3,3-d_4

Eizi HIROTA, Masaharu FUJITAKE, and James S. CHICKOS *(Univ. Missouri–St. Louis)*

In order to get detailed information on the structure and puckering motion of cyclobutane, the *cis* and *trans* 1,2-d_2 and 1,1,3,3-d_4 species were investigated by microwave spectroscopy. The *trans* 1,2-d_2 species was shown to consist of two forms, ax-ax and eq-eq, and both forms exhibited rotational spectra that could be fit to the ordinary asymmetric rotor pattern. The puckering in the *cis* form makes its spectra complicated; as the molecule starts to pucker, the a and b inertial axes suddenly rotate by nearly + or −45°. This means that the ring puckering and the molecular asymmetry are coupled strongly. In fact, inclusion of the $(R/2)(J_xJ_y+J_yJ_x)$ term, in addition to the ordinary asymmetry term $[(A-B)/2](J_x^2-J_y^2)$, in the rotation Hamiltonian explains nicely the unusual splittings, K-type as well as puckering, observed for the "c-type" R branch transitions of J=17–16 up to 19–18, allowing us to estimate the puckering splitting to be 87.0 MHz. The 1,1,3,3-d_4 species is an ideal molecule to study the puckering, because the puckering and the overall rotation are not coupled to the first order. Each transition was, in fact, found to be split into two with the splitting almost independent of rotational levels. Table I summarizes the rotational and centrifugal distortion constants derived from the average frequencies of the doublets and also the splitting parameters; the splitting in each rotational state was fitted to $\Delta+\delta_a\langle J_a^2\rangle+\delta_b\langle J_b^2\rangle+\delta_c\langle J_c^2\rangle$.

Table I. Molecular Constants of Cyclobutane-1,1,3,3-d_4 (MHz)[a]

A	9975.725(14)	Puckering splitting	
B	8105.376(13)	Δ	34.47(10)
C	5536.091(44)	δ_a	0.000 11(32)
Δ_J	0.002 512(78)	δ_b	0.001 91(22)
Δ_{JK}	−0.001 72(23)	δ_c	0.005 17(25)
Δ_K	0.004 19(14)		
δ_J	0.000 432(38)		
δ_K	0.001 11(12)		

a. Values in parentheses denote three standard errors and apply to the last digits of the constants.

II-C-2 Submillimeter Wave Spectrum of $k=\pm1 \leftarrow \mp2$ Transitions of NH_3

Keiichi TANAKA *(Kyushu Univ.)*, **Yasuki ENDO, and Eizi HIROTA**

[*Chem. Phys. Lett.*, **146**, 165 (1988)]

"Forbidden" rotational transitions of NH_3 with the selection rules $\Delta J=0$ and $k=\pm1 \leftarrow \mp2$ were measured in the submillimeter-wave region. The C_0 rotational constant for the lower component of the inversion doublet in the ground vibrational state is obtained from the observed spectrum as 186 695.815±0.053 MHz. The observed line intensity agrees well with that calculated from the centrifugal-distortion-induced dipole moment.

II-C-3 Submillimeter Wave Spectrum of the Vibrationally Induced Rotational Transitions of Allene in the Degenerate Vibrational States

Keiichi TANAKA *(Kyushu Univ.)*, **Masaharu FUJITAKE, and Eizi HIROTA**

Vibrationally induced rotational transitions of allene in the degenerate vibrational states with the selection rules $\Delta K=0$ and $\Delta \ell=\pm 2$ were measured in the submillimeter wave region. Six R-branch transitions were observed for the $K=0$ stack in each of the ν_9, ν_{10}, and ν_{11} states. Twelve transitions obeying the $\ell=\pm 1 \leftarrow \mp 1$ selection rules in the $K=2$ stack of the ν_{10} state were also observed. The A_0 rotational constant in the ground vibrational state was determined to be 144 259.8 ± 3.5 MHz from the analysis of the present results combined with those of a Fourier transform infrared study.

II–D Laser Investigation of High-Lying Doubly Excited States of Atoms

Doubly excited states of atoms are one of the interesting problems in atomic physics, because they are typical models for quantum-mechanical Coulomic three-body problems, in which a strong electron correlation effect is generally expected to play an important role. Although the electron correlation effect has theoretically been predicted to be more remarkable in high-lying doubly excited states, their behavior has not been fully understood and there have been few experimental studies. Laser spectroscopic investigation of those states has a great advantage since it has a high spectral resolution which is of general importance in the study of highly excited states. From these viewpoints, we have started experimental studies on high-lying doubly excited states of atoms with laser spectroscopic method.

II-D-1 Laser Spectroscopy of Doubly Excited 9*sns* ($11 \leq n \leq 20$) and 8*dns* ($10 \leq n \leq 20$) States of Ca

Norio MORITA, Toshifumi SUZUKI and Keiichi SATO

[*Phys. Rev. A* **38**, 551 (1988)]

Doubly excited *mlns* (*ml*=9*s* and 8*d*) states of Ca atoms have been produced by three-step four-photon laser excitation via 4*sn's* one-electron Rydberg states, and they have been observed by detecting photoionization current of Ca^{2+} yielded from the doubly excited states. Although the electron correlation effect is expected to be the most remarkable in the $m=n$ states, only the states with $m+3 \leq n$ have been observed in the preceeding works. In this work, for the first time, we have successfully observed some resonance peaks which are quite likely to be interpreted as transitions to the states with $n=m+1$ and $n=m$. In addition, remarkable interference patterns and considerable line narrowing caused by the interaction with other autoionizing Rydberg series have been observed in some states. The quantum defects of the observed states have also been obtained and discussed. The behavior of the quantum defects is very complicated in the $m \approx n$ states, and it will be an interesting future work to analyze these states.

II-D-2 Spectroscopic Observation of Doubly Excited 8*sns* and 7*dns* States of Ca with Multistep Laser Excitation

Norio MORITA and Toshifumi SUZUKI

[*J. Phys. B* **21**, L439 (1988)]

Using multistep laser excitation via 4*sn's* Rydberg states, doubly excited *mlns* (*ml*=8*s and* 7*d*; $m+1 \leq n \leq 20$) states of Ca atoms have been observed. Quantum defects of the observed states have been obtained and discussed. For the states with $m \ll n$, the quantum defects are almost independent of n in both 8*sns* and 7*dns* series. For the $m \approx n$ states, however, the quantum defect of the 7*dns* state remarkably increases as n decreases to approach m, while that of the 8*sns* state does not significantly change but rather tends to decrease with decreasing n. An electron correlation effect is expected to play an important role in the $m \approx n$ states.

II-D-3 Spectroscopic Observation and Theoretical Analysis of High-Lying Doubly Excited states of Ca atoms

Norio MORITA and Toshifumi SUZUKI

With multistep laser excitation, we have observed a number of doubly excited *mlns* states over $6 \leq m \leq 10$ for $l=s$, $5 \leq m \leq 9$ for $l=d$, and $m \leq n \leq 20$. The spectra of the $m \ll n$ states are well understood with the theory assuming the absence of the electron correlation, although some of them exhibit considerable reduction of the autoionization rate as well as remarkable splitting patterns. The latter behaviors have been analyzed with the multichannel quantum-defect theory. Consequently, they have been well reproduced by the theoretical calculation and have been interpreted as those which are due to the interaction with other autoionizing Rydberg series. The quantum defect averaged over the principal quantum number of the outer electron depends linearly on that of the inner electron for both *msns* and *mdns* states. This linear dependence has been well reproduced by a theoretical calculation assuming a potential constituted by a frozen closed-core plus an inner electron's wavefunction. The calculated relative slope, however, has not agreed with the observed one. This fact may suggest the existence of an electron correlation effect even in the $m \ll n$ states. The analysis for the $m \approx n$ states is now in progress.

II-E Construction of Coherent VUV Light Source with Narrow Bandwidth, High Intensity and Wide Tunability

Toshifumi SUZUKI and Norio MORITA

We are constructing a coherent vacuum ultraviolet (VUV) light source using two-photon-resonant four-wave difference-frequency mixing. This method of VUV generation is expected to have not only high efficiency and high spatial quality but also broader tunability than other methods. The latter property is due to less restriction of the phase-matching condition. We are using the 4p-5p two-photon transition of Kr atom to generate as short wavelength as possible. The input light for the mixing is produced by four-stage amplification of a single-mode cw-dye-laser in order to obtain as narrow band VUV as possible. While we usually use a pulsed-dye-laser as the other input light for the mixing, we are also preparing another cw-dye-laser with an amplifier chain. This scheme is expected to generate 120–200nm VUV light with high intensity and uniform tunability. Another generation scheme using sum-frequency mixing with Mg atoms is also being prepared to generate further short wavelength and/or to obtain more intense light in a particular wavelength. As a preliminary result, we have generated coherent VUV light at around 140nm with high efficiency by using the above scheme with Kr atoms. Further improvement and application of this VUV source are in progress.

II-F Raman Spectroscopy and Its Application

Raman spectroscopy reveals the vibrational spectrum of a molecule which is sensitive to changes of geometrical structure and bond strength. We have applied this technique to study the following three projects; 1) elucidation of the structure-function relationship of biological molecules, particularly the proton and electron transfer through proteins, 2) structure of short-lived species, 3) solution structure. The first project utilizes resonance enhancement effect of Raman intensity, which enables us to observe the vibrational spectra of chromophores of large molecules with a small amount of dilute solution. Various kinds of heme proteins, flavoproteins, retinoid proteins, metalloproteins, and their model compounds have been investigated. Currently we focus our attention to reveal the

resonance Raman spectra of reaction intermediates of bacteriorhodopsin, cytochrome *c* oxidase, peroxidase, and cytochrome P-450. We have also investigated photoreduction of heme proteins by visible light. So far we have used mainly visible lasers to obtain the spectra of chromophores, but we are extending the excitation wavelength to UV region (~200 nm) to enhance selectively the Raman bands of aromatic amino acid residues of proteins. The second project aims to determine resonance Raman spectra of transient states in the time region of $10^{-7} - 10^{-11}$ sec. The pump-probe technique with two pulsed lasers is applied to this project. In order to reject fluorescence in the measurements of Raman spectra, we developed an improved method for fluorescence rejection by using a gated diode array detector. The third project intends to evaluate a relative size of solvent-solvent and solvent-solute interactions for various binary mixtures of liquids and to explore a concentration-dependent cluster structure of solutions. A Raman difference spectrometer constructed in this lab have been applied to this problem.

II-F-1 Observation of Resonance Raman Spectra of S_1-, T_1-, and S_0- Pyrene in Solution: Application of a Fluorescence Rejection Technique

Takashi FUJII, Keiji KAMOGAWA, and Teizo KITAGAWA

[*Chem. Phys. Lett.* **148**, 17 (1988)]

Our new technique of fluorescence rejection in Raman measurements described previously was applied to observe transient resonance Raman (RR) spectra of pyrene in electronically excited states and a UV RR spectrum in its ground state. This method gave well-defined spontaneous RR spectra with a ns laser source despite the strong fluorescence.

II-F-2 A Novel Optical Device for Simultaneous Measurements of Raman and Absorption Spectra: Application to Photolabile Reaction Intermediates of Hemeproteins

Takashi OGURA and Teizo KITAGAWA

[*Rev. Sci. Instr.* **59**, 1316 (1988)]

Resonance Raman studies on transient molecules have raised a problem about characterization of a photolabile species. Therefore, in order to observe the Raman and absorption spectra of the same spatial region of the sample at the same time, we have constructed a novel device and applied it successfully to monitor the transient species involved in an enzymic reaction of horseradish peroxidase and in photodissociation of carbonmonoxide adduct of hemoglobin.

II-F-3 Resonance Raman Studies of Hydrogenase-catalysed Reduction of Cytochrome c_3 by Hydrogen; Evidence for Heme-Heme Interactions

Alan L. VERMA, Keisaku KIMURA, Asaro NAKAMURA, Tatsuhiko YAGI, Hiroo INOKUCHI, and Teizo KITAGAWA

[*J. Am. Chem. Soc.* **110**, 6617 (1988)]

We observed splittings of Raman bands for a multi-heme protein for the first time. In the resonance Raman studies of hydrogenase-catalyzed reduction of a tetraheme protein cytochrome c_3 (Cyt-c_3) with hydrogen, certain Raman bands show clear splittings in the intermediate redox states obtained under controlled pressure of hydrogen, while apparently nonstructured bands were observed in the fully oxidized or fully reduced states. This suggests either non-equivalence in the environments of the four hemes or an exciton-like splitting of vibrational modes. Since various C-type cytochromes at neutral pH which have different amino acid compositions but the same axial ligands, do not give a wide variety of frequencies for a given mode and furthermore, a bandwidth of the Soret band was much narrower with Cyt-c_3 than with various single-heme cytochromes *c*, it is more likely to assume that the four hemes in the protein interact directly with each other, giving rise to exciton-like splitting. Observation of well-defined Raman lines in the partialy reduced states at the characteristic frequencies for the reduced or the oxidized form indicates that the electron exchange rates either intramolecular within the four hemes or intermolecular between different Cyt-c_3 molecules is much slower than the time scale of the RR scattering process while the recent NMR studies indicate that the intra-

molecular electron-exchange rates are faster than 10^9 s^{-1}. We have attempted to estimate the relative importance of the dispersion, induction, orientational and repulsive interactions for understanding the splitting of the Raman bands. The dipole-dipole coupling mechanism can be ruled out while the dispersion type interactions may contribute predominantly for it.

II-F-4 Structural Characterization of Fibroblast Human Interferon-β1-m

Kazuo HOSOI, Jun UTSUMI, Teizo KITAGAWA, Hirohiko SHIMIZU, Shigeyasu KOBAYASHI

[*J. Interferon Res.* **8**, 375 (1988)]

The complete amino acid sequence of fibroblast human interferon-β1 (IFN-β1) was determined and the higher-order structure of the protein was characterized with Raman spectroscopy. That amino acid sequence was identical to the entire sequence deduced from cDNA nucleotide sequence, showing there are no proteolytic cleavages of carboxy-terminal residues in constrast with natural human IFN-α and natural human IFN-γ. The *N*-glycosylation site was confirmed in Asn80 from the detection of glucosamines in the peptide contained Asn80. A *S*-carboxymethyl Cys17 was detected in the *S*-carboxymethylated protein suggesting that Cys17 is unpaired. Raman spectra of this protein indicated a predominance of α-helical backbone, existences of one unpaired Cys residue and one disulfide bond which are consistent with existence of three Cys residues in the protein. These results bear some evidences for the primary and higher-order structures of natural IFN-β1 which have been predicted till now.

II-F-5 Origin of Raman Spectral Difference Between the Spinning-cell and Flow-cell Measurements for Bacteriorhodopsin Photointermediates

Masao NAKAGAWA, Akiko MAEDA, Takashi OGURA, and Teizo KITAGAWA

[*J. Raman Spectrosc.* in press]

Previous resonance Raman works with the spinning-cell technique pointed out that the L_{550} intermediate gave a doublet at 1552 and 1539 cm^{-1} for the C=C stretching mode while the results from the flow-cell technique claimed that the two bands arised from different intermediates on the basis of different kinetic behaviors. This study explored the origin of the discrepancy by using the double-beam flow apparatus as well as the spinning cell for observing transient resonance Raman spectra. It turned out that the presence of a very small amount of dark adapted species caused the apparent differences in kinetic behaviors of those two bands.

II-F-6 Transient Resonance Raman Spectra of Neutral and Alkaline Bacteriorhodopsin Photointermediates by Using Double-Beam Flow Apparatus: Presence of Very Fast Decaying M_{412}

Masashi NAKAGAWA, Takashi OGURA, Akiko MAEDA, and Teizo KITAGAWA

[*Biochemistry* in press]

Time-resolved resonance Raman spectra were observed for neutral and alkaline bacteriorhodopsin (bR) by using a double-beam flow apparatus. The delay time (t_d) between the pump and probe beams were changed from 15 to 1200 μs, and the probe-only spectra were observed before and after individual pump-probe spectra in order to rectify the bleaching effect of bR during the measurements. In the 457.9 nm-probed spectra, the intensity of the 1566 cm^{-1} band of M_{412} increased until t_d= 190 μs and then decreased with a decay constant (τ_d) of 1.7 ms at pH 7.0. However, at pH 10.5, its intensity was maximum at t_d=15 μs and decayed monotonously. In the first 300 μs, ca. 40% of M_{412} decayed with τ_d=0.39 ms whereas its decay curve at later time was very close to that of neutral M_{412}. The slower decay component in this study corresponds to the so-called fast decay component of M_{412} (M^f). The reversal of positions of the pump and probe beams gave a spectrum similar to the probe-only spectrum, indicating that a possible long-lived intermediate (τ_d>3s) little contributes to the present spectrum. Accordingly, the presence of a very fast decaying M species (M^{vf}) was deduced at alkaline pH. In the 514.5 nm-probed spectra, the 1190 cm^{-1} band characteristic of the N (or

P or L') intermediate did not grow in conformity with the decay of M^{vf}, suggesting that M^{vf} is not converted into N. The two C=C stretching bands of L_{550} at 1551 and 1542 cm^{-1} decayed similarly and this decay behavior agreed with the rising kinetics of the 1566 cm^{-1} band and also with the reported kinetics of the slow rising component of M_{412}. The efficiency for a practical photoreaction appeared 1.6 times higher at pH 10.5 than at pH 7.0 and the increment is ascribable to generation of M^{vf}.

II-F-7 Photoreduction of Cytochrome *c* and Its Mechanism Monitored by Resonance Raman Spectroscopy

Alan L. VERMA and Teizo KITAGAWA

Purified monomeric cytochrome *c* (Cyt-c) at neutral pH exhibited extensive photoreduction under anaerobic conditions (a fore pressure 10^{-5} Torr) upon laser irradiation in the 400–440 nm region and the resonance Raman (RR) spectrum of the photoreduced species was identical with that of the chemically reduced species. However, only partial photoreduction occurred at pH 10.1 where the axial methionine ligand is replaced probably by lysine, and no photoreduction took place after the transitions with pK_a=12.76 and 2.5 where axial histidine ligand is replaced by other residue. The photoreduction was completely inhibited in the presence of oxygen for monomeric Cyt-c, suggesting active participation of a triplet state in this process. When the monomeric Cyt-c was left at room temperature for a month, its absorption spectrum, which lacked the 695 nm band characteristic of the methionine coordination, indicated the formation of aggregated forms. This species was photoreduced even in the presence of oxygen, and the resultant RR spectrum was identical with that of the monomeric reduced species. The monomer and aggregated forms exhibited different luminescence pattern in the oxidized form. Immediate electron donors to the heme and a plausible mechanism of the photoreduction are discussed.

II-F-8 Resonance Raman Spectra of Intermediate Ligated Forms of Hemoglobin: The $\nu_{Fe\text{-}His}$, $\nu_{Fe\text{-}CO}$, δ_{FeCO}, and ν_{OO} Modes of Cross-linked Fe-Co Hybrid Hemoglobins

Shoji KAMINAKA, Takashi OGURA, Keiko KITAGISHI, Takashi YONETANI and Teizo KITAGAWA

[*J. Am. Chem. Soc.* in press]

Asymmetrically Co-substituted Fe-Co hybrid hemoglobins were prepared by cross-linking Hb A to mutant Hb C (Gluβ6 $\rightarrow$ Lys) through bis(3,5-dibromosalicyl) fumarate and their resonance Raman (RR) spectra were observed for various ligated forms. In order to explore the band position of the Fe-histidine stretching mode ($\nu_{Fe\text{-}His}$) which was distorted due to a tail of Rayleigh scattering, the spectrum of the fully oxygenated form was subtracted from each spectrum. With regard to the fully deoxy form, the $\nu_{Fe\text{-}His}$ mode gave an asymmetric band at 206 (and 215) cm^{-1} for the mono-α(Fe) tetramer and it was intensified without a change of the band shape for di-α(Fe) tetramer, while both mono- and di-β(Fe) tetramers yielded a symmetric and more intense band at 216 cm^{-1}. The $\nu_{Fe\text{-}His}$ band of the photodissociated transient FeCO subunit of the mono-α(Fe) tetramer was observed at 206 (and 216) cm^{-1} similar to the fully deoxy Hb but that of the mono-β(Fe) tetramer was shifted to 220 cm^{-1}, and they were observed at 219 and 222 cm^{-1}, respectively, when three Co subunits were oxygenated. Accordingly, it was confirmed that the binding of a ligand to a single β subunit causes a large structural change of the protein but that to a single α subunit has much less effect. COFe subunits of di-α(Fe) and di-β(Fe) tetramers were observed at 220–223 cm^{-1} which were unaltered by oxygenation to the remaining two Co subunits. This suggested that a structural change of the heme is almost completed upon binding of two ligands. The Fe-CO stretching ($\nu_{Fe\text{-}CO}$) and bending (δ_{FeCO}) frequencies were slightly lower and higher, respectively, for the β than α subunit for all ligation states. This implied that the anticipated steric hinderance by Val-Ellβ was not important. The OO stretching (ν_{OO}) frequency was the same between the α(Co) and β(Co) subunits for all the ligation states. Therefore, the hydrogen bonding to the bound oxygen is deduced to be similar between the α and β subunits.

II-F-9 Resonance Raman Evidence for Symmetric Coodination of Peroxide Ion in Binuclear Copper(II) Complexes as in Oxyhemocyanin

Nobumasa KITAJIMA, Takayuki KODA, Kiyoshi FUJIWAWA, Chisato FUJIMOTO, Yoshihiko MOROOKA, Shinji HASHIMOTO, and Teizo KITAGAWA

The coordination structure of dioxygen on the binuclear site of hemocyanin (Hc) has attracted much attention. The resonance Raman study on oxy-Hc with unsymmetrically labeled dioxygen proved that the dioxygen (peroxide) binds to the two Cu^{2+} ions in symmetric mode (μ-1,2). However, there has been no synthetic example of such binuclear copper-peroxide moiety until very recently. Karlin and coworkers [*J. Am. Chem. Soc.* **110**, 3690 (1988)] reported the synthesis and crystal structure of $[CuL]_2(O_2)^{2+}$ (L=tris [2-pyridyl (methyl)] amine) which definitely established the presence of trans μ-1,2 coordination of peroxide ion. However, the Cu-Cu distance and electronic spectrum of the complex is significantly different from those of oxy-Hc and the O-O stretching mode of the complex has not been explored yet. Herein, we present resonance Raman evidence for the similarity in a coordination mode of peroxide ion between the synthetic analogue 1~3 and oxy-Hc.

II-F-10 Functional Activity of Haemoglobins Adsorbed on Collodial Silver: A SERRS Study

Jeff DE GROOT, Ronald E. HESTER, Shoji KAMINAKA and Teizo KITAGAWA

[*J. Phys. Chem.* **92**, 2044 (1988)]

Surface enhanced resonance Raman spectra from submicromolar concentrations of human and carp haemoglobins adsorbed on collodial silver are reported. The adsorbed haemoglobins show reversible dioxygen and carbon monoxide binding and undergo a reversible R- to T-state transition. The Fe-N_{His} stretching vibration is unperturbed by adsorption at the silver surface, indicating that the intact haem environment is preserved and the tetrameric structure is retained, even at submicromolar concentrations. Molecular graphics representations of haemoglobins indicate that the propionate groups attached to the porphyrin macrocycle provide suitable binding groups for adsorption of the haemoglobin at the positively charged silver surface.

II-F-11 Characteristics in Tyrosine Coordinations of Four Hemoglobins M Probed by Resonance Raman Spectroscopy

Masao NAGAI, Yoshimasa YONEYAMA, and Teizo KITAGAWA

[*Biochemistry* in press]

Resonance Raman spectra of four Hbs M with tyrosinate ligand, that is, Hb M Saskatoon (β distal His $\rightarrow$ Tyr), Hb M Hyde Park (β proximal His $\rightarrow$ Tyr), Hb M Boston (α distal His $\rightarrow$ Tyr) and Hb M Iwate (α proximal His $\rightarrow$ Tyr) were investigated in order to elucidate structural origins for distinctly facile reducibility of the abnormal subunits of Hb M Saskatoon in comparison with other Hbs M. All of them exhibited the fingerprint bands for the Fe-tyrosine proteins around 1600, 1500, and 1280 cm^{-1}. However, only Hb M Saskatoon displayed the Raman spectral pattern of a six-coordinate heme for the β abnormal subunit while others displayed that of a five-coordinate heme, and its Fe-tyrosinate stretching frequency was the lowest among them. The absorption intensity of Hb M Saskatoon at 600 nm indicated a transition with a midpoint pH at 5.2, but that of Hb M Boston showed no change until pH 4.8. The fingerprint bands for the tyrosinate coordination as well as the Fe-tyrosinate stretching band disappeared for Hb M Saskatoon at pH 5.0 and the resultant Raman spectrum bore close resemblance to that of metHb A, while those bands were clearly observed for Hb M Boston at pH 5.0 and for two Hbs M at pH 10.0. From these observations we deduce that the characteristics in the heme structure of the abnormal β chains of Hb M Saskatoon lie in the weak feature of the Fe-tyrosinate bond, which makes the strain for pulling the heme iron toward the tyrosinate weaker and thus allows weak coordination of proximal histidine at its trans position, giving rise to the six-coordinate high-spin state at pH 7, but at pH 5 the coordination geometry is reversed due to protonation of the tyrosinate.

II-F-12 Resonance Raman Characterization of N-methyl-Octaethylporphyrinato-cobalt(II)

Yukihiro OZAKI, Katsuhiro AOYAGI, Keiji IRIYAMA, Hisanobu OGOSHI and Teizo KITAGAWA

[*J. Phys. Chem.* in press]

Resonance Raman (RR) spectra were observed for Co(N-CH_3OEP)AcO (N-CH_3OEP: N-methyl-octaethylporphyrin, AcO: acetate), Co(N-CH_3OEP-d_4)AcO, Co(N-CH_3OEP-$^{15}N_4$)AcO, and Co(N-CD_3-OEP)AcO, and their vibrational assignments have been investigated. Frequencies of the $C_\alpha C_m$ stretching RR bands of Co(N-CH_3OEP)AcO were generally much lower than those of Co(OEP) (OEP: octaethylporphyrin). Two $C_\alpha C_m$ stretching frequencies (ν_{10} and ν_3) were in good agreement with the values expected from the average core-size of 2.042 Å, while two $C_\beta C_\beta$ stretching modes (ν_2 and ν_{11}) exhibited large separation in comparison with those of Co(OEP) and thus deviated from the expected values. Contrary to Co(OEP) with one intense totally symmetric $C_\alpha N$ stretching mode (ν_4) at 1379 cm^{-1}, Co(N-CH_3OEP)AcO gave two ^{15}N sensitive bands at 1374 and 1361 cm^{-1}. Three bands at 309, 203 and 179 cm^{-1} were deduced to arise from the out-of-plane deformation modes of the N-methylated pyrrole ring and therefore to be sensitive to structural changes of the N-methyl group. Some RR bands which are symmetrically forbidden for Co(OEP) were observed with Co(N-CH_3OEP)AcO. The RR data imply that the replacement of the axial ligand from AcO to imidazole, pyridine, or 2-methylimidazole induced slight changes in the tilt angle of the N-methylated ring and/or in the orientation of the N-methyl group.

II-F-13 Effect of Urea on Hydrophobic Interaction: Raman Difference Spectroscopy on the C-H Stretching Vibration of Acetone and the C-N Stretching Vibration of Urea

Yasuhisa MIZUTANI, Keiji KAMOGAWA, and Koichiro NAKANISHI

Mixing state of urea in urea-water binary system and those of urea and acetone in urea-acetone-water ternary system are investigated with Raman difference spectroscopy. Frequency shift of the C-N stretching vibration, $\Delta\nu_{CN}$, in the former linearly depends on the mole fraction of urea, χ_U, and changes little at lower χ_U. In the ternary system, frequency shift, $\Delta\nu_{CH}$, is determined as a function of χ_A and χ_U, from which transfer shift from water to aqueous urea solution, $\Delta\nu_{CH}^{trans}$, is evaluated as a function of χ_U. $\Delta\nu_{CH}^{trans}$ is found to give major contribution to the $\Delta\nu_{CH}$ and it is almost in proportion to χ_U. The results reveal that urea molecules attractively solve acetone single molecule in a close vicinity to themselves without modifying water structure, and decrease acetone-acetone interaction to some extent. This is also confirmed by $\Delta\nu_{CN}$ behavior. The present study provides important experimental evidence for the solvation effect of urea which has been discussed extensively.

II-F-14 SERR Evidence for Preservation of Physiological Function of Cytochrome c_3 Adsorbed on Ag Colloids.

Alan L. VERMA, Keisaku KIMURA, Asaro NAKAMURA, Tatsuhiko YAGI, Hiroo INOKUCHI, and Teizo KITAGAWA

Surface-Enhanced resonance Raman (SERR) spectra excited near the Soret as well as the α and β bands are reported for a tetraheme protein cytochrome c_3 (Cyt-C_3) adsorbed on colloidal silver particles. The adsorbed protein in Ag sol could be fully reduced by hydrogen in the presence of hydrogenase but not in its absence, providing direct evidence that the physiological function of Cyt-C_3 and hydrogenase in bulk are well preserved in the adsorbed state. We confirmed an adsorption induced partial transition from the low-spin to high-spin state in both the oxidized and reduced forms similar to observations for cytochrome *c* by Hildebrandt and Stockburger [*J. Phys. Chem.* **90**, 6017 (1986)]. The relative populations of the low- and high-spin forms was temperature-dependent, suggesting a thermal spin equilibrium of the protein adsorbed on the Ag sol.

II–G Structure of Noncrystalline Solids by EXAFS

It is very important to know the structure of supported catalyst in order to understand the roles of catalysts in catalytic reactions. EXAFS is best suited for the purpose because the local structure around the selected elements can be determined irrespective of the phase. Very tiny metal or metal oxide clusters in the supported catalyst, which TEM and XRD fail to observe, can be studied. Especially, the structure under the reaction conditions can be probed by the use of an *in situ* cell, since EXAFS measurement can be done with the presence of reacting gas.

In the past years, our effort was mainly concentrated on the determination of the structures of several supported mono- and bimetallic catalysts. Structural changes at the several stages of the preparation procedure and under the presence of reacting gases have also been investigated. Studies above these lines have been continued and extended to try to make relationship between catalyst structure and catalytic activity. Local structures around metals in amorphous solids or in solution have been studied as joint studies program.

A possibility of x-ray Raman spectroscopy as a new method for structure determination has been continuously pursued in laboratory as well as with synchrotron radiation facility, and it was confirmed that structural parameters can be extracted. Resonance effect in x-ray Raman scattering was also studied.

The followings are the abstracts of the manuscripts submitted to several journals in the past year.

II-G-1 X-Ray Raman Scattering as a Substitute for Soft X-ray EXAFS

Kazuyuki TOHJI and Yasuo UDAGAWA

[*Phys. Rev. B,* in press]

We have recorded x-ray Raman scattering spectra from graphite and diamond with high resolution and good S/N ratio by the excitation of hard x-rays from synchrotron radiation. The scattering spectra show characteristics predicted by the theory. Especially, oscillations identical with those found in extended x-ray absorption fine structure (EXAFS) spectrum[1] are observed for diamond as is shown in Figure 1. From an analysis employing the formula used for EXAFS, interatomic distances can be determined. Thus, it is experimentally confirmed for the first time that x-ray Raman spectroscopy by hard x-rays can supply the same information as the soft x-ray EXAFS. It can be a substitute for EXAFS to determine the local structure around low atomic number elements whose EXAFS study is plagued with various experimental difficulties.

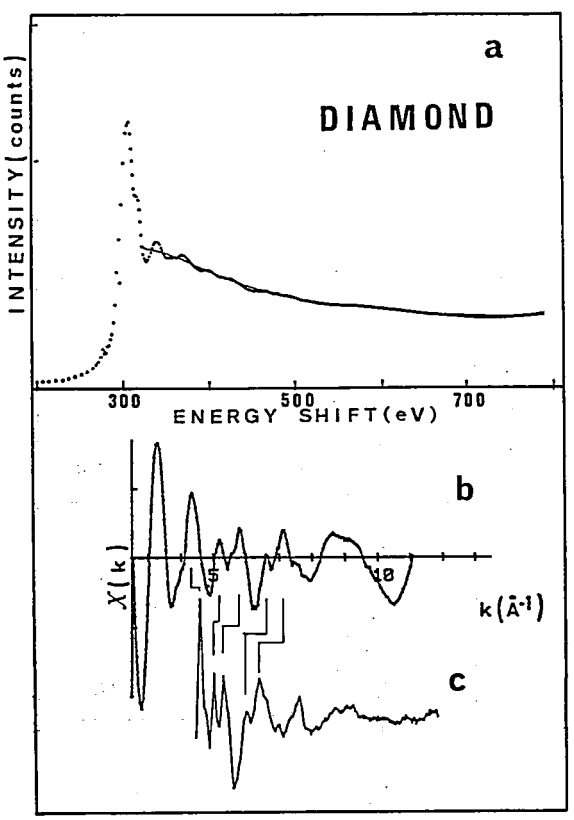

Figure 1. (a) X-ray Raman scattering spectrum of diamond at scattering angle of 60°. (b) Extracted oscillation from (a). (c) Extracted oscillation from soft x-ray absorption spectrum of diamond.

Reference

1) G. Comelli, J. Stohr, W. Jark, and B.B. Pate, *Phys. Rev.* **B37**, 4393 (1988).

II-G-2 Observation on X-ray Resonant Raman Spectra and Transition to Resonant Fluorescence

Yasuo UDAGAWA and Kazuyuki TOHJI

[*Chem. Phys. Lett.* **148**, 101 (1988)]

X-ray Raman spectra of transition metal compounds, copper, cuprous oxide, and cupric oxide are reported in the resonant, pre-resonant, and non-resonant conditions for the first time. As an example, Figure 1a shows Raman spectra of CuO excited by X-rays from 8958 to 8988 eV. In this compound K absorption starts at ca. 8985 eV. In the off-resonant condition, a sharp edge is observed to the higher energy side for each compound, and the energy differences between the edge and the exciting light corresponds to L_{III} absorption of copper (935 eV).

Upon approaching the resonant condition the spectra show remarkable changes. When excited by X-rays above 8988 eV, the same spectrum, namely the well-known K_α doublet of copper atom is observed. With detuning the excitation energy, the scattering intensity decreases drastically, and the shape of the two components of the doublet becomes more and more asymmetric, having a tail to the lower energy side. Peak energies shift toward lower energy in accordance with the decrease in excitation energy.

The transition from the near resonance Raman spectrum to K fluorescence can be nicely reproduced by a simple calculation using well known Kramers-Heisenberg equation by employing one electron approximation as is shown in Figure 1b.

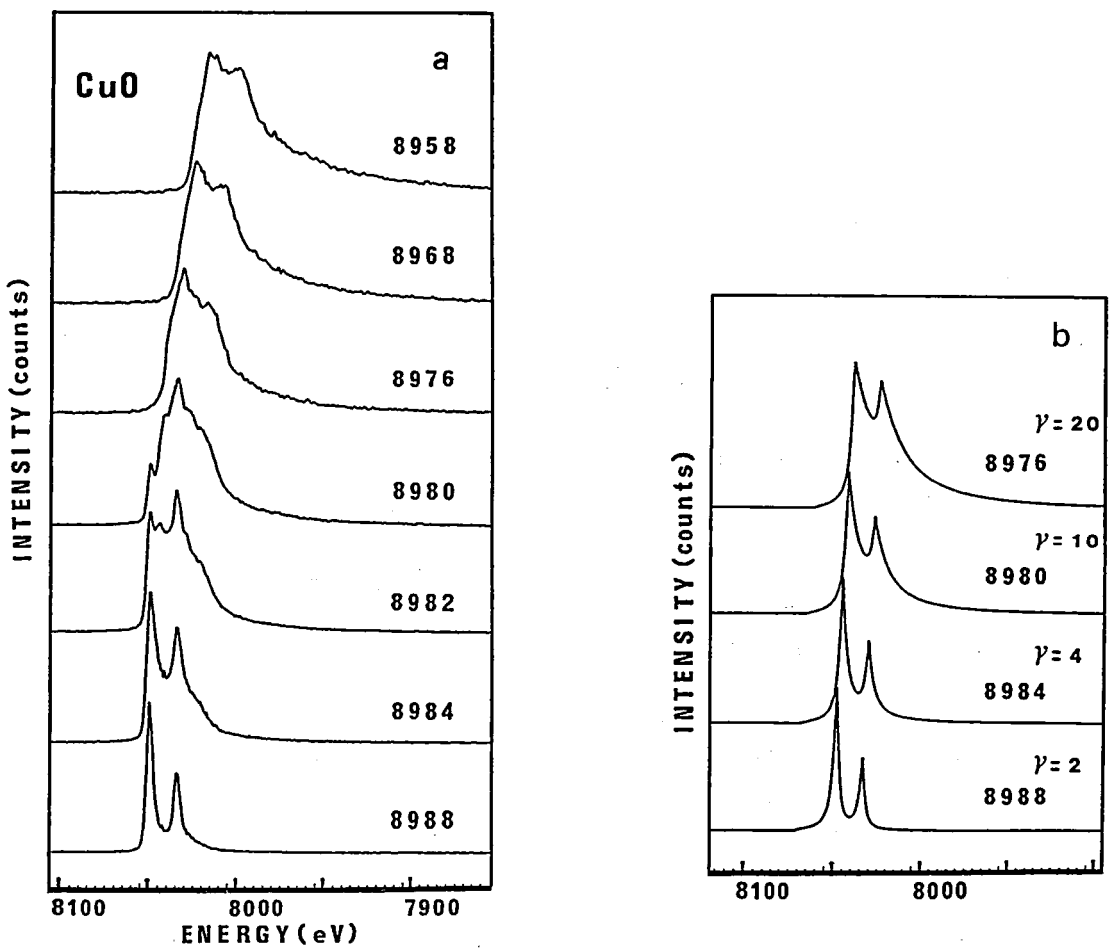

Figure 1. (a) Excitation energy dependence of scattering spectra from cuprous oxide. Inserted numbers indicate excitation energy in eV. The ordinate does not represent the relative intensity of the spectra. (b) Calculated excitation energy dependence of the scattering. Inserted numbers indicate excitation energy and dumping factor γ in eV. E_f-E_g was fixed to 8986 eV in the calculation.

II-G-3 An EXAFS Study on the Morphology Change of Ru Catalyst by CO Adsorption

Takanori MIZUSHIMA, Kazuyuki TOHJI, and Yasuo UDAGAWA

[*J. Am. Chem. Soc.* **110**, 4459 (1988)]

Highly dispersed $Ru/\gamma\text{-}Al_2O_3$ catalyst was prepared from $Ru_3(CO)_{12}$ and morphology change of Ru clusters before and after CO adsorption was studied. The dispersion of the catalyst was estimated to be 0.8 from the hydrogen adsorption. Figure 1a shows the Ru EXAFS spectrum, extracted oscillation, and the associated k^3 weighted Fourier transform of the reduced 2 wt % catalyst. For comparison, those of Ru powder as a reference are shown in Figure 1c. From the analysis of the EXAFS spectra, it is concluded that the coordination number is about 4, which indicates that Ru clusters in the catalyst consist of less than 10 atoms. In addition, the nearest neighbor interatomic distance reduces to 2.55 Å, which is shorter than the bulk value by as much as 0.13 Å.

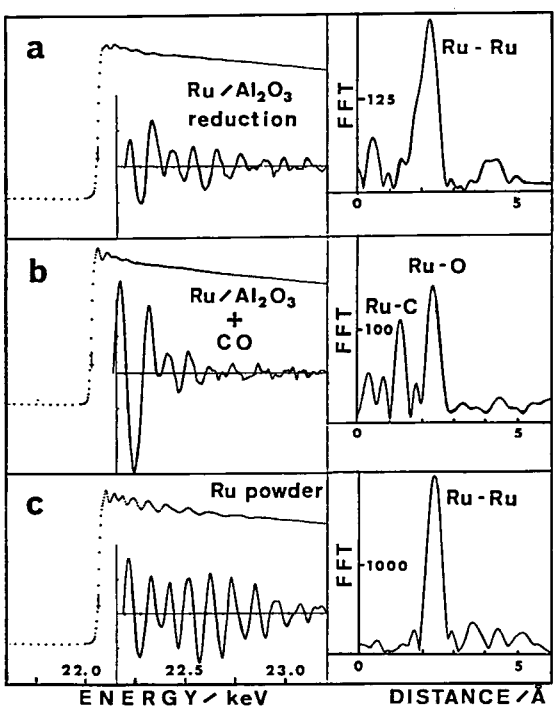

Figure 1. Observed Ru K edge EXAFS spectra, extracted oscillations, and associated Fourier transforms of (a) $Ru/\gamma\text{-}Al_2O_3$ reduced at 723 K in H_2, (b) after admission of 200 Torr CO, and (c) Ru powder. All the spectra were obtained at room temperature.

The adsorption of CO on the catalyst thoroughly changes the local structure around Ru atoms as evidenced in Figure 1b. The associated Fourier transform shows two peaks which should be assigned to Ru-C and Ru-O of the adsorbed CO molecules. The spectrum change between spectrum a and b is completely reversible by repeated adsorption/desorption cycles.

The following conclusions can be drawn from the present study. First, ultradispersed Ru clusters are formed on alumina support. Second, Ru-Ru bonds in the very tiny Ru clusters are disrupted by CO adsorption, leading to the formation of a new species like $Ru(CO)_n$. Third, the tiny Ru clusters are recovered by CO desorption.

II-G-4 Characterization and Catalytic Properties of Silica Supported Iron-Nickel Catalysts through EXAFS and Formic Acid Decomposition

Takanori MIZUSHIMA, Kazuyuki TOHJI, Yasuo UDAGAWA, Akifumi UENO*, and Mutsumi HARADA* *(*Toyohashi University of Technology and IMS)*

[*Material Research*, in press]

Bimetallic Fe-Ni catalysts with various compositions were prepared according to two procedures; alkoxide (A) and impregnation (I) methods. The catalyst structure as well as the surface composition are studied by EXAFS and the reactivity was compared. From EXAFS study it is concluded that alloy with fcc structure is always formed in the concentration range studied (1:3 – 3:1) for both catalysts A and I and that Fe tends to be exposed on the surface. The surface concentration of Fe is more pronounced in A than in I.

On the other hand, it is found that the selectivity over the formic acid decomposition reaction is completely different for the two catalysts. In the 1:1 catalyst prepared by the alkoxide method the selectivity to dehydration is 50–60 % depending on the temperature, which can be compared with 70–80 % in the pure iron. On the other hand, in the 1:1 catalyst by the impregnation method the selectivity is about 10 %, which is almost the same as 5 % of the pure nickel. The selectivity varies in a complicated manner with concen-

tration and preparation procedure, but on the whole, the selectivity can be understood by the surface composition and selectivity of individual component.

II-G-5 Local Structure around Y atoms in Y_2O_3 Stabilized Tetragonal ZrO_2

Hideki MOIRIKAWA*, Y. SHIMIZUGAWA*, Fumiyuki MARUMO*, H. HARASAWA, Kazuyuki TOHJI, and Yasuo UDAGAWA *(*Tokyo Institute of Technology)*

[*J. Jpn. Ceramic Soc.* **96**, 253 (1988)]

Local structures around Y^{3+} ions in stabilized ZrO_2 with the chemical composition of $94ZrO_26YO_{1.5}$(Y6) and $86ZrO_24YO_{1.5}10CeO_2$(Y4) were studied by Y K EXAFS analysis. Using Y_2O_3 crystal (Y-O=2.28 Å, six-fold coordination) as a reference sample, average Y-O distances for Y6 and Y4 samples were estimated to be 2.31 and 2.35 Å by the curve fitting method, respectively. Y atoms in the tetragonal zirconia seem to locate at seven-fold coordination sites, judging from the atomic distances. The average Y-cation distances for Y6 and Y4 samples were calculated to be 3.70 and 3.73 Å, respectively. They are longer than the average cation-cation distances calculated from the lattice dimensions, but shorter than the average Y-Y distance of 3.77 Å in the Y_2O_3 crystals. A $Zr_2Y_2O_7$ cluster was proposed as a model for local structures around Y^{3+} ions. The cluster consists of two ZrO_7 and two YO_7 polyhedra which share one oxygen vacancy. If one oxygen vacancy is introduced into the atomic arrangement of tetragonal ZrO_2, four equivalent cation sites change to two bigger and two smaller sites which are respectively positioned along the a axis. A pair of Y^{3+} ions probably occupies the bigger sites and as a result the c/a axial ratio decreases. Therefore this model is consistent with the fact that the c/a axial ratio decreases with an increase of Y_2O_3 concentration when Y^{3+} ions are added to tetragonal ZrO_2.

II-G-6 Unusual Long Distances of Germanium-Carbon Bond of Organogermyl-alkali Metal Probed by EXAFS

Kunio MOCHIDA*, Tsuyoshi KUGITA*, Kazuyuki TOHJI, and Yasuo UDAGAWA *(*Gakushuin Univ.)*

[submitted to *Organometallics*]

Extended X-ray absorption fine structure spectra were analyzed for series of organogermylalkali metals in solutions; Me_3GeLi, Me_3GeNa, Me_3GeK, Et_3GeLi, and Ph_3GeLi as well as related reference Ge compounds. The distances of germanium-carbon bond of the germylalkali metals were found to be longer about 10 % than those of the corresponding neutral species. The longer germanium-carbon bond distances of organogermyl-alkali metals may be explained to be a consequence of charge polarizaion of $Ge^{\delta-}$-$C^{\delta+}$ induced by a large negative charge on germanium atom.

RESEARCH ACTIVITIES III
Department of Electronic Structure

III–A Role of Hot Molecules in UV Single- and Multiphoton Chemistry

Irradiation of molecules with UV or VUV light often induces photodissociation. Besides direct and pre-photodissociation, we have been invesitgating another type of photodissociation, which consecutively involves excitation of electronically excited state, efficient internal conversion to the ground state, and dissociation or isomerization. The ground electronic state produced by a single photon has a very high vibrational energy, in other words the corresponding vibrational temperature is thousands Kelvin. These states can absorb another photon and get excited to even higher excited states, which cause dissociation. In this chapter we mainly discuss a new mechanism of multiphoton processes, hot-molecule mechanism of dissociation, which could be important in neutral radical formation.

III-A-1 Hot Toluene as an Intermediate of UV-Multiphoton Dissociation

Nobuaki NAKASHIMA, Noriaki IKEDA and Keitaro YOSHIHARA

[*J. Phys. Chem.*, **92**, 4389 (1988)]

We have demonstrated that hot molecules are the intermediates in UV dissociation of alkylbenzenes.[1),2)] This paper describes that S_0^{**} has another role in UV laser photochemistry. It can be one of the intermediates in UV multiphoton dissociation. Decomposition of toluene with the ArF laser light (193.2 nm) is a typical example. Hot toluene shows strong absorption in the UV region and hence absorbs a second photon. The second photon dissociates S_0^{**} into a benzyl radical. We believe that a third photon decomposes the benzyl radical. This is the first observation of UV multiphoton chemistry via hot molecule.

UV multiphoton chemistry via hot molecule has a different aspect from that via excited singlet or lowest triplet state. In the case of the hot molecule mechanism the second absorbed photon does not ionize the hot toluene, because the energy of the first photon has been distributed in vibrational modes. It should be noted that neutral rather than ion fragmentation takes place as shown in Figure 1.

References

1) N. Ikeda, N. Nakashima, and K. Yoshihara, *J. Chem. Phys.*, **82**, 5285 (1984).
2) Y. Kajii, K. Obi, I. Tanaka, N. Ikeda, N. Nakashima, and K. Yoshihara, *J. Chem. Phys.*, **86**, 6115 (1987).

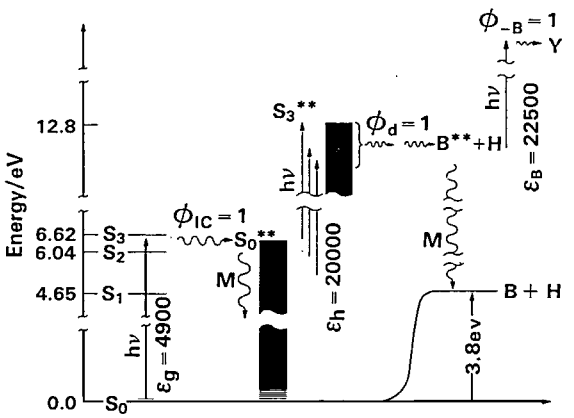

Figure 1. Schematic diagram of UV multiphoton dissociation via hot toluene, ArF laser light (193.2 nm) excites the S_3 state of toluene. Internal conversion finally leading to S_0^{**} takes place. The second photon excites S_0^{**} during collisional relaxation with 800 Torr of added nitrogen. The excitation of S_0^{**} leads to toluene dissociation into a benzyl radical. The benzyl radical is assumed to disappear on absorption of a third photon. A set of well-fitting parameters is also shown.

III-A-2 Role of Hot Molecule in UV Single- and Multiphoton Chemistry

Nobuaki NAKASHIMA *(Osaka Univ.)* **and Keitaro YOSHIHARA**

[*J. Phys. Chem.*, submitted]

The UV photochemistry of benzenes, alkylbenzenes, and olefins is described from a new point of view: the hot molecule mechanism. The hot molecule (denoted as S_0^{**}) is formed by internal conversion to the ground state in gas phase upon irradiation with UV light. Thus produced S_0^{**} has a very high equivalent tempeterature and a narrow energy distribution, therefore, specific reactions can be driven by thermal energy. We have measured dissociation reaction via the hot molecule mechanism (Figure 1(a)) for more than 60 molecules. It can be stated that the hot molecule mechanism is one of general reaction routes of unsaturated hydrocarbons. For the first time, it has been found that the hot molecule (S_0^{**}) has another role. It can be an intermediate in UV multiphoton dissociation (Figure 1(b)). S_0^{**} shows strong absorption in the UV region and hence efficiently absorbs a second photon which causes dissociation. Radical fragmentations are major reactions of this new multiphoton chemistry. The reaction with this mechanism is particularly important for neutral radical formation.

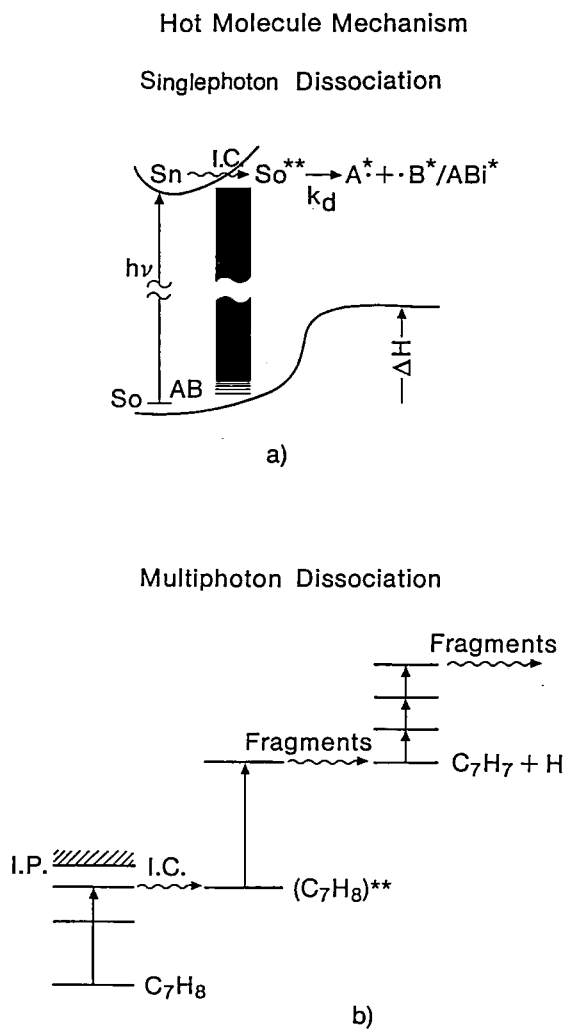

Figure 1. Hot molecule mechanism of single- and multiphoton chemistry. (a) Upon irradiation with UV-VUV light, rapid internal conversion can occur from the absorbed state to the ground electronic state. The vibrationally hot molecule, S_0^{**}, dissociated to A* + B* and/or isomerizes to AB_i^*. (b) Hot molecule mechanism of multiphoton dissociation. Taking an example of exciting toluene with ArF laser light (193 nm), the first photon produces S_0^{**} after efficient internal conversion from the absorbing state. The second photon excites S_0^{**} and excitation leads dissociation to a benzyl radical. The benzyl radical is assumed to disappear on absorption of a third photon. Neutral fragmentation is the major reaction.

III-A-3 UV Multiphoton Dissociation of Benzene

Limin ZHANG, Andrew H. CAMPEN *(Univ. of Southampton)*, **and Keitaro YOSHIHARA**

The mechanism of acetylene formation via multiphoton dissociation of benzene has been observed for the first time. The hot benzene is probably an intermediate in UV multiphoton dissociation.[1] The major products are acetylene, fulvene and biacetylene, the quantum yield of acetylene formation being 0.30 ± 0.01 with an excitation by ArF at 50 mJ/cm^2, and 0.29 ± 0.01 with resonant multiphoton excitation by a tunable dye laser at 9 mJ/cm^2. With excitation by KrF at 80 mJ/cm^2, the major products are acetylene and biacetylene, the quantum yield of former being 0.12 ± 0.01. In the case of excitation with ArF, in the region of higher laser fluence, considerable amounts of polymeric or carbonaceous deposits on the cell wall are observed. Saturation effects of product is seen in Figure 1.

Typical results of power dependence on yield of acetylene formation are shown in Figure 1. A cubic relation holds between the acetylene yield versus laser fluence for the three kinds of laser light sources and benzene was most likely to be dissociated through three photon process.

Reference
1) N. Nakashima, N. Ikeda, N. Shimo, and K. Yoshihara, *J. Chem. Phys.* **87**, 3471 (1987).

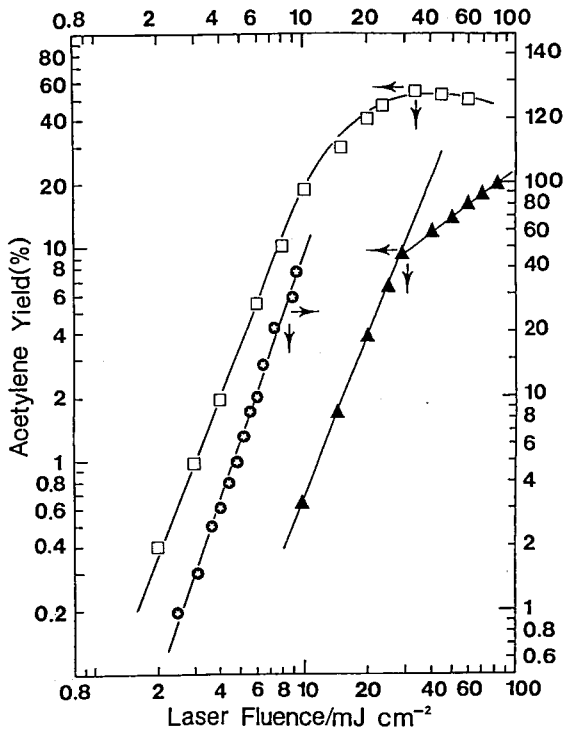

Figure 1. Power dependence of acetylene formation. (□) 2 Torr of benzene and 760 of Torr N_2 irradiated with 193 nm light from an ArF laser. (○) 2 Torr of benzene and 760 Torr N_2 irradiated with 241.7 nm dye laser. (▲) 2 Torr of benzene and 760 Torr N_2 irradiated with 248 nm light from a KrF laser.

III–B Photochemical cis-trans Isomerization of Isolated Olefinic Molecules

The photochemical *cis-trans* isomerizaion of an olefinic carbon bond is a fundamental chemical transformation that is important in chemical and biological sciences. Although much work has been done in this field, especially on model systems such as stilbenes, the isomerization dynamics and the photochemical intermediates are poorly understood. The fluorescence excitation spectrum of supersonically cooled *cis*-stilbene in Ne, Ar, Kr, and N_2 clusters has been measured in order to determine whether there exists a local minimum in the S_1 state of *cis*-stilbene. *Trans*-Stilbene in clusters shows previously unobserved photochemistry. The fluorescence excitation spectrum of supersonically cooled diphenylsuberene, which has electronic structure that is similar to *cis*-stilbene but cannot isomerize, is measured in order to study the electronic structure of *cis*-stilbene like molecules.

III-B-1 Fluorescence Excitation Spectroscopy of *cis*-Stilbene in Inert Gas Clusters

Hrvoje PETEK, Yoshihisa FUJIWARA *(Kanazawa Univ.)*, **Dongho KIM** *(Korea Standards Res. Inst.)* **and Keitaro YOSHIHARA**

[*J. Am. Chem. Soc.*, **110**, 6269 (1988)]

Strong evidence for a minimum on the S_1 surface of *cis*-stilbene from which the molecule decays on 20 ns time scale is found for *cis*-stilbene-inert gas clusters. In *trans*-stilbene, isomerization is inhibited by a 1,200 cm^{-1} barrier. By contrast, at ~300 K in gas and solution, *cis*-stilbene is non-emissive presumably because the S_1 state decays by barrierless isomerization on time scale of *ca.* 1 ps. In viscous solutions, a marked increase in *cis*-stilbene fluorescence quantum yield has been ascribed to retardation of isomerization by solvent-dependent viscosity barrier. In this work, some of these ideas are challenged by observation of the same emission spectrum from inert-gas *cis*-stilbene clusters formed by supersonic expansion. Namely, the macroscopic viscosity of inert gas clusters (e.g. Ar) is more than 10^6 times smaller than in viscous solutions; therefore, viscosity may not be the controlling factor, rather it is proposed that *cis*-stilbene in a cluster vibrationally relaxes into an inherent minimum on the S_1 surface, from where it decays with the observed 20 ns lifetime. Fluorescence excitation spectrum of *cis*-stilbene seeded in several gases support these conclusions (Figure 1).

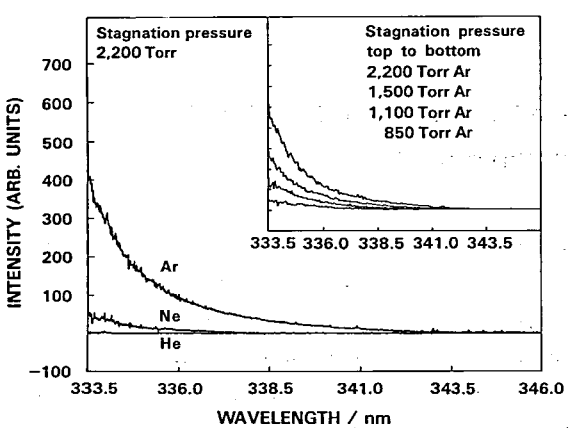

Figure 1. The fluorescence excitation spectrum of *cis*-stilbene near the origin. Changing the seeding gas and the stagnation pressure should not influence the *cis*-stilbene density, rather the fluorescence intensity under different expansion conditions reflect changes in *cis*-stilbene emission quantum yield.

III-B-2 Photochemistry of *cis*- and *trans*-Stilbene in Inert Gas Clusters

Hrvoje PETEK, Yoshihisa FUJIWARA *(Kanazawa Univ.)*, **and Keitaro YOSHIHARA**

The unexpected observation of strong fluorescence from *cis*-stilbene in inert gas clusters (see above), was explained by rapid vibrational relaxation that allows trapping of *cis*-stilbene in a minimum on the S_1 surface. To test this hypothesis, *trans*-stilbene fluorescence excitation and emission spectra in inert clusters were measured. The observation of completely relaxed *trans*-stilbene emission spectra indicates that *trans*-stilbene can dissipate into the cluster bath as much as 17,000 cm^{-1} excess energy on time scale which is significantly faster than the 2.7 ns fluorescence lifetime. A surprising result is that three distinct spectral components are observed – one is the expected UV emission from planar *trans*-stilbene S_1 minimum, while the other two components, which are at lower energy and have longer emission lifetimes, have **not** previously been observed with optical excitation of *trans*-stilbene. The origins of these additional components are not known but may be due to previously unobserved photochemical pathways in *trans*-stilbene or due to the interaction of *trans*-stilbene with the cluster environment.

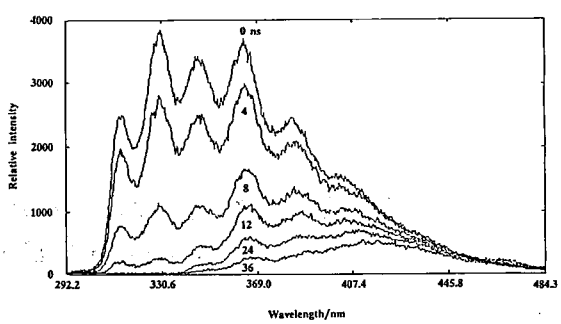

Figure 1. The time-resolved emission spectra of *trans*-stilbene in 1,600 Torr Ar expansion following 266 nm excitation measured with OMA using a nominal 5 ns gate. The shortest lived component in uv is due to *trans*-stilbene S_1 state emission. The two components to the red have not been observed in optical excitation of *trans*-stilbene.

III-B-3 Fluorescence Excitation Spectroscopy of Supersonically Cooled Selectively Deuterated Dibenzosuberene

Hrvoje PETEK, Yoshihisa FUJIWARA *(Kanazawa Univ.)*, **and Keitaro YOSHIHARA**

The fluorescence excitation spectrum of 2:3, 6:7-dibenzocyclo-hepta-2:4:6-triene, a fluorescent isomorph of *cis*-stilbene which cannot isomerize, has been investigated in order to obtain better understanding of *cis*-stilbene electronic structure and isomerization dynamics. The fluorescence excitation spectrum of $C_{15}H_{12}$ consists almost exclusively of two essentially harmonic progressions with 31 cm^{-1} vibrational frequency that extend for least 30 quanta.[1] In order to test whether these vibrations are due to the out-of-plane bending motion of the bridging methylene group, the spectrum is measured for dibenzosuberene which is selectively deuterated on the methylene. The modest decrease of the vibrational frequency to 29 cm^{-1} (Figure 1) indicates that the Franck-Condon active modes do not involve large amplitude motion of the methylene group, rather they most likely reflect the large amplitude motion of the phenyl groups as would be expected for the cis-trans isomerization coordinate.

Reference

1) H. Petek, Y. Fujiwara, D. Kim, and K. Yoshihara, *Ann. Rev. Inst. Mol. Sci.*, p. 47 (1987).

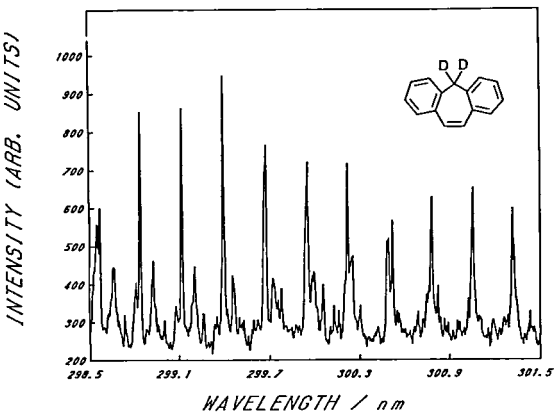

Figure 1. A portion of the fluorescence excitation spectrum of selectively deuterated dibenzosuberene.

III–C Dynamic Behavior of Excited States

Optical excitation of molecules to electronically excited states causes a variety of dynamical behavior, depending upon the nature of electronic structures and environments, such as energy transfer, proton transfer, chemical reaction, radiationless transition, ionization, and others. Most of these processes fall into the nanosecond, picosecond and femtosecond timescales. Firstly we discuss on the picosecond kinetics of excited-state proton transfer reaction of 2,5-bis-(2-benzoxazolyl)-hydroquinone and confirm a rapid equilibrium in the excited-state tautomers. Secondly we discuss the picosecond photochemistry of photosystem I of highly enriched reaction center of spinach. Particularly the effect of the presence and absence of primary electron acceptor vitamin K was examined.

III-C-1 Picosecond Kinetics of the Excited State Intramolecular Proton Transfer Reaction: Confirmation of the Intrinstic Potential Barrier in 2,5-Bis-(2-benzoxazolyl)-hydroquinone

Anna GRABOWSKA, Andrzej MORDZINSKI *(Inst. Phys. Chem., Polish Acad. Sci.)*, **Naoto TAMAI** *(Instrum. Center)*, **and Keitaro YOSHIHARA**

[*Chem, Phys. Lett.*, in press]

Intramolecular proton transfer (PT) reactions occurring within the lifetime of an electronically excited state are objects of current interest. 2,5-Bis-(2-benzoxazolyl)-hydroquinone (2,5-BBHQ) was studied and (i) stationary emission spectra and (ii) kinetic measurements in the picosecond time scale were undertaken. The sample shows two fluorescences, the primary and tautomeric fluorescence, observed at 450 nm and 620 nm, respectively. The data in Table 1 clearly show that the decay of the primary species (enol tautomer) contains two components, $\tau_1 = 17 \sim 23$ ps and $\tau_2 = 950 \sim 970$ ps. Both, within the experimental error, are reproduced in the rise (negative amplitude) and the decay of the fluorescence of the non-symmetric single ketotautomer.[1] The data unambiguously confirm the bimodal kinetics of the excited 2,5-BBHQ as well as the common decay of the two reaction partners being in equilibrium. The detection of the fast component, $\tau_1 = 20$ ps, is an example of rather unique case of the direct observation of the proton transfer process in the excited intramolecular system.

Table 1. Kinetic parameters of the PT reaction of the excited 2,5-BBHQ: N°, number of experiment; τ_{ex}, τ_{obs} denote the excitation and observation wavelengths, respectively, $\tau_{1,2}$ are lifetimes, the corresponding amplitudes being given in parantheses. Time resolution, ps/ch, is shown in the last row.

N°	τ_{ex} (nm)	τ_{obs}	τ_1(A) (ps)		τ_2(A) (ps)		ps/ch (ps)
1	305	450	20.1	(14.29)	950	(17.06)	5.6
		620	21.4	(−18.68)	945	(20.60)	
2	300	450	16.9	(21.77)	977	(17.84)	2.5
		620	17.5	(−15.16)	972	(17.51)	
3	314	450	20.4	(8.26)	972	(12.61)	2.5
		620	23.1	(−13.97)	942	(13.99)	

Reference

1) A. Mordzinski, A. Grabowska, and K. Teuchner, *Chem. Phys. Lett.*, **111**, 383 (1984).

III-C-2 Picosecond Photochemistry of Photosystem I in the Absence of Vitamin K-1

Dongho KIM *(Korea Standards Res. Inst.)*, **Keitaro YOSHIHARA, and Isamu IKEGAMI** *(Teikyo Univ.)*

[*Plant Cell Physiol.*, submitted]

Photosystem-I (PS-I) particles usually have a large amount of antenna chlorophylls, which makes it difficult to select out the primary processes without any screening of antenna chlorophyll molecules. Thus, the highly enriched PS-I particles where antenna chlorophyll molecules have been extracted by a treatment with wet diethyl ether, has a good advantage for an investigation of the primary photo-induced processes. The bound vitamin K-1 can also be completely removed from PS-I particles by the ether treatment, which is expected to block out the electron transfer to the terminal electron acceptors, because vitamin K-1 is believed to act as A_1. In addition, the externally added naphthoquinones act as an efficient electron acceptor without perturbing any other photoinduced processes. In Figure 1, we show the picosecond transient absorption changes of PS-I in the highly enriched PS-I particles which were totally devoid of vitamin K-1. The effect of exogenously added vitamin K-3 on picosecond absorption changes are also shown. Spectral profile of the bleaching is quite similar to the absorption spectra, as have been shown previously.[1] Assignment of the picosecond transient absorption spectra was given.

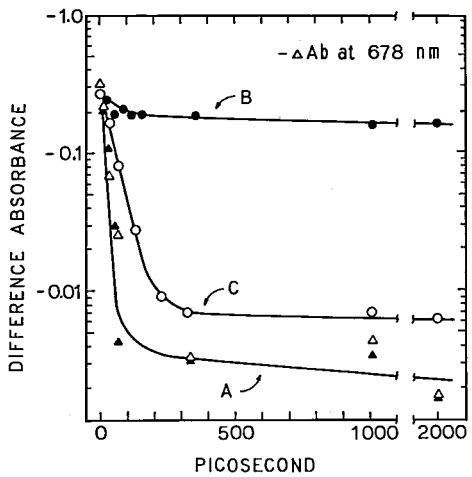

Figure 1. Decay kinetics of the bleaching at 678 nm in the oxdized (triangles, curve A) and in the reduced (circles, curve B and C) PS-I particles. Vitamin K-3 was added to the reduced (open circles, curve C) and the oxidized (open triangles, curve A) particles.

Reference

1) K. Kamogawa, A. Namiki, N. Nakashima, K. Yoshihara, and I. Ikegami, *Photochem. Photobiol.*, **34**, 511 (1981).

III–D Development of New Experimental Methods for Ultrafast Spectroscopy

Development of new instruments or new methods is often necessary for deeper understanding of dynamic behavior of molecules. Development of laser science and technology had enormous impact on time-resolved spectroscopic studies of molecular dynamics in the picosecond and femtosecond time domains. The application of ultrafast spectroscopy is extending to a wider wavelength region, higher sensitivity, faster time resolution, higher accuracy, and more variety of experimental conditions. In this chapter, we firstly describe the first direct observation of photodynamics in opaque materials with a picosecond diffuse reflectance detection of transient intermediates. Secondly, picosecond dynamics of adsorbates detected by time-resolved surface second harmonic generation is described and dynamics of surface isomerization and desorption are reported. Thirdly development of a femtosecond laser system for molecular vibrational spectroscopy is described.

III-D-1 Direct Observation of Photodynamics in Opaque Organic Microcrystals: A Picosecond Diffuse Reflectance Laser Photolysis Study

Noriaki IKEDA, Masanori KOSHIOKA, Hiroshi MASUHARA *(Kyoto Inst. Tech.)*, **Nobuaki NAKASHIMA, and Keitaro YOSHIHARA**

[*Ultrafast Phenomena IV*, in press]

In recent years, a diffuse reflectance laser photolysis method has been developed.[1] This method is powerful because it gives absorption spectra of transient species in opaque and scattering meterials such as organic microcrystals, semiconductors, insoluble polymer powders, dyed fabrics, molecules adsorbed on silica gel, *etc.*

Figure 1 shows a series of time-resolved absorption spectra of benzil in microcrystal and in solution. Although the obtained spectra were broader and red shifted in microcrystal than in solution, a similar spectral change occurred but with a different time constant. The fast and slow transients can be assigned to S_1 and T_1 states, respectively. The geometry of the excited states is reported to be skewed in crystal and trans-planar in solution. As can be seen in Figure 1, the intersystem crossing rate of benzil in microcrystal is faster than in solution. However, in the case of benzophenone there was no appreciable difference of the triplet rise curves between solid and solution phases.[2] We have demonstrated for the first time a picosecond transient absorption spectral and kinetic measurement of singlet excited states of organic microcrystals by the diffuse reflectance laser photolysis method.

References

1) F. Wilkinson, *J. Chem. Soc. Faraday Trans. 2*, **82**, 2073 (1986).
2) N. Ikeda, K. Imagi, H. Masuhara, N. Nakashima, and K. Yoshihara, *Chem. Phys, Lett.* **140**, 281 (1987).

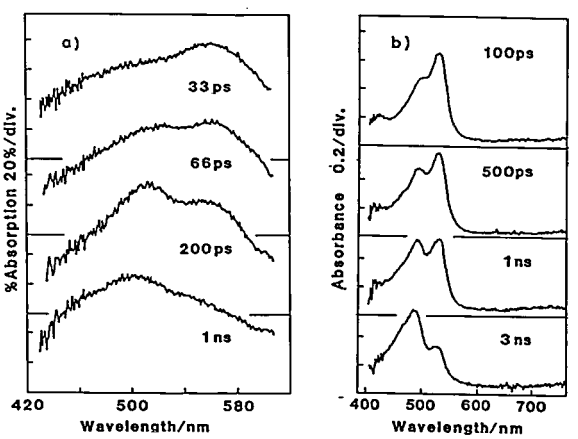

Figure 1. Transient absorption spectra of benzil in microcrystal (a) and in cyclohexane solution (b).

III-D-2 Picosecond Dynamics of Adsorbates by Time-Resolved Surface Second Harmonic Generation

Stephen R. MEECH, and Keitaro YOSHIHARA

[*Chem. Phys. Lett.*, in press]

The technique of time-resolved surface-second harmonic generation has been developed to study the dynamics of adsorbate reactions.[1] Both intramolecular (isomerisation) and desorption dynamics have been observed. The TRSSHG method is less sensitive than fluorescence, but has the great advantage that the signal is surface specific; the signal arises only from the interface.[2]

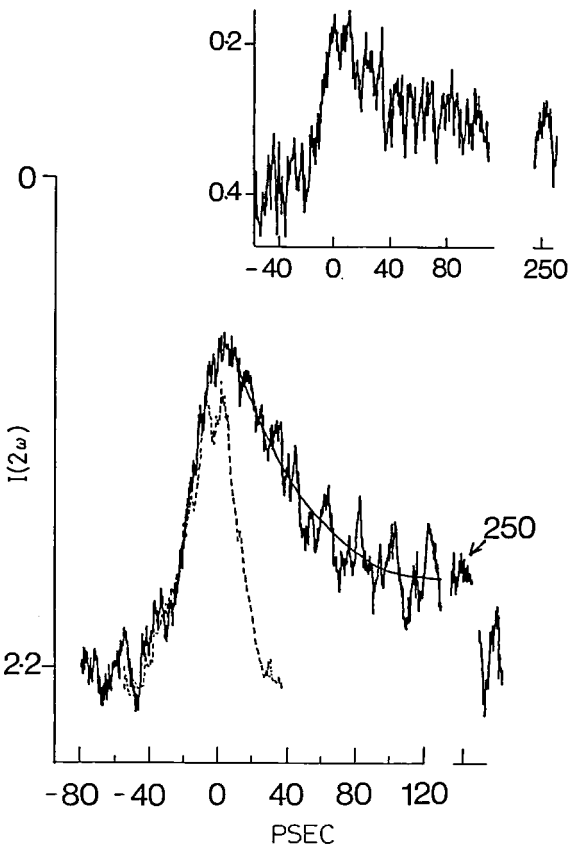

Figure 1

A frequency doubled mode locked Nd: YAG laser (25 psec pulse, 10 mJ, 2Hz) is used in a normal pump and probe configuration. The signal, measured reflexion, is processed by a boxcar and divided by the square of the incident intensity. The square root of the result is output as $I(2\omega)$, where $I(2\omega) \propto N_a\alpha_s^{(2)}$, the product of the adsorbate number density and the molecular hyper-polarizability.

In the simplest case the pump pulse creates two populations on the surface transient (N_T) and ground (N_a-N_T), which have different $\alpha_s^{(2)}$. The probe pulse arriving some time t later will probe the relaxation back to the ground state,

$$I(2\omega, t) = N_0\alpha_{s,G}^{(2)} + N_T(t)\,(\alpha_{s,T}^{(2)} - \alpha_{s,G}^{(2)})$$

so the dynamics $N_T(t)$ can be recorded as a function of probe delay. An example, showing the excited state isomerisation of pyridine 2 on quartz is shown in Figure 1.

References

1) S.R. Meech and K. Yoshihara, submitted to *Chem. Phys. Lett.*
2) Y.R. Shen in "Annual Review of Material Science" **16**, 69 (1986).

III-D-3 Construction of Femtosecond Tunable Dye Laser System

Hiromi OKAMOTO, Yoshihiro TAKAGI, and Keitaro YOSHIHARA

Construction of high power high repetition rate femtosecond tunable dye laser system with excitation by a CW mode-locked YAG laser and amplification with a copper-vapor laser is described in section Special Research Projects.

III–E Solar Energy Conversion by Using Photocatalytic Effects of Semiconductors and Dyes — Decomposition of Water and Application to Organic Synthesis —

Essential roles are played by semiconductors and dyes in the photocatalytic effects to which particular attention has been paid in connection to the direct conversion of solar energy to chemical energy. One of the most important application is the water splitting reaction. Photocatalytic reactions of water with various organic compounds are also interesting not only from the view point of hydrogen production but also from that of the application to organic

synthesis. In order to elucidate the mechanism of these photocatalytic reactions, we need detailed knowledges on the electronic structures of adsorbed molecules, the fundamental processes of photoinduced electron transfer at the semiconductor-liquid interface and catalysis on the surface. Work on the following topics is in progress with the purpose of clarifying the photocatalytic effects of semiconductors and dyes from the view point of solar energy conversion.

III-E-1 Electrochemical Reduction of Carbon Dioxide at Low Temperature on Various Metal Electrodes

Masashi AZUMA, Kazuhito HASHIMOTO, Masahiro HIRAMOTO, Tadayoshi SAKATA, Masahiro WATANABE *(Yamanashi Univ.)*

Electrochemical reduction processes of CO_2 were investigated at around 0°C on various metal electrodes by measuring reduction products after potentiostatic electrolysis.

Table 1 shows current efficiencies for reduction products at around 0°C. These reduction products depended on the electrode materials and the electrolyte temperature. It is reported that CO_2 reduction is not observed and only hydrogen evolution reaction occurs on Ni or Fe metal electrode at room temperature, whereas very efficient CO_2 reduction into CO and HCOOH was observed on Ni electrode in our condition and the total current efficiency exceeded 30%. Moreover it must be noted that CH_4, C_2H_4, C_2H_6 were detected for all metal electrodes used in the present experiments. These high reduction efficiencies were obtained in these conditions probably because the solubility of CO_2 into aqueous solution at low temperature is greater than that at room temperature and the stability of the reduction intermediates are higher so as to promote multi-electron reduction. It was observed also that the ratio of reduction products at low temperature on Cu electrode is quite different from those at room temperature, clearly showing that the adsorption states at these conditions of CO_2 are different from each other.

Table 1. Current efficiencies (%) for CO_2 reduction products at −2.2 V vs. SCE (193°C) in a CO_2-saturated 0.05 M $KHCO_3$ aqueous solution at about 2°C. Both gaseous and liquid products were analyzed by using gas chromatography and liquid chromatography.

Electrode	CH_4	CO	C_2H_4	C_2H_6	HCOOH	H_2	sum
C	0.11		0.0064	0.0070			
Al	0.012		0.00022	0.00040			
Ti	t	13.5	t		5.2	69.4	83
V	0.02	1.3	t		2.6	91.9	96
Cr	0.74	0.49	0.050	0.18	0.15	92.2	94
Mn	1.5	0.34	0.093	0.29	0.03	90.9	93
Fe	0.07	2.2	t		1.1	89.8	93
Co	0.13	0.47	0.0057	0.032	0.85	92.9	94
Ni	0.14	20.5	t		12.9	62.9	96
Cu	24.7	16.5	6.5		3.0	49.3	100
Zn	0.23	9.8	t		19.5	68.1	98
Zr	0.49	0.42	0.021	0.055	t	99.9	101
Nb	0.16	0.46	0.0088	0.042	0.03	97.3	98
Ag	0.042	49.4	0.0085	0.0052	24.3	23.1	97
In	t	3.8	t		72.9	20.0	97
Pt	0.29	1.2	t		5.5	92.6	100
Au	t	16.9	t		10.3	73.4	101

t: trace

III-E-2 Photocatalytic Asymmetric Synthesis of Hydroxy Acid with Asymmetric Catalyst and Powdered Semiconductor Photocatalyst

Hanghein WANG *(Institute of Photographic Chemistry, Beijing)*, **Tadayoshi SAKATA, Masashi AZUMA, Tetsuo OHTA and Hidemasa TAKAYA** *(Kyoto Univ.)*

Asymmetric synthesis of various organic compounds is one of the important subjects in organic chemistry and a remarkable progress has been made these years. It has been demonstrated that BINAP asymmetric catalysts have quite high enantioselectivity to various asymmetric hydrogenations. However most asymmet-

ric reactions investigated so far are mostly dark reactions. As for photochemical asymmetric reactions very few results have been reported. Here we would like to report a clear result of photocatalytic asymmetric synthesis of 2-hydroxy-3-methyl-butyric acid using an organo-metalic asymmetric catalyst, BINAP-Rh (II) complex, and powdered semiconductors such as TiO_2 and CdS.

Table 1 shows one of the results in the case of TiO_2 photocatalyst. As shown in this table, 2-hydroxyl-3-methyl-butyric acid were produced enantioselectively from 3-methyl-2-oxo-butanoic acid in an aqueous methanol solution through photocatalytic hydrogenation with asymmetric catalyst, BINAP-Rhodium (II) complex and semiconductor (CdS and TiO_2) photocatalyst. The highest enantiomeric excess amounts to 60%. The chirality of the products are controlable by changing the chirality of the BINAP catalyst.

Table 1. Asymmetric Synthesis by TiO_2

Run	Photocat.	Asym. cat.	React. time	Product (μmol)	Asym. Ratio	Enantio. Excess (% ee)
1	Pt/TiO_2	Rh(COD)[(R)-binap]ClO4	15h	D-hydroxy acid (25μmol)	78%	56% ee
				L-hydroxy acid (7μmol)	22%	
2	Pt/TiO_2	Rh(COD)[(S)-binap]ClO4	15h	D-hydroxy acid (15μmol)	20%	60% ee
				L-hydroxy acid (60μmol)	80%	
3	TiO_2	——	5h	D-hydroxy acid (87μmol)	50%	0% ee
				L-hydroxy acid (87μmol)	50%	

TiO_2: Furuuchi, rutile
Pt: TiO_2=3:100 mol%
Hydroxy acid: 2hydroxy-3methyl-butyric acid

III-E-3 Ultramicrostructured Photoelectrode System Composed of TiO_2 Single Crystal, Layered SiO_2 and Pt Thin Film

Masahiro HIRAMOTO, Kazuhito HASHIMOTO and Tadayoshi SAKATA

The ultramicrostructured photoelectrode system composed of TiO_2 single crystal, SiO_2 and Pt thin films was prepared by exposing the vertical section of the layered SiO_2 and Pt films. Distance between semiconductor and metal electrodes, *i.e.*, thickness of SiO_2 layer is very small, 140 nm. Under various gas atmosphere, this microstructured electrode shows a photoresponse. For example, Figure 1 shows the photocurrent (i)- voltage (U) curves under 19 Torr H_2O vapor. Under irradiation with UV light, stable photocurrent was observed. Under vacuum, no photocurrent was detected. The photocurrent depends strongly on the vapor pressure. Various gases such as ammonia, ethanol and acetone also give a photocurrent. Moreover the vapor pressure dependence varies with a kind of vapor. These results clearly show that the adsorbed gases are directly photodecomposed on the electrode system. This is due to very small distance between counter and working electrodes. Moreover, any kind of ion can serve as a charge carrier. This is one of the most important characteristics of the present ultramicrostructured electrode compared to the solid electrolyte in which the type of charge carrier ion is restricted. This ultramicrostructured electrode system can be used for gas-phase electrochemical reactions. Moreover, low temperature photoelectrochemistry becomes possible.

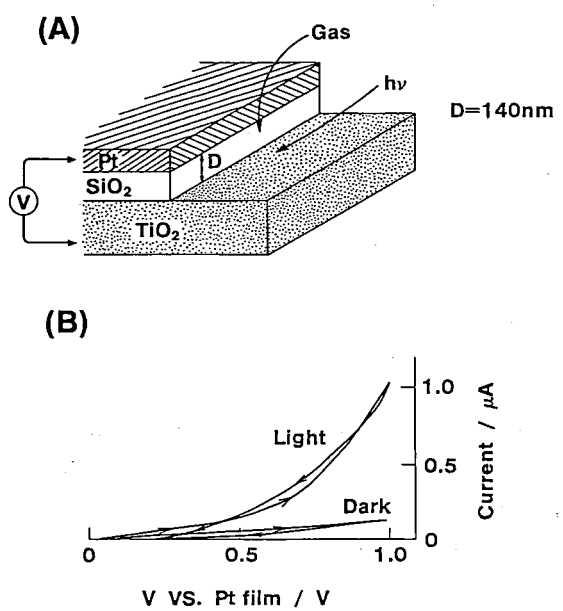

Figure 1.
(A) Ultramicrostructured electrode system prepared from the vertical section of alternating layers of metal and insulator. In this work one metal was replaced by semiconductor (TiO_2). (B) Photocurrent (i)- voltage (U) curves of $TiO_2/SiO_2/Pt$ microstructured electrode under water vapor (19 Torr).

III-E-4 Photovoltage Transient Signal at Semiconductor Electrolyte Interface

Hasuck KIM *(Seoul National Univ. Korea)*, **Kazuhito HASHIMOTO and Tadayoshi SAKATA**

Although much progress has been made in recent years in understanding the events which occur in photoelectrochemical cells, a well established mechanism about the interfacial charge transfer is still needed. In this regard, the fast transient voltage or current measurement was carried out to understand the dynamic properties involved in the photo-assisted processes. Photovoltage transients were obtained with nano- or pico-second laser pulses. It was found that the slow part in the rise of photo-transient is dependent on the concentration of electrolyte. Effect of the nature of electrolyte, concentration as well as different electrolyte was examined. The rise becomes very slow with decreasing the concentration of electrolyte. The effect was very significant and cannot be explained by normal photovoltage sources such as semiconductor space charge layer or electrical double layer at the interface. Since the concentration of the electrolyte exhibited the most significant changes in transient signal, it's behavior was explained by the movement of ions in the diffuse double layer near the electrode. A simple model which can explain well this behavior is proposed. One of the results obtained by this model is shown in Table 1.

Table 1. Comparison of experimental values with theoretical one based on a diffusion layer model

PLOTS	ELECTRODE	Experimental rate (sec^{-1}) KI soln.	KCl soln.	Theoretical rate (sec^{-1})
	InP	1.08×10^{8} (7.66×10^{7})	2.07×10^{8}	
$1/\sqrt{\tau}$ vs C_d	TiO_2	3.4×10^{7} (3.2×10^{7})	1.06×10^{8}	5.7×10^{8}
	p-n Si	8.5×10^{7}	1.89×10^{8}	
C_d vs $\sqrt{C^*}$		535 (ϕ_0=78mv) 608 (ϕ_0=84mv)	167	228zcosh (19.5ϕ_0)
	InP	3.56×10^{9}	1.46×10^{9}	1.68×10^{10}
$1/\tau$ vs C^*	TiO_2	4.1×10^{8}	$3.0-3.7\times10^{8}$	
	p-n Si	2.37×10^{9}	1.15×10^{9}	

τ : rise time of slow transient potential
C_d : Capacitance of diffuse double layer
C^* : Concentration of electrolyte
ϕ_0 : potential of diffuse double layer

III-E-5 Photoluminescence Quenching of Single Crystalline CdS Electrode

Masahiro HIRAMOTO, Kazuhito HASHIMOTO and Tadayoshi SAKATA

Two kinds of emissions for a single crystalline CdS were observed. One is the red emission around 730 nm which is essentially the same emision as the red emission from CdS particles deposited on porous Vycor glass (CdS/PVG).[1] The other is so called "green emission" at 510 nm which is not observed for CdS/PVG. Both red and green emissions of the single crystalline CdS electrode, which is kept at certain potential, are efficiently quenched by Fe^{3+}. Without electron acceptors, the intensity of both emissions depends strongly on the potential. When the potential becomes negative, the intensities of both emission become stronger without changing the spectral shape. However, the addition of the electron acceptor such as benzoquinone, methylviologen and Fe^{3+} causes further drastic quenching of the both emissions at any potentials from −1.05 V to −0.6 V vs SCE as shown in Figure 1. Recently, Ferrer *et al.*[2] and Uchihara *et al.*[3] reported that photoluminescence quenching of CdS electrode by anodic polarization is presumably due to

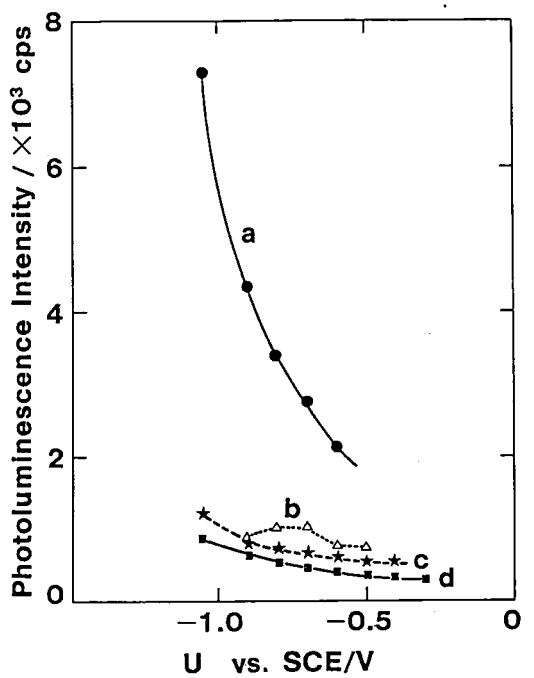

Figure 1. Electrode potential vs. red emission intensity at 730 nm of the single crystalline CdS in the solution without electron acceptor (a), with MV^{2+} (b), benzoquinone (10^{-3}M) (c), and Fe^{3+} (10^{-2}M) (d).

the electric field effect. However, the present results clearly show that the interfacial electron transfer also plays an important role in the photoluminescence quenching.

References

1) M. Hiramoto, K. Hashimoto, and T. Sakata, *Chem. Phys. Lett.*, **133**, 440 (1987).
2) I.J. Ferrer and P. Salvador, *Chem. Phys. Lett.*, **142**, 399 (1987).
3) T. Uchihara, M. Matsumura, and H. Tsubomura, *J. Phys. Chem.*, submitted.

III-E-6 Photo-induced Electron Transfer from Adsorbed Rhodamine B to Oxide Semiconductor Substrates *in Vacuo*: Semiconductor Dependence

Kazuhito HASHIMOTO, Masahiro HIRAMOTO and Tadayoshi SAKATA

[*Chem. Phys. Lett.*, **148**, 215 (1988)]

Adsorbate-substrate electron transfer (ET) relates to fundamentally important problem of how the discrete levels of molecules and the bulk continuous or surface localized levels of substrate interact each other. However, very few systematic studies on the dynamics of this ET process have been done, although ET among molecules in homogeneous solution has been studied very well and great advances have been made both theoretically and experimentally.

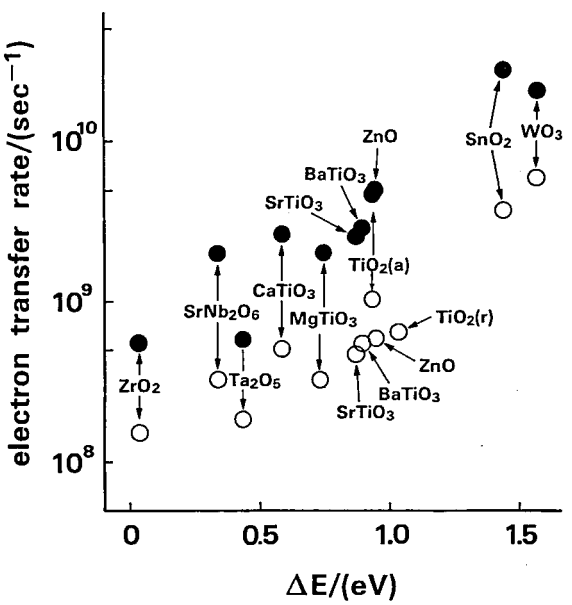

Figure 1. Dependence of the ET rate constant from Rh B to oxide S.C. on the energy difference ΔE.
●: fast decay component ($k_{et,1}$)
○: slow decay component ($k_{et,2}$)

Here we studied the ET process by measuring luminescence decays of rhodamine B (Rh B) adsorbed on various kinds of oxide semiconductor (S.C.) powders *in vacuo*. The decay curves depended strongly on the substrates. By comparing the decay rates with those on insulator substrates, the electron transfer (ET) rates were determined. The ET rates increased with the energy difference of the excited state of Rh B and the flat-band potential of the S.C. It was shown clearly that the energy gap dependence for molecule to semiconductor surface ET is quite different from that observed in molecular systems in homogeneous solution. It is suggested that the electron acceptor levels in S.C. are continuous levels in the conduction band, and that the distribution of the continuous levels is related to the ET rate.

III-E-7 Energy Gap Law of Electron Transfer Rate on Semiconductor Surfaces

Tadayoshi SAKATA, Masahiro HIRAMOTO and Kazuhito HASHIMOTO

In investigation of dynamical ET (electron transfer) processes in the dye sentitized semiconductor systems, we have found a new type of energy gap dependence of ET rates:[1),2)] the ET rate increases with increasing energy gap, ΔE. Here ΔE is defined as the difference between the energy level of the excited dye and the bottom of the conduction band. This energy gap dependence is quite different from that for molecular systems, where the inverted region is observed. This anomolous behavior is explained well by ET from the excited dye to the conduction band of the semiconductors. In such a case, ET rate is expressed by the following general equation.

$$k_{et} = (2\pi/\hbar)\, v^2 \int D_{-}(E)\, \varrho(E)\, dE \qquad (1)$$

Here $D_{-}(E)$ and $\varrho(E)$ represent the distribution function of electrons in the excitated dye and the state density of the conduction band of the semiconductor, respectively. After reasonable approxmations, the following relation is obtained.

$$k_{et} = (2\pi/\hbar)\, v^2 \varrho(\Delta E - \lambda) \qquad (2)$$

This theory explains well the experimental results as shown in Figure 1.

References

1) K. Hashimoto, M. Hiramoto, A.B.P. Lever, and T. Sakata, *J. Phys. Chem.*, **92**, 1016 (1988).
2) K. Hashimoto, M. Hiramoto and T. Sakata, *Chem. Phys. Lett.*, **148**, 215 (1988).

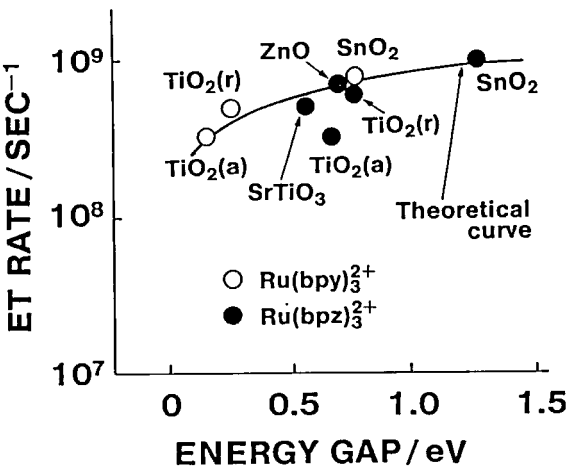

Figure 1. The energy gap dependence of electron transfer rate from the excited Ru complexes to various oxide semiconductors. The solid line represents the theoretical curve calcurated from eq. (2).

III-E-8 Temperature Independent Electron-Transfer: Rhodamine B/Oxide Semiconductor Dye-Sensitization System

Kazuhito HASHIMOTO, Masahiro HIRAMOTO, and Tadayoshi SAKATA

[*J. Phys. Chem.* **92**, 4272 (1988)]

The fluorescence spectrum and decay of rhodamine B (Rh B) adsorbed on insulator (SiO_2) and oxide semiconductors (ZrO_2, TiO_2 (anatase)) were measured *in vacuo* at temperatures in the range 4 to 300 K. The effect of temperature on both the intensity and decay rates of the fluorescence is very weak, indicating that the electron-transfer (ET) from Rh B in the excited state to those semiconductors (S.C.) is almost an activationless process. The ET rate can be expressed by two terms. One is an electron-exchange matrix element and the other is a Franck-Condon term. The latter is responsible for the temperature dependence. According to the conventional ET theory which describes ET between discrete-discrete levels, a negative activation energy might appear when $-\Delta G^0$ is equal to the reorganization energy. Therefore, almost activationless ET in the present system cannot be explained with the discrete-discrete ET theory. The observation leads to the conclusion that continuous levels in the conduction band of the S.C. serve as the electron acceptor state. The energy level density distribution of the S.C. must be taken into account to explain the temperature dependence.

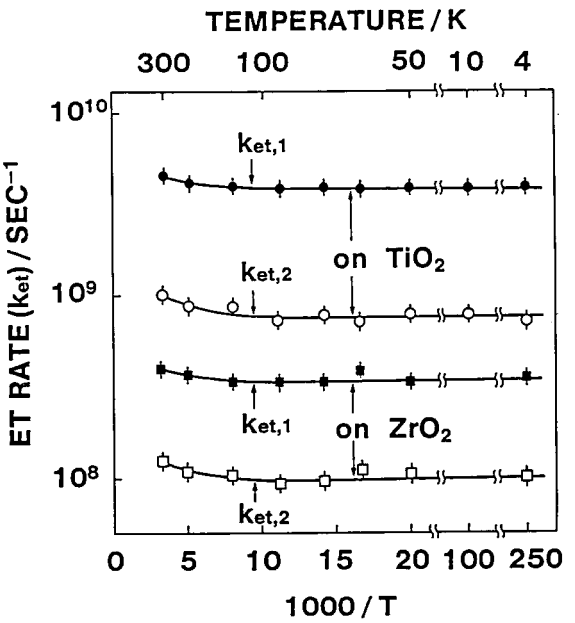

Figure 1. Temperature dependence of the electron transfer rates determined from the fluorescence decay rates.

III-E-9 A New Origin of Activation Energy of Electron Transfer on Solid Surfaces

Tadayoshi SAKATA, Kazuhito HASHIMOTO and Masahiro HIRAMOTO

In the case of ET between molecule and the conduction band of a semiconductor temperature-independent ET is expected. Recently, we reported temperature-independent ET in the case of RhB/TiO_2 and RhB/ZrO.[1)] Many experimental data are now being accumulated in this laboratory. On the other hand, an ET process with an activation energy has also been observed in several dye sensitization systems,

even though the activation energy is generally very small, in the order of 10^{-2}eV. The existence of activation process looks strange, because the excited energy level is enough higher than the bottom of the conduction band even in those cases. Even in the temperature independent ET cases careful examination reveals a very small increase of ET rate above 150K. These results suggest that there is another origin of activation energy on solid surface. Since the FC term disappears on the surface, the only possibility is the exchange energy term. Since the exchange energy term is attenuated exponentially with increasing the distance between the molecule and the surface, a thermal vibration of the adsorbed molecule can give an influence on the magnitude of the exchange energy. A simple quantum mechanical model can explain well the temperature dependence. An example is shown in Figure 1.

Reference

1) K. Hashimoto, M. Hiramoto and T. Sakata, *J. Phys. Chem.* **92**, 4272 (1988).

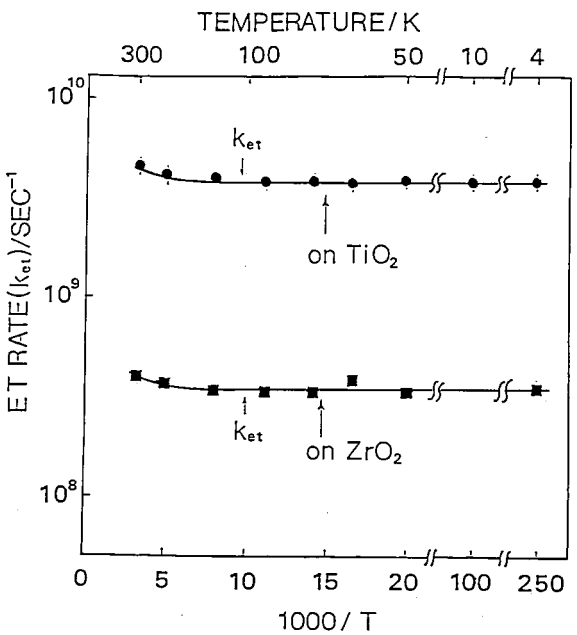

Figure 1. Temperature dependence of electron transfer rate from Rhodamine B to semiconductors (TiO_2 and ZrO_2). The solid lines represent theoretical curves.

III-E-10 Pico- and Nano-second Time-Resolved Resonance Raman Scattering of Photochemical Intermediate on Semiconductor Surface *in Vacuo*

Kazuhito HASHIMOTO, Patrick J. CARROLLE *(AT & T Bell Labs.)*, **and Louis E. BRUS** *(AT & T Bell Labs.)*

Time-resolved resonance Raman spectra of a photochemical intermediate on semiconductor surface *in vacuo*, semioxidized eosin Y (E^+) on dried TiO_2 powder, were observed in pico- and nano-second time scales by the irradiation of adsorbed eosin Y whose surface coverage is about one seventieth of a monolayer. E^+ is formed in two different time regions, less than several tens of pico-seconds, and several nano-seconds. The same was observed for eosin Y adsorbed on colloidal TiO_2. It is considered that the slower process of E^+ formation corresponds to the electron transfer from photoexcited eosin Y to the substrate TiO_2. The back electron-transfer process from TiO_2 to produce E^+ is slower than 20 ns. By the comparison of the resonance Raman spectra of E^+ on dried powder to those on wet and colloidal TiO_2, it is suggested that the dye molecules are still semi-solvated on the dried powder by physisorbed water. Actually long-time evacuation at 82°C changes the resonance Raman spectra drastically and only very broad peaks were detected.

The Raman scattering measurement of adsorbate on dried surface is experimentally very difficult because the adsorbate is easily decomposed by an intense laser light. To our knowledge, this is the first study of the time-resolved resonance Raman scattering of the reaction intermediate adsorbed on *dried* solid surface.

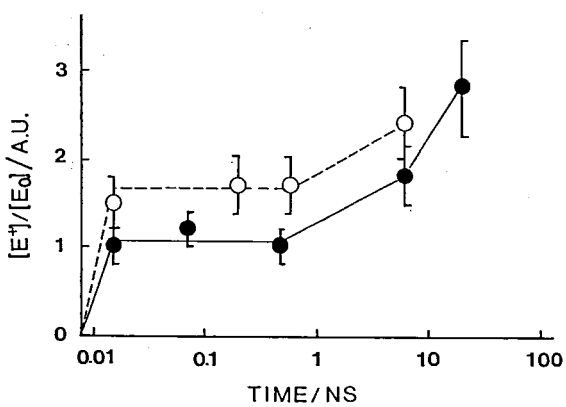

Figure 1. Relative Raman intensities of semioxidized eosin Y and eosin Y ($[E^+]/[E_0]$) as a function of delay time. Data at 15 ps and 6 ns were obtained by high fluence single-pulse experiments with pico- and nano-sec lasers, respectively. Other data were obtained by two-pulse experiments. The values of $[E^+]/[E_0]$ are saturated under these conditions. See the text.
The value at 6 ps for dry system is normalized to unity.
●: dried TiO_2 system.
○: colloidal TiO_2 system.
The lines are drawn to guide the eye.

III-E-11 Study of Electron-Transfer Between Molecule and Semiconductor by Time-Resolved Resonance Raman Scattering and Fluorescence Measurements.

Kazuhito HASHIMOTO, Patrick J. CARROLLE *(AT & T Bell Labs)*, **Tadayoshi SAKATA, and Louis E. BRUS** *(AT & T Bell Labs)*

Pico- and nano-second time-resolved resonance Raman spectra of adsorbed, semioxidized eosin Y (E^+) *in vacuo* have been obtained following excitation of adsorbed eosin Y (E_0) on *fourteen* kinds of metal oxide powders. The transient Raman intensity of E^+ on the surfaces changes depending on the delay time after the excitation of E_0. It also depends strongly on the substrate. The fluorescence decay from photoexcited eosin Y (E^*) was also measured. From those observations, two different energy-gap dependences of ET between adsorbed molecule and substrate semiconductor *in vacuo* are obtained. One is the energy-gap dependence of the photo-induced ET from eosin Y in the excited-state to semiconductor. The dependence is quite different from that for molecular system. The ET rate increases with a larger energy-gap between energy level of eosin Y in the excited-state and the band edge of conduction band of semiconductor, indicating that the density of energy levels in conduction band plays an important role in ET rate. The other is the energy-gap dependence of the dark ET from semiconductor to semioxidized eosin Y. The ET rate decreases with a larger energy-gap. This process is presumably treated as the discrete-discrete levels ET, so the energy-gap dependence is the same as molecular system. The energy-gap studied is larger than reorganization energy. Therefore it is considered that the inverted region of the ET is observed.

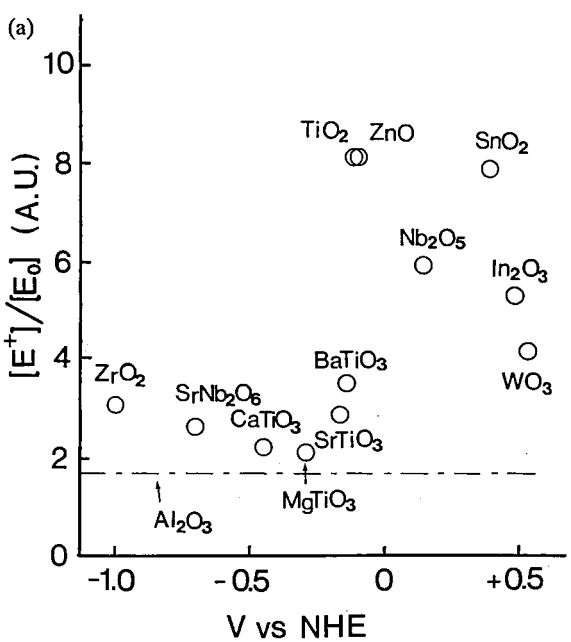

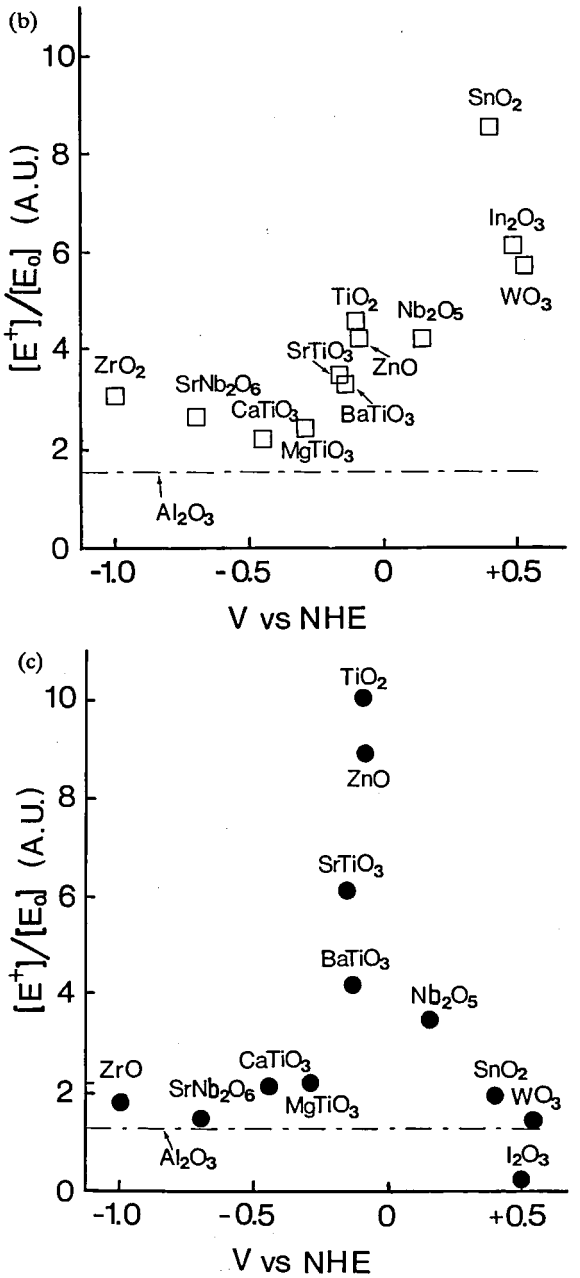

Figure 1. Plot of the Raman intensity ratio R of semioxidized eosin Y (1456 cm^{-1} and 1591 cm^{-1}) and eosin Y (1515 cm^{-1}) as a function of energy-gap between excited state of eosin Y and conduction band edge of semiconductors. Averaged values of those two lines were plotted. The lines represent the values for insulator (Al_2O_3) as a substrate.
(a) 20-ps high flux one-pulse (447 nm, 1 mJ/pulse).
(b) 10-ns high flux one pulse (447 nm, 1 mJ/pulse).
(c) Two-pulse with 20 ns time delay (532 nm (3 mJ/pulse) followed 447 nm (0.15 mJ/pulse)).

III–F Dynamical Processes in Electronically and/or Vibrationally Excited Molecules

III-F-1 Construction of Apparatus for Investigating Laser-Induced Half-Reaction in van der Waals Complexes

Hiroshi OHOYAMA, Masao TAKAYANAGI, Teruhiko NISHIYA and Ichiro HANAZAKI

An apparatus for the title purpose was constructed. The system consists of conventional pulsed valve, reaction chamber, a quadrupole mass filter, a gated photon counting system, timing circuit, and two laser systems. This apparatus was applied to N_2O·HI system. N_2O·HI was generated by supersonic expansion of He containing 2.6% HI and 4.4% N_2O through a pulsed valve operated at 10Hz. The typical duration of the gas pulse was 300μs. The cluster size distribution in the free jet and the beam profile were measured 50cm downstream using the quadrupole mass spectrometer, which was mounted in a separated chamber differentially pumped by a liquid nitrogen trapped diffusion pump. 266nm light from the fourth harmonic of YAG laser (Quanta-Ray DCR-2A, HG-2) was used to induce the half-reaction. Resulting OH was probed by LIF. The probe light was provided by frequency doubled tunable dye laser (Quantel TDL-50, UVT-3) pumped by YAG laser (Quantel YG571C-10). The fluorescence of OH was collected by a concave mirror and lens system, and focused onto the photomultipiler (HAMAMATSU R943-02). The portion of OH fluorescence signal arriving between 150–800 ns after the probe laser excitation was counted by the gated-photon counting method. The timing for two laser system, counter gate and pulsed valve driver were controlled by the circuit with a maximum jitter of 5ns. To normalize the LIF signal, the intensity of probe laser was monitored with a photodiode, whose output was converted to a frequency, summed in an ORTEC counter and stored in a microcomputer. The LIF spectrum of OH v=0 state is shown in Figure 1.

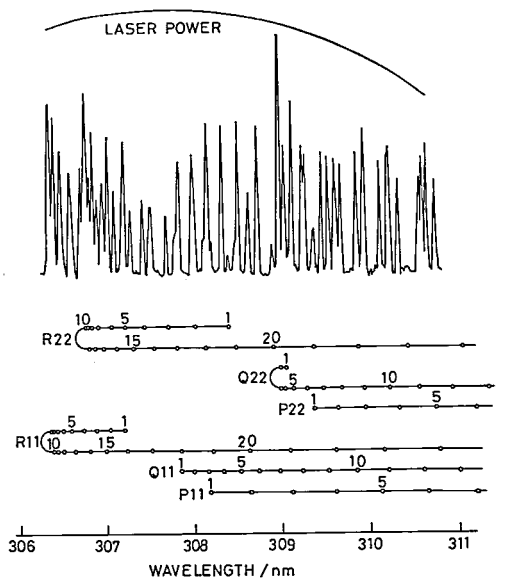

Figure 1. OH $A^2\Sigma$–$X^2\Sigma$(0,0) LIF spectra obtained from the half reaction in HI·N_2O complex.

III-F-2 Orientation Selected Chemical Reaction Using van der Waals Molecules

Hiroshi OHOYAMA, Masao TAKAYANAGI, Teruhiko NISHIYA and Ichiro HANAZAKI

By laser-induced fluorescence, the rotational, spin-orbit, and Λ-doublet population was determined for OH produced from the reaction H + N_2O via a reactant pair I···H·N_2O induced from the 266 nm excitation of complex HI·N_2O which has two types of geometric isomers. The results were compared with the bulb experiment. The rotational population of OH derived from the reaction via complex differs from that obtained under bulb condition. Figure 1 shows the Boltzmann plot for the R-branch rotational distribution arising from the two spin-orbit components. Except for an additional distribution with low temperature of 80K for the F_1 state, the distributions under both conditions are well represented by two Boltzmann distributions. They are, however, mixed with different ratio. This bimodality can be attributed to the different reaction mechanisms predicted by theoretical calculation. The

mixing ratio of two reaction mechanisms depends on the population ratio of two geometric isomers. The Q-branch rotational distribution exhibits little difference between jet and bulb conditions, suggesting Π^- was generated via similar intermediate with poor memory for entrance channel specificity. For both bulb and jet conditions, the population ratio for Λ doublet (Π^+/Π^-) are larger than unity, indicating preference for Π^+ formation. This implies the importance of a planar intermediate. The ratio for bulb experiment is slightly larger than that for jet experiment.

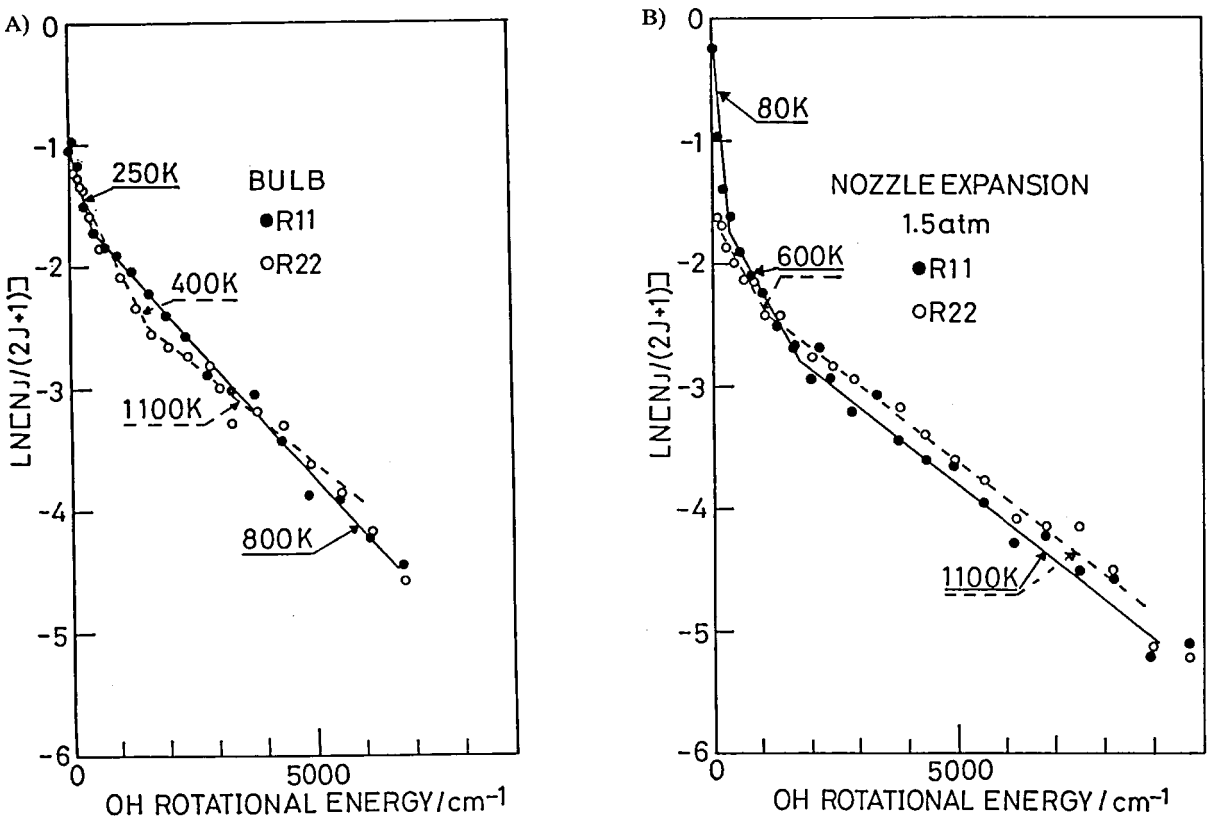

Figure 1. Boltzmann plots for the R-branch rotational distribution of OH in the v=0 state, for A) bulb, and B) jet conditions. The bulb and jet cases are normalized separately. N_J is the population of the rotational level J, and (2J+1) the rotational degeneracy.

III-F-3 Infrared Photodissociation Spectra of Benzene-2,2,2-trifluoroethanol Complex

Masao TAKAYANAGI and Ichiro HANAZAKI

The infrared photodissociation spectra of benezene-2,2,2-trifluoroethanol (TFE) complex were measured using a cw molecular beam apparatus. The photodissociation was monitored by observing the attenuation of the mass signal due to the complex. In order to investigate the excitation mode dependence of the infrared photodissociation, three vibrational modes of the complex (*i.e.* a band at 1040 cm^{-1} of benzene, and two bands at 945 cm^{-1} and 1080 cm^{-1} of TFE) were excited by a CO_2 laser. As far as we know, there have been only a few examples of measuring photodissociation spectra of hetero dimers by exciting vibrational modes of each constituent.

The laser fluence dependence of the photodissociation was examined. For all three vibrational modes, the photodissociation yield at fixed frequency shows second order dependence on the laser fluence: the dissociation occurred after two-photon absorption and the dissociation energy is below 1890 cm^{-1}.

The bands at 945 cm^{-1} and 1040 cm^{-1} show

Lorentzian profiles with linewidths (FWHM) about 13 cm^{-1} and 17 cm^{-1}, respectively. Although the dissociation yield for the band at 1080 cm^{-1} was so small that we cannot obtain the clear profile of the band, it spreaded over about 20 cm^{-1}. If these linewidths are assumed to be homogeneous, the lifetimes of vibrational relaxation or predissociation obtained from the widths are about 0.4 ps.

In this measurement, we could not find clear mode dependence of the photodissociation.

III-F-4 Fluorescence Dip Spectra of van der Waals Molecules Containing Benzonitrile

Masao TAKAYANAGI and Ichiro HANAZAKI

Fluorescence dip spectra of benzonitrile (C_6H_5CN) and some van der Waals complexes containing benzonitrile [$C_6H_5CN{\cdot}H_2O$, $C_6H_5CN{\cdot}(H_2O)_2$ and $C_6H_5CN{\cdot}Ar$] were measured using a pulsed molecular beam apparatus and a Nd:YAG-pumped dye laser system. The molecules are excited by the pump light whose frequency was fixed to the 0–0 transition of the molecule. Fluorescence dip spectra were obtained by measuring the decrease of the fluorescence from excited state induced by the scanning dump light. With this method, the spectra of each species can be obtained separately, for each species has different frequency of the 0–0 transition.

The depth and width of the fluorescence dip spectra are expected to contain the information on the relaxation of the excited states. Figure 1 shows the bands at 1004 cm^{-1} and 1028 cm^{-1} observed in the fluorescence dip spectra of benzonitrile monomer and three complexes. For all species, the widths (FWHM) of the band at 1004 cm^{-1} is 3–4 cm^{-1}, which is presumably inhomogeneous broadening due to the rotational contour. The corresponding lifetime (~1.5 ps) gives therefore a lower limit for the lifetime of the vibrational relaxation or vibrational predissociation. Complex formation and/or predissociation of the complexes cause little effect on the linewidth.

This time we measured spectra only in the region around 1000 cm^{-1}. We are now trying to measure fluorescence dip spectra in the higher energy region to examine excitation energy dependence.

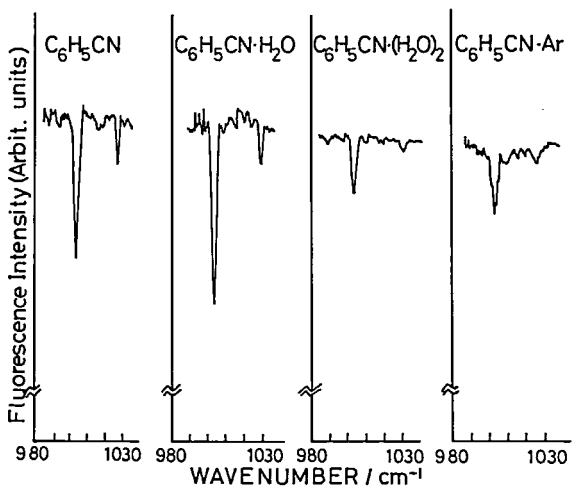

Figure 1. Fluorescence dip spectra of benzonitrile monomer and three van der Waals complexes (not normalized).

III–G Mass Spectrometrical Study of Molecular Association in Aqueous Solutions through Adiabatic Expansion and Fragmentation of Liquid Jets

In the well-known model of liquid water, it was assumed that water consists of a continuous distribution of all possible cluster sizes in equilibrium. There will be present isolated molecules, pairs of molecules close together forming dimers, groups of three molecules (trimers), four molecules (tetramer), and so on. These clusters are in mutual equilibrium associating and dissociating. In binary aqueous solutions, formation of hydrate clusters is expected to play very important role in the physical and chemical properties of the solutions, such as solubility, heat capacity, surface tension, and so forth. The understanding of such properties of aqueous solutions in terms of "fragments" is highly necessary for analyzing the real situation since measurement of overall average properties of a solution does not provide realistic information on the local structure which determines the various properties of

liquid. Adiabatic expansion of a droplet of liquid in vacuum causes its immediate fragmentation by dissociating molecules which are weakly bound to hydrogen-bonded clusters or rotationally excited due to the hydrogen-hydrogen repulsive force field at higher temperatures. Inevitably this process is accompanied with evaporation of unstable surface molecules that causes substantial cooling of the fragment clusters. Mass spectroscopic analysis of the isolated clusters makes it possible to study molecular association in aqueous solution.

III-G-1 Molecular Association in Ethanol-Water Mixtures Studied by Mass Spectrometric Analysis of Clusters.

Nobuyuki NISHI, Kunimasa KOGA†, Chikako OHSHIMA†, Kazunori YAMAMOTO, Umpei NAGASHIMA, and Kenzo NAGAMI† *(†Suntory Research Center)*

[*J. Am. Chem. Soc.* **110**, 5246 (1988)]

Molecular association in ethanol-water solutions with various ethanol concentrations was studied mass-spectrometrically. The spectral pattern of the clusters changed sensitively depending on the ethanol concentration region. In the region of x (ethanol mole fraction) < 0.04, ethanol monomer and polymer signals are followed by long water sequences of hydrated species $(C_2H_5OH)_m(H_2O)_n$. At low temperatures, ethanol-ethanol hydrogen bond formation becomes predominant and water molecules tend to participate in hydrophobic hydration of the ethyl groups of the polymer chains. This water shell was not seen for the mixtures with $x > 0.04$. At $x = 0.08$, the growth of ethanol polymers is almost saturated, and in the region of $0.08 \leq x \leq 0.5$ the spectral pattern showed little change although the polymer intensity was strongest for the solution with $x = 0.42$ at 35°C. In ethanol rich solutions, the intensity of the polymers becomes weaker with decreasing water content. Neat ethanol did not produce large polymers any more. The observed changes of the cluster spectra coincided nicely with the reported NMR data and thermodynamic properties of this system. The present study makes the nature of ethanol-water mixtures clearly understandable at a molecular level: (1) the hydrophobic hydration of ethanol is so strong that pure water clusters are not detectable at $x > 0.04$ and (2) ethanol molecules tend to form ethanol polymers with surrounding water molecules.

III-G-2 Formaldehyde in Water

Nobuyuki NISHI and Kazunori YAMAMOTO

Formaldehyde shows UV absorption at 300 nm in gas phase, that disappears or becomes weaker in aqueous solvents. From proton magnetic resonance measurements and Raman spectra, the reason has been attributed to the presence of the hydration reaction equilibrium: $H_2CO + H_2O \rightleftarrows H_2C(OH)_2$. (1) Gruen and McTigue obtained an ethalpy change (ΔH) of 5.7 kcal/mol for the above reaction from the sophisticated van't Hoff plots of the absorption intensity in 3.4~13.3M solutions.[1] Adiabatic expansion of aqueous formaldehyde solutions isolates both H_2CO and $H_2C(OH)_2$ in vacuum. The latter species forms relatively strong hydrated clusters, while the former one (H_2CO) is only weakly coordinated by water molecules in the solution. This is seen by a collisional desolvation procedure. On dehydration of the hydrated clusters, the intensity of H_2COOH^+ at mass 47 greatly increases in contrast with that of H_2CO^+ and HCO^+. Ionization of $H_2C(OH)_2$ produces H_2COOH^+ and H_2COH^+. The spectra of the solution fragments shows a hydration sequence of $H^+(H_2C(OH)_2)(H_2O)_n$. At 10 eV ionization energy, the intensities of these solvated ions decreases, and H_2CO^+ and $H_2C(OH)_2$ are the main signals. The slope of the van't Hoff plots of the ion intensity ratios $[H_2COOH^+]/[H_2CO^+]$ and $[H_2COH^+]/[H_2CO^+]$ provides the enthalpy change of the reaction equilibrium (1). The present analysis gives 5.7 ± 0.5 kcal/mol. This value is exactly the same as that reported by Gruen and McTigue,[1] although this value was once claimed to be uncertain.

Reference

1) L.C. Gruen and P.T. McTigue, *J. Chem. Soc.* 5217 (1963).

III-G-3 Formaldehyde in "Formalin" Solution

Nobuyuki NISHI and Kazunori YAMAMOTO

Commercial "formalin" solution contains formaldehyde, methanol and water in the molar ratio of 4:1:10. Methanol is added to prevent polymerization of formaldehyde which produces polyoxymethylene, H-(O-CH_2-)$_n$-OH. Fragmentation of this solution to molecules and clusters in vacuum isolated the main monomer species of H_2O, H_2CO, $H_2C(OH)_2$, CH_3OH, and $H_2COH(OCH_3)$ in order of increasing mass number. The last compound is a hemiacetal, although in literature it is written that hemiacetals are generally too unstable to be isolated. Nevertheless, an aqueous solution of formaldehyde mixed with alcohol contains an equilibrium amount of the hemiacetal:

$$H_2CO + CH_3OH \rightleftarrows HOCH_2(OCH_3). \quad (1)$$

On ionization the hemiacetal dissociates a hydrogen atom leaving an $H_2CO(OCH_3)^+$ ion (mass 61). Figure 1 shows a cluster mass spectrum of a commercial formalin solution at 60°C. No pure water or hydrate clusters is seen at this temperature. At mass 77, the dehydrogenated ion of the smallest polyoxymethylene, HO-CH_2-O-CH_2-OH (mass 78), appears as well as that of HO-CH_2-O-CH_2-OCH_3 (mass 92). The strongest peak in the high mass region ($\geq$ 100) is seen at mass 125, which is the protonated ion of the hemiacetal dimer, $H^+(HOCH_2(OCH_3))_2$. The protonated hemiacetal trimer, $H^+(HOCH_2(OCH_3))_3$, appeared at mass 187. Main cluster signals in the mass spectrum are assigned to the mixed clusters:

$$H^+\{HOCH_2(OCH_3)\}_m\{H_2C(OH)_2\}_n\{H_2CO\}_p,$$

where $m \geq 1$ and $n+p \geq 1$. Insertion of hemiacetal in the mixed clusters may prevent the growth of polyoxymethylene chains in the solution.

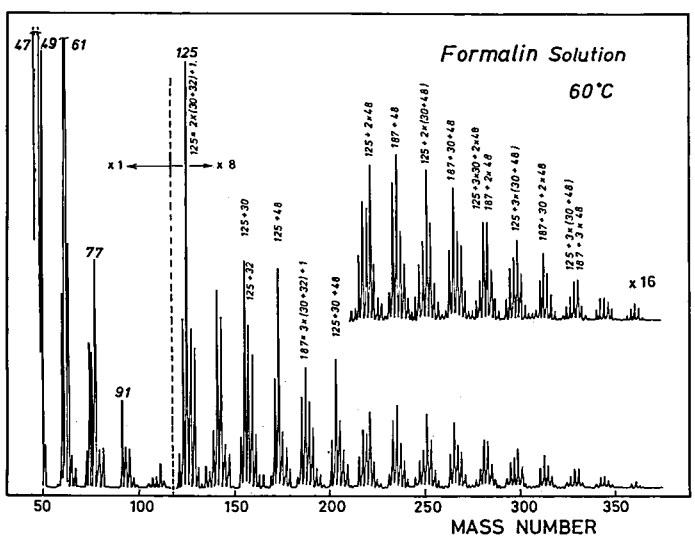

Figure 1. Mass spectrum of cluster fragments of "formalin" solution at 60°C.

III-G-4 Primary Process of Formaldehyde Oligomerization in Water

Nobuyuki NISHI and Kazunori YAMAMOTO

Formaldehyde shows very efficient oligomerization and polymerization in gas phase or on condensation in a nitrogen cooled trap from gaseous state. The products were attributed to polyoxymethylene, (H-(O-CH_2)$_n$-OH, and cyclic polymers such as trioxane, $\ulcorner(O\text{-}CH_2)_3\urcorner$. In diluted aqueous solutions, this oligomerization is strongly inhibited by the formation of dioxymethylene, $H_2C(OH)_2$. However, since this hydration reaction is an equilibrium process, increase of formaldehyde concentration enhances dehydration yielding free formaldehyde species. Thus the concentrated solution with a solute to water ratio of 1:2.5 (the concentration in "formalin") contains oligomer species particularly

at high temperatures. Figure 1 shows the temperature dependence of the cluster mass spectrum taken by the fragmentation through adiabatic expansion of the solution. The spectrum taken at 60°C showed a regularly spaced structure with a mass deference of 6. This is just because the main structure of the spectrum is composed of the hydration sequences: $H^+(H_2C(OH_2))(H_2O)_n$;mass=49 + nx18, $H^+(H\text{-}(O\text{-}CH_2)_2\text{-}OH)(H_2O)_n$;mass=79 + nx18, and $H^+(H\text{-}(O\text{-}CH_2)_3\text{-}OH)(H_2O)_n$;mass=109 + nx18. At 90°C, oligomerization became dominant in destroying hydration networks. The main component in the lower spectrum is $H^+[H\text{-}\{O(H_2O)\text{-}CH_2\text{-}\}_nOH - m\cdot H_2O]$, where m=1~3. It is found that each oxymethylene unit of the oligomers in aqueous solution is strongly associated with a water molecule. Relative abundance of such oligomers in the concentrated solution was less than 5%.

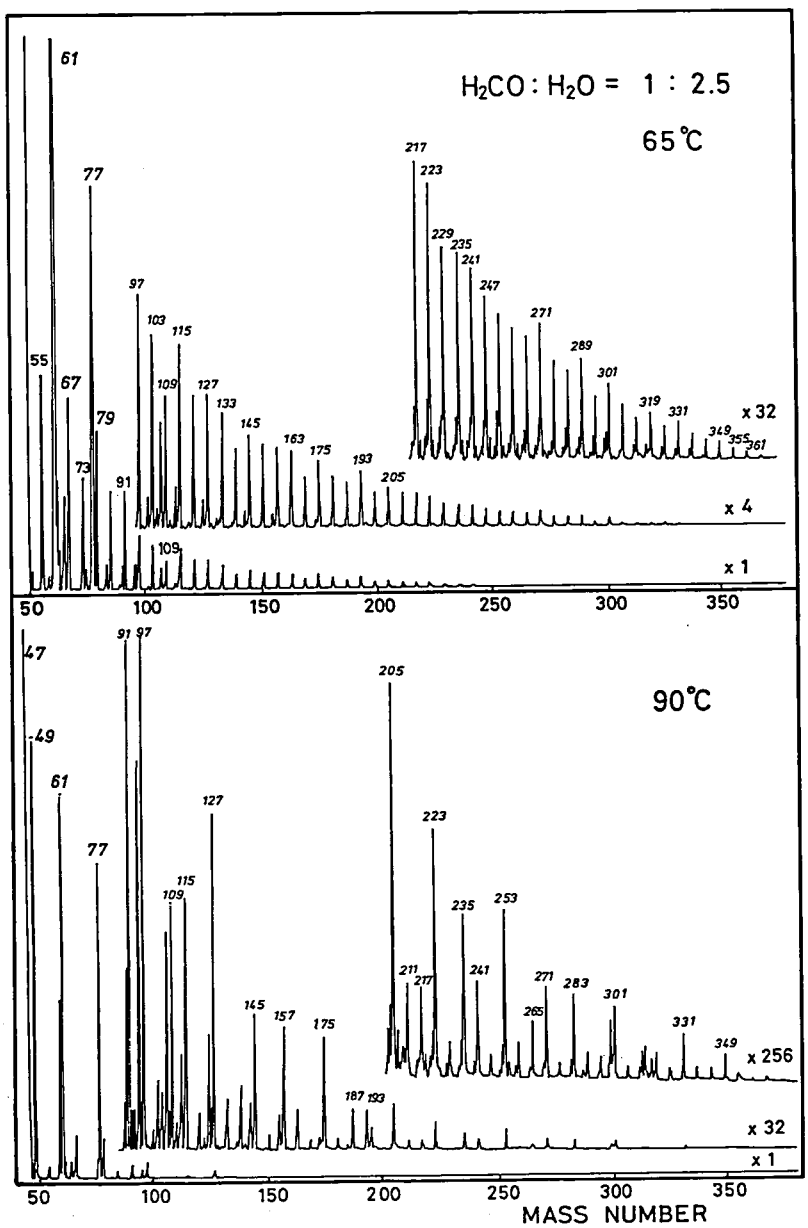

Figure 1. Mass spectral change of cluster fragments with temperature increase of a concentrated formaldehyde solution, whose solute concentration is the same as that of "formalin".

III-G-5 Dimer Formation of Carboxylic Acids in Aqueous Solutions: Effect of Alkyl Group

Kazunori YAMAMOTO and Nobuyuki NISHI

Aqueous solutions of carboxylic acid with acid molar fractions of 0.005 ~ 0.00125 were fragmented to cluster beams in vacuum and investigated by mass spectrometrical analysis. The change of the cluster composition results in the shift of the equilibrium of cluster formation-dissociation processes in a solution. An equilibrium for acid dimer hydrate formation is:

$$RCOOH(H_2O)_n + RCOOH(H_2O)_{n-1} \rightleftarrows (RCOOH)_2(H_2O)_{n-1} + (H_2O)_n. \quad (1)$$

Although eq. (1) neglects acid monomer with no hydrogen-bond in solution, it may describe the acid dimer formation process more properly. It is possible to determine the stability constant $\varkappa_D$, the enthalpy change $\Delta\bar{H}_D$ and the entropy changes $\Delta\bar{S}_D$, which are independent of the water number n. The stability constant $\varkappa_D$ and the enthalpy change $\Delta\bar{S}_D$ are defined as $\varkappa_D = K_D/2$ and $\Delta\bar{S}_D = \Delta S_D + R\ln 2$, where K_D and ΔS_D are the equilibrium constant and the entropy change for eq. (1). Stability constant $\varkappa_D$ is expressed by $\ln \varkappa_D = (-\Delta\bar{H}_D/R)(1/T) + (\Delta\bar{S}_D/R)$. Therefore the logarithmic plots of the stability constant $\varkappa_D$ against T^{-1} gives the enthalpy and entropy of dimerization of carboxylic acid. The results obtained from this treatment are listed in Table I. It is observed that the value of $\varkappa_D$ increases almost linearly with the chain length of alkyl residue, which is accompanied by the increases of entropy. For alkyl carboxylic acid, the increase of entropy overcomes the increase of enthalpy, shifting eq. (1) to the right direction. The association of alkyl carboxylic acid in aqueous solution is, therefore, a pure entropic effect.

Table I Stability constant, enthalpy change and entropy change for the acid dimer hydrate formation process: $RCOOH(H_2O)_n + RCOOH(H_2O)_{n-1} \rightleftarrows (RCOOH)_2(H_2O)_{n-1} + (H_2O)_n$.

solute species	$\varkappa_D$[a]	ΔH_D[b]	ΔS_D[c]
HCOOH	0.84	0.0	−0.4
CH_3COOH	1.28	0.0	0.6
C_2H_5COOH	1.42	0.0	0.7
C_3H_7COOH	1.43	0.6	2.5
C_4H_9COOH	1.92	0.7	3.4
$C_5H_{11}COOH$	1.80	1.1	4.3

[a] Stability constant for acid dimer formation.
[b] Enthalpy of dimerization in $kcal.mol^{-1}$.
[c] Entropy of dimerization in $cal.mol.^{-1}K^{-1}$.

III-G-6 Molecular Association in a Ternary System: Aqueous Solution of Two Carboxylic Acids

Kazunori YAMAMOTO and Nobuyuki NISHI

Molecular association in aqueous solution with formic and propionic acids was studied by means of mass spectrometry of the cluster beams generated through the adiabatic expansion of the ternary system ($HCOOH : C_2H_5COOH : H_2O = 1 : 1 : 200$). A stability constant $\varkappa_m^k(RCOOH)$ of the hydrate cluster $(R'COOH)_k(RCOOH)_m(H_2O)_{n-1}$ against $(R'COOH)_k(RCOOH)_{m-1}(H_2O)_n$, are determined from the intensity ratio of the clusters as:

$$\varkappa_m^k(RCOOH) = \frac{[H^+(R'COOH)_k(RCOOH)_m(H_2O)_{n-1-s}]}{[H^+(R'COOH)_k(RCOOH)_{m-1}(H_2O)_{n-s}]} \frac{m}{n} \frac{X(H_2O)}{X(RCOOH)} \quad (1)$$

Table I Stability constants of solute(s) hydrate clusters $(R'COOH)_k(RCOOH)_m(H_2O)_{n-1}$ against $(R'COOH)_k(RCOOH)_{m-1}(H_2O)_n$ in aqueous solutions of formic acid and propionic acid at 68°C.

Solutions $HCOOH : C_2H_5COOH : H_2O$	Stability Constants[a]
1 : 1 : 200	$\varkappa_1^0(HCOOH) = 7.5$
	$\varkappa_1^1(HCOOH) = 7.3$
	$\varkappa_1^2(HCOOH) = 7.7$
1 : 0 : 200	$\varkappa_1^0(HCOOH) = 7.4\pm0.3$
	$\varkappa_2^0(HCOOH) = 6.5\pm0.3$
1 : 1 : 200	$\varkappa_1^0(C_2H_5COOH) = 11.2$
	$\varkappa_1^1(C_2H_5COOH) = 10.7$
	$\varkappa_2^0(C_2H_5COOH) = 16.3$
	$\varkappa_2^1(C_2H_5COOH) = 16.9$
0 : 1 : 200	$\varkappa_1^0(C_2H_5COOH) = 11.1\pm0.3$
	$\varkappa_2^0(C_2H_5COOH) = 14.8\pm0.5$

[a] $\varkappa_m^k(RCOOH)$ corresponds to the equilibrium constant $K_{m,n}^k$ for the following molecular exchange process: $(R'COOH)_k(RCOOH)_{m-1}(H_2O)_n + RCOOH \rightleftarrows (R'COOH)_k(RCOOH)_m(H_2O)_{n-1} + H_2O$ by the relation: $\varkappa_m^k(RCOOH) = (m/n)K_{m,n}^k$.

where s is the number of water molecules lost on the cluster-ion formation processes, and X(H_2O) and X(RCOOH) are molar fractions of H_2O and RCOOH in solution. $\varkappa_m^k$(RCOOH) is related to the equilibrium constant $K_{m,n}^k$ (see the footnote of Table I). Table I summerizes the results thus obtained for three different solutions at 68°C. For the ternary system, three stability constants $\varkappa_1^k$(HCOOH) (k=0~2) have similar value, which are equal to $\varkappa_1^0$(HCOOH) for aqueous solution of formic acid (HCOOH : H_2O = 1 : 200). The stability constant $\varkappa_1^0(C_2H_5COOH)$ has a similar value to $\varkappa_1^1(C_2H_5COOH)$ for the ternary system, which is nearly equal to $\varkappa_1^0(C_2H_5COOH)$ for aqueous solution of propionic acid (1 : 200). Stability constants $\varkappa_2^0(C_2H_5COOH)$ and $\varkappa_2^1(C_2H_5COOH)$ in the ternary system are slightly larger than $\varkappa_2^0(C_2H_5COOH)$ in the binary system. Molecular association in the ternary system is, therefore, regarded as the superposition of the binary systems.

III–H Study of Molecular Clusters through Wavelength-Selected Multi-Photon Ionization Method

III-H-1 Higher Electronically Excited States of Benzene Clusters

Hisanori SHINOHARA and Nobuyuki NISHI

[*Chem. Phys.*, in press]

Van der Waals clusters of benzene in a supersonic jet are resonantly two-photon ionized (RE2PI) via the second excited singlet state S_2 by using a tunable (205–220 nm) pulsed UV dye laser, and the resultant cluster ions are subjected to time-of-flight mass analysis. Benzene ionizes very inefficiently at these wavelengths in agreement with previous studies, whereas benzene clusters are effectively resonantly ionized via the S_2 state. The RE2PI excitation spectra of benezene clusters with the S_2 excitation (between 211.5 and 218.5 nm) are obtained for the first time. The spectra show specific large red-shifts relative to the presumed (0,0) band of the benzene monomer. The large stability of the S_2 state of benzene upon clustering is ascribed to formation of the benzene excimer whose electronic state can be pictured as a tightly bound state due primarily to the configuration mixing with the so-called charge-resonance state. Direct experimental evidence of the main photo-fragmentation channel leading to the $C_6H_6^+$ ion, $(C_6H_6)_2^+ \rightarrow C_6H_6^+ + C_6H_6$, in addition to the dimer ion $(C_6H_6)_2^+$ production, is also presented.

III-H-2 Intra-cluster Ion-Molecule Reaction in Benzene-Water Mixed Clusters

Hisanori SHINIHARA and Nobuyuki NISHI

[*Z. Phys. D*, in press]

Benzene-water mixed clusters showed intriguing ion-molecule reactions inside of the hydrate clusters. Figure 1 shows the time-of-flight mass spectrum of the mixed cluster beams excited at 261.3 nm. At least two series of water progressions are seen in the spectrum, which originate from mass 91 ($C_7H_7^+$; tropylium ion) and mass 95 ($C_6H_5OH_2^+$). One more interesting feature is the appearance of protonated benzene dimer and trimer ions, although these ions are not accompanied with the water sequence. The reaction schemes will be expressed as follows.

$$C_6H_6\cdot(H_2O)_n \xrightarrow{m\cdot h\nu} [C_6H_6^+(H_2O)_n]^* \rightarrow C_6H_5OH_2^+(H_2O)_{n-s} + H + s\cdot H_2O \quad (1)$$

$$(C_6H_6)_2(H_2O)_n \xrightarrow{m\cdot h\nu} [(C_6H_6)_2^+(H_2O)_n]^* \rightarrow C_7H_7^+(H_2O)_{n-t} + C_5H_5 + t\cdot H_2O \quad (2)$$

$$(C_6H_6)_p(H_2O)_n \xrightarrow{m\cdot h\nu} [(C_6H_6)_p^+(H_2O)_n]^* \rightarrow (C_6H_6)_{p-q}H^+ + OH + q\cdot C_6H_6 + (n+1)H_2O \quad (3)$$

The appearance of the protonated benzene clusters requires the dissociation of H-O bond of the water molecule.

$$C_6H_6^+\cdot H_2O \rightarrow (C_6H_6\text{–}H)^+\text{---}OH \rightarrow C_6H_7^+ + OH \quad (4)$$

The proton affinity of benzene (182.5 kcal/mol) is larger than that of water (164 kcal/mol). Actually, the $C_6H_7^+$ ion was observed even in a static gas cell experiment as the second-most abundant ion species at high pressures (>0.1 Torr). In a water rich environment, protonated benzene clusters could be more preferably formed.

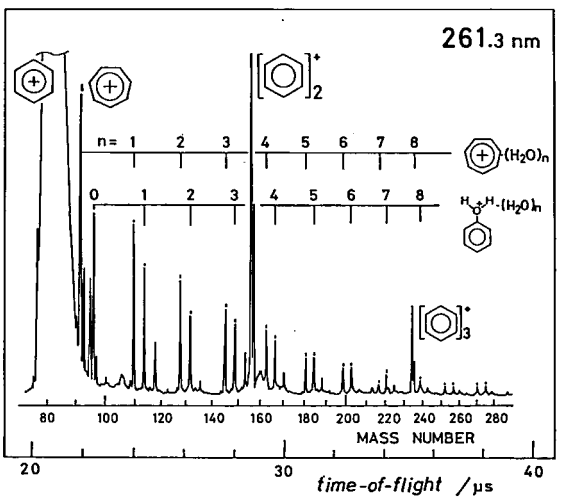

Figure 1. REMPI time-of-flight mass spectrum of a benzene-water mixed cluster beam at 261.3 nm. The cluster beam was produced by bubbling Ar gas flow (350 Torr) through a benzene-water (4:1) mixture. Laser power ≈ 1mJ/pulse.

III-H-3 Resonance-Enhanced Multiphoton Ionization Studies on Benzene-Carbon Tetrachloride Binary Clusters

Fuminori MISAIZU, Hisanori SHINOHARA, Nobuyuki NISHI, Tamotsu KONDOW *(Univ. Tokyo)*, **and Minoru KINOSHITA** *(ISSP, Univ. Tokyo)*

Benzene-carbon tetrachloride clusters, $(C_6H_6)_m(CCl_4)_n$, are produced in a nozzle expansion and ionized by multiphoton excitation with a tunable laser light (209–212 nm) in the accerelation region of a time-of-flight mass spectrometer. Figure 1 shows typical mass spectra of the binary clusters for the mixtures with C_6H_6:CCl_4 = 1:4 (a) and 9:1 (b). Figure 1-a exhibits intense ion signals of CCl^+ and $C_6H_6^+$, whereas some additional ions, for example, $C_6H_6Cl^+$, $C_7H_6Cl_x^+$ (x=1, 3, 4), and $C_7H_5Cl_2^+$, are also seen for the benzene rich mixture (b). The fragment ion, CCl^+, is not observed for a pure CCl_4 beam. This suggests that the ion is produced mostly from the binary cluster, $C_6H_6 \cdot CCl_4$. The ion signal intensity dependence on the laser power reveals that the CCl^+ ion is produced by four-photon excitation.

At the wavelengths around 210 nm, the binary clusters are two-photon ionized via the S_2 state of benzene. The chloro-substituted tropylium ion, $C_7H_6Cl^+$, which is considered to be a stable species, may be produced by the third-photon absorption, and the CCl^+ ion can be produced by photodissociation of this ion. The seven-membered ring ions, $C_7H_6Cl^+$ and $C_7H_5Cl_2^+$, must be characteristic to the present MPI experiment and are ascribed to intracluster ion-molecule reactions within the binary clusters.

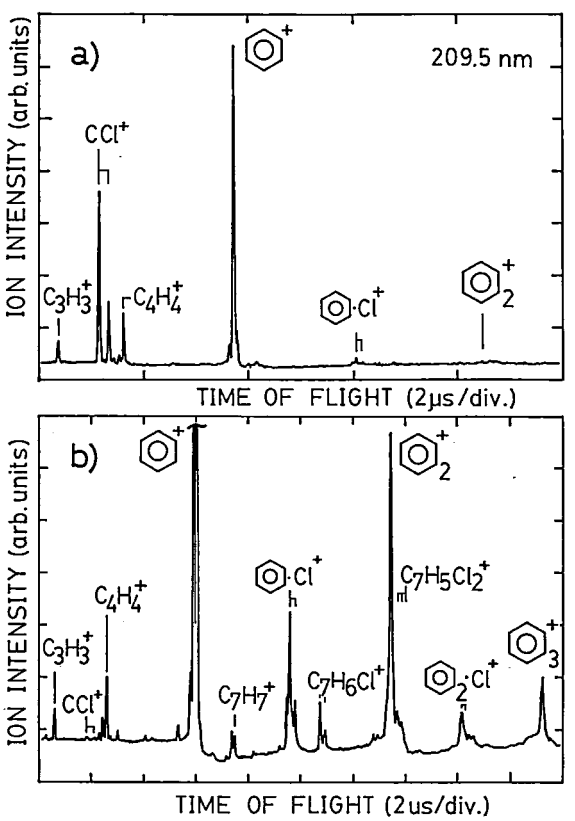

Figure 1. Resonance-enhanced multiphoton ionization mass spectra of benzene-carbon tetrachloride binary clusters. a) sample mixing ratio, C_6H_6:CCl_4 = 1:4, b) 9:1.

III–I Resonance Enhanced Two-Photon Ionization Study of Unimolecular Reaction Processes

III-I-1 Nanosecond Two-Color RE2PI Study of Benzene in the Channel Three Region

Teijiro ICHIMURA *(Tokyo Inst. Tech.)*, **Hisanori SHINOHARA, and Nobuyuki NISHI**

The so-called "third channel" process occuring in the first excited singlet state $S_1(^1B_{2u})$ of benzene has been an intriguing topic in view of the study of non-radiative processes. The sudden decrease in the fluorescence quantum yield under collisionless conditions has been observed at an excess energy of 2800 cm^{-1} above the origin. The present study shows that the photoionization yield observed with the pump and probe (two-color) method also decreases at the onset of the channel three region in the nano-second time scale similar to the fluorescence quantum yield.

Figure 1 shows a two-color resonance-enhanced two photon-ionization (RE2PI) excitation spectrum of benzene around the onset of the channel three region. A dramatic decrease of the relative ion intensity ($6_0^1 1_0^2$ vs. $6_0^1 1_0^3$) in the present work is evident in comparison with our previous one-color RE2PI results.[1] The fact that the normalized intensity for the 7^1 band in one-color scheme is larger than in two-color study with a longer delay time indicates that the 7^1 band is clearly involved in channel three. This tendency is much salient for the $6_0^1 1_0^3$ band, which obviously is due to the enhanced internal conversion.

Reference

1) T. Ichimura, H. Shinohara, and N. Nishi, *Chem. Phys. Lett.* **146**, 83 (1988).

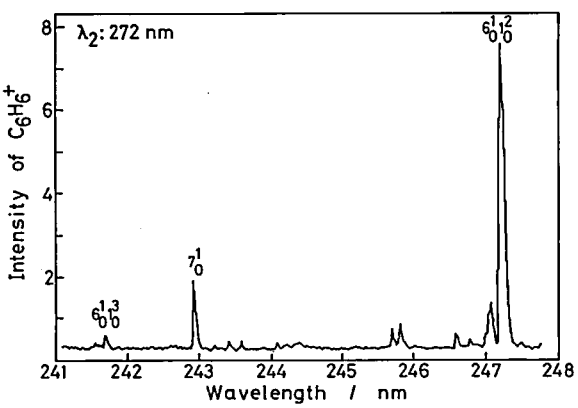

Figure 1. Two-color resonance-enhanced two photon-ionization excitation spectrum of benzene around the onset of the channel three region. The probe laser is tuned to 272.0 nm. The beam condition is Ar-seeded 2 atm with a nozzle temperature of 46°C.

III–J External Magnetic Field Effects upon Chemical Reactions

Magnetic field effects upon chemical reactions provide us with useful methods for elucidating reaction mechanism and techniques for controlling reaction rates, product yields, and concentration of a certain isotope. In the recent decade, the magnetic field effects upon photochemical reactions have been extensively studied by a variety of methods, *i.e.* magnetic-field-modulated fluorescence measurement, kinetic spectroscopy of reaction intermediates by laser photolysis and its modification two-step laser excitation, and chemical analysis of photoproducts obtained by steady-state irradiation. In particular, the photochemistry of aromatic carbonyls and bifunctional chain molecules in the solution phase has been investigated in some detail. In addition, we have also examined the magnetic field effects on afterglow activated by a microwave discharge and the mechanism of magnetic quenching of CS_2 fluorescence in the gaseous state.

III-J-1 Magnetic Field Effects upon Photochemistry of Bichromophoric Chain Molecules Containing Nitro-aromatic and Arylamino Moieties: Elucidation of Reaction Mechanism and Control of Reaction Yields.

Ryoichi NAKAGAKI, Kiyoshi MUTAI *(Univ. of Tokyo)*, **Mitsuo HIRAMATSU** *(Hamamatsu Photonics, K.K.)*, **Hideyuki TUKADA** *(Univ. of Tokyo)*, **and Saburo NAGAKURA**

[*Can. J. Chem.*, in press]

The photochemistry of bichromophoric species containing nitro-aromatic and arylamino moieties has been studied in the presence and absence of an external magnetic field. Photolysis products are an unsubstituted arylamine, a nitroso-aromatic species (cage product), and a nitro-aromatic compound (escape product). On application of the magnetic field, the formation yield for the cage product decreases and that for the escape product correspondingly increases, whereas the consumption of the starting material and the release of the unsubstituted arylamine are independent of the magnetic field. Analysis of the magnetic field effects shows photoreaction takes place in the triplet manifold of the nitro-aromatic moiety. Application of the magnetic field may cause an appreciable change in the relative yield of cage and escape products, *i.e.* the branching ratio of competitive processes.

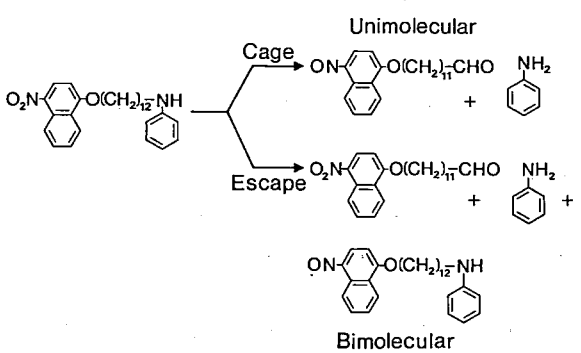

Figure 1. A typical example of photoredox reactions observed for bifunctional chain molecules containing nitro-aromatic and arylamino moieties.

III-J-2 Magnetic Field Effect on Monophotonic Ionization of *N,N,N′,N′*-Tetramethylbenzidine in Propionitrile and *n*-Butyronitrile

Toshiro SAITO *(Osaka Univ.)*, **Yoshinori HIRATA** *(Osaka Univ.)* **and Noboru MATAGA** *(Osaka Univ. and IMS)*

[*Chem. Phys Lett.*, **145**, 509 (1988)]

N,N,N′,N′-Tetramethylbenzidine (TMB) in propionitrile and *n*-butyronitrile (RCN) undergoes monophotonic ionization from fluorescent state and forms a long lived ion pair which shows a geminate recombination type of decay in a few hundreds of microseconds.[1] At least two kinds of ion pairs, an initially formed short lived and a long lived one formed from the short lived one, are involved in the relaxation process of the excited state in these systems. Studies of external magnetic field effect showed that the yield of the triplet (^{3}TMB) due to the recombination of initially formed ion pair decreased under the magnetic field strength of 0–500 G. No magnetic field effect was observed for the long lived ion pair. The monophotonic ionization mechanism is given by the following reaction scheme where the initially formed singlet ion pair is converted to the triplet ion pair by hyperfine interaction and the dimer anion $(RCN)_2^-$ grows into polymer anion to form the long lived ion pair.

$$\left.\begin{array}{l} TMB\ (S_0) \xrightarrow{h\nu} TMB^*(S_1) \\ \rightarrow {}^1(TMB^+ \ldots (RCN)_2^-) \\ \qquad \uparrow\downarrow \\ {}^3(TMB^+ \ldots (RCN)_2^-) \end{array}\right\} \rightarrow TMB^+ \ldots (RCN)_n^- \downarrow TMB(S_0)$$

Reference

1) T. Saito, Y. Hirata and N. Mataga, *J. Phys. Chem.* **90**, 4017 (1986).

III-J-3 Long-Lived Triplet Radical Ion Pairs State of Porphyrin-Methylviologen Combined Systems as Revealed by a Large Magnetic Field Effect on Its Lifetime

Toshiro SAITO *(Osaka Univ.)*, **Yoshinori HIRATA** *(Osaka Univ.)*, **Hisashi SATO** *(Osaka Univ.)*, **Toshikatsu YOSHIDA** *(Univ. Osaka Prefecture)*, **and Noboru MATAGA** *(Osaka Univ. and IMS)*

[*Bull. Chem. Soc. Jpn.*, **61**, 1925 (1988)]

The external magnetic field effect on the lifetime of the ion pair state has been examined for the porphyrin-methylviologen combined systems in polar solvents by using nanosecond laser flash photolysis techniques. Applying the external magnetic field, a drastic increase in the lifetime has been observed. For $P11MV^{2+}$ in DMSO under the magnetic field of 50 mT, the ion pair lifetime was almost three times longer than the zero field value, which can be deemed the ideal case of the external magnetic field effect due to the hyperfine interaction mechanism. The results clearly showed that the long-lived ion pair was formed by the intramolecular electron transfer from the triplet state of porphyrin (k_{et}^3), of which the relaxation is affected by the external magnetic field as indicated by the magnetic field dependent rate constant $k(B)$ in the following reaction scheme.

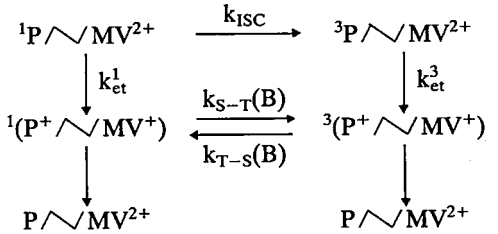

III-J-4 External Magnetic Field Effect on CS_2 Banded Emission. Laser Excitation in the Wavelength Region of Nitrogen Laser

Takashi IMAMURA, Saburo NAGAKURA, Haruo ABE *(Inst. of Phys. and Chem. Res. and IMS)*, **Yoshio FUKUDA, Hisaharu HAYASHI** *(Inst. of Phys. and Chem. Res.)*

[*J. Phys. Chem.*, in press]

External magnetic field effects on the banded emission of gaseous CS_2 were measured at room temperature by the excitation near the nitrogen laser wavelengths with a ns dye laser. The magnetic field effects observed below 8.3 kG have the following characteristics: 1) a magnetic field affects only the emission intensity without changing its lifetime, 2) the integrated intensity of the excitation spectrum of the banded emission is reduced by a magnetic field (see Figure 1 for 9U band), 3) magnetic field effects can be observed even under supersonic jet condition, and 4) magnetically induced decrease in the integrated intensity of the excitation spectrum is independent of the Zeeman splitting in the absorption spectrum.

These experimental results indicate that the Zeeman detuning model is not applicable to the present case but a magnetic field affects intramolecular energy redistribution processes. The possible mechanisms for the novel magnetic field effect on the CS_2 banded emission are discussed.

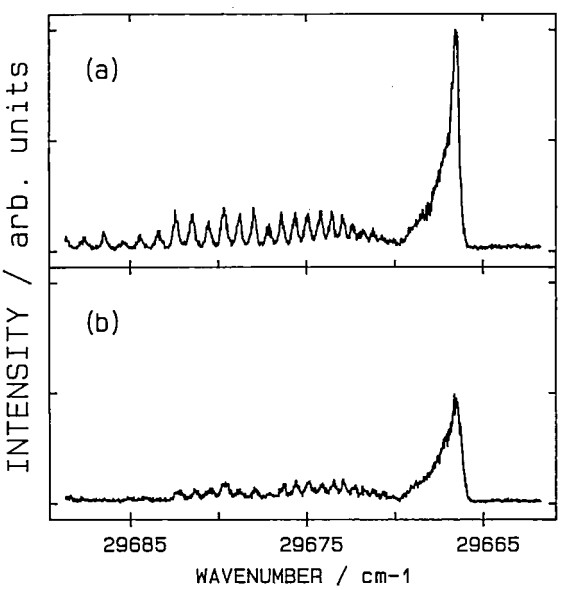

Figure 1. Excitation spectra in the 9U band region observed (a) at H=0 kG and (b) at H=8.3 kG. CS_2 pressure was 45 mTorr. Emission was monitored at 23213 cm^{-1}.

RESEARCH ACTIVITIES IV
Department of Molecular Assemblies

IV-A Studies of Ion-Molecule Reactions by a Threshold Electron-Secondary Ion Coincidence (TESICO) Technique

The knowledge of the microscopic reaction cross sections for evolution of a system in a single reactant quantum state (translational, rotational, vibrational, and electronic) to a single product quantum state is essential for a complete understanding of a chemical reaction. Ion-Molecule reactions are particularly suited for studying such microscopic cross sections since ions can readily be prepared in various internal states in the initial ionization processes, such as photoionization, and the emitted photoelectrons provide information on the distribution among these states.

In this project, we study state-selected ion-molecule reactions by the use of a photoionization technique which utilizes the threshold photoelectron-secondary ion coincidence. The technique allows direct determination of $\sigma(i,v)$, i.e., the reaction cross section as a function of the internal and collisional energies of reactants. The selection of electronic, vibrational, rotational, and fine-structure states are possible by this technique.

IV-A-1 Separation of Two Microscopic Reaction Mechanisms in the Reaction $CH_3F^+ + CH_3F \rightarrow CH_4F^+ + CH_2F$

Shinzo SUZUKI and Inosuke KOYANO

The ion-molecule reaction $CH_3F^+ + CH_3F \rightarrow CH_4F^+ + CH_2F$ has been investigated using the TESICO technique.[1] Two peaks observed in the time-of-flight coincidence spectra of the mass-selected product ion CH_4F^+ at collision energies $E_{cm} = 2.4$ and 3.6 eV were interpreted as corresponding to the hydrogen atom abstraction and proton transfer mechanisms for the CH_4F^+ formation. Figure 1 shows the TOF coincidence spectrum for $E_{cm} = 3.6$ eV, where the separation of the two peaks is the largest among three energies studied. The collision energy dependence of the separation is in good agreement with the calculated result based on the assumption that the difference in the initial forward velocity of the product ions between these two mechanisms causes the difference in overall TOF. After correcting the peak intensities for background signals, relative cross sections have been determined for each of the two microscopic reaction mechanisms as a function of the internal energy of the reactant ion at two c.m. collision energies. The results show that the fraction of the proton transfer mechanisms slightly increases as the total (internal + collisional) energy of the reactants increases.

Reference

1) I. Koyano and K. Tanaka, *J. Chem. Phys.* **72**, 4858 (1980).

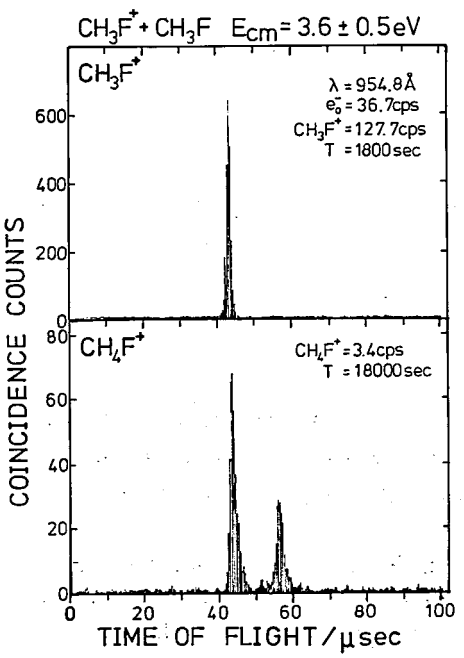

Figure 1. TOF coincidence spectra of the primary and secondary ions of the reaction $CH_3F^+ + CH_3F \rightarrow CH_4F^+ + CH_2F$.

IV-A-2 State Selected Dissociative Charge Transfer Reactions: $Ne^+(^2P_J)$ +OCS

Shinzo SUZUKI, Kazuhiko OKUNO *(Tokyo Metropolitan Univ.)*, **Takashi IMAMURA, and Inosuke KOYANO**

[*Rev. Sci. Instrum.*, in press]

Performance of a dodecapole collision chamber, constructed for the study of state-selected ion-molecule reactions using synchrotron radiation, has been examined utilizing the Ne^+ ions produced by photoionization of Ne at the $^2P_{3/2}$ threshold. Figure 1 shows the change of the intensity of the primary ion $Ne^+(^2P_{3/2})$ as a function of the potential difference between the ionization region (fixed) and the center of the collision chamber (varied). From Figure 1, it can be seen that the ion intensity rises sharply from zero to a certain finite value as the potential difference reaches zero, and then becomes almost constant below −2 V. It is confirmed that the ion collecting efficiency remains unchanged when ion kinetic energy is varied within a certain range of interest. The ion-molecule reactions,

$$Ne^+(^2P_J) + OCS \rightarrow CO^+ + S + Ne$$
$$\rightarrow S^+ + CO + Ne$$

has been investigated at the collision energy E_{cm} = 1.7 eV using this apparatus. The ratio of the cross sections for these two reaction channels, $I(CO^+)/I(S^+)$, obtained from the time-of-flight coincidence spectra, has been found to be almost 2, independent of the initial spin-orbit state of Ne^+.

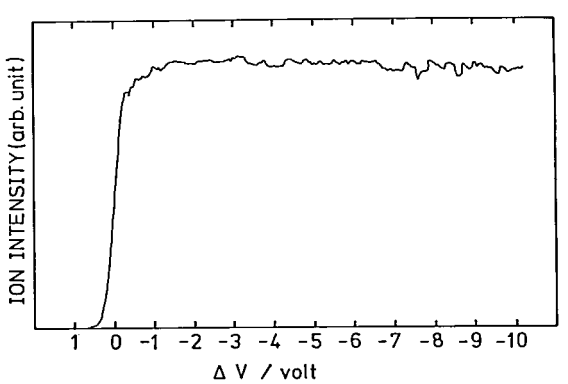

Figure 1. The change of the intensity of the primary ion $Ne^+(^2P_{3/2})$ as a function of the potential difference between the ionization region and the center of the collision chamber.

IV-A-3 State Selected Ion-Molecule Reactions by a Coincidence Technique. XV. Hydrogen atom Abstraction as an Electron Jump Followed by Proton Transfer in the $ND_3^+(v) + NH_3$ and $NH_3^+(v) + ND_3$ Reactions

Shinji TOMODA *(Osaka Univ.)*, **Shinzo SUZUKI, and Inosuke KOYANO**

[*J. Chem. Phys.* **89**, in press (1988)]

The effects of the vibrational excitation of the ν_2 mode of ND_3^+ and NH_3^+ on the three channels of their reaction with NH_3 and ND_3, respectively, are studied up to v=12, in the c.m. collision energy range from 0.9 to 4.8 eV using the TESICO technique. The observed variation of the ratio γ of the hydrogen/deuterium atom abstraction cross section over the competing deuteron/proton transfer cross section as a function of the vibrational quantum number[1] is interpreted by a new reaction model proposed on the basis of the calculated potential energy surfaces for the ammonia dimer cation.[2] The hydrogen/deuterium atom abstraction reaction is interpreted as a near resonant electron jump

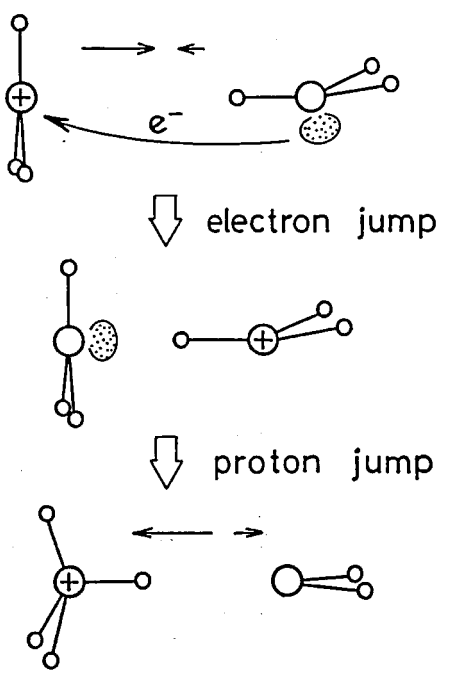

Figure 1. Microscopic reaction mechanism for the phenomenological hydrogen/deuterium atom abstraction reaction. Large and small circles represent a nitrogen and a hydrogen atom, respectively.

at large intermolecular separations followed by a proton/deuteron transfer which proceeds on the "charge-transferred" potential surface, as schematically illustrated in Fig. 1.

References

1) S. Tomoda, S. Suzuki, and I. Koyano, IMS *Ann. Rev.* **1987**, 87.
2) S. Tomoda, *Chem. Phys.* **110**, 431 (1986).

IV-B Studies of Photo-Induced Ion-Molecule Reactions

Exploration of chemical reactions coupled with radiation field has paved the way for a deeper understanding of the structure and potential energy surfaces. In this project, we attempt to investigate the ion-molecule reactions induced by the resonant and/or non-resonant laser irradiation to obtain some information on the intermediate states of reactions, as well as on the reactions of excited ions. The reaction paths of electronically-excited ions are expected to be quite different from those of the ground state ions. Detection of stimulated transitions in colliding systems induced by the non-resonant laser irradiation might provide new information on the reaction path and potential energy surfaces, and is expected to open a new area in the reaction dynamics.

IV-B-1 Construction of a Tandem Mass Spectrometer for Probing Transition State in Ion-Molecule Reactions

Takashi INAMURA, Toshio HORIGOME, Shinzo SUZUKI, Takashi IMAJO, and Inosuke KOYANO

An apparatus for the title purpose is under construction. The system consists of a 60° sector magnetic analyzer which serves as a source of mass-selected primary ion beams, collision chamber, and a quadrupole mass filter as a detector. The ions produced by a duoplasmatron with high current density are directed into the magnetic analyzer through an electrostatic lens system with the asymmetric triple-cylinder lens and a pair of quadrupole deflectors. The mass-selected ion beam is retarded to an energy of tens of eV using another electrostatic lens system which consists of a matching lens with a quadrupole lens pair and an exponential decelerator. The ions injected into the collision chamber, held in an octahedral aluminum housing, then collide with the target molecule in the presence of photon field. The effects of laser irradiation at various wavelengths upon ion-molecule reactions are probed by monitoring the variation in the secondary ion intensity.

IV-B-2 Collisional Removal Rates for Vibronically Excited Molecular Ions: CO^+ (A, v=1)

Takashi IMAJO, Takashi IMAMURA, and Inosuke KOYANO

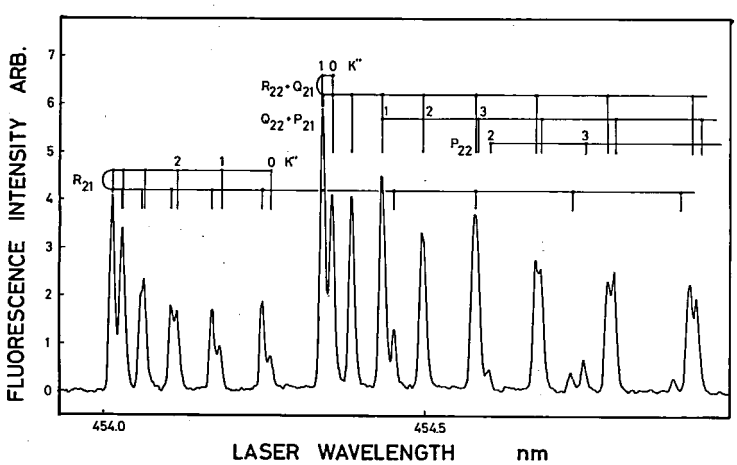

Figure 1. Laser induced fluorescence excitation spectrum of the $CO^+A^2\Pi(v'=1) \leftarrow X^2\Sigma^+(v''=0)$ transition.

Although extensive studies have been performed on the ion-molecule reactions both experimentally and theoretically, little is known about the reactions of electronically excited ions. In order to study such reactions, we have measured collisional removal rates of vibronically excited ions by a flowing afterglow/time resolved laser induced fluorescence technique. Ion-molecule reactions are expected to constitute a main part of the removal rate of electronically excited ions.

Figure 1 shows a fluorescence excitation spectrum for the CO^+ $A^2\Pi(v'=1)\leftarrow X^2\Sigma^+(v''=0)$ transition. In measuring removal rates, the wavelength of the dye laser was fixed at the bandheads of $R_{22}+Q_{21}$ branches and the lifetime measurements were performed at various pressures of collision partners. A Stern-Volmer plot for the $CO^+(A)+N_2$ collision is shown in Figure 2 from which the collisional removal rate was obtained to be $(1.9\pm0.1)\times10^{-9}$ $cm^3molec^{-1}s^{-1}$. In the same manner, the collisional removal rates for the systems of $CO^+(A)+Ar$ and $CO^+(A)+CO$ were determined to be $(1.1\pm0.1)\times10^{-9}$ and $(1.5\pm0.1)\times10^{-9}cm^3molec^{-1}s^{-1}$, respectively. In all these systems, the collisional deactivation is very fast and the rate constants exceed gas kinetic rates. Ion-molecule reactions and charge transfer processes are expected to be responsible for such large deactivation rates.

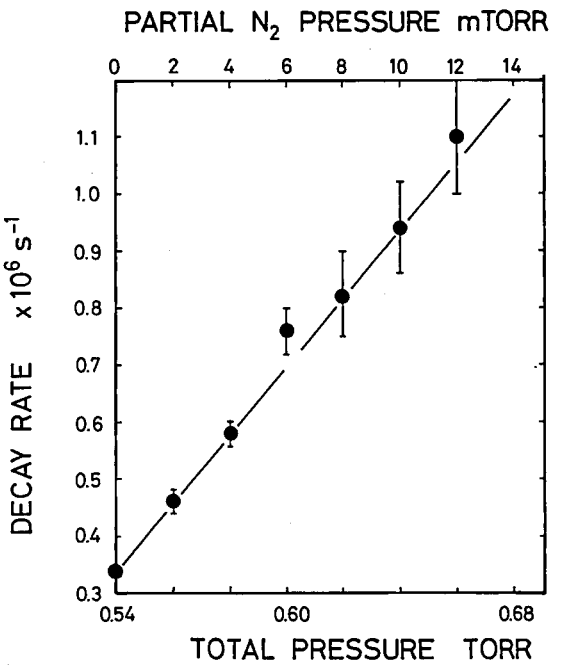

Figure 2. Stern-Volmer plot of the $CO^+(A)$ + N_2 system.

IV-C Studies of Unimolecular Decomposition of Simple and Complex Molecular Ions

The TEPSICO and the TEPSICO-II apparatus which we have developed for the study state selected ion-molecule reactions (see **IV-A** above and **IV-F-4** of IMS Ann. Rev. 1984) are also applicable to the study of unimolecular decomposition of molecular ions. In this technique, ions can be prepared with defined amounts of internal energy and their subsequent decomposition investigated. In the present project, we study unimolecular decomposition of both simple and complex molecular ions mainly following valence and inner valence photoionization. Both laboratory and synchrotron light sources are used. Processes following core photoionization constitute another project (see **IV-D** below).

IV-C-1 Dissociation of State Selected OCS^+ Ions

Shinzo SUZUKI, Kazuhiko OKUNO *(Tokyo Metropolitan Univ.)*, **Takashi IMAMURA, and Inosuke KOYANO**

To make a comparison between ionic dissociation process of OCS^+ initiated by the charge transfer reaction $Ne^+ + OCS \rightarrow$ products and by photoionization of OCS at the same energies, the branching ratios of the dissociation products (CO^+, S^+) from the state-selected OCS^+ ions have been investigated with the TEPSICO-II apparatus installed in the UVSOR synchrotron radiation facility.

The experimental results show that the ratio of the intensities of the two dissociation products, $I(CO^+)/I(S^+)$, takes the value of about 0.1, which is significant-

ly smaller than the corresponding value by the dissociative charge that transfer reaction (see **IV-A-2**). The discrepancy between these branching ratios suggests that the crossing of the $OCS^+(C)$ surface with the repulsive surface correlating to $CO^+ + S$ occurs at a relatively high vibrational state of $OCS^+(C)$.

IV-C-2 Dissociation of State Selected NO_2^+ Ions

Kazuhiko SHIBUYA *(Tokyo Inst. of Tech.)*, **Shinzo SUZUKI, Takashi IMAMURA, and Inosuke KOYANO**

A detailed study of dissociation processes of state selected NO_2^+ ions has been performed using synchrotron radiation and a TOF coincidence technique. Branching ratios for the two dissociation channels $NO_2^+ \rightarrow NO^+ + O$ and $NO_2^+ \rightarrow O^+ + NO$, as well as for the production of stable parent ion NO_2^+ (nondissociative channel) have been determined at eight wavelengths between 40 and 100 nm, corresponding to the initial preparation of the parent NO_2^+ ions in the electronic and vibronic states 2^3A_1, $2^3B_2(100)$, $2^3B_2(000)$, $1^3A_1(200)$, $a^3B_2(030)$, $1^3B_2(020)$, $1^3B_2(010)$, and $1^3B_2(000)$. It has been found that the dissociation rate of the $NO_2^+(1^3B_2)$ ions increases dramatically (exponentially) with increasing vibrational quantum number v of the ν_2 mode in the range v = 0-3, as shown in Fig. 1. This fact has been discussed in conjunction with the quantum mechanical tunnelling. Possibility of radiative stabilization of some electronically excited parent ions has also been discussed.

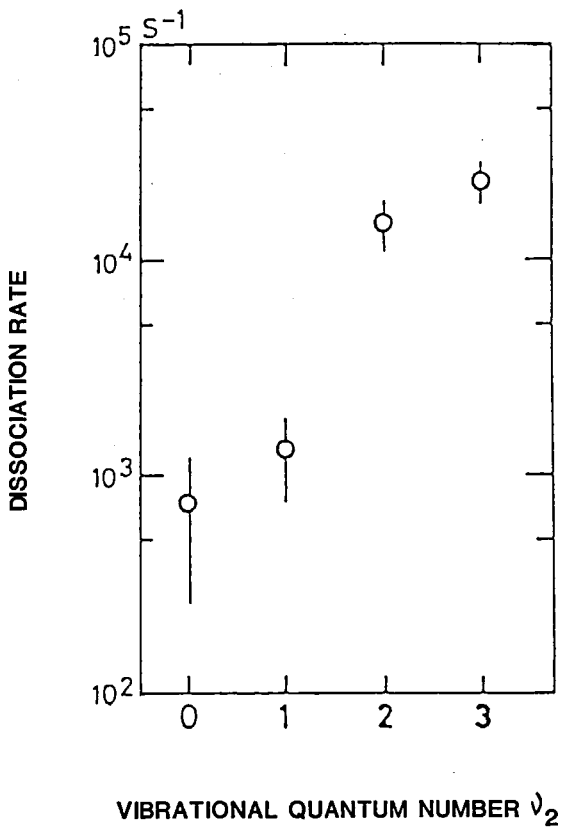

Figure 1. Dependence of the dissociation rate of $NO_2^+(1^3B_2)$ on the quantum number of the ν_2 vibration.

IV–D Investigation of Ionic Fragmentation Following Core Level Ionization in the Vapor Phase Using Synchrotron Radiation

Shallow valence level ionization and subsequent fragmentation of molecules have been studied extensively using various kinds of light source in recent years. However, the investigation of processes following core level excitation have not been so extensive, because, for the purpose of such investigation, the conventional light sources are insufficient both in photon energy and intensity. Synchrotron radiation is expected to provide a powerful means to obtain information about the core level excitation. In contrast to the case of the valence electrons delocalized over the molecule, the core electrons in a molecule are localized near the atom to which they belonged originally. As a result, the photoionization from the core levels is expected to produce dissociation pathways quite different from those following valence photoionization.

IV-D-1 Investigation of Fragmentation Processes Following Core Photoionization of Organometallic Molecules in the Vapor Phase

Shin-ichi NAGAOKA, Shinzo SUZUKI and Inosuke KOYANO

[*Nucl. Instrum. Methods.* **A266**, 699 (1988)]

Ionic Fragmentation processes following (n−1)d core level photoionization of organometallic molecules have been studied in the vapor phase using synchrotron radiation. Results on tetramethyllead, tetramethyltin and tetramethylgermanium are reported. The threshold electron spectra and the photoionization efficiency curves of these molecules are presented and discussed. It is concluded that the $[(n-1)d]^9$ core-hole state of $M(CH_3)_4$ (M = Pb, Sn or Ge) is split into five sublevels owing to both the spin-orbit coupling and the electrostatic perturbations by the methyl groups, and that the M^+ ions are predominantly produced following (n−1)d photoionization.

IV-D-2 Ionic Fragmentation Following the 3d Core-Level Excitation of $Sn(CH_3)_4$ by Soft-X Ray

Kiyoshi UEDA *(Tohoku Univ.)*, **Eiji SHIGEMASA** *(Tohoku Univ.)*, **Yukinori SATO** *(Tohoku Univ.)*, **Shin-ichi NAGAOKA, Inosuke KOYANO, Akira YAGISHITA** *(National Lab. High Energy Phys.)*, **Tetsuo NAGATA** *(Meisei Univ.)*, **and Tatsuji HAYAISHI** *(Univ. of Tsukuba)*

Ionic fragmentation following the photoionization of $Sn(CH_3)_4$ has been studied in the photon energy region between 400–600 eV using synchrotron radiation and time-of-flight mass spectromerty. Photoionization efficiency curves for various ionic fragments are presented and discussed in relation to the correlated Sn:3d subshell phtoionization. Vacancy-relaxation and dissociation processes following the 3d photoionization are also discussed.

IV-D-3 Ionic Fragmentation Following Inner-Core Level Excitation of $Pb(CH_3)_4$ in the Vapor Phase

Shin-ichi NAGAOKA, Inosuke KOYANO, Kiyoshi UEDA *(Tohoku Univ.)*, **Eiji SHIGEMASA** *(Tohoku Univ.)*, **Yukinori SATO** *(Tohoku Univ.)*, **Akira YAGISHITA** *(Natural Lab. High Energy Phys.)*, **Tetsuo NAGATA** *(Meisei Univ.)*, **and Tatsuji HAYAISHI** *(Univ. of Tsukuba)*

Ionic fragmentation following inner-shell (Pb:5p and 4f, C:1s) excitation of $Pb(CH_3)_4$ has been studied in the vapor phase by use of synchrotron radiation and time-of-flight mass spectrometry. The C:1s ionization is followed by a KVV Auger process, and results in formation of the double charged parent ion. The Pb:5p or 4f ionization is followed by a cascade of Auger events, and results in formation of the triple or higher multiple charged parent ions. For these reasons, the fragmentation pattern changes drastically depending on the nature of the core-electrons to be excited.

IV-D-4 Investigation of Fragmentation Processes Following Core Photoexcitation of Trimethylgallium in the Vapor Phase

Shin-ichi NAGAOKA, Shinzo SUZUKI, Umpei NAGASHIMA, Takashi IMAMURA, and Inosuke KOYANO

[*Rev. Sci. Instrum.*, in press]

Ionic fragmentation following 3d core level photoexcitation of trimethylgallium has been studied in the vapor phase using synchrotron radiation. The threshold electron spectrum, phtoionization efficiency curves, and TPEPICO spectra are presented and discussed. The Ga^+ and $GaMe^+$ ions are predominantly produced following 3d photoexcitation. The fragmentation patterns following the 3d core level excitation can be explained by considering the hybrid orbitals constructed from the 3d, 4s and 4p atomic orbitals for both parent ions and neutrals.

IV-D-5 Ionic Fragmentation Processes in Organometallic Molecules Following (n−1)d Core Photoionization

Shin-ichi NAGAOKA, Shinzo SUZUKI, Umpei NAGASHIMA, Takashi IMAMURA, and Inosuke KOYANO

Ionic fragmentation following photoionization from the shallowest d core orbital in organometallic molecules with a group II-V element [$ZnMe_2$, $GaMe_3$, $GaMe_4$, $SnMe_4$, $PbMe_4$, and $BiMe_3$ (Me=CH_3)] has been studied in the vapor phase. The (n−1)d core-ionized state of the tetramethyl compound of a group IV element ($PbMe_4$ and $SnMe_4$) has been found to be split into five sublevels owing to both the spin-orbit coupling and the electrostatic perturbation from the methyl groups. By use of the threshold photoelectron-photoion coincidence technique, it has been shown that in the molecules studied here (except $BiMe_3$), the excitation to the $[(n-1)d]^9$ hole-state produces dissociation pathways quite different from those following valence photoionization. The metal ions are predominantly produced following the excitation to the $[(n-1)d]^9$ hole-state. The monomethyl metal ions are likely to be produced following both the excitation to the hole-state and the photoionization from the valence orbitals. The dimethyl and trimethyl metal ions are shown to originate from the valence-ionized states. The fragmentation processes following the 5d ionization of $BiMe_3$ is considered to be statistical. The quintet splitting of the (n−1)d core-ionized states of the tetramethyl compounds of a group IV element and their fragmentation patterns can be explained in terms of the crystal field theory and the hybrid orbitals constructed from the (n−1)d, ns, and np atomic orbitals.

IV-D-6 Ionic Fragmentation of Tetramethyl Tin Following the Photoionization in the range between 60–160 eV

Kiyoshi UEDA *(Tohoku Univ.)*, **Yukinori SATO** *(Tohoku Univ.)*, **Shin-ichi NAGAOKA, Inosuke KOYANO, Tatsuji HAYAISHI** *(Univ. of Tsukuba)*, **and Akira YAGISHITA** *(National Lab. High Energy Phys.)*

Ionic Fragmentation processes following the photoionization of $Sn(CH_3)_4$ in the photon energy region between 60–160 eV have been studied using synchrotron radiation and time-of-flight mass spectrometry. The yield curves of various ionic fragments are presented and discussed in relation to the correlated atomic 4d, 4p and 4s sub-shell photoionization. Vacancy-relaxation and dissociation processes following the 4d and 4p sub-shell photoionization are also discussed.

IV−E Application of Excited-State Photoelectron Spectroscopy to Photophysics and Photochemistry

Pulse Laser Photoelectron spectroscopy for studying excited molecules in the gas phase has been developed in this Institute by K. Kimura and his coworkers since 1980 [IMS Annual Review (1980–88); Adv. Chem. Phys. **60**, 161 (1985)]. Since any electronically excited states can in principle be ionized by an appropriate pulse laser, the laser photoelectron spectroscopic technique is especially powerful for studying non-radiative excited states. The technique is also useful to find new ionic states of molecules. In this project, we have been further improving the technique and applying it for various molecular excited states associated with photophysical and photochemical processes.

IV-E-1 Optical-Optical Double Resonance MPI Photoelectron Spectroscopy of the NO Molecule via the $C^2\Pi$ (v=4) State: *n*s and *n*d Rydberg Series

Yohji ACHIBA *(Tokyo Metropolitan Univ.)* **and Katsumi KIMURA**

[*Chem. Phys.*, in press]

In order to study autoionization mechanism, two-color MPI ion-current and photoelectron spectra of NO have been measured by means of a double resonance technique. A series of the *n*dδ autoionizing Rydberg states were selectively produced via the $C^2\Pi(v'=4)$ Rydberg state. The observed MPI spectrum shows very sharp peaks attributable to the vibrationally excited *n*dδ Rydberg series converging to the NO^+ $X^1\Sigma^+(v^+=4)$ state. The photoelectron vibrational branching ratios observed for n = 5–14 have clearly

indicated the break-down of the so-called $\Delta v=-1$ propensity rule for pure vibrational autoionization. It has been concluded that the Rydberg-valence multi-state interaction in the ionization continuum plays an essential role in the present autoionization. The mechanism suggested here is that electronic autoionization proceeds by continuum-continuum interaction via the dissociative valence excited state. The vibrational-state population of the ion thus induced can be described in terms of the Franck-Condon overlap of the vibrational wavefunctions between the repulsive potential of the dissociative valence excited state and the bound potential of the NO^+ ion.

Figure 1 shows the potential curve of the ion, the vibrational wave functions, the repulsive portion of the potential curve deduced from the present photoelectron data.

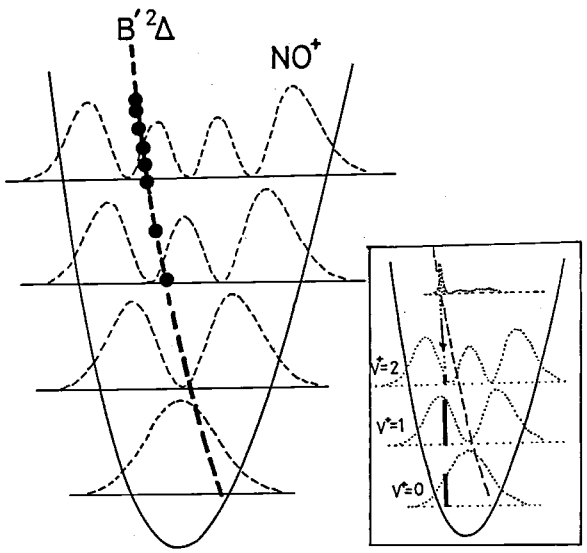

Figure 1. A potential energy curve of the NO^+ $X^1\Sigma^+$ state and the probability distribution of the vibrational wave functions. The dotted curves were calculated by assuming a Morse function with known molecular parameters. Black circles were obtained by a procedure schematically illustrated in the inserted drawing. The broken curve crossing the NO^+ potential curve is a repulsive portion of the potential curve expected for the $B'^2\Delta$ state, obtained with the present photoelectron data.

IV-E-2 MPI Photoelectron Study of Photoionization of NO Molecule via the Valence Excited State $B'^2\Delta$

Masahiko TAKAHASHI, Katsuhiko OKUYAMA, Katsumi KIMURA

Previously, Achiba, Sato, and Kimura[1] have studied (2+1) MPI photoelectron spectra of NO molecule via the valence excited state $B^2\Pi$ ($v'=9$), indicating that the photoelectron vibrational peaks can be interpreted in terms of electronic autoionization.

In the present work, we have carried out (2+1) MPI experiments, selecting the higher valence excited state $B'^2\Delta$ at the $v'=3$ and 4 levels as resonant intermediates. Photoelectron spectra of this valence state are quite interesting, since one-photon "direct ionization" from the $B'^2\Delta$ valence state to the ground state ion is forbidden in the sense of one-electron Hamiltonian. Figure 1 shows the photoelectron spectrum observed at the main rotational MPI peak in the $B'^2\Delta$ $v'=3$ region.

The calculated Franck-Condon factors between B'-3 (NO) and $X(NO^+)$ are in good agreement with the experimental ones of the $v^+=0$–4 photoelectron peaks, so that these weak bands may be due to direct ionization in spite of two-electron transition. However, the $v^+=7$–9 peaks cannot be explained by direct ionization or the $\Delta v=-1$ autoionization. Electronic autoionization is considered to occur through the repulsive portion of a neutral bound potential. One of possible candidates for this repulsive portion may be the $I^2\Sigma^+$ state.

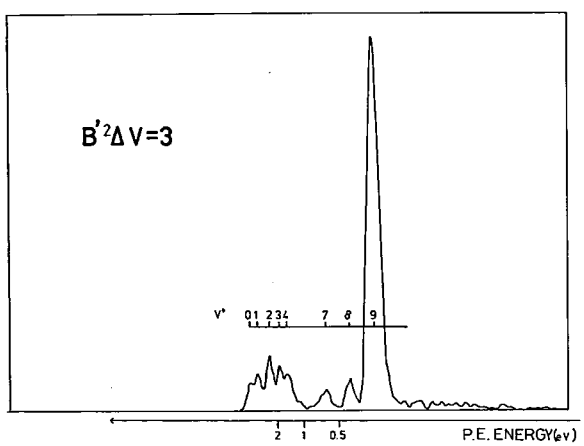

Figure 1. Photoelectron spectrum obtained for the $B'^2\Delta$ $v'=3$ state.

Reference
1) Y. Achiba, K. Sato, and K. Kimura J. Chem. Phys., **82**, 3959 (1985).

IV-E-3 Two-Color MPI Ion-Current Spectrum of Isolated Triplet Pyrazine

Katsuhiko OKUYAMA, Masahiko TAKAHASHI, Shin-ichi NAGAOKA, Katsumi KIMURA, Seigo YAMAUCHI *(Kyoto Univ.)*, **Toshihiro KAMEI** *(Kyoto Univ.)*, **and Minoru HIROTA** *(Kyoto Univ.)*

Application of the MPI spectroscopy to excited triplet molecules is quite attractive. Recently, triplet pyrazine molecule has been studied by means of phosphorescence excitation and one-color (3-photon) MPI techniques.[1)–3)] In the MPI study through its one-photon resonant excited state, however, there would be another possibility of resonance at the 2-photon state.

In the present work, using a two-color technique we have been able to obtain an ion-current spectrum of jet-cooled triplet pyrazine molecule, as shown in Figure 1. Pyrazine was excited to its T_1 state by ω_1, and then ionized by ω_2 (ArF 193 nm). The ion current spectrum resembles the phosphorescence excitation spectrum. The band rotational contour belongs to the parallel type, clearly indicating that the spectrum is due to $T_1(^3B_{3u}(n\pi^*))$ and there is no evidence for existence of other electronic states.

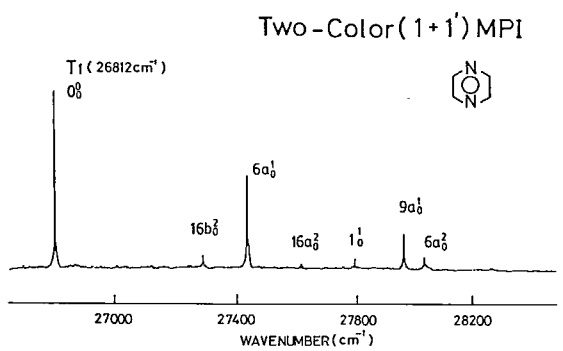

Figure 1. Two-color ion-current spectrum of jet-cooled pyrazine.

Reference
1) J.L. Tomer, K.W. Holtzclaw, and D.W. Pratt, J. Chem. Phys. **88**, 1528 (1988).
2) N. Ohmori, T. Suzuki, and M. Ito, J. Phys. Chem. **92**, 1086 (1988).
3) E. Villa, M. Terazima, and E.C. Lim, Chem. Phys. Letters **129**, 336 (1986).

IV-E-4 Photoelectron Spectrum of Isolated Triplet Pyrazine

Katsuhiko OKUYAMA, Masahiko TAKAHASHI, and Katsumi KIMURA

A laser two-color technique is especially useful for photoelectron spectroscopic studies of excited molecules to obtain their spectroscopic and dynamic informations. In such photoelectron studies, the ionization process of the excited state to be studied should be single-photon ionization.

In the present work, we have carried out photoelectron spectrum measurements for triplet pyrazine molecule, using combining two nanosecond lasers (UV laser and ArF 193-nm laser). Initially we have observed an MPI ion-current spectrum in the T_1 region (see IV-E-3) of this molecule, and then we have measured photoelectron spectra at the T_1 ion-current peak. Figure 1 shows the photoelectron spectrum obtained for the first time for the lowest excited triplet state (T_1:$^3B_{3u}(n\pi^*)$, 0^0 level) of isolated pyrazine, together with possible vibrational assignments of the partially resolved vibrational structure. The energy diagram relevant to the two-step ionization is also shown in Figure 1. The

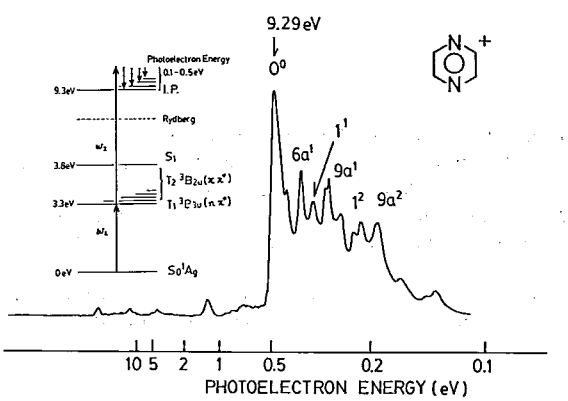

Figure 1. Two-color ionization photoelectron spectrum of jet-cooled pyrazine and the energy level diagram relevant to two-photon two-step ionization.

vibrational assignments shown have been carried out on the basis of the available information of the pyrazine cation.

IV-E-5 Picosecond Pulse Laser Photoelectron Spectra of Some Molecular Excited States

Katsumi KIMURA, Kenji SATO, Katsuhiko OKUYAMA, Masahiko TAKAHASHI

It is quite attractive to employ a picosecond pulse UV laser in photoelectron spectroscopy to study the excited-state dynamics of molecules. Excited-state photoelectron spectra have been obtained successfully with a picosecond pulse laser at the Rydberg A state (v'=2) of ammonia and at different vibronic levels of the first singlet state of benzene in jets at 208.8, 228.7, and 252.7 nm. Some spectra are possibly assigned to resonant/non-resonant ionization before and after vibrational relaxation.

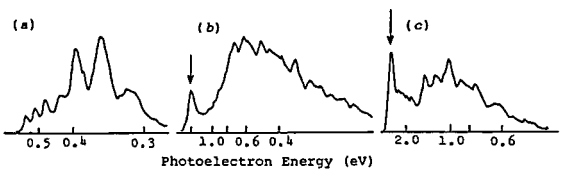

Figure 1. The picosecond photoelectron spectra of the benzene S_1 state. (a) λ = 252.7 nm, the $6^1 1^1$ level; (b) λ = 228.7 nm, the $6^1 1^4$ level (4200 cm^{-1}); (c) λ = 208.8 nm, a higher vibronic level (8300 cm^{-1}). Arrows show the 2-photon non-resonance.

Photoelectron spectra obtained by (1+1) resonant ionization through the S_1 state of benzene at 252.7, 228.7, and 208.8 nm are shown by spectra (a–c) in Figure 1.

IV-E-6 Resonant MPI Photoelectron Study on Direct Ionization and Autoionization of Nitric Oxide Molecule

Katsumi KIMURA and Yohji ACHIBA *(Tohyo Metropolitan Univ.)*

[Advances in Multiphoton Processes and Spectroscopy, in press]

One of the most puzzling and confusing problems in MPI photoelectron studies of nitric oxide is the observation of slow photoelectrons which sometimes appear in (n+1) and (n+2) MPI experiments. From a systematic comparison of the photoelectron data so far published for nitric oxide, recently the present authors have realized that information about slow photoelectrons is an important key to understand the electronic autoionization processes of this molecule.

In this review article, we have surveyed mainly the excited-state photoelectron studies of nitric oxide molecule, paying special attention to the formation of slow photoelectrons. Our interpretation for the slow electron formation have been described in connection with electronic autoionization.

IV–F Synchrotron Radiation Researches of Molecules and Molecular Clusters: Photoionization and Photoelectron Spectroscopy

The use of synchrotron radiation from the 750-MeV Electron Storage Ring (UVSOR) of this Institute is attractive for studying higher electronic states and various ionic states of gaseous molecules and molecular clusters by photoionization and photoelectron spectroscopy, because of its continuous character of the radiation in the wide VUV region. Therefore we have recently completed the construction of our molecular-beam apparatus on beamline BL2B2 in the UVSOR Facility. In this experimental station, we are using a multi-stage differential pumping system, so that no window materials are used between the molecular-beam apparatus and the storage ring.

In this project we have carried out synchrotron radiation photoionization experiments with our molecular-beam apparatus in which molecular clusters are produced in supersonic jets.

IV-F-1 Synchrotron Radiation Apparatus for Supersonic-Jet Experiments

Katsumi KIMURA, Yohji ACHIBA *(Tokyo Metropolitan Univ.)*, **and Haruo SHIROMARU** *(Tokyo Metropolitan Univ.)*

Supersonic molecular beams have been widely used in studies of molecular complexes such as van der Waals complexes or molecular clusters by VUV sources. Photoionization experiments of moleular complexes by SR (synchrotron radiation) are quite attractive, because of its continuous character with respect to the wavelength. The SR source is ideal to measure photoionization efficiency (PIE) curves and threshold photoelectron spectra as a function of the wavelength in a wide VUV region.

The 750-MeV electron storage ring (UVSOR) of the Institute for Molecular Science has been dedicated to synchrotron radiation studies in the field of molecular science. Under such circumstances, we have constructed a molecular-beam photoionization apparatus in the UVSOR Facility for studying molecular complexes in the gas phase.

In the present paper we have described the layout of our VUV beamline including a VUV monochromator and a molecular-beam photoionization apparatus. This experimental system has recently been completed. Several experimental results are also demonstrated to show the characteristics of the apparatus.

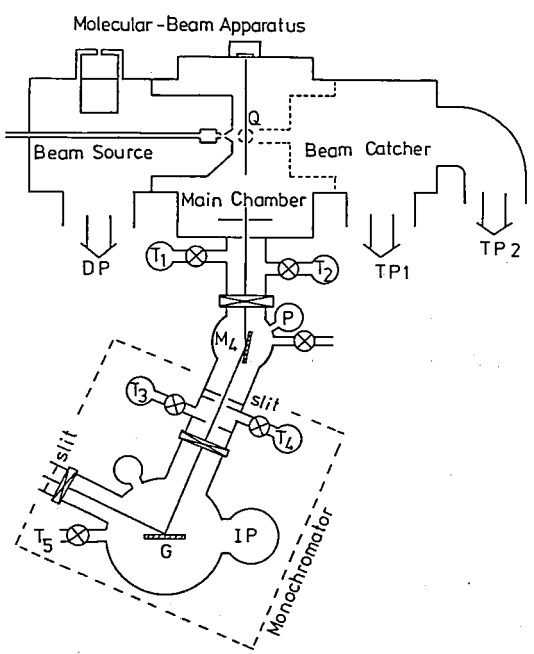

Figure 1. The VUV monochromator and the molecular-beam apparatus.

IV-F-2 Synchrotron Radiation Study on Small Binary Molecular Clusters. Ar-Water and CO_2-Water Systems

Haruo SHIROMARU, Hideyuki SUZUKI *(Mi'e Univ.)*, **Hiroyasu SATO** *(Mi'e Univ.)*, **Shin-ichi NAGAOKA, and Katsumi KIMURA**

[*J. Phys. Chem.*, in press]

With synchrotron radiation we have carried out measurements of photoionization mass spectra and photoionization efficiency (PIE) curves for Ar-water and CO_2-water binary clusters produced in a supersonic jet. From the mass spectra obtained for the CO_2-H_2O system at 60 nm, we have detected the following cluster ions: $[(H_2O_m]^+$ (m = 1–5), $[(H_2O)]_mH^+$ (m = 1–5), $[(CO_2)_m]^+$ (m = 1, 2), $[(CO_2)_m(H_2O)_n]^+$ (m = 1; n = 1,

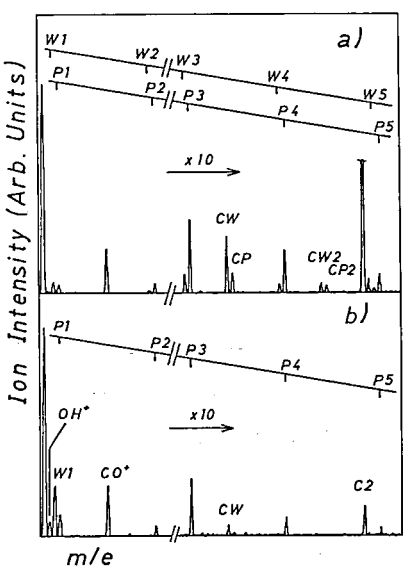

Figure 1. Photoionization mass spectra obtained in supersonic jets of CO_2-seeded water mixtures at 60 nm at different stagnation pressures of CO_2: (a) 3.9 atm, (b) 1.3 atm. No optical filters were used in the mass-spectrum measurements. The peak assignments are indicated by: $W_n = [(H_2O)_n]^+$, $P_n = [(H_2O)_n]H^+$, $C_n = [(CO_2)_n]^+$, $CW_n = [(CO_2)(H_2O)_n]^+$, $CP_n = [(CO_2)(H_2O)_n]H^+$. (A strong peak due to $[CO_2]^+$ is omitted.)

2), $[(CO_2)_m(H_2O)_n]H^+$ (m = 1; n = 1, 2).

The PIE curves of producing several neat and mixed water cluster ions for the Ar-H_2O system show monotonically increasing tendency in the 75–100 nm region, whereas the corresponding PIE curves obtained for the CO_2-H_2O system mostly show broad peaks due to photoionization of the CO_2 site. From such differences between the two system, it has been suggested for the CO_2-H_2O system that intra-cluster charge transfer takes place from the CO_2 site to the H_2O site before the formation of the neat and mixed water cluster ions.

Evaporation processes of the neat and mixed water clusters have been discussed.

IV-F-3 Threshold Photoelectron-Ion Coincidence Technique for Synchrotron Radiation Study of Gaseous Atomic and Molecular Clusters

Takato HIRAYAMA, Shin-ichi NAGAOKA and Katsumi KIMURA

We have designed and constructed a threshold-electron photo-ion coincidence (TEPICO) spectrometer for studying the photoionization processes of atomic and molecular clusters by synchrotron radiation. This spectrometer has been installed in the molecular-beam apparatus on the beamline BL2B2 (with a 1-m Seya-Namioka monochromator) in the UVSOR Facility. Application of the TEPICO technique to the synchrotron radiation photoionization study of a cluster system is particularly useful, as the cluster system contains various cluster components with different masses.

Although there are several methods of measuring threshold photoelectron spectra, in the present work we have adopted an angular discrimination technique using a capillary array plate (HAMAMATSU PHOTONICS), in which each hole is 12 μm in diameter and 1 mm in length.

Figure 1 shows our preliminary result of the threshold photoelectron spectrum of O_2 in the wavelength region 65–80 nm, clearly indicating vibrational bands of O_2^+.

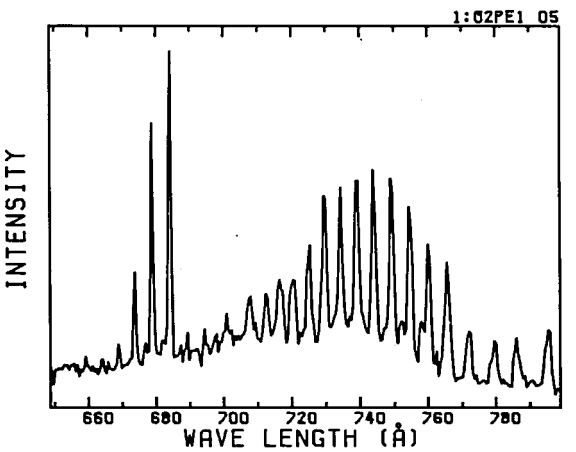

Figure 1. Threshold electron spectrum of O_2 in the wavelength range 65 – 80 nm.

IV–G Production, Characterization, and Spectroscopic Studies of Molecular Complexes and Clusters

There are several techniques to investigate physics and chemistry of molecular complexes and clusters. One of the most powerful techniques for producing such weakly bound complexes is supersonic expansion of a high pressure gas through a small nozzle hole, by which one can produce a large numbers of exotic molecules. However, quantitative characterization of van der Waals complexes is hard because of its weak bonding character.

In this project we apply laser induced fluorescence spectroscopy combined with a nanosecond time resolved fluorescence technique to study dynamics of electronically excited rare gas clusters and solvated molecules of substituted anthracenes produced in a free jet expansion.

IV-G-1 Vibronic-Level Specific Heavy Atom Effect on the Fluorescence Decays of the Rare-Gas Complexes of 9-Methoxyanthracene

Satoshi HIRAYAMA *(Kyoto Inst. of Tech.)*, **Fujio TANAKA** *(Univ. of Osaka Prefecture)*, **and Kosuke SHOBATAKE**

[*Chem. Phys. Lett.* in press]

Van de Waals complexes of 9-Methoxyanthracene (MEOA) with Ar, Kr, and Xe formed in supersonic free jets are studied by laser induced fluorescence spectroscopy and fluorescence decay measurements. The fluorescence decay features of these rare-gas complexes vary widely depending on their number of the coodinated atoms as well as the vibronic levels of MEOA. The heavy atom effect noticed for the Kr and Xe complexes in the electronic origin is manifested more strongly in the vibrationally excited 12_0^1 and 12_0^2 levels which are 383 and 853 cm^{-1}, respectively, above the 0_0^0 origin. The excitation to the 12_0^3 (or 8_0^1) (1157 cm^{-1} above 0_0^0 origin) and 6_0^1 levels (1402 cm^{-1}) is found to yield non-exponential fluorescence decays with long-lived components (15–25 ns), the lifetimes of which are comparable to those of bare MEOA molecules. These findings are explained in terms of vibrational predissociation of the 1:1 complexes.

IV-G-2 Fluorescence Decays of 9,10-Dichloroanthracene and its van der Waals Complexes with Rare gas Atoms in Supersonic Free Jets

Fujio TANAKA*, Shigeru YAMASHITA* *(Univ. of Osaka Prefecture)*, **Satoshi HIRAYAMA**, Akiho ADACHI**** *(Kyoto Inst. of Tech.)*, **and Kosuke SHOBATAKE**

The fluorescence lifetimes of 9,10-dichloroanthracene (DCA) and its van der Waals complexes with Ar, Kr, and Xe atoms were measured in supersonic free jets. For bare DCA the origin of the S_1 state ($S_1(0)$) shows a long lifetime of 24.8 ns while the 403 cm^{-1} band undergoes intersystem crossing (ISC) to a nearby triplet state (T_n) as implied by its shortened lifetime of 13.1 ns. The electronic origin of T_n is located between $S_1(0)$ and 403 cm^{-1} levels. The fluorescence lifetime shows an oscillatory dependence on the excess vibrational energy (E_v) up to *ca.* 1200 cm^{-1} while it becomes very short in the range of $E_v > 1390$ cm^{-1}. This oscillatory behavior is discussed in terms of the Franck-Condon factor between the S_1 vibrational level and the isoenergetic T_n vibrational level in the sparse level structure. The electronic origins of the vdW complexes show long lifetimes, nearly the same as the bare DCA. The absence of the heavy atom effect on the ISC for the vdW complexes in a low E_v range is explained by a microscopic solvent shift and relaxation. The fluorescence decays of the vdW complexes with 1390 cm^{-1} or higher E_v become dramatically slow in comparison with those of the corresponding bare bands. It is suggested from a nonexponential fluorescence decay that the fragments DCA produced by vibrational predissociation are distributed among two or more vibrational levels. The fragment complexes DCA-Xe_m produced from predissociation of DCA-Xe_n ($m<n$) also do not exhibit the heavy atom effect on the ISC.

IV–H Molecular Beam Studies of Chemical Reaction Dynamics

In this project we investigate the dynamics of (1) chemical reactions involving reactive species such as N, B, O, and C atoms, (2) dissociative excitation transfer reactions involving metastable rare gas atoms, and (3) molecule-molecule reactions, using a crossed molecular beams technique. For the studies of (1) and (2) chemiluminescence spectroscopy is applied. For the study of dynamics of molecule-molecule reactions a crossed molecular beams apparatus with a rotatable mass spectrometer detector is used.

IV-H-1 Crossed Molecular Beam Study of Dynamics of Molecule-Molecule Reaction: $C_6D_6 + F_2 \rightarrow C_6D_6F + F$

Ye WEN, J. Robb GROVER *(Brookhaven Natl. Lab. and IMS)*, **Yuan T. LEE** *(Univ. of Calif., Berkeley and IMS)*, **Kiyohiko TABAYASHI, and Kosuke SHOBATAKE**

The endoergic molecule-molecule reaction

$$C_6D_6 + F_2 \rightarrow C_6D_6 + F$$

is investigated by a crossed molecular beam scattering technique over a collision energy range from 15 to 31 kcal/mol. The collision energy was controlled by changing the stagnation temperatures of the two reactant beams. The TOF velocity distributions of the product, C_6D_6F, were measured at the parent mass (m/e=103) for two nominal collision energies, 26.0 and 31.0 kcal/mol. The angular and the TOF distribution data were analyzed, assuming that the product center-of-mass (c.m.) differential cross section is represented by the product of the angular- and energy- dependent distribution functions. Figure 1 illustrates the deconvoluted contour diagrams of the C_6D_6F products produced for the two collision energies. From the contour diagrams it is clear that the reaction proceed via a direct mechanism, the C_6D_6F product being forward scattered, and that the anisotropy increases as the collision energy is raised. The dependence of the total reactive cross section upon c.m. collision energy and the internal energy of C_6D_6 as measured at two masses, m/e=103 (parent) and 101 (daughter $C_6D_5F^+$ ion) indicates that the internal energy of C_6D_6 molecule enhances the reaction than the collision energy.

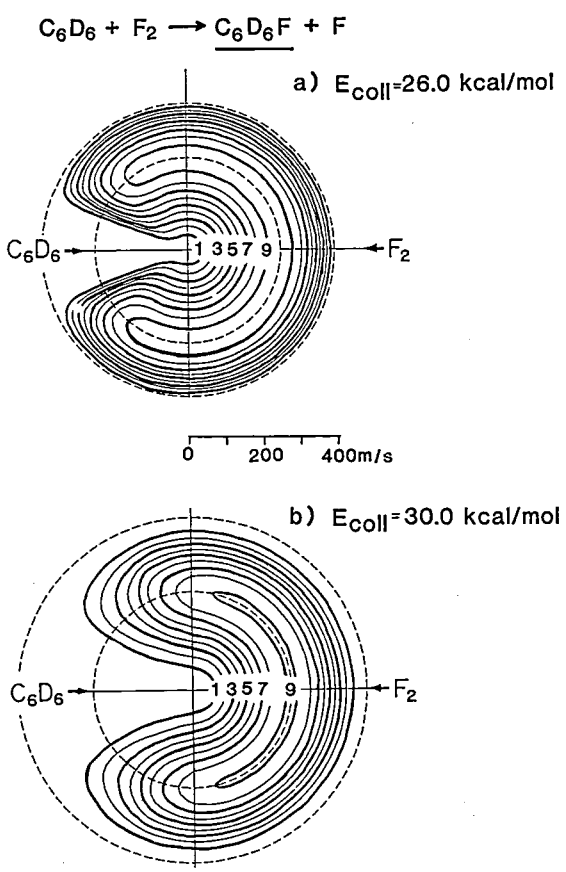

Figure 1. Product contour diagrams of C_6D_6F formed from the reactive collision of F_2 with C_6D_6 at two c.m. collision energies, (a) 26.0 kcal/mol and (b) 31.0 kcal/mol. The center-of-mass scattering angle θ = 0 degree corresponds to the forward scattering of C_6D_6F product relative to the incident c.m. F_2 velocity.

IV-H-2 Microwave Discharge Plasma Beam Source for Production of Active Species.

Kiyohiko TABAYASHI and Kosuke SHOBATAKE

We have constructed a new beam source for production of active species such as atoms and free radicals with translational energies in the sub-eV region. Here, the new beam source employs a microwave plasma discharge of a dilute mixture of molecules in rare gas at relatively high pressures (< 200 Torr). A cross sectional view of the microwave discharge source is shown in Figure 1.

So far a variety of atomic beams, O, N, H, C, etc, have been successfully generated from the admixed

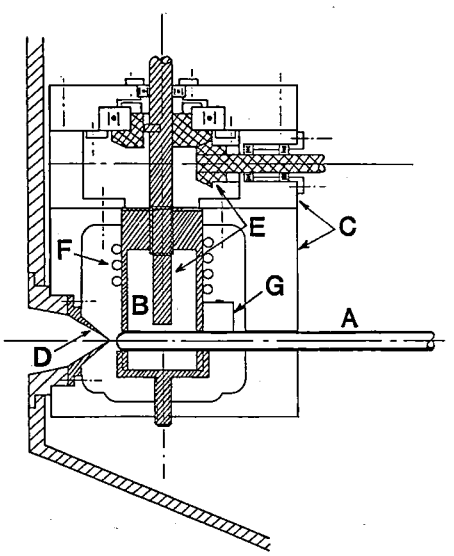

Figure 1. Microwave discharge beam source.
(A) discharge nozzle-tube, (B) microwave cavity, (C) supporting frame, (D) skimmer, (E) tuning electrode and its driving-shaft assembly, (F) water cooling tube, (G) MW power connector.

molecules with high degrees of dissociation. Although the beam stagnation temperature does not exceed 2500 K, average translational enegies can be varied by a proper choice of buffer gas. Under our normal operation conditions (80 W input), atomic beams with average translational energies up to 0.6 eV and Mach number < 5 have been easily produced when He is used as a buffer gas. From the intensity levels of crossed beam-chemiluminescence observed by using this beam source, we find that it is also applicable for production of electronically excited species, eg. metastables of rare gas and nitrogen atoms.

IV–I Vacuum UV Photochemistry of Molecules and Clusters

Photochemistry by vacuum UV (VUV) light has recently become a very active field owing to the rapid progress in and the relatively easy access to the VUV light sources such as synchrotron orbital radiation (SR) and VUV laser as well as conventional atomic resonance lines. In the present project we seek to obtain more detailed information about, 1) photodissociation dynamics of simple molecules, 2) production of emitting species from highly excited molecules, and 3) excited states of clusters formed in a supersonic free-jet, applying absorption and fluorescence (polarized-) spectroscopy by means of the tunable, stable, and polarized VUV light from SR.

IV-I-1 Photochemistry of CCl_3F and CCl_2F_2 in the 106–200 nm Region

Toshio IBUKI *(Kyoto Univ.)*, **Atsunari HIRAYA** *(UVSOR)*, **and Kosuke SHOBATAKE**

The photoabsorption cross section and fluorescence excitation spectra of CCl_3F and CCl_2F_2 were measured using SR at 106–200 nm. The observed absorption bands were accounted as Rydberg transitions. The emission was attributed to $CClF(\tilde{A}^1A'' \rightarrow \tilde{X}^1A')$ and CF_2 $(\tilde{A}^1B_1 \rightarrow \tilde{X}^1A_1)$ transitions, respectively, and their radiative lifetimes were found to be 635 ± 35 and 58 ± 2 ns. The fluorescence excitation spectra of CCl_3F and CCl_2F_2 indicated that the electronically excited CClF and CF_2 radicals are formed by the elimination reaction of Cl atoms but not by the molecular Cl_2 releasing process. In the $CClF(\tilde{A} \rightarrow \tilde{X})$ transition the occurence of collision-induced intersystem crossing between the excited $^1A''$ and the lower $^3A''$ states of CClF radical was suggested.

IV-I-2 Photoexcitation of $M(CH_3)_2$ (M = Zn, Cd, Hg) Compounds in the 106–270 nm Region

Toshio IBUKI *(Kyoto Univ.)*, **Atsunari HIRAYA** *(UVSOR)*, **and Kosuke SHOBATAKE**

The photoabsorption cross sections and Fluores-

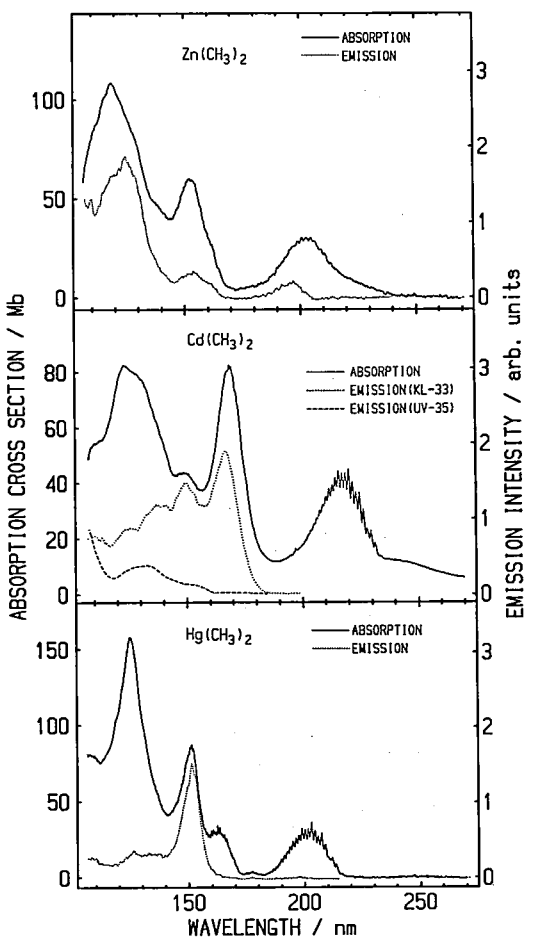

Figure 1. Absorption and fluorescence excitation spectra of $Zn(CH_3)_2$ (top), $Cd(CH_3)_2$ (middle) and $Hg(CH_3)_2$ (Bottom) at 106–270 nm.

cence excitation spectra of group IIb dimethylmetals were measured using synchrotron radiation at 106–270 nm. The observed absorption bands were accounted for in terms of Rydberg transitions. The fluorescence spectra of $MCH_3(\tilde{A}^2E–\tilde{X}^2A_1)$ transitions were observed and the radiative lifetimes determined were 41 ± 2 and 54 ± 2 ns for M = Zn and Cd, respectively. The excited M(np $^3P_0^1$) atoms were detected in the photolyses of demethylcadmium and dimethylmercury but not in dimethylzinc. The formations of $MCH_3(\tilde{A}^2E)$ and M(np $^3P_0^1$) states are characteristic for the Rydberg excitations of the C-H in methyl and M-C bonding electrons, respectively.

IV-I-3 Photodissociation Dynamics of HCN in the 105–125 nm Range

Takashi NAGATA*, Tamotsu KONDOW* *(*Univ. of Tokyo)*, **Kozo KUCHITSU** *(Tech. Univ. of Nagaoka)*, **Atsunari HIRAYA** *(UVSOR)*, **and Kosuke SHOBATAKE**

Photodissociation of hydrogen cyanide

$$HCN + h\nu \rightarrow (HCN)^* \rightarrow H + CN(B^2\Sigma^+),$$

was studied by measurements of absorption, fluorescence excitation, and optical polarization of subsequent CN(B-X) emission in the wavelength range from 105 to 125 nm. The dispersed SR was introduced through a LiF window along the Z axis into a flow cell containing HCN gas of ~20 mTorr. Its polarization vector was parallel to the X axis. Emission from the product CN(B) radical was collected in the direction of the Y axis. The emission intensities polarized along the X and Z axes, denoted as I_X and I_Z respectively, were measured by use of a photoelastic modulator (HINDS).

Figure 1 shows the observed degree of polarization P, defined by $P = (I_x - I_z)/(I_X + I_Z)$ of the CN(B-X) emission as a function of the wavelength of the incident radiation along with the absorption and the fluorescence excitation spectra. The prominent peaks appearing in the absorption spectrum were assigned to Rydberg transitions where the 1π electron is excited to the $3s\sigma$, $3p\sigma$ and $3d\sigma$ highlying valence states. Positive polarization was observed in the entire wavelength range studied. Below 116 nm, the polarization varies almost smoothly with the wavelength, while above 116 nm the polarization curve shows two minima which coincide with the absorption bands of the 1π–$3s\sigma$ Rydberg transition. The positive values of P below 116 nm indicate that the high-lying valence states belong to A′ symmetry. In case of direct dissociation, P should be 1/7. The observed values of P, which are smaller than 1/7, are explained by depolarization due to predissociation. The predissociation lifetime of the valence states was estimated to be 0.1–0.3 ps from the degree of depolarization. The minima at 118 and 122 nm result from the fact that the $(1\pi)^3$ Rydberg state has a linear geometry of Π symmetry.

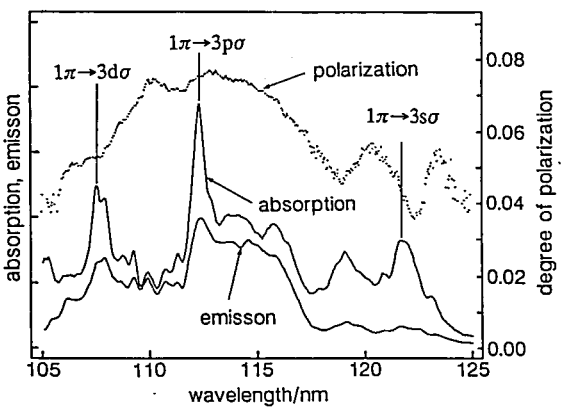

Figure 1. Absorption, fluorescence excitation and polarization spectra of CN(B–X) radicals formed from photodissociation of HCN.

IV-I-4 Direct Absorption Spectrum of Benzene in a Free Jet

Atsunari HIRAYA *(UVSOR)* **and Kosuke SHOBATAKE**

Direct absorption spectra of benzene in a supersonic free-jet have been obtained, for the first time, in the wavelength range of the S_1, S_2, S_3 and up to the first ionization limit by using SOR as a light source. Figure 1 shows a direct absorption spectrum of jet-cooled benzene seeded in He. The absolute value of molar extinction coefficient (ε) was determined by normalizing the value at 200.1nm band of the S_2 to that measured in room temperature vapor, assuming the invariance of absorption coefficient in both conditions for such a broad band. In the S_1 region, the vibrational progression of $6_0^1 1_0^n$ (n = 0–4) is observed without any

congestions arose from vibrationally hot-bands. The maximum value of ε for the S_1 in this spectra (spectral bandwidth = 0.065nm) is 1430 at 252.9nm ($6_0^1 1_0^1$), which is fairly larger than that in room temperature vapor.

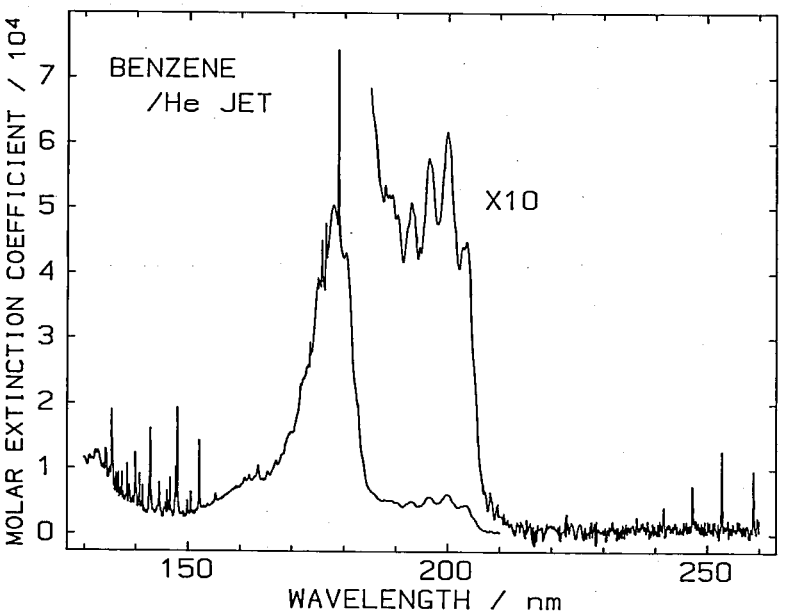

Figure 1. Absorption spectrum of benzene seeded in a He supersonic free-jet (total stagnation pressure 400 Torr). Spectral bandwidth is 0.065nm.

IV-I-5 Absorption Spectra of Benzene Clusters in a Free Jet

Atsunari HIRAYA *(UVSOR)* **and Kosuke SHOBATAKE**

Absorption spectra of benzene clusters have been observed, for the first time, in a supersonic free jet using SOR. Figure 1 shows absorption spectra of benzene in the free jets under different conditions: (a) without carrier gas, (b) with 653 Torr Xe as a carrier gas. The spectrum (a) obtained without carrier gas is quite similar to that for room temperature vapor. In the spectrum (b) obtained with carrier gas, absorption starts to appear at longer wavelength (218nm) than the spectrum (a) and increases monotonically toward shorter wavelength while the spectrum (a) exhibits rather flat region at about 190nm. By subtracting spectrum (a) from (b), with appropriate factors (0.84) to cancel out the vibrational structures in spectrum (b), a spectrum (c) is obtained. This difference spectrum shows two broad absorption bands with maxima at 186 and 207nm. There are two candidates for the absorbing

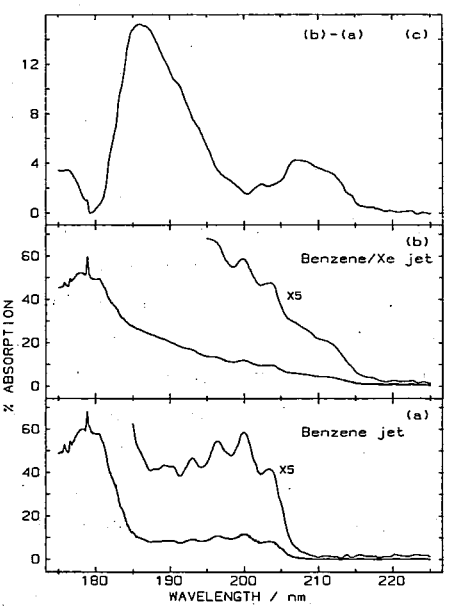

Figure 1. Absorption spectra of benzene and its clusters in a supersonic free-jet. Spectral bandwidth is 0.2nm: (a) 107 Torr benzene without carrier gas, nozzle temperature = 20°C, (b) with 653 Torr Xe gas (total 760 Torr), nozzle temperature is 21.6°C. Difference spectrum (c) is obtained by subtracting spectrum (a) with scaling factor of 0.84 from spectrum (b).

species which gives these broad absorption bands in difference spectrum, one is benzene cluster and another is benzene-Xe cluster. However, these broad bands are also found in the difference spectra for both He and Ar carrier with the same feature as observed for Xe carrier. Therefore, the observed two broad absorption bands are assigned, at least as the major species, to the benzene clusters not to the benzene-rare gas clusters. By comparing spectrum (a) and (c), the red-shift of absorption transition by cluster formation are estimated to be about 1700 cm^{-1} for both the S_2 and S_3 electronic states.

IV–J Synchrotron Orbital Radiation-Assisted Surface Reactions

Synchrotron orbital radiation (SR) is still a new light beam source from the viewpoint of promoting chemical reactions on solid surfaces although lithography of resist materials by means of SR has been known for about a decade. We have initiated the title project in order to explore the possibilities of promoting surface reactions or making new types of thin films using SR as a light source, and furthermore to understand the mechanisms of photochemical reactions which occur on solid surfaces. The experiments are done using an apparatus for photochemical surface reaction installed on the Beam Line BL8A at UVSOR facility. The unfocused synchrotron radiation is irradiated upon the solid sample at 5.85 m from the souce point.

IV-J-1 Synchrotron Radiation-Assisted Etching of SiO_2 by SF_6. Quantum-Yield of Etching

Kosuke SHOBATAKE, Nobuo HAYASAKA, Haruo OHASHI *(Toyohashi Univ. of Tech.)*, **Hiroshi KUME** *(Niigata Univ.)*, **and Kiyohiko TABAYASHI**

Synchrotron radiation assisted-etching of SiO_2 surface has been studied using unfocused SR as a light source and SF_6 as an echant. This process has been studied by Urisu and Kyuragi[1] using focused SR for the pressure range 10^{-4}–0.12 Torr of SF_6. The merit of our experiment is that one can estimate the absolute number of photons which are irradiated upon the SiO_2 sample. Figure 1 shows the etching rate (Å/min·mA) against the SF_6 pressure along with the data obtained by Urisu and Kyuragi. Since the number of photons irradiated upon the SiO_2 crystal surface of 3 mm in diameter is calculated to be 1.0 x10^{13} photons per min·mA stored current. The fraction of SiO_2 removed per irradiated photon below 1600Å is estimated from the right-hand scale of ordinate in Figure 2. The results indicate that, because the etching rate does not depend on the SF_6 pressure, i.e. the concentration of radical species such as F atoms in the range of higher pressures (P>0.1 Torr), the rate determining step for the etching reaction is the removal of the adsorbed molecule as the result of irradiation.

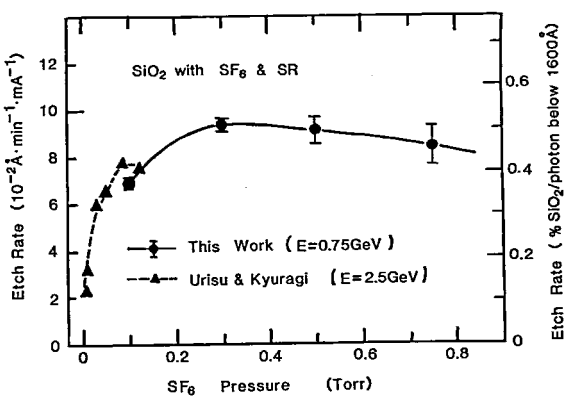

Figure 1. SR-assisted etching rate of SiO_2 against vapor pressure of SF_6. The unit of the left-hand ordinate is Å per min·mA stored current. The unit of the right-hand ordinate is % SiO_2 removed per photon at the wavelengths below 1600 Å.

Reference

1) T. Urisu and H. Kyuragi, *J. Vac. Sci. Technol.* **B5**, 1436 (1987)

IV-J-2 Synchrotron Radiation-Assisted Etching of Various Si Samples Using Cl_2, SF_6 and NF_3

Kosuke SHOBATAKE, Nobuo HAYASAKA, Haruo OHASHI *(Toyohashi Univ. of Tech.)*, **Hiroshi KUME** *(Niigata Univ.)*, **and Atsunari HIRAYA** *(UVSOR)*

Synchrotron radiation-assisted eching of various

samples of Si semiconductor materials is studied using Cl_2, SF_6, and NF_3 as echant gas. The unfocused SR with or without a Ti filter is irradiated upon the solid sample 5.85 m from the source point. The etching rate is determined by measuring the depth of etched material. Figure 1 shows the cross section of an etched sample of P-doped amorphous Si (n^- Si) using SF_6 as an echant at a pressure of 0.5 Torr. The result for SiO_2 is also illustrated to show the difference between the etching behaviors for the two samples, n^- Si and SiO_2. The mechanisms of synchrotron radiation-assisted etching reactions are being studied.

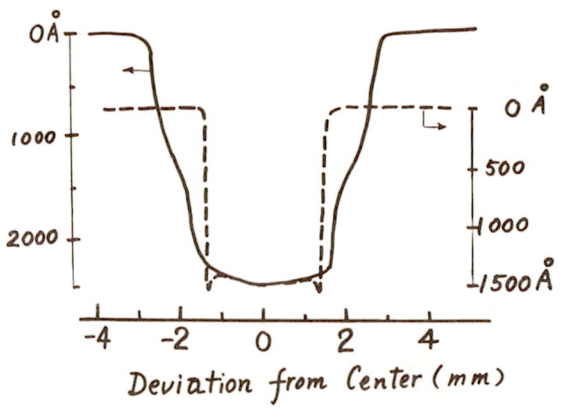

Figure 1. The cross sectional profile of n^- poly Si surface etched with unfiltered SR and SF_6 gas at 0.5 Torr (——) along with that of SiO_2 etched with unfiltered SR and SF_6 at 0.5 Torr (.....).

IV-J-3 Synchrotron Radiation-Assisted Deposition of Carbon Films

Haruhiko OHASHI*, Katsushi INOUE*, Yoji SAITO*, Akira YOSHIDA*, *(Toyohashi Univ. of Tech.)*, **Hiroshi OGAWA** *(Saga Univ.)*, **and Kosuke SHOBATAKE**

Photo-chemical vapor deposition from n-butane at room temperature successfully formed carbon film for the first time using SR as a light source. Emissions from a light-green glow of the source gas irradiated by the unfiltered SR are assigned to the electronically excited CH and C_2 molecules, and H atom (which are formed by photochemical processes). The IR spectra of the deposited films show that they are hydrogenated amorphous carbon films with sp^3 hybridization. The positive ions formed by photoionization are found to be effective in depositing films. Figure 1 illustrates a scanning electron micrograph (SEM) of the carbon film formed.

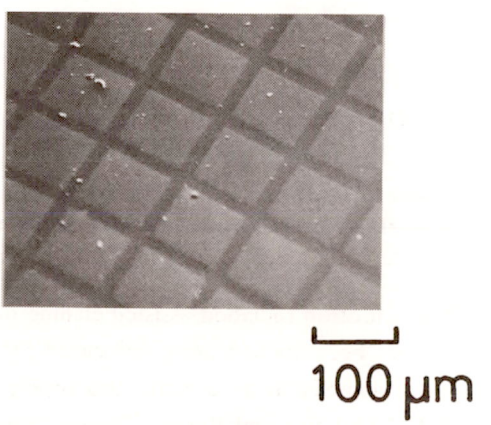

Figure 1. The SEM immage of the carbon film formed on a single crystal of Si. The Ni mesh with 100 μm mesh unit and 20 μm wire size is used. Only the irradiated area through the mesh (80 μm square) has deposit of carbon film. The thickness of the deposited film is 2000 Å.

IV–K Black Phosphorus

Black phosphorus is a layered structure semiconductor. We have prepared iodine intercalated compounds of black phosphorus and revealed their metallic character. Recently, inclusion or doping of silicon, gallium, or germanium to black phosphorus has been undertaken.

IV-K-1 Electrical Conductivities of Black Phosphorus-Silicon Compound

Yusei MARUYAMA, Tamotsu INABE, Toshifumi NISHII *(Mitsubishi Peterochemical Co. Ltd.)*, **Lin HE** *(General Institute for Colored Metal, China and IMS)*, **Anthony John DANN** *(Univ. of Nottingham and IMS)*, **Ichimin SHIROTANI** *(Muroran Inst. of Technology and IMS)*, **Michael Richard FAHY** *(Univ. of Nottingham and IMS)*, **and Martin Richard WILLIS** *(Univ. of Nottingham)*

[*Synth. Metals*, in press]

A new material, black phosphorus-silicon compound has been prepared, and the temperature dependence of its electrical conductivity has been measured at low temperature region. Silicon atoms are included in black phosphorus in the course of single crystal preparation by a bismuth-flux method. Silicon ion implantation has been also tried to introduce much amount of silicon atoms into the surface of black phosphorus single crystals. The electrical resistivities of the some samples prepared by a bismuth-flux method and ion implantation technique show somewhat metallic character at low temperatures, just like the iodine intercalated black phosphorus. Moreover, some of them exhibit a sharp drop of the resistivity at around 1.5 K. Temperature dependence of the thermoelectric power of the crystals is also definitely different from that of pure black phosphorus. The electron accepting character of the doped silicon may be effective for these effects.

IV–L Ultra-Thin Organic Multi-Layer Films Prepared by the Molecular Beam Epitaxy Technique

As a strategy for the development of new types of organic materials, we have undertaken the fabrication of ultra-thin organic multi-layer films with the "MBE" technique. We are expecting new types of charge transfer compounds and/or intercalation compounds (hybrid compounds), and also the realization of novel low-dimensional properties in such materials. As the first step of the study, we have prepared ultra-thin well-oriented monolayers on several substrates.

IV-L-1 Ultra-Thin Organic Layers Prepared by the Molecular Beam Epitaxy Technique

Hajime HOSHI, Anthony John DANN *(Univ. of Nottingham and IMS)*, **Yusei MARUYAMA, Tamotsu INABE, and Martin Richard WILLIS** *(Univ. of Nottingham)*

μ-bridged (-F-) metallo (Al) phthalocyanine polymer films have been deposited on silicon, quartz, KCl, KBr, NaCl, and KI, and characterized by a variety of techniques including ESCA, SEM, TEM, X-ray diffraction, UV-VIS and IR spectroscopy. It has been found out that epitaxially-grown crystalline films are obtainable on alkali halide substrates. The next step for multi-layer film preparation is now in progress.

IV-L-2 Electrical and Optical Properties of Ultra-Thin Phthalocyanine Polymer Films

Anthony John DANN *(Univ. of Nottingham and IMS)*, **Hajime HOSHI, Yusei MARUYAMA, Tamotsu INABE, and Martin Richard WILLIS** *(Univ. of Nottingham)*

The films grown by the MBE technique are studied by transmission spectroscopy. Differences in the IR properties are found for films grown on different substrates reflecting the orientation of the molecule on the surface. New absorption is found in the visible region due to a constrained pseudomorphic layer at the substrate-film interface. The electrical properties of the films are studied in-situ using the DC technique.

IV–M Preparation and Characterization of Metal Oxide High T_c Superconductor Films

After the discovery of novel high T_c superconductors, a lot of works including the film preparation have been carried out. We also have started to fabricate thin films of such superconductors by a sputtering method with the purpose of searching out new compositions, structures, and elements for higher T_c superconductivity.

IV-M-1 Thin Films of the Y-Ba-Cu-O and the Bi-Sr-Ca-Cu-O Systems Prepared by RF-Magnetron Sputtering

Yoichiro KAWAI *(Toyota Motor Corp. and IMS)*, **Yusei MARUYAMA, Toshifumi TERUI*, and Ichimin SHIROTANI*** *(*Muroran Inst. of Technology and IMS)*

[*Synth. Metals*, in press]

Thin films of both the Y-Ba-Cu-O and Bi-Sr-Ca-Cu-O systems have been prepared by RF-magnetron sputtering using targets which are composed of simply mixed powders of each component material. Superconductivity has been observed in both systems without any post-heat treatment. The highest critical temperatures for zero resistivity in each system were 77 K and 31 K, respectively.

IV–N Synthesis and Electrical Properties of Organic Conductors

In order to obtain the knowledge required for the future development of new organic conductors, charge-transfer complexes of OCNAQ and AzaTCNQ have been prepared and their structures and electrical properties have been studied. Also, some electrical properties of a new organic superconductor, $(BEDT\text{-}TTF)_2Cu(NCS)_2$, have been examined.

IV-N-1 A Twin-TCNQ-Type Acceptor. Synthesis of 11,11,12,12,13,13,14,14-Octacyano-1,4:5,8-anthradiquinotetramethane and Structures of the Tetraethylammonium Salts of Its Mono- and Dianion

Tsutomu MITSUHASHI *(Univ. of Tokyo)*, **Midori GOTO** *(Nat. Chem. Lab. for Industry)*, **Kazumasa HONDA** *(Nat. Chem. Lab. for Industry)*, **Yusei MARUYAMA, Tamotsu INABE, Tadashi SUGAWARA** *(Univ. of Tokyo)* **and Tokuko WATANABE** *(Tokyo Univ. of Fisheries)*

[*Bull Chem. Soc. Jpn.*, **61**, 261 (1988)]

The title compound (OCNAQ) was synthesized. Treatment of 1,2,3,4,5,6,7,8-octahydroanthracene with *N*-bromosuccinimide (NBS) under irradiation using a 100-W light bulb in refluxing CCl_4 followed by dicyanomethylation with excess of $NaCH(CN)_2$ in Me_2SO gave an isomeric mixture of 1,4,5,8-tetrakis(dicyanomethyl) derivatives. The mixture was subjected by repetition of the successive bromination-dehydrobromination procedure giving OCNAQ in 20% overall yield. The cyclic voltammogram of OCNAQ exhibits four redox waves ($E_{1/2}^1$ 0.26, $E_{1/2}^2$ 0.05, $E_{1/2}^3$ −0.44, and $E_{1/2}^4$ −0.53 V vs. SCE in MeCN), indicating that OCNAQ is a stronger acceptor than tetracyanoquinodimethane (TCNQ, $E_{1/2}^1$ 0.17 V vs SCE). Both 1:1 and 2:1 salts, $(Et_4N)(OCNAQ)$ and $(Et_4N)_2(OCNAQ)$, were obtained from reactions of Et_4NI with potassium and lithium salts of OCNAQ, respectively. The X-ray crystal analyses of these salts indicate that the TCNQ moieties are boat-shaped bent to opposite directions. With the 1:1 salt, which behaves as a semiconductor ($4\times10^{-4}\Omega^{-1}cm^{-1}$ at room temperature, E_a 0.22 eV), the OCNAQ molecules are arrayed in the segregated stacking mode, while the 2:1 salt

($10^{-7}\Omega^{-1}cm^{-1}$) has no columnar structure of the OCNAQ molecules.

IV-N-2 New Organic Conductor $(TTT)_2$-OCNAQ(DMF). Transverse Interaction through the OCNAQ Molecules

Tamotsu INABE, Tsutomu MITSUHASHI *(Univ. of Tokyo)*, **and Yusei MARUYAMA**

[*Chem. Lett.*, **1988**, 429]

A new organic conductor $(TTT)_2OCNAQ(DMF)$, where TTT is 5,6:11,12-bis(epidithio)naphthacene, OCNAQ is 11,11,12,12,13,13,14,14-octacyano-1,4:5,8-anthradiquinotetramethane, and DMF is *N,N*-dimethylformamide, has been prepared electrochemically. The crystal consists of one-dimensional TTT stacks with the OCNAQ and DMF molecules lying between the TTT columns. There exist short S···N contacts, and the transverse interaction has been demonstrated by the small anisotropy of the electrical conductivity.

IV-N-3 Charge-Transfer Complexes Based on the Twin-TCNQ-Type Acceptor 11,11,12,12,13,13,14,14-Octacyano-1,4:5,8-anthradiquinotetramethane (OCNAQ)

Tamotsu INABE, Tsutomu MITSUHASHI *(Univ. of Tokyo)*, **and Yusei MARUYAMA**

[*Bull. Chem. Soc. Jpn.* in press]

Charge-transfer complexes of OCNAQ with pyrene, PT (phenothiazine), TMTTF (tetramethyltetrathiafulvalene), TTT (5,6:11,12-bis(epidithio)naphthacene), and TTF (tetrathiafulvalene) have been prepared. The pyrene and PT complexes are electrically insulating and the ground state is neutral. In most of the other complexes OCNAQ is fully charged. One of the TTT complexes, $(TTT)_2OCNAQ(DMF)$, where DMF is *N,N*-dimethylformamide, has been found to show metallic conductivity. The structural study has revealed that short S···N contacts exist between TTT and OCNAQ in addition to one-dimensional TTT stacks. This transverse interaction has been demonstrated by the small anisotropy of the conductivity. The 2:1 TTF complex is also metallic down to 43 K, where a metal-to-insulator transition occurs. A structure analysis and thermoelectric power data suggest that the charge conduction in this crystal takes place not only through the TTF stacks but also through the two-dimensional network of the OCNAQ molecules.

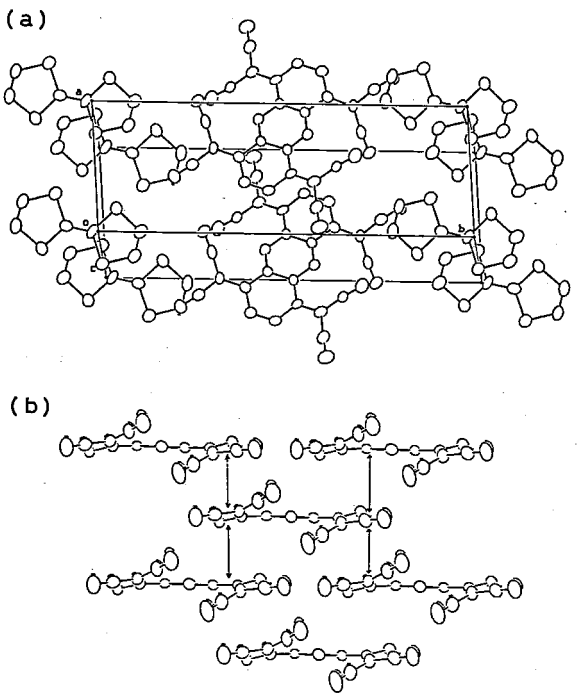

Figure 1. Crystal structure of $(TTF)_2OCNAQ$ (a) and the two-dimensional network composed of the OCNAQ molecules (b).

IV-N-4 Crystal Structures and Electronic Properties of Organic Conductors Based on AzaTCNQ

Hatsumi URAYAMA *(ISSP, Univ. of Tokyo)*, **Tamotsu INABE, Takehiko MORI, Yusei MARUYAMA, and Gunzi SAITO** *(ISSP, Univ. of Tokyo)*

[*Bull. Chem. Soc. Jpn.*, **61**, 1831 (1988)]

AzaTCNQ((4-dicyanomethyl-1-pyridinio)dicyanomethanide) is employed as an organic acceptor to form new organic conductors with a TTF family such as TTF, TMTTF, TMTSF, HMTTF, and DBTTF. Among them, TMTTF and TMTSF give 2:1 single crystals and the latter affords the most conductive complex, showing a metallic characteristic down to 150 K. This can be

observed by measuring the thermoelectric power and the ESR spectra. A crystal structure analysis indicates that only TMTSF molecules stack to form one-dimensional conduction pathways, while AzaTCNQ molecules are arranged side-by-side and oriented almost perpendicular to the donor molecules. There exists an orientational disorder of the nitrogen atom in the pyridine skeletone of an AzaTCNQ molecule, which may be associated with the weak temperature dependence of the electrical conductivity.

IV-N-5 Crystal Structures of Organic Superconductor, (BEDT-TTF)$_2$Cu(NCS)$_2$, at 298 K and 104 K

Hatsumi URAYAMA *(ISSP, Univ. of Tokyo)*, **Hideki YAMOCHI** *(ISSP, Univ. of Tokyo)*, **Gunzi SAITO** *(ISSP, Univ. of Tokyo)*, **Shoichi SATO** *(ISSP, Univ. of Tokyo)*, **Atsushi KAWAMOTO** *(Nagoya Univ.)*, **Jiro TANAKA** *(Nagoya Univ.)*, **Takehiko MORI, Yusei MARUYAMA, and Hiroo INOKUCHI**

[*Chem. Lett.*, **1988**, 463]

The crystal structures of an organic superconductor (BEDT-TTF)$_2$Cu(NCS)$_2$ (T_c=10.4 K) at 298 K and 104 K are determined by X-ray analysis. The packing pattern of donors is nearly analogous to $\varkappa$-(BEDT-TTF)$_2$I$_3$. The counter anion, Cu(NCS)$_2^-$, has no positional disorder and constructs a peculiar sheet where a copper ion is coordinated with a sulfur and two nitrogen atoms to form a one-dimensional polymer with a permanent dipole moment.

IV-N-6 Valence State of Copper Atoms and Transport Property of an Organic Superconductor, (BEDT-TTF)$_2$Cu(NCS)$_2$, Measured by ESCA, ESR, and Thermoelectric Power

Hatsumi URAYAMA *(ISSP, Univ. of Tokyo)*, **Hideki YAMOCHI** *(ISSP, Univ. of Tokyo)*, **Gunzi SAITO** *(ISSP, Univ. of Tokyo)*, **Minoru KINOSHITA** *(ISSP, Univ. of Tokyo)*, **Tamotsu INABE, Takehiko MORI, Yusei MARUYAMA, and Hiroo INOKUCHI**

[*Chem. Lett.*, **1988**, 1057]

ESCA, ESR, and thermopower were measured in crystals of an organic superconductor, (BEDT-TTF)$_2$Cu(NCS)$_2$ (T_c=10.4 K), to examine a valence state of Cu and a transport property. The Cu^{I} state was confirmed at 298 K by ESCA. ESR indicates a broad Lorentzian signal of a BEDT-TTF cation radical and no Cu^{II} signal at 298-4 K. The thermopower is anisotropic in the two-dimensional bc plane, which is originated from the anisotropy of the band structure.

IV-N-7 Tunneling Spectroscopic Study on the Superconducting Gap of (BEDT-TTF)$_2$Cu(NCS)$_2$ Crystals

Yusei MARUYAMA, Tamotsu INABE, Hatsumi URAYAMA *(ISSP, Univ. of Tokyo)*, **Hideki YAMOCHI** *(ISSP, Univ. of Tokyo)*, **and Gunzi SAITO** *(ISSP, Univ. of Tokyo)*

[*Solid State Commun.*, **67**, 35 (1988)]

The superconducting gaps of newly discovered organic superconductor, (BEDT-TTF)$_2$Cu(NCS)$_2$, have been measured with a tunneling spectroscopic method. One of the observed gap data, 4meV, gives 4.5 for the $2\Delta/kT_c$ (2Δ=4meV and T_c=10.4 K) which is a little larger than that of BCS ratio, 3.52. The other spectra observed in different crystals, however, are exhibiting much smaller gap electronic structure. This fact is suggestive of the anisotropic nature of the superconductivity in this crystal.

IV–O Synthesis and Characterization of Proton-Transfer/ Charge-Transfer System

This study deals with hydrogen-bonded systems, in which the proton transfer is coupled with the π-electron configurational change. In such a system the proton transfer converts a component molecule into a different chemical species. The component molecule itself can be utilized as memory or switching devices. Furthermore, if the intermolecular interaction is sufficiently strong, the proton transfer is expected to modulate the solid-state properties, especially expected is the coupling between the electronic properties and the proton motion. In order to examine such a possibility, compounds which have a framework of salicylideneaniline have been synthesized as the intramolecular proton transfer system. Also some intermolecular hydrogen-bonded systems have been prepared for this study.

IV-O-1 Structure and Optical Properties of a Thermochromic Schiff Base. Thermally Induced Intramolecular Proton Transfer in *N,N'*-Bis-(salicylidene)-*p*-phenylenediamine Crystals

Naomi HOSHINO, Tamotsu INABE, Tadaoki MITANI, and Yusei MARUYAMA

[*Bull. Chem. Soc. Jpn.*, in press]

A thermochromic derivative of salicylideneaniline, *N,N'*-bis(salicylidene)-*p*-phenylenediamine (BSP), has been prepared and subjected to structural and optical studies in the crystalline state. An X-ray crystallographic analysis has shown that the molecules are planar and are stacked in a parallel fashion to form one-dimensional columns. The interplanar spacing has been found to be quite short, suggesting the existence of an intermolecular charge-transfer interaction. The molecule contains fairly short O-H···N hydrogen bonds, the strength of which is manifested in an OH stretching absorption band in the infrared region, showing considerable broadening and a low-frequency shift. The BSP crystals are remarkably thermochromic, and visible absorption and emission spectral changes with temperature have been interpreted in terms of an intramolecular proton transfer from the hydroxyl oxygen to imine nitrogen through the O-H···N hydrogen bond. The emission spectra have also been examined under high pressures.

IV-O-2 Structure and Optical Properties of a Thermochromic Schiff Base. Low-Temperature Structural Studies of the *N,N'*-Bis(salicylidene)-*p*-phenylenediamine and *N,N'*-Bis(salicylidene)-1,6-diaminopyrene Crystals

Tamotsu INABE, Naomi HOSHINO *(Hokkaido Univ.)*, **Tadaoki MITANI, and Yusei MARUYAMA**

The crystal structure of *N,N'*-bis(salicylidene)-*p*-phenylenediamine (BSP) has been determined at 108 K. This compound shows thermochromic behavior in the crystalline state, and this chromism is interpreted in terms of an intramolecular proton transfer from the hydroxyl oxygen to imine nitrogen through the O-H···N hydrogen bond. In comparison with the room temperature structure, significant differences in the molecular structure and the molecular packing in the lattice have not been observed. The room temperature and low-temperature structures of another salicylideneaniline derivative, *N,N'*-bis(salicylidene)-1,6-diaminopyrene (BSDAP), have also been determined. In contrast to BSP, absence of the thermal proton-transfer process in BSDAP is suggested by the optical measurements. The comparative studies of these two compounds indicate that the conjugation system which does not undrego a π-electron configurational change by the proton transfer is needed to be co-planar with the hydrogen-bonded chelate ring for the thermal proton transfer.

IV-O-3 Structure and Optical Properties of a Thermochromic Schiff Base. Intra/Intermolecular Charge Transfer System *N*-Tetrachlorosalicylidene-1-aminopyrene

Tamotsu INABE, Naomi HOSHINO *(Hokkaido Univ.)*, **Tadaoki MITANI, and Yusei MARUYAMA**

The title compound has been synthesized as a member of the intramolecular proton transfer system. Especially this molecule is designed to increase the intramolecular charge-transfer interaction. As a consequence of this chemical modification, the charge-transfer interaction has also been found to operate between the molecules in the crystalline state. The equilibrium position of proton in the hydrogen-bonded chelate ring is largely influenced by this chemical modification, namely the proton is located at the middle of the hydrogen bond and the bond with the proton is not localized at either oxygen site or nitrogen site.

IV-O-4 Effect on the Intramolecular Proton Transfer by Complexation with Various Acceptors

Tamotsu INABE, Naomi HOSHINO *(Hokkaido Univ.)*, **Hiroshi OKAMOTO, Tadaoki MITANI, and Yusei MARUYAMA**

Some salicylideneaniline derivatives have been employed as a donor component to form charge-transfer complexes with various acceptors. Main effect on the structure by complexation appears in the hydrogen-bonded chelate ring. The equilibrium position of the proton changes from the oxygen side to the nitrogen side upon formation of charge-transfer complexes. Furthermore, there seems to be some correlation between the position of the proton and the ionicity of the molecule. These facts indicate that the π-electron system is strongly coupled with the hydrogen-bonding structure, and further investigation is in progress.

IV-O-5 Intermolecular Hydrogen-Bonded Charge-Transfer Complexes

Tamotsu INABE, Hiroshi OKAMOTO, Tadaoki MITANI, and Yusei MARUYAMA

In order to explore the possibility of an intermolecular proton transfer, some intermolecular hydrogen-bonded charge-transfer complexes of 1,6-diaminopyrene have been prepared. This approach is also convenient to introduce a conduction electron system into the hydrogen-bonded system. At the present stage the complexes with *p*-chloranil have been studied structurally, and the formation of the hydrogen-bonded network in the lattice has been indicated. The dependence of the electrical properties on the structures and that on pressure are studied now.

IV–P High Temperature Oxide Superconductors

As we felt at the very beginning of the study on the high-T_c oxides through the electron tunneling exteriment and the estimation of the coherence length, almost all of their superconducting characteristics except for the very high transition temperatures can universally be explained within the framework of BCS's mean field description, that is the qualitative superconducting behaviors do not depend on the origin of the electron-electron pairing force. Therefore, for the assignment of the mechanism of the superconductivity or the origin of the attractive force, it would be necessary to carry out the quantitative studies which are based on the detailed but broad knowledge of the various physical properties. Then, continuous effort has been made this year to accumulate various detailed data of the physical properties of the high-T_c oxides. We studied the transport, magnetic, thermal and optical properties. Structure determination by X-ray four circle diffraction and neutron inelastic measurement have also been carried out. It should be emphasized that through the success in growing large single crystals, rather detailed studies became possible. We also paid much attention to the correct characterization of the specimens. Electron probe micro analyzer (EMPA) and SQUID magnetometer were quite useful for the purpose. Search for new oxide superconductors has also been carried out continuously, which is, we think, to be quite important because it gives us the information on what kinds of oxides exhibit high-T_c superconductivity. As a result of this effort, the

superconductivity of the systems with Tl was first found here. Below the abstracts of the published papers and preprints are shown.

IV-P-1 Electron Tunneling Studies of High-T_c Superconductors $YBa_2Cu_3O_{7-\delta}$

Masafumi SERA, Shin-ichi SHAMOTO and Masatoshi SATO

[*Solid State Commun.* **65** 997 (1988)]

Electron Tunneling Measurements have been carried out on high T_c superconductor $YBa_2Cu_3O_{7-\delta}$ at temperatures between 4.2K and 110K. By analyzing the experimental data the following results are obtained. The values of $2\Delta/kT_c$ at low temperatures are 3~4 close to that expected from BCS theory. The temperature variation of the energy gap also seems to be consistent with that of BCS theory.

IV-P-2 Optical Studies of High-T_c Oxide Superconductors

Shinji SUGAI*, Shin-ichi UCHIDA$^+$, Hidenori TAKAGI$^+$, Koichi KITAZAWA$^+$, Shoji TANAKA$^+$, Masatoshi SATO and Syoichi HOSOYA** *(*Osaka Univ., $^+$Tokyo Univ., **Institute for Materials Research, Tohoku Univ.)*

[*Physica* **148B** 282 (1987)]

Oxygen deficiency effects on the superconductivity of $YBa_2Cu_3O_{7-\delta}$ are investigated by the electrical resistivity and the infrared reflection spectroscopy. On increasing the quenching temperature the sample changes to a semiconductor from a metal. The superconducting gap of the slowly cooled sample is anisotropic and the minimum gap is $2\Delta/k_BT_c$~1.6. The anisotropy of the sample quenched from 600°C is very small in the proximity-coupled superconducting region and the $2\Delta/k_BT_c$~1.

IV-P-3 Superconducting and Electronic Properties of $Bi_{1-x}La_xSrCuO_y$ System

Masashige ONODA, Masafumi SERA, Kenji FUKUDA, Shinji KONDOH, Masatoshi SATO, Toru DEN*, Hiroshi SAWA* and Jun AKIMITSU* *(*Aoyama-Gakuin Univ.)*

[*Solid State Commun.* **66** 189 (1988)]

Electrical resistivity, Hall coefficient, superconducting critical magnetic field and magnetic susceptibility are measured for crystals and sintered specimens nominally described as $Bi_{1-x}La_xSrCuO_y$. The compounds with x=0.0 exhibit midpoint superconducting transition temperatures of 7–9K, while the other compounds exhibit higher midpoint values of 16–20K. It is found that the present system has the characteristic features of low hole carrier concentration, two-dimensional electrical conduction and anisotropic susceptibility, which are similar to those of well-known high-T_c superconductors $(La_{1-x}Sr_x)_2CuO_4$ and $YBa_2Cu_3O_7$.

IV-P-4 Anisotropy of Magnetic Behavior of High-T_c Oxides

Kenji FUKUDA, Shin-ichi SHAMOTO, Masatoshi SATO and Kunihiko OKA

[*Solid State Commun.* **65** 1323 (1988)]

Recent results of the magnetic susceptibility χ of crystal specimens of $(La_{1-x}M_x)_2CuO_4$ (M=Sr and Ba) and $YBa_2Cu_3O_{7-\delta}$ are reported. The anisotropy of χ seems to be a common characteristic of the Cu-O layers. The spin canting model associated with the tetragonal-orthorhombic transition is proposed to explain the observed nonlinear magnetization vs. the magnetic field curve.

IV-P-5 Doping Effect on Magnetic Behaviors of La_2CuO_4

Kenji FUKUDA, Masafumi SERA and Masatoshi SATO

[*Solid State Commun.* **65** 1157 (1988)]

Effect of the La or Cu substitution by various elements on the magnetic properties of La_2CuO_4 have been studied. The La-substitution by Y which does not introduce hole carriers was found to be quite different from that of Bi, which turned out to introduce holes. The typical linear temperature dependence of the magnetic susceptibility was found for $(La_{1-x}Bi_x)_2CuO_4$ with $x>0.02$. The nonlinear behavior of the magnetization vs. the magnetic field curve was found to take place only for the orthorhombic specimens.

IV-P-6 Magnetic Susceptibility of Ca_2CuO_3

Shinji KONDOH, Kenji FUKUDA and Masatoshi SATO

[*Solid State Commun.* **65** 1163 (1988)]

Magnetic susceptibility and electrical resistivity of $(Ca_{1-x}Na_x)_2CuO_3$ with corner-linked planar CuO_4 chains have been experimentally studied to compare these behaviors with those of La_2CuO_4 with two dimensional Cu-O network. Above 100K, the susceptibility increases with temperature. An anomalous behavior of the susceptibility has beeen observed at low temperatures. Metallic conduction could not be maintained by the Na-doping.

IV-P-7 Superconductivity in Tl-Ba-Cu-O System

Shinji KONDOH, Yoshiyasu ANDO, Masashige ONODA, Masatoshi SATO and Jun AKIMITSU* *(*Aoyama-Gakuin Univ.)*

[*Solid State Commun.* **65** 1329 (1988)]

A new high-T_c superconductor Tl-Ba-Cu-O system is found by resistivity and Meissner diamagnetism measurements. The onset transition temperature becomes as high as 20K when small amount of the Tl-substitution by other trivalent elements is carried out. The superconducting phase may be described as $Tl_{1+y}Ba_{1-y}CuO_x$ with $y \ll 1$.

IV-P-8 Single Crystal Growth of High-T_c Superconductors

Shin-ichi SHAMOTO, Syoichi HOSOYA and Masatoshi SATO

[*Solid State Commun.* **66** 195 (1988)]

Crystal growth methods of high-T_c superconductors, $(\widetilde{La}, M)_2CuO_{4-\delta}$ (M=Sr or Ba) and $YBa_2Cu_3O_{7-\delta}$, are described in detail. For both kinds of oxides, crystals with superconducting transition were successfully obtained. The maximum crystal sizes of $(\widetilde{La}, M)_2CuO_{4-\delta}$ and $YBa_2Cu_3O_{7-\delta}$ are about $25\times20\times5mm^3$ and $6\times6\times3mm^3$, respectively.

IV-P-9 Growth and Properties of Single Crystals of High-T_c Oxides

Masatoshi SATO

[*Physica C* 153–155 38 (1988)]

A brief review on single crystal preparation of the high-T_c oxides is presented. Results of studies on the physical properties carried out mainly for these crystal specimens are also given. Characteristics of newly found high-T_c oxides are discussed. Because the existence of Cu-O layers seems to be a necessary condition at the present stage for exhibiting high-T_c superconductivity, it is quite important to use single crystal specimens to extract the detailed informations on such low dimensional systems.

IV-P-10 On the Structure of High-T_c Oxide System Tl-Ba-Cu-O

Masafumi SERA, Shinji KONDOH, Yoshiyasu ANDO, Kenji FUKUDA, Shin-ichi SHAMOTO, Masashige ONODA and Masatoshi SATO

[*Solid State Commun.* **66** 707 (1988)]

The X-ray powder diffraction data of high-T_c oxide system, Tl-Ba-Cu-O have been re-examined and found that the oxide has an orthorhombic cell with the lattice parameters a=5.52(2)Å, b=5.49(1)Å and c=23.33(3)Å. The structure seems to be similar to that of other high-T_c oxide, Bi-Sr-Cu-O. We have also found a sharp resistivity decrease around 70K in Tl-Ba-Sr-Cu-O system as temperature decreases, which

indicates the existence of high-T_c phase reminiscent of Bi-Sr-Ca-Cu-O recently found by Maeda et al.

IV-P-11 Growth and Characterization of $YBa_2Cu_3O_{7-\delta}$ Single Crystals

H. KATAYAMA-YOSHIDA*, T. YONEZAWA*, H. HIROOKA*, Y. OKABE*, T. TAKAHASHI*, T. SASAKI*, M. HONGOH*, K. YAMADA*, T. SUZUKI*, S. HOSOYA, M. SATO, T. CISZEK*** and S.K. DEB***** *(*Tohoku Univ., **Institute for Materials Research, Tohoku Univ., ***Solar Energy Research Institute, U.S.A.)*

[*Physica* C153–155 425 (1988)]

Large single crystals of high-T_c superconductor $YBa_2Cu_3O_{7-\delta}$ (T_c=90K) have been successfully grown in the cavity of the bulk materials with a CuO flux. We have also grown single crystals of $(La_{1-x}Sr_x)_2CuO_{4-\delta}$ (T_c=20K). Resistivity, Meissner effect and photoemission spectrum were measured for the single crystals. We also studied the newly discovered superconductor $BiSrCaCu_2O_x$ with T_c of 75~110K, and proposed the method to produce the single phase.

IV-P-12 Photoemission Study of Single-Crystalline $(La_{1-x}Sr_x)_2CuO_4$

Takashi TAKAHASHI*, Fumio MAEDA*, Hiroshi KATAYAMA-YOSHIDA*, Yutaka OKABE*, Takashi SUZUKI*, Atsushi FUJIMORI, Syoichi HOSOYA***, Shin-ichi SHAMOTO and Masatoshi SATO** *(*Tohoku Univ., **National Institute for Research in Organic Materials, ***Institute for Materials Research, Tohoku Univ.)*

Ultraviolet and x-ray photoemission measurements have been performed on single-crystalline $(La_{1-x}Sr_x)_2CuO_4$ with x=0.0 and 0.04. Considerable differences have been found in the photo-emission spectra when compared with the results for sintered samples: a single-peak structure for the O 1s level and the absense of the peak at 9 eV of unknown origin reported for sintered samples, etc. Comparison is also made with band-structure calculation.

IV-P-13 Absence of the T-Linear Term in Low Temperature Specific Heat of High-T_c Oxide, Bi-Sr-Ca-Cu-O System

Masafumi SERA, Shinji KONDOH, Kenji FUKUDA and Masatoshi SATO

[*Solid State Commun.* **66** 1101 (1988)]

The specific heat of high-T_c oxide system, Bi-Sr-Ca-Cu-O was measured in a temperature range between 1.7K and 20K. The used specimen has a nominal formula of $Bi_4(Sr_{0.6}Ca_{0.4})_6Cu_4O_y$ and exhibits superconductivity below 70K with rather large Meissner volume fraction. In contrast to the results reported for other high-T_c system, there is no appreciable T-linear term in the specific heat of the present system, which seems to negate the argument that a pseudo Fermi surface exists even in the superconducting phase of the high-T_c oxides.

IV-P-14 Superlattice Structure of Superconducting Bi-Sr-Cu-O System

Masashige ONODA and Masatoshi SATO

[*Solid State Commun.* **67** 799 (1988)]

Superlattice structure of superconducting Bi-Sr-Cu-O system with onset transition temperature of about 10K is determined by single crystal X-ray diffraction. The unit cell is described by a face-centered monoclinic lattice with space group C2 and the lattice parameters are a=26.856Å, b=5.380Å, c=26.908Å and β=113.55°. The estimated chemical formula is $Bi_{10}Sr_{10}Cu_5O_{29}$ with Z=4, which is reduced to $Bi_2Sr_2CuO_{6-\delta}$ with δ=0.2 as the ideal phase. The structural unit consists of the five oxide layers, -Bi-Sr-Cu-Sr-Bi-, stacked along the a*-direction. A long-period sinusoidal modulation with very large amplitude can essentially explain the structure of this compound. The large deviations of Cu atom positions from the ac-plane caused by this modulation may be one of the origins of the rather low T_c value of the compound.

IV-P-15 Two Magnon Raman Scattering in $(La_{1-x}Sr_x)_2CuO_4$

Shinji SUGAI*, Shin-ichi SHAMOTO and Masatoshi SATO *(*Osaka Univ.)*

[*Phys. Rev. B* submitted]

The 2-dimensional 2-magnon peak in $(La_{1-x}Sr_x)_2CuO_4$ decreases rapidly from $x=0$ to $x=0.01$, and at $x>0.03$ scattering still remains in a very wide energy region from low energy to over 4000 cm^{-1}. This indicates that the correlation length of the 2-dimensional spin order decreases rapidly from $x=0$ to $x=0.01$, which is related with the rapid decrease of the 3-dimensional T_N, and at $x>0.03$ the correlation still retains a short length and a short time. At $x<0.01$ the scattering is in a resonant state with narrow electronic levels with transition energy of about 18000 cm^{-1}. The narrowness of these energy levels and the simultaneous extinction of resonance and the 2-magnon scattering suggests that these are localized levels relating to the Cu spins.

IV-P-16 Antiferromagnetic Spin Correlation in Insulating, Metallic and Superconducting $La_{2-x}Sr_xCuO_4$

R.J. BINGENEAU*, D.R. GABBE*, H.P. JENSSEN*, M.A. KASTNER*, P.J. PICONE*, T.R. THURSTON*, G. SHIRANE$^+$, Y. ENDOH, M. SATO, K. YAMADA*, J. JODALA^{++}, M. ODA^{++}, Y. ENOMOTO^{++}, M. SUZUKI^{++} and T. MURAKAMI^{++}** *(*Massachusetts Institute of Technology, $^+$Brookhaven National Laboratory, **Tohoku Univ., $^{++}$NTT Electrical Communications Laboratories)*

[*Phys. Rev. B* submitted]

We have carried out elastic, quasielastic ($\int dE$) and inelastic neutron scattering studies of the antiferromagnetic spin correlations in $La_{2-x}Sr_xCuO_4$ with x varying between 0.02 and 0.18. The crystals which were grown in three different laboratories, exhibit behavior which varies smoothly with x. In all cases antiferromagnetic correlations with a scattering amplitude corresponding to a fully occupied Cu^{2+} square lattice are observed. However, the Néel state is destroyed by the doping and the spin-spin correlation length ξ is quite short, varying from ~35Å to ~8Å as x varies between 0.02 and 0.18. The fluctuations are dynamic in character as in pure La_2CuO_4 above the Néel Temperature T_N. To a first approximation, $\xi=3.8/\sqrt{x}$ Å, the average separation between the holes introduced by the Sr^+ doping. The x=0.08 sample exhibits superconductivity with T_c=10 K and with a Meissner fraction exceeding 15% at 5K; no important differences in the magnetic scattering are observed in the normal and superconducting states. In an appendix we present additional data on the spin dynamics in pure La_2CuO_4 at T = 300K in a sample with T_N = 235K.

IV-P-17 Neutron Scattering Study of the Transition from Antiferromagnetic to Weak Ferromagnetic Order in La_2CuO_4

M.A. KASTNER*, R.J. BIRGENEAU*, T.R. THURSTON*, P.J. PICONE*, H.P. JENSSEN*, D.R. GABBE*, M. SATO, K. FUKUDA, S. SHAMOTO, Y. ENDOH, Y. YAMADA** and G. SHIRANE***** *(*Massachusetts Institute of Technology, **Tohoku Univ., ***Brookhaven National Laboratories)*

[*Phys. Rev. B* submitted]

Neutron scattering studies provide direct evidence for a field-driven magnetic transition which originates from the canting of spins out of the CuO_2 planes: at the transition between antiferro- and ferromagnetic ordering of the canted component of the spins in the layers, the (100) Bragg peak vanishes while the (201) peak appears. Detailed measurements and analysis suggest that the phase transition can be described by the mean-field theory of Thio et al. only close to the Néel temperature.

IV-P-18 Two Dimensional Antiferromagnetic Excitations from a Large Single Crystal of $YBa_2Cu_3O_{6.2}$

M. SATO, S. SHAMOTO, J.M. TRANQUADA*, G. SHIRANE* and B. KEIMER** *(*Brookhaven National Laboratory, **Massachusetts Institute of Technology)*

[*Phys. Rev. Letters* **61** 1317 (1988)]

A large single crystal (7×7×3 mm^3) of $YBa_2Cu_3O_{6.2}$ has been successfullly grown and its magnetic excitations have been observed by neutron scattering techniques. A two-dimensional magnetic ridge, similar to that

observed for La_2CuO_{4-y}, has been clearly identified by triple-axis measurements. The slope of the dispersion curve for spin-wave excitations is very large ($\gtrsim$ 0.5 eV-Å), consistent with the result of spin-pair Raman scattering by Lyons *et al.*

IV-P-19 Study on Normal and Superconducting Properties of $Bi_4Sr_3(Ca_{1-x}Y_x)_3Cu_4O_y$

Yoshiyasu ANDO, Kenji FUKUDA, Shinji KONDOH, Masafumi SERA, Masashige ONODA and Masatoshi SATO

[*Solid State Commun.* **67** 815 (1988)]

Carrier concentration of high-T_c oxide, $Bi_2(Sr,Ca)_3Cu_2O_8$ has been successfully varied by the substitution of Ca atoms with Y and by a thermal treatment at relatively low temperatures in (0.9Ar + $0.1H_2$) gas flow. Various physical properties have been measured through the metal-insulator boundary, the results of which indicate that these properties are quite similar to those of other well known high-T_c oxides. The relationship between the magnetic susceptibility and the hole concentration seems to have a crossover behavior at the metal (superconducting)-insulator boundary from the one which may be expected for localized and fluctuating electron spin systems to that of band electron spin systems.

IV-P-20 Structural Aspects of Charge Density Waves in the Blue Bronzes

J.P. POUGET*, S. GIRAULT*, A.H. MOUDDEN*, B. HENNION, E. ESCRIBE-FILLIPPINI$^+$ and M. SATO** *(*Univ. Paris-Sud, **Laboratory Lëon Brillouin, $^+$C.N.R.S. Grenoble)*

[*Physica Scripta* in press]

This summarizes the spatial and dynamical aspects of the Peierls transition of the blue bronzes. For the first time the q dispersion of the amplitude and phase excitations of an incommensurate CDW modulation have been measured. From the experimental data the microscopic parameters of the Peierls transition have been obtained. In this respect it appears that the Peierls transition of the blue bronzes is governed by a sizeable electron-phonon coupling and that the electron-electron interactions do not have a pertinent influence, at the difference of the quasi 1D organic conductors. Although the blue bronzes do not exhibit a true regime of 1D fluctuations below T_c^{MF}, these fluctuations show substantial deviations, in their dynamics, from the simple predictions of the mean field theory.

IV-P-21 Synthesis of Superconducting Ba-K-Bi-O System with Perovskite Structure

Shinji KONDOH, Masafumi SERA, Yoshiyasu ANDO, Kenji FUKUDA and Masatoshi SATO

[*Solid State Commun.* **67** 879 (1988)]

Superconducting system of Ba-K-Bi-O with perovskite structure was synthesized in silver tubes. One of the as-reacted samples was found, for the first time by resistivity measurement, to exhibit a sharp superconducting transition. Subsequent low temperature annealing in flowing oxygen gas did not improve the transport and superconducting properties of the samples. The paramagnetic component of the magnetic suceptibility due to the mobile electrons has been found to be much smaller than the diamagnetic one of ion cores, which suggests that the electronic properties of the present system is rather similar to those of $BaPb_{1-x}Bi_xO_3$ than those of high-T_c oxides with Cu atoms.

IV-P-22 Gd^{3+} EPR of High Temperature Superconductor $GdBa_2Cu_3O_x$

Hiromitsu KIKUCHI*, Yoshitami AJIRO*, Yutaka UEDA*, Koji KOSUGE*, Mikio TAKANO$^+$, Sasuo TAKEDA and Masatoshi SATO** *(*Kyoto Univ., $^+$Institute for Chemical Research, Kyoto Univ., **Mie Univ.)*

[*J. Phys. Soc. Jpn.* **57** 1887 (1988)]

EPR measurements of Gd^{3+} were performed in the superconducting and non-superconducting $GdBa_2Cu_3O_x$. There is no distinct difference between the EPR behaviors of the two samples. The results show that even in the superconducting sample, the Gd

ions behave as paramagnetic local moments with a mutual exchange interaction of 0.1 K.

IV-P-23 Anisotropic Thermoelectric Powers of $YBa_2Cu_3O_{7-\delta}$ and $(La_{1-x}Sr_x)_2CuO_4$ Single Crystals

Masafumi SERA, Shin-ichi SHAMOTO and Masatoshi SATO

[*Solid State Commun.* submitted]

Thermoelectric powers of $YBa_2Cu_3O_{7-\delta}$ and $(La_{1-x}Sr_x)_2CuO_4$ single crystals have been studied systematically. Their magnitudes and temperature dependence are quite anisotropic. Within the CuO_2 planes, they exhibit a positive broad maximum at 200~300K and along the direction perpendicular to the CUO_2 planes, they are positive and nearly T-linear. It is suggested that these characteristic behaviors of the thermoelectric powers are due to anomalous scattering of the conduction holes associated with the magnetic scattering by the Cu spins.

IV-P-24 Thermoelectric Power of Superconducting Ba-K-Bi-O with Perovskite Structure

Masafumi SERA, Shinji KONDOH and Masatoshi SATO

[*Solid State Commun.* submitted]

Thermoelectric power of a sintered specimen with a nominal formula of $K_{0.75}Ba_{0.7}BiO_3$ with $T_c \simeq 30$K was studied. It is positive and nearly T-linear above ~100K as in the case of usual metals, which has clear contrast to the anomalous T-dependence observed in high-T_c oxides with CuO_2 planes. A hump is observed around 50K which may be due to a phonon-drag effect.

IV-P-25 Structural Study of Superconducting Tl-Ba-Ca-Cu-O System

Masashige ONODA, Shinji KONDOH, Kenji FUKUDA and Masatoshi SATO

[*Jpn. J. Appl. Phys.* **27** L1234 (1988)]

Crystal structure of Tl-Ba-Ca-Cu-O system with superconducting onset transition temperature higher than 100K which is systematically characterized by electron probe micro analysis and electron diffraction, is determined by single crystal X-ray diffraction. The unit cell is described by a body-centered tetragonal lattice with space group I4/mmm. The structural unit consists of the seven oxide layers, -Ca-Cu-Ba-Tl-Tl-Ba-Cu-, stacked along the c-direction. The expected chemical formula is $Tl_{1.95}Ba_2Ca_{0.85}Cu_{2.18}O_8$, which is slightly deviated from the stoichiometric composition $Tl_2Ba_2CaCu_2O_8$. It is suggested that the hole carrier of this system may be given by the nonstoichiometric composition of cation.

IV-P-26 Growth and Annealing Effect of Single Crystals of High-T_c Superconductors

Shin-ichi SHAMOTO

[*Solid State Commun.* **66** 1151 (1988)]

Detailed informations on the crystal preparations of $(La_{1-x}Sr_x)_2CuO_{4-\delta}$ and $YBa_2Cu_3O_{7-\delta}$ are reported. The Sr content x in $(La_{1-x}Sr_x)_2CuO_{4-\delta}$ crystals is shown as a function of the Sr content in the initial mixtures. For $YBa_2Cu_3O_{7-\delta}$, the conditions to get three types of crystals, thin plate, rectangular cube and irregular block shapes are described. Annealing effect on the resistivities of these crystals is also reported.

IV-P-27 Lattice Instability in Single-Crystal $La_{2-x}Sr_xCuO_4$

P. BÖNI*, J.D. AXE, G. SHIRANE**, R.J. BIRGENEAU+, D.R. GABBE+, H.P. JENSSEN+, M.A. KASTNER+, P.J. PICONE+, T.R. THURSTON+, S. SHAMOTO and M. SATO** *(*Paul Scherrer Institute, **Brookhaven National Laboratory, +Massachusetts Institute of Technology)*

[*Phys. Rev.* submitted]

The structural phase transition from the tetragonal to the orthorhombic phase of doped and undoped samples of $La_{2-x}Sr_xCuO_4$ has been investigated by using inelastic neutron scattering techniques. The rotational nature of the soft mode leads to moderate

electron-phonon coupling and the mode is unlikely to enhance significantly conventional phonon mediated superconductivity.

IV-Q Photoelectron Spectroscopy of Organic Solids in Vacuum Ultraviolet Region

Ultraviolet photoelectron spectroscopy (URS) of organic solids and graphite compounds has been carried out. Photoelectron spectroscpoy with synchrotron radiation (UVSOR-UPS) was applied to observe the electronic structure of condensed organic/inorganic materials.

IV-Q-1 X-Ray Photoelectron Spectroscopy of Tetrathiofulvalene- and Tetrathiotetracence- Tetracyanoquinodimethane Charge-Transfer Complexes in Reticulate Doped Polymers

J.K. JESZKA *(Polish Academy of Science and IMS)*, **Keisaku KIMURA, A. TRACZ** *(Polish Academy of Science)*, **Hiroo INOKUCHI, and M. KRYSZEWSKI** *(Polish Academy of Science)*

[*J. Molecular Electronics*, **3**, 157 (1987)]

Charge-transfer (CT) TTF-TCNQ and TTT-TCNQ complexes in reticulate doped surface-conductive and bulk-conductive polymers have been investigated by X-ray photoelectron spectroscopy (XPS). The N 1s peak from the acceptor and S 2p from the donors were analyzed. In spite of a very low concentration of N and S atoms in the investigated systems, it was possible to obtain for some of them information on the concentration of the additatives in the surface layer and also on the electronic state of the CT complex. It was found that in the case of the surface-conductive system polycarbonate + TTF-TCNQ the concentration of the CT complex in the conductive surface layer is considerably enhanced compared with the average concentration. XPS spectra for the N 1s and S 2p regions are similar to those of TTF-TCNQ. In bulk-conductive films of polycarbonate doped with TTT-TCNQ, the CT complex concentration was found to be different on the top and bottom surface of the film. The stoichiometry and the electronic state of the additive were found to be related to the morphology of the conductive network.

IV-Q-2 Ultraviolet Photoemission Study of Oligothiophenes: The Effect of Irregularity on π-Electron Systems

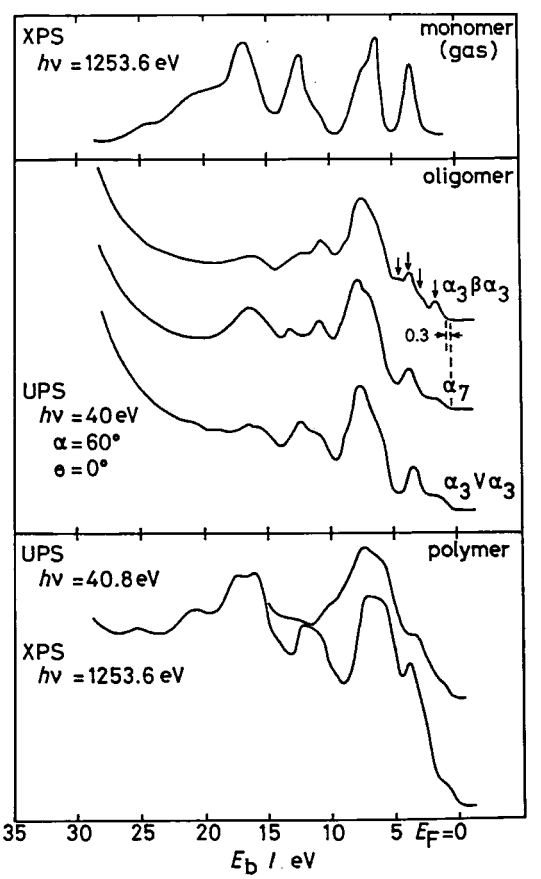

Figure 1. UPS spectra of three oligothiophenes. For a comparison, UPS and X-ray photoelectron (XPS) spectra of polythiophene[2] and an XPS spectrum of gas phase thiophene[3] are shown in the upper and lower panels. Arrows show the peak positions of π bands of $\alpha_3\beta\alpha_3$.

Hitoshi FUJIMOTO, Umpei NAGASHIMA, Hiroo INOKUCHI, Kazuhiko SEKI *(Hiroshima Univ.)*, **Hiroo NAKAHARA** *(Saitama Univ.)*, **Junzo NAKAYAMA** *(Saitama Univ.)*, **Masamatsu HOSHINO** *(Saitama Univ.)*, **Kiyoshige FUKUDA** *(Saitama Univ.)*

[*J. Chem. Phys.*, **89**, 1198 (1988)]

We report on the effect of irregularity on the π-electron systems by the ultraviolet photoelectron spectroscopy (UPS) for several oligothiophenes: α_7, $\alpha_3\beta\alpha_3$, $\alpha_3V\alpha_3$.[1] Our purpose is to investigate the electronic structure of these oligomers, to check the quality of α_7 as a model compound of polythiophene, and to examine the effects of introducing β linkages and a different π system between α-linked parts.

References

1) In IUPAC, α_7 is 2,2′:5′,2″:5″,2‴:5‴,2⁗:5⁗,2⁗′:5⁗′,2⁗″-septithiophene, $\alpha_3\beta\alpha_3$ is 2,2′:5′,2″:5″,3‴:4‴,2⁗:5⁗,2⁗′:5⁗′,2⁗″-septithiophene, and $\alpha_3V\alpha_3$ is (E)-bis-(2,2′:5′2″-terthiophene-5yl)ethylene.
2) C.R. Wu, J.O. Nilsson, O. Inganäs, W.R. Salaneck, J.E. Osterholm, and J.L. Brédas, *Synth. Met.*, **21**, 197 (1987).
3) U. Gelius, C.J. Allan, G. Johansson, H. Siegbahn, D.A. Allison, and K. Siegbahn, *Phys. Scr.*, **3**, 237 (1971).

IV-Q-3 Evidence from Angle-Resolved Resonant Photoemisson for Oxygen-2p Nature of the Fermi-Liquid States in $Bi_2CaSr_2Cu_2O_8$

Takashi TAKAHASHI *(Tohoku Univ.)*, **Hiroyoshi MATSUYAMA** *(Tohoku Univ.)*, **Hiroshi KATAYAMA-YOSHIDA** *(Tohoku Univ.)*, **Yutaka OKABE** *(Tohoku Univ.)*, **Shoichi HOSOYA** *(Tohoku Univ.)*, **Kazuhiko SEKI** *(Hiroshima Univ.)*, **Hitoshi FUJIMOTO, Masatoshi SATO, Hiroo INOKUCHI**

[*Nature*, **334**, 691 (1988)]

Photoemission measurements with synchrotron radiation have been performed on single crystal $Bi_2CaSr_2Cu_2O_8$. Two energy bands with dispersion of 0.2–0.5 eV were observed in the vicinity of the Fermi level and one of them crosses the Fermi level midway between the center and boundary of the Brillouin zone, giving a clear evidence for existence of a Fermi surface. The Fermi-edge peak exhibits a pronounced enhancement at photon energy of the O 2s core threshold, meaning a dominant O 2p nature of Fermi-edge states. These results indicate existence of Fermi-liquid states with dominant O 2p nature in the high-Tc superconductor. The superconductivity is supposed to be driven by formation of Cooper-pairs of the O 2p holes in the Fermi-liquid states, probably through the spin or charge fluctuation.

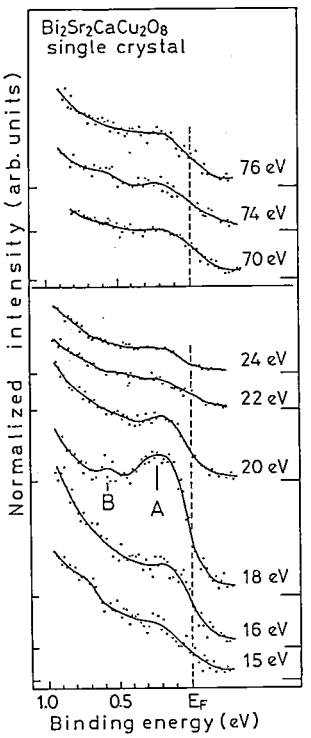

Figure 1. Photoemission spectra of single crystal $Bi_2CaSr_2Cu_2O_8$ in the vicinity of the Fermi level measured with photon energies near the O 2s (lower) and Cu 3p (upper) core thresholds in the normal emission arrangement. The photon energy used is indicated on each spectrum. The intensity of photoemission is normalized to the incident photon flux, independently for the O 2s and Cu 3p regions.

IV-Q-4 Ultraviolet Photoelectron Spectra of Hexamethylene-tetratellurafulvalene (HMTTeF) in the Gaseous and Solid States

Naoki SATO *(Univ. Tokyo)*, **Gunzi SATIO** *(Univ. Tokyo)*, **and Hiroo INOKUCHI**

[*Chem. Phys.*, in press]

Ionizatoin potentials of HMTTeF in the gaseous and solid states were determined to be 6.81 and 4.8_7 eV, respectively, from the photoelectron spectra. The origin of the first ionization was estimated by compar-

ing with the assignment of photoelectron spectra of unsaturated compounds containing chalcogen atoms. The differential ionization energy between the two phases, 1.9_4 eV, was compared with the polarization energies of other tetrathiafulvalene derivatives, in particular, of sulfur and selenium, congeners of HMTTeF. A capability of HMTTeF as a donor forming highly conductive salts was discussed by examining the energy parameters obtained and the molecular polarizability.

IV-R Electrical Conduction of Organic Solids

Physico-chemical properties — electrical, thermal and structural — of tetrakis alkylchalcogeno substituted tetrathiafulvalene have been observed extensively.

IV-R-1 Electrical Properties of the Organic Conductor, $(BEDT\text{-}TTF)_3(ClO_4)_2$

Kenichi IMAEDA, Toshiaki ENOKI, Gunzi SAITO *(Univ. of Tokyo)*, **and Hiroo INOKUCHI**

[*Bull. Chem. Soc. Jpn.*, **61**, 3332 (1988)]

The anisotropy and pressure effect of electrical conductivity, and thermoelectric power have been measured for $(BEDT\text{-}TTF)_3(ClO_4)_2$. The electrical conduction is two-dimensional in the bc plane with the small anisotropy ($\varrho_b/\varrho_c \sim 2$) at room temperature. The metal-insulator transition temperature (T_{MI}) of 172 K at 1 bar is lowered to 145 K, 115 K, and 95 K under 4.1 kbar, 7.2 kbar, and 9.8 kbar, respectively. The suppressing rate of T_{MI} by pressure is estimated to be about -8 K kbar^{-1}. The thermoelectric power at room temperature is ~ 0 μV K^{-1} (Figure 1), which is in complete agreement with the calculated value from the formalism for a system with strongly interacting electrons. This fact indicates that $(BEDT\text{-}TTF)_3(ClO_4)_2$ is the system with large on-site Coulomb repulsion.

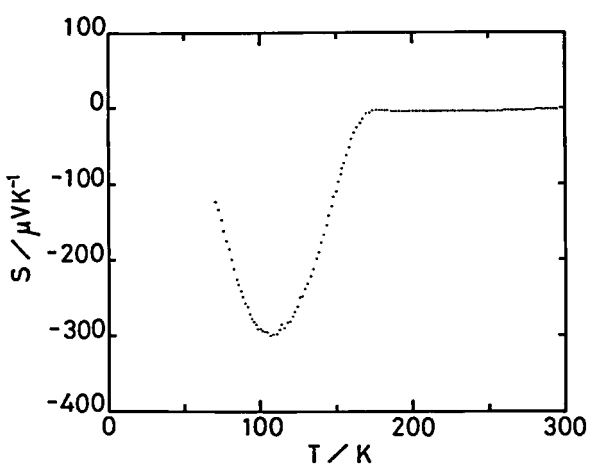

Figure 1. Temperature dependence of the thermoelectric power for $(BEDT\text{-}TTF)_3(ClO_4)_2$.

IV-R-2 Thermal Properties of Tetrakis(alkylthio)tetrathiafulvalenes

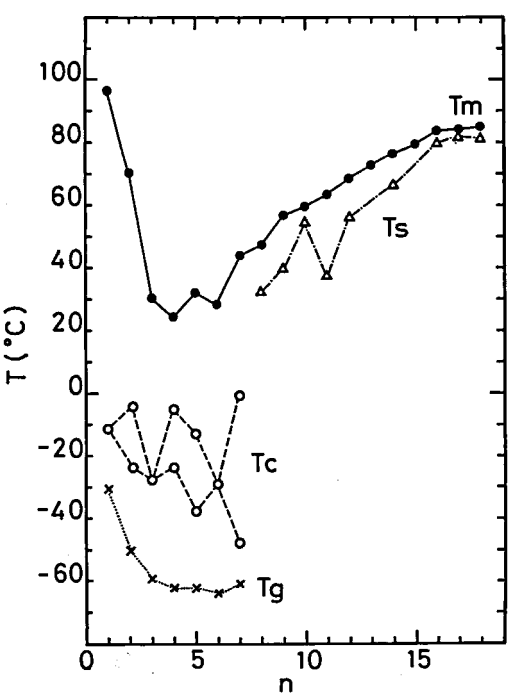

Figure 1. Carbon number dependence of glass transition temperature (T_g), crystallization transition temperature (T_c), solid-solid phase transition temperature (T_s), and melting point (T_m) for $TTC_n\text{-}TTF$.

Zurong SHI*, Toshiaki ENOKI, Kenichi IMAEDA, Kazuhiko SEKI, Peiji WU* *(*IMS and Inst. Chem., Academia Sinica, China)*, **Gunzi SAITO** *(Univ. of Tokyo)*, **and Hiroo INOKUCHI**

[*J. Phys. Chem.*, **92**, 5044 (1988)]

Thermal properties have been investigated for a series of tetrakis(alkylthio)tetrathiafulvalenes (abbreviated TTC_n-TTF's(n=1–18)), by means of differential scanning calorimetry. The linear n dependence of the enthalpy and entropy changes at the melting point, ΔH_m and ΔS_m, are observed, which is consistent with the behavior of flexible molecules reflecting the contribution from the configurational change in alkyl chains of TTC_n-TTF's to the entropy change at the melting point. The n dependence of the melting point (Figure 1), in addition to that of ΔH_m and ΔS_m, suggests that the series of TTC_n-TTF's are divided into two subgroups depending on n. In one subgroup with smaller $n \leq 7$, the intermolecular interaction between adjacent TTF skeletons dominates the crystal structures, while in the other subgroup with $n>7$, van der Waals intermolecular interaction associated with alkyl chain groups works to reduce the interplanar distance between adjacent TTF's in the crystal. The reduction in the interplanar distance is also suggested by the investigation of crystal density in the latter subgroup.

IV-R-3 Crystal Structure and Electrical Properties of $TSeC_n$-TTF (n=2 and 4)

Ping WANG *(Inst. Chem., Academia Sincia, China and IMS)*, **Takehiko MORI, Chikako NAKANO, Yusei MARUYAMA, Hiroo INOKUCHI, Naoko IWASAWA*, Hideoki YAMOCHI*, Hatsumi URAYAMA*, and Gunzi SAITO*** *(*ISSP, Univ. of Tokyo)*

[*Bull. Chem. Soc. Jpn.* **61**, 3455 (1988)]

An organic compound $TSeC_n$-TTF [tetrakis (alkylseleno)tetrathiafulvalenes] with n=2, crystallizes in the monoclinic space group $P2_1/a$, a=23.218(5), b=8.960(3), c=10.489(3) Å, β=96.61(2)°, V=2168(1) Å^3 and Z=4; the compound with n= crystallizes in the triclinic space group P1, a=9.198(1), b=10.539(2), c=8.248(2) Å, α=113.16(2), β=96.02(2), γ=90.61(2)°, V=729.9(3) Å^3 and Z=1. The molecule with n=2 has a bent structure like a boat; and the molecule with n=4 has a structure in which each of the four alkyl chains is stretched towards different directions. The temperature dependence of electrical resistivity and the charge-carrior mobility have been measured, and the resistivities at room temperature are $\varrho_a/\varrho_b/\varrho_c$ = 3.3 × 10^9 / 2.0 × 10^9 / 6.0 × 10^{11} and 2.2 × 10^{11} / 1.0 × 10^{11}/ 1.3 × 10^{11} (Ωcm) for $TSeC_2$-TTF and $TSeC_4$-TTF, respectively. The quite isotropic character in the resistivities of a $TSeC_4$-TTF crystal may originate from its rather strange molecular structure.

IV-S Electron Transport in Cytochromes

The electrical conduction of proteins in the solid state has been reported by many investigators with interest in the carrier transport in biological systems. We have already found that a great difference in the electrical conductivity between hemoproteins and simple proteins with no heme as a prosthetic group: The electrical conductivity of cytochrome c_3 is enormously large as 1.6 × 10^{-1} Scm^{-1}. Recently, we found more peculiar conduction phenomena in the series of cytochromes and are accumulating their detailed experimental findings.

IV-T Physics and Chemistry of Graphite Intercalation Compounds

Graphite-alkali metal intercalation compounds absorb hydrogen chemisorptively, leading to the occlusion of hydrogen in intercalate layers. The introduction of hydrogen gives effects on the electronic and lattice properties of the compounds due to the strong electron affinity of hydrogen and the occupation of the sites by hydrogen species in the intercalate layer. We investigate the properties of the alkali metal-hydrogen-graphite ternary intercalation

compounds by means of measurements of ultra-violet photoelectron spectra, c-axis thermal expansion, and positron annihilation.

IV-T-1 Ultraviolet Photoemission Spectroscopy of Ternary Graphite Intercalation Compound C_8KH_x

Hiromichi YAMAMOTO, Kazuhiko SEKI, *(Hiroshima Univ.)*, **Toshiaki ENOKI,** *(Tokyo Ins. of Tech.)*, **and Hiroo INOKUCHI**

The electronic structure of potassium-hydrogen-graphite ternary intercalation compound C_8KH_x is studied by UV photoemission spectroscopy, Comparison of C_8KH_x and potassium-graphite binary intercalation compound C_8K reveals indicate a distinct hydrogen-induced (H-induced) state around 2.0 eV below the Fermi level. E_F, as shown in Fig.1. Furthermore, the rise of E_F from graphite to C_8KH_x is obtained to be 1.4 eV. From the rise of E_F, the charge-transfer rate of hydrogen is estimated to be 0.62–0.89 using Blinowski model. This value indicates the existence of small vacancy in the H 1s band in C_8KHx, which is consistent with the results of the previously reported H-NMR and thermoelectric power measurements. Therefore, judging from the H 1s band just below E_F and the incomplete anion state of hydrogen, the H 1s band is supposed to be widely spread due to the strong H-H interactions in the two-dimensional hydride lattice in the dense state as well as the K-H interactions in the intercalate space, and furthermore, to distribute across E_F. The present UPS study and previously reported H-NMR results strongly suggest a possibility that the two-dimensional metallic hydrogen sheets are formed in C_8KH_x.

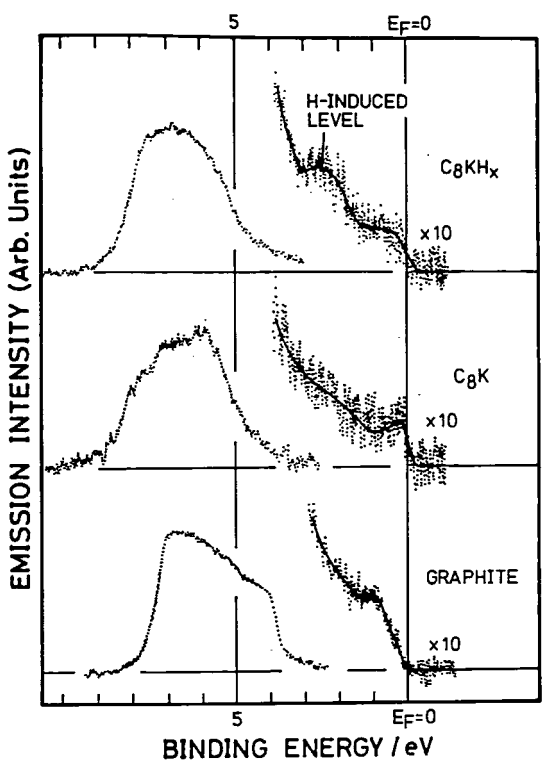

Figure 1. The UPS spectra of graphite, C_8, and C_8KH_x using the ArI (11.7 eV) resonance line. The abscissa is the binding energy relative to E_F.

IV-T-2 C-Axis Thermal Expansion of Donor Graphite Intercalation Compounds

Toshiaki ENOKI, Jeremiasz JESZKA, Hiroo INOKUCHI and Mizuka SANO *(Kumamoto Univ.)*

Temperature dependence of linear thermal expansion coefficients parallel to c-axis α_c has been investigated for donor graphite intercalation compounds, C_8K, C_4KHg and $C_{4n}KH_x$ (n=1,2 for stage-1 and 2) in the temperature region between 4.2K and room temperature. The c-axis linear thermal expansion coefficient α_c can be related to the (001) longitudinal acoustic phonon. α_c increase in the order of C_8KH_x < HOPG < C_4KH_x < C_8K < C_4KHg. The experimental results are analysed using data of specific heat and inelastic neutron diffraction measurements, as shown in Table I. Taking into account the lattice stiffness of these comounds, the anharmonicity of the lattice vibration relevant to α_c increases in the order of HOPG < C_4KH_x < C_4KHg < C_8K. The high concentration of conduction electrons is considered to enhance anharmonicity in C_8K and C_4KHg, while the ionic nature of the K^+-H^--K^+ intercalate results in the less anharmonicity in C_4KH_x. The KH-GICs show negative or very small thermal expansion coefficient at low temperatures.

Table I. Elastic constant C_{33}, Debye temperature Θ_D and c-axis thermal expansion coefficient α_c (at 250K).

	$C_{33}(x10^{11})$ (dyne/cm^2)	Θ_D (K)	$\alpha_c(x10^5)$ (K^{-1})
HOPG	3.65 ± 0.1[a)]	427[b)]	2.63[c)]
KH	—	—	2.97
C_8K	4.85 ± 0.14[d)]	393.5[e)]	4.67 ± 0.04
C_4KHg	2.3 ± 0.1[f)]	269[g)]	7.31 ± 0.55
C_4KH_x	3.4[h)]	—	3.73 ± 0.11
C_8KH_x	—	350.3[e)]	2.36 ± 0.18

a, b, c, d, e, f, g, h: other works

IV-T-3 Two-Dimensional Electron Momentum Distribution in Graphite Revealed by Means of Angular Correlation of Positron Annihilation

Ikuzo KANAZAWA *(Tokyo Gakugei Univ.)*, **Shoichiro TANIGAWA** *(Univ. Tsukuba)*, **Ryoichi SUZUKI** *(Univ. Tsukuba)*, **Yoji MIZUHARA** *(Univ. Tsukuba)*, **Mizuka SANO** *(Kumamoto Univ.)* **and Hiroo INOKUCHI**

[*J. Phys. Chem. Solids*, **48**, 701 (1987)]

Two-dimensional angular correlation measurements with positron annihilation radiation (2D-ACAR) on a single crystal of Kish graphite reveal that the motion of the annihilating electrons is nearly free along the graphite layers and restricted within some distance shorter than the lattice constant in the direction perpendicular to the layers. The hollows appearing on the 2D-ACAR surfaces are explained in terms of preferential annihilation of positions with π-electrons in graphite.

IV-T-4 Hydrogen in a Graphite-Rubidium Intercalation Compound RbC_8 Studied by Positron Annihilation

Hideoki MURAKAMI *(Tokyo Gakugei Univ.)*, **Ikuzo KANAZAWA** *(Tokyo Gakugei Univ.)*, **Mizuka SANO** *(Kumamoto Univ.)*, **Toshiaki ENOKI** *(Tokyo Institute Tech.)* **and Hiroo INOKUCHI**

[*J. Phys. Chem. Solids*, **49**, 457 (1988)]

Doppler-broadened spectra of positron-annihilation radiation have been measured on RbC_8 absorbing hydrogen at 300 or 373 K. The spectrum of RbC_8 was composed of a narrow component and a broad one. The intensity of the narrow component was suppressed through hydrogen absorption at 300 K, while it decreased at first and then increased through the absorption at 373 K. From the change in line-shape of the spectra, the hydrogen accomodated in RbC_8 is considered to be atomic at 300 K and to be in the form of hydride ion at 373 K. The spectrum was compared with that calculated for the lattice accommodating hydrogen atoms.

IV-U Organic Metals

In an attempt to develop a new organic superconductor and to explore the related phenomena, several new organic charge-tansfer complexes are prepared, and their structural and physical properties are investigated.

IV-U-1 Structural and Electrical Properties of $(BEDT\text{-}TTF)_5Hg_3Br_{11}$

Takehiko MORI, Ping WANG, Kenichi IMAEDA, Toshiaki ENOKI, and Hiroo INOKUCHI

[*Solid State Communn.*, **64**, 733 (1987)]

New organic conductors, $(BEDT\text{-}TTF)_5Hg_3Br_{11}$ and $(BEDT\text{-}TTF)HgBr_3$ (BEDT-TTF: bis(ethylenedithio)tetrathiafulvalene) are prepared, and their crystal structures, transport properties, and ESR are investigated. In the former complex, 3/10 of the BEDT-TTF molecules are incorporated in the anion sheet as $BEDT\text{-}TTF^{2+}$ (Fig. 1). This complex shows, in spite of its complicated 7-fold periodicity, metallic conductivity down to 120 K.

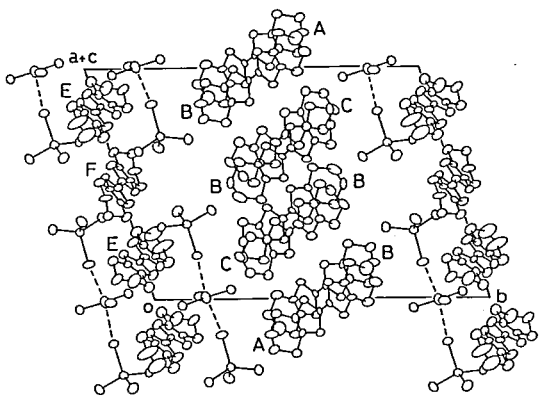

Fig 1. Crystal Structure of $(BEDT\text{-}TTF)_5Hg_3Br_{11}$. The anions are composed of $HgBr_4^{2-}$-$HgBr_3^{-}$-$HgBr_4^{2-}$ unit. The divalent donors ($BEDT\text{-}TTF^{2+}$) E and F are sandwiched by these anions. The central donor layer around y= 0.5 is the conducting sheet with the 7-fold periodicity.

IV-U-2 A BEDT-TTF Complex Including a Magnetic Anion, $(BEDT\text{-}TTF)_3(MnCl_4)_2$

Takehiko MORI and Hiroo INOKUCHI

[*Bull. Chem. Soc. Jpn.*, **61**, 591 (1988)]

The title charge-transfer complex is prepared and its crystal structure is determined. One third of the donors is incorporated in the anion sheet, and holds about 2+ charge. The remaining donors from a conducting sheet with a similar arrangement to β'-$(BEDT\text{-}TTF)_2ICl_2$. The spin susceptibility investigated by ESR obeys the Curie law down to 5 K, and no magnetic phase transition coming from the Mn^{2+} spin is observed.

IV-U-3 Electrical Conductivity, Thermoelectric Power, and ESR of a New Family of Molecular Conductors, $(DCNQI)_2M$

Takehiko MORI, Hiroo INOKUCHI, Akiko KOBAYASHI *(Univ. of Tokyo)*, **Reizo KATO*, and Hayano KOBAYASHI*** *(*Toho Univ.)*

[*Phys. Rev. B* **38**, 5913 (1988)]

A family of organic molecules, R_1R_2DCNQI (R_1, R_2 = CH_3, CH_3O, Cl, Br; DCNQI = *N,N'*-dicyanoquinonediimine; Fig. 1) works as a ligand as well as an eletron acceptor to form highly-conducting charge-transfer/coordination compound as $(R_1R_2DCNQI)_2M$(M = Cu, Ag, Li, Na, K, NH_4). These salts are investigated by the measurements of electrical conductivity, thermoelectric power, and ESR. The salts containing cations, M, other than Cu undergo the Peierls transitions at 50 – 100 K. The Cu salts of the halogen-containing DCNQI also exhibit the Peierls transitions between 150 K and 250 K, followed by antiferromagnetic transitions around 10 K. The Cu salts with the substitutents, R_1 = R_2 = CH_3 or CH_3O are especially interesting because these salts retain metallic conductivity down to (at least) 1.5 K, whereas ESR of $(DMDCNQI)_2Cu$ indicates occurrence of a short-range magnetic order at 30 K succeeded by a long-range three-dimensional order at 5.5 K. This may be the first organic conductor where metallic conduction and a magnetic order are coexisting.

	R_1	R_2
DMDCNQI	CH_3	CH_3
DMODCNQI	CH_3O	CH_3O
MeBrDCNQI	CH_3	Br
DBrDCNQI	Br	Br
MeClDCNQI	CH_3	Cl
DClDCNQI	Cl	Cl

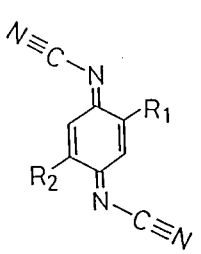

Figure 1. Molecular structures of the investigated DCNQI series molecules.

IV-U-4 Coexistence of a Magnetic Order and Metallic Conduction in an Organic System, $(DMDCNQI)_2Cu$

Takehiko MORI, Shunji BANDOW, Hiroo INOKUCHI, Akiko KOBAYASHI *(Univ. of Tokyo)*, **Reizo KATO*, and Hayao KOBAYASHI*** *(*Toho Univ.)*

[*Solid State Commun.*, **67**, 565 (1987)]

A magnetic molecular metal, $(DMDCNQI)_2Cu$ is investigated by the measurements of ESR, static susceptibility, and specific heat. The large Pauli paramagnetism and the large electronic specific heat indicate a significant contribution of the mixed-valent Cu

orbitals to the conduction bands and the essentially itinerant character of the d-electrons. The increase of magnetic susceptibility below 70 K and a magnetic order below 5.5 K, however, demonstrate the development of small magnetic moments on the Cu sites at low temperatures.

IV-U-5 Electronic Properties of New Organic Conductors Based on 2,7-Bis(methylthio)-1,6-dithiapyrene (MTDTPY) with TCNQ and p-Benzoquinone Derivatives

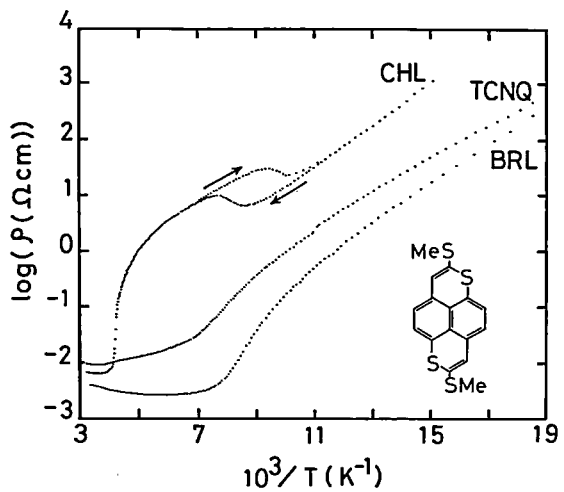

Figure 1. Temperature dependence of the resistivities for β-MTDTPY-TCNQ, MTDTPY-CHL, and MTDTPY-BRL. The inset shows the molecular structure of MTDTPY.

Kenichi IMAEDA, Toshiaki ENOKI, Takehiko MORI, Hiroo INOKUCHI, Mitsuru SAKAKI*, Kazuhiro NAKASUJI*, and Ichiro MURATA* *(*Osaka Univ.)*

[*Bull. Chem. Soc. Jpn.* in press]

Electronic properties of charge-transfer complexes based on 2,7-bis(methylthio)-1,6-dithiapyrene (MTDTPY) with TCNQ and p-benzoquinone derivatives (fluoranil (FLL), chloranil (CHL), bromanil (BRL), and DDQ) have been investigated by means of electrical conductivity, thermoelectric power, ESR, and band calculation. α-MTDTPY-TCNQ, MTDTPY-FLL, and MTDTPY-DDQ are semiconductors. β-MTDTPY-TCNQ shows a metallic conduction owing to uniform segregated stacks and partial charge-transfer, as shown in Figure 1. The metal-insulator transition takes place around 110 K. The sharp ESR linewidth and large anisotropy of transfer integral suggest one-dimensionality of β-MTDTPY-TCNQ. Thus this transition is considered to be caused by a Peierls instability. MTDTPY-CHL and MTDTPY-BRL are also metallic and show sharp metal-insulator transitions at 240 K and 125 K, respectively. The results of ESR and band calculation for MTDTPY-CHL are suggestive of one-dimensional metal as well as β-MTDTPY-TCNQ.

RESEARCH ACTIVITIES V
Department of Applied Molecular Science

V-A Synthesis and Properties of Novel Type Transition Metal Oxide and Sulfide Clusters

A new type of organometallic oxide and sulfide clusters have been synthesized by using oxo and thiometalate as a metal oxide and sulfide building block, respectively. We have shown that some of them have multi-electron transfer properties and the highly selective catalyses for oxidation of olefines as well as unique structures being viewed as a fragment structure of metal oxide.

We have continued to study such new type of organometallic oxide clusters with a particular interest in the cooperative effect due to multi-metal center on reactivities and physicochemical properties.

V-A-1 Synthesis and Molecular Structure of Organometallic Oxide Clusters with a Quadruple-Cubane Core Structure: $[(MCp^*)_4V_6O_{19}]$ (M=Rh and Ir; $Cp^*=C_5Me_5$)

Yoshihito HAYASHI, Yoshiki OZAWA, and Kiyoshi ISOBE

The structure of neutral organometallic oxide clusters, which is constructed by the interaction of oxometalates and organometallic groups, depends mainly on the charges of both groups and the number of available coordination site on organometallic groups.

The use of the dianion oxometalate $M'O_4^{2-}$ (M'=Mo, W) as the building block of oxides with MCp* groups gave the novel triple cubane-type cluster.[1] We have employed the monoanion oxometalate, VO_3^-, to synthesize the title clusters.

X-ray analysis of $[(RhCp^*)_4V_6O_{19}]\cdot 4CH_3CN\cdot H_2O$ revealed that the structure consists of six vanadium atoms and four $[RhCp^*]^{2+}$ groups which are located octahedrally and tetrahedrally, respectively, around a central oxygen atom. Each vanadium is bonded peripherally to neighboring vanadium atoms through oxygen bridge to form the cage-like structure. Four alternate faces of the octahedron composed of six vanadium atoms are capped by $[RhCp^*]^{2+}$ groups through three Rh-O bonds to give an unique neutral molecule having overall Td symmetry. Alternatively, the structure can be visualized as formed from four cubic cores (RhV_3O_4) that have condensed so that they all share a common vertex as shown in Figure 1.

Reference

1) Y. Hayashi, K. Toriumi, and K. Isobe, *J. Am. Chem. Soc.*, **110**, 3666 (1988); *IMS Ann. Rev.*, 121 (1987).

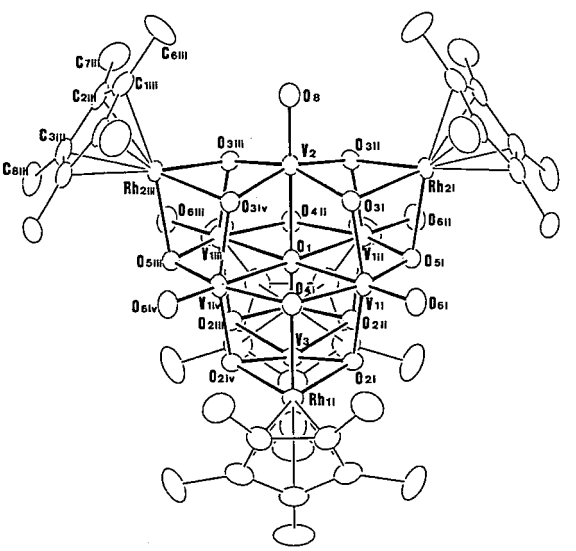

Figure 1. Molecular structure of the oxide cluster, $[(RhCp^*)_4V_6O_{19}]$. Important bond lengths (Å) and angles (deg) are given with e.s.d.'s in parentheses: Rh1(i)-O2(i), 2.114(9); V1(i)-O6(i), 1.60(1); V1(i)-O1, 2.248(3); V1(i)-O2(i), 1.918(9); V2-O1-V3, 180(1); Rh1(i)-Rh1(ii)-Rh2(i), 60.29(3); V1(i)-V2(i)-V1(ii), 60.2(1); V1-O1-V3, 90.5(6).

V-A-2 Reactivities and Properties of the Organometallic Oxide Cluster, $[(MCp^*)_4V_6O_{19}]$ (M=Rh and Ir)

Yoshihito HAYASHI and Kiyoshi ISOBE

In metal cluster chemistry, the cooperative effect due to multi-metal center is a most interesting phenomenon. We have found the rhodium oxide cluster, $[(RhCp^*)_4V_6O_{19}]$ **1**, shows a site selective oxygen atom exchange reaction caused by this effect.

Cluster (**1**) has a cage-like structure of V_6O_{19} made up of six distorted VO_6 octahedra as shown in Figure 1 in V-A-1. Within each of these octahedra the vanadium atom is involved in three distinct types of bonding: One bond is to a terminal oxygen atom (Ot), four are to bridging oxygen atoms (Ob) which are shared by an other vanadium and rhodium atoms, and one is to a central oxygen atom (Oc) which is shared by all the six vanadium atoms.

Sample of **1** enriched in ^{17}O have been prepared in ^{17}O-enriched water. It displays three completely resolved ^{17}O NMR signals (C) in $CDCl_3$ as shown in Figure 1. These signals are assigned using the general correlation between chemical shift and π-bond order which is assumed to increase as bond length decreases. Cluster **1** gives also a similar ^{17}O NMR spectral pattern (B) in H_2O at 25°C. After heating in H_2O at 90°C for 4h the Ob resonance displayed an anomalous intensity decrease, although intensity of the Ot and Oc signals remained constant (A). This suggests that a site selective oxygen exchange with free H_2O takes place. The averaged bond distance of V-Ob bonds is 1.910 Å, longer than that of the typical V-O bond (1.85 Å). The V-Ob bond is not only weakened but also activated kinetically by the capping RhCp* groups.

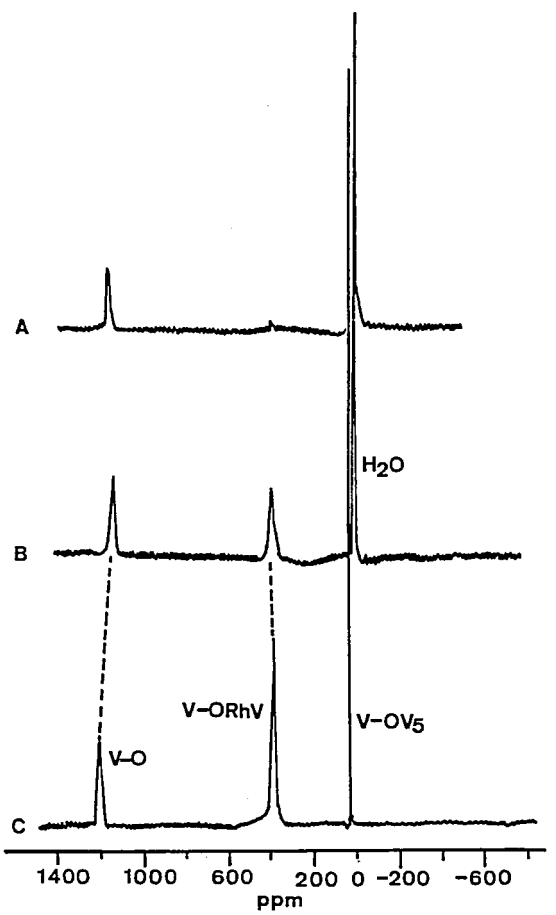

Figure 1. ^{17}O NMR spectra of $[(RhCp^*)_4V_6O_{19}]$ in $CDCl_3$ (C), in H_2O (B), and in H_2O after heating at 90°C for 4 h (A).

V-A-3 Synthesis and Molecular Structure of a Novel Metal-Sulfido Cluster: $[Ir(\eta^5\text{-}C_5(CH_3)_5)\text{-}WOS_2(S_2)]_2$.

Yoshiki OZAWA, Yoshihito HAYASHI, and Kiyoshi ISOBE

Recently transition-metal sulfido clusters have been studied as model compounds of active site in iron-molybdenum enzymes, and as industrial hydrodesulfurizing catalysts. These compounds have been exclusively synthesized by the "spontaneous self-assembly" method. We have used tetrathiometalates as bidentate ligands for organometals to develop a synthetic method for new heterometal sulfido clusters.

The title compound was prepared by the reaction of $[IrCp^*Cl_2]_2$ ($Cp^*=C_5Me_5$) with $(NH_4)_2WS_4$ reduced by

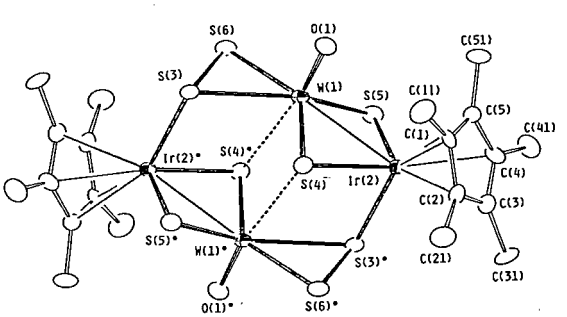

Figure 1. Molecular Structure of $[IrCp^*WOS_2(S_2)]_2$ with OPTEP drawing. Selected bond distances (Å) and angles (°) are given as follows: Ir-W 2.816(1), Ir-S 2.378(3) 2.349(3) 2.401(3), W-O 1.708(8), W-S 2.306(3) 2.275(3), W-S(persulfido) 2.417(3) 2.490(3), S-W-S(persulfido) 50.4(1), W-S-Ir 74.0(1), 74.5(1).

$NaBH_4$ in methanol. Air stable deep red crystals were obtained from the reaction mixture re-oxidized with oxygen.

Crystallographic data: monoclinic, $P2_1/n$, a= 9.708(1), b=17.773(4), c=8.609(1) Å, β=100.36(1)°, V=1461.2(4) Å^3, Z=2, Dx=2.89 g cm^{-3}, μ (Mo Kα)= 176.37 cm^{-1}. The R value of 0.031 is obtained by using 2263 independent reflections in the range 2θ <65° for structure determination and refinement.

The tetranuclear cluster (Figure 1) having an inversion center consists of two equivalent $IrCp^*WOS_2(S_2)$ moieties. Each W atom has a distorted tetragonal pyramidal coordinaiton with one terminal O atom at the apex, a persulfido S_2^{2-} ligand (S(3),S(6)), and two S atoms (S(4),S(5)) shared by the Ir atom. The Ir atom is also bound to one S atom (S(3)*) of a persulfido molecule in the other moiety. The short W-Ir distances of 2.817(7) Å indicate a metal-metal bond.

V–B Carbon-Carbon Bond Formation Employing Fe-C and Pd-C Bond

Among organotransition metal compounds with significant metal-carbon covalent character, organo iron and palladium have been found to be remarkable useful compounds for organic synthesis based on C-C bond formation. The formation of C-C bond consists of a variety of elemental reactions such as reductive coupling, migratory insertion, oxidative addition, etc. We now show two unique but fundamental C-C bond formations due to oxidative solvolysis of Fe-C bond and intermolecular reductive coupling of Pd-C bond.

V-B-1 Reactivity of Cumulene Complexes. Two Competing Pathways in Oxidative Solvolysis of Tetramethylbutatriene(hexacarbonyl)diiron

Syun-ichi KIYOOKA *(Kochi Univ.)*, **Takuya ATAGI** *(Kochi Univ.)*, **Ryoji FUJIYAMA** *(Kochi Univ.)*, **and Kiyoshi ISOBE**

[*Chemistry Lett.*, 891 **(1988)**]

The oxidation of tetramethylbutatriene(hexacarbonyl)diiron (**1**) in alcohols by ceric ammonium nitrite gives regioselectively diene-diesters (**2**) and acetylene-diethers (**3**) in moderate yields. The reaction is the first example showing that both the carbonylation and etherification of the cumulene ligand with solvent alcohols take place concurrently on a cationic 17-electron species.

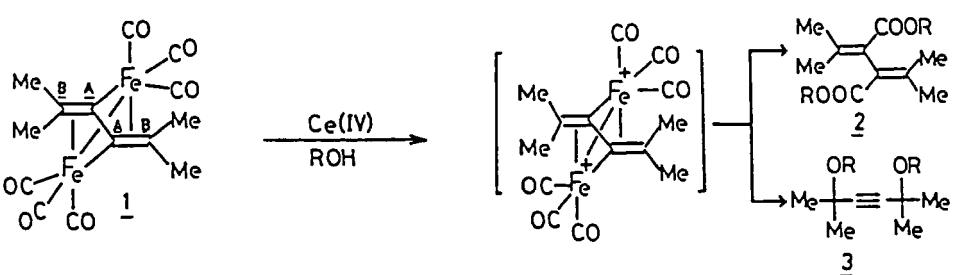

V-B-2 Thermolysis of [(η^3-allyl)PdMe(PPh_3)]: An Unexpected Evolution fo Ethane Gas as a Main Product

Yoshihito HAYASHI *(Osaka City Univ.)*, **Yukio NAKAMURA** *(Osaka City Univ.)*, **and Kiyoshi ISOBE**

[*J. Chem. Soc., Chem. Commun.*, 403 **(1988)**]

The title complex (**3**) which is synthesized according to Scheme 1 thermally decomposes with preferential evolution of ethane rather than but-1-ene, the allilic alkylation product, indicating that the binuclear methyl-bridged intermediate formed by phosphine dissociation predominantly participates in this thermolysis (Scheme 2).

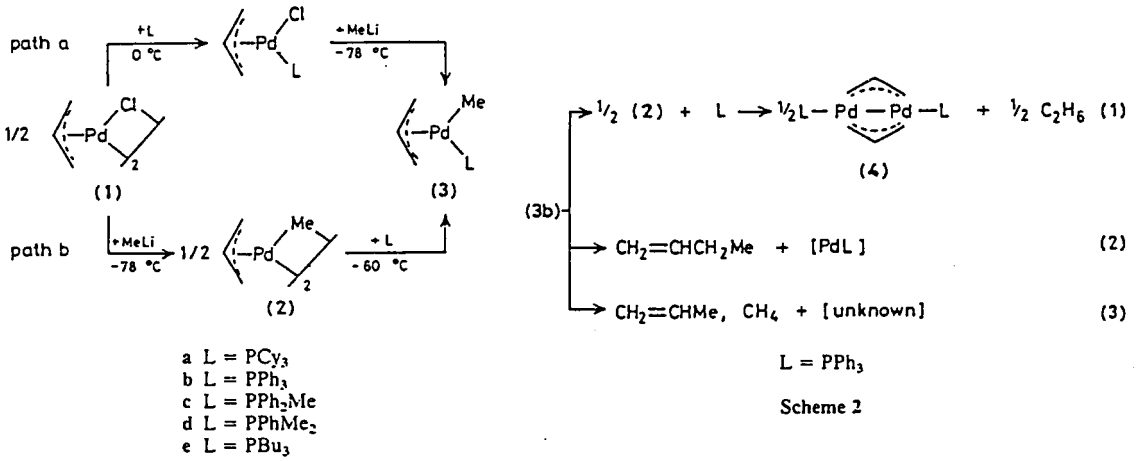

a L = PCy_3
b L = PPh_3
c L = PPh_2Me
d L = $PPhMe_2$
e L = PBu_3

Scheme 1

Scheme 2

V–C Halogen-Bridged M^{II}-M^{IV} Mixed-Valence Compounds

In the past ten years, crystal structures and solid state properties of the halogen-bridged M_1^{II}-M_2^{IV} mixed valence compounds with a one-dimensional chain structure (M_1=Pt, Pd, Ni; M_2=Pt, Pd) have been extensively studied because of their characteristic physical and chemical properties such as the strong charge transfer absorption and the luminescence with large Stokes shift. They are well interpreted in terms of the strong electron-lattice interaction in quasi-one-dimensional systems.

Recently, we succeeded in the preparation of a bromo-bridged Ni^{III}-Ni^{III} compound of $\{[Ni(R,R\text{-chxn})_2Br]Br_2\}$, which have a similar structure to the mixed valence compound but have no Peierls distortion [See *IMS Ann. Rev.*, **124** (1987)]. The magnetic behavior and crystal structure suggest strong diamagnetic interaction between Ni^{III} atoms through a bridging Br atom, and further two-dimensionality of the structure.

V-C-1 Crystal Structures of Bromo-Bridged One-Dimensional M^{II}-M^{IV} Mixed-Valence Compounds with a Cyclohexanediamine Ligand, $[M(R,R\text{-chxn})_2][MBr_2(R,R\text{-chxn})_2]Br_4$ (M=Pt and Pd)

Koshiro TORIUMI, Masahiro YAMASHITA *(Nagoya Univ.)*, **Hans TOFTLUND** *(IMS and Odense Univ.)*, **Jin SONGCHUN** *(Tohoku Univ.)*, **and Tasuku ITO** *(Tohoku Univ.)*

Structure and solid state properties of halogen-bridged mixed-valence compounds are highly dependent on a manner of hydrogen-bond network in the crystal. Crystal structures of the title compounds have been determined by X-ray diffractometry. Crystallographic data are: orthorhombic, I222, Z=2; for Pt compound, a=23.865(5), b=5.372(2), c=7.022(1) Å, V=900.3(4) $Å^3$, R=0.020 for 1914 reflections; for Pd compound, a=23.884(5), b=5.296(1), c=7.067(2) Å, V=893.8(4) $Å^3$, R=0.021 for 1727 reflections. Their crystal structures are isomorphous with those of $[Pt(R,R\text{-chxn})_2][PtCl_2(R,R\text{-chxn})_2]Cl_4$ and $\{[Ni(R,R\text{-chxn})_2Br]Br_2\}$. Figure 1 shows the chain structure of the Pd compound. The Pd^{2+} and Pd^{4+} moieties in the linear chain are linked by charge transfer interaction through the Br atoms, and also linked by hydrogen-bonds (NH···Br). Those in the neighboring chains are also linked by the hydrogen bonds, constructing a two-dimensional structure. On the other hand, Weissenberg photographs for the Pd compound show diffuse lines with indexes (−, k+0.5, 1), which suggest two dimensional order of the crystal structure. This result is well corresponding to the two dimensional hydrogen bond network.

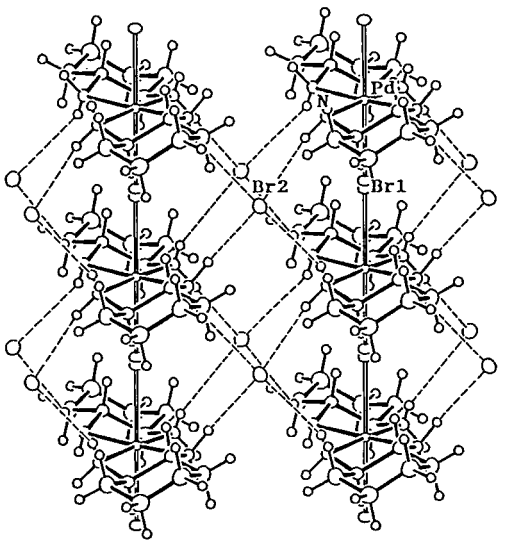

Figure 1. Portion of the infinite chains along the b axis with surrounding Br^- ions. The dashed lines correspond to hydrogen bonds.

V-C-2 Crystal Structures of New Hetero-Metal Mixed Valence Cu^{II}-Pt^{IV} Complexes with One Dimensional Chain Structure

Hiroki OSHIO and Koshiro TORIUMI

It is well known that charge transfer properties between two metal ions or molecules can be used to design a molecular ferromagnet or high electric conducting material. The introduction of paramagnetic hetero-metal ions to the Wolfram's type one dimentional chain system is expected to give us the insight of the charge transfer properties between hetero-metal ions. Here we report the crystal structure of new hetero-metal one dimentional compounds, $[Cu(en)_2][PtX_2(en)_2](ClO_4)_4$ (X=Cl (**1**) and Br (**2**)).

The X-ray crystal structure analysis reveals a halogen-bridged linear chain structure, and the octahedral six-coordinate $Pt^{IV}X_2(en)_2$ and square-planar four-coordinate $Cu^{II}(en)_2$ units are arranged alternately, constructing a linear chain structure along the b-axis. Crystalographic data are: for (**1**), orthorhombic, Icma, Z=2, a=13.645(1), b=10.787(1) c=9.645(1) Å, V=1419.6 $Å^3$, R=0.025 for 991 relections; for (**2**), orthorhombic, Icma, Z=2, a=13.559(1), b=10.917(1), C=9.657(1) Å, V=1433.6(2) $Å^3$, R=0.022 for 884 reflections. Defects of copper and halogen atoms depending on the preparation condition was found. The ratios of the Pt, Cu, and halogen atoms were estimated to be 1.11:0.89:2 and 1.44:0.56:1.70 for (**1**) and (**2**), respectively. The bond distances of Pt^{IV}-X and Cu^{II}-X for (**1**) and (**2**) were determined to be 2.313(3), 3.081(3), and 2.453(1), 3.005(1) Å, repsectively.

V-C-3 Magnetic Properties of $[Cu(en)_2][PtX_2(en)_2](ClO_4)_4$ (X=Cl adn Br)

Hiroki OSHIO, Koshiro TORIUMI and Shunji BANDO

A single crystal EPR spectrum measured at 10 K for X=Cl (**1**) is shown in Figure 1. Hyperfine splitting and zero-field splitting were not observed. Anisotropic g values for perpendicular and paprallel components are obtained; 2.048, 2.167 and for 2.044, 2.167 for both (**1**) and (**2**). The EPR spectrum indicates that an electron spin on the copper atom occupies the $d_{x^2-y^2}$ orbital which is perpendicular to the chain direction. The temperature dependence of the magnetic susceptibility for the compounds was measured in the temperature range (2.7-300 K). The susceptibility obeys the Curie-Weiss law, and the Curie and Weiss constants were determined to be 0.415 emu mol^{-1} K and −1.2 K for (**1**), and 0.495 emu mol^{-1} and −2.95 K for (**2**). Both the EPR and magnetic data show that there is no strong magnetic interaction between the paramagnetic copper ions.

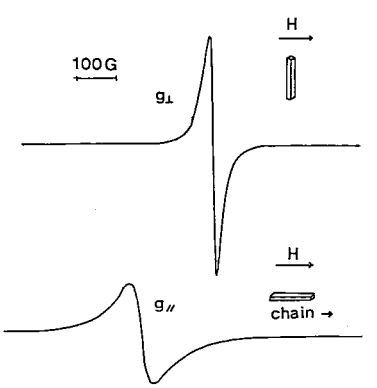

Figure 1. Single crystal X-band EPR spectrum of $[Cu(en)_2][PtCl_2(en)_2](ClO_4)_4$

V-D Synthesis and Reactivities of New Class of Transition Metal Polyhydride Complexes

Transition metal hydrides are implicated in the variety of stoichiometric and catalytic organic transformations such as alkene isomerization, hydrogenation, and hydroformylation. The hydrides especially polyhydrides are also known to have the potential for generating coordinative unsaturation by eliminating molecular hydrogen. The reactivities of the resulting coordinative unsaturated species therefore caputured the imagination of many investigators. In recent years, polyhydride complexes with electron donating ligands have been shown to be of importance as the precursors of active species for alkane C-H activation reaction.

Investigation in our group have been centered on the synthetic and reactivity study of a new class of polyhydride complexes having only pentamethylcyclopentadienyl groups as the auxiliary ligands. Recently, we have isolated a novel dinuclear tetrahydride bridged ruthenium complex. We are striving now to get the penetrating understanding on the C-H and C-C activation reaction promoted by the ruthenium tetrahydride.

V-D-1 A Novel Dinuclear Tetrahydride Bridged Ruthenium Complex, $(\eta^5\text{-}C_5Me_5)Ru(\mu\text{-}H)_4Ru(\eta^5\text{-}C_5Me_5)$

Hiroharu SUZUKI and Hideki OMORI *(Tokyo Inst. of Tech.)*

The ruthenium tetrahydride complex, $(\eta^5\text{-}C_5Me_5)Ru(\mu\text{-}H)_4Ru(\eta^5\text{-}C_5Me_5)$ (**2**), was prepared by treatment of $[(\eta^5\text{-}C_5Me_5)RuCl_2]_2$ (**1**) with $LiAlH_4$ in Et_2O and the subsequent protonolysis with ethanol. Complex **2** is the first example of the binuclear tetrahydride bridged complex having no phosphine or arsine ligands. The structure of **2** is unambiguously assigned on the basis of ^1H NMR, ^{13}C NMR, FD-MS, and X-ray diffraction study (Fig. 1).

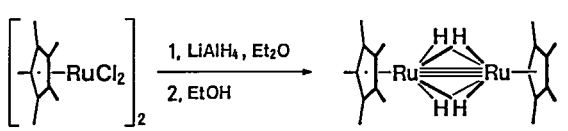

1 2

While complex **2** is hardly decomposed upon irradiation of UV light, **2** evolves H_2 to generate the coordinatively unsaturated species by heating or by the addition of acid. Treatment of **2** in toluene solution with atmospheric pressure of ethylene resulted in the formation of a binuclear vinyl complex via a vinylic C-H activation reaction.

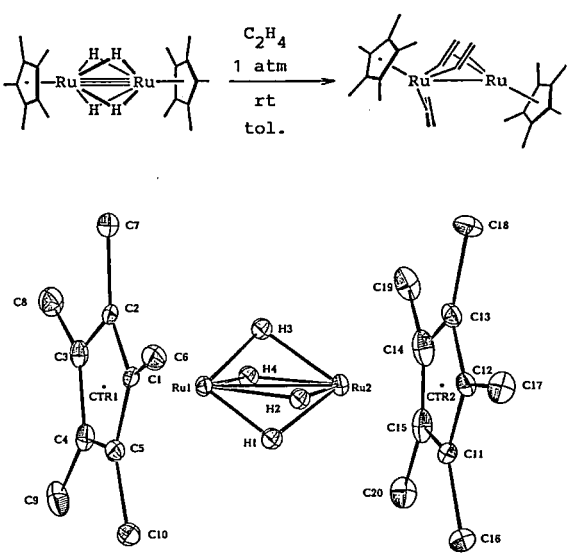

Figure 1. Molecular structure of $[(\eta^5\text{-}C_5Me_5)Ru]_2(\mu\text{-}H)_4$

RESEARCH ACTIVITIES VI
Coordination Chemistry Laboratories

New staffs came to the laboratories after April, 1988, since Professor K. Saito retired in March, 1987 and Professor S. Kida and Associate Professor S. Ishiguro moved back to their original Institutes, from which they had been transferred, in March 1988. Two previous Adjunct Professors, Dr. T. Saito and Dr. H. Takei, and two previous Adjunct Associate Professors, Dr. S. Funahashi and Dr. S. Tero finished their terms and were replaced by new Adjunct Professors and Associate Professors, respectively, from April, 1988, also.

One of the new members of the Coordination Chemistry Laboratories is Professor H. Ohtaki, who moved from Tokyo Institute of Technology in April, 1988, and was appointed to be the Director of the Laboratories in June. Thus, X-ray diffraction and EXAFS investigations of the structure of complexes in solution became new subjects of the Laboratory of Complex Catalysts. Molecular dynamics simulations were also applied to the solution system by his group to elucidate the micro-structure and dynamic properties of electrolyte solutions, as well as solvents themselves.

Professor E. Kimura and Associate Professor R. Ikeda were transferred from Hiroshima University and Nagoya University, respectively, to develop new synthetic chemistry of metal complexes with macrocyclic ligands and structural chemistry of various complexes, as well as their dynamic properties, in the solid and solution states.

New Adjunct Professors, Dr. T. Yoshida and Dr. A. Uehara and new Adjunct Associate Professors, Dr. R. Kuroda and Dr. H. Ōkawa started new projects concerning syntheses of low and/or mixed valent complexes of new types and structural studies of nucleic acids and their interactions with small molecules. Thermochemistry was introduced as a tool for investigating reactions of metal complexes in solid, as well as solution calorimetry which has been employed in the laboratories.

VI–A Structural Studies of Metal Complexes in Solution and in the Glassy State by the X-Ray Diffraction and EXAFS Methods

Structures of solvated ions, metal complexes and clusters, and solvents themselves in solution and in the glassy state are investigated by the X-ray diffraction and EXAFS methods.

VI-A-1 Thermodynamic and Structural Studies of Metal Complexes in Various Solvents

Shin-ichi ISHIGURO, and Hitoshi OHTAKI

[*J. Coord. Chem.*, **15**, 237–306 (1987)]

Complexation of various metal-ligand systems has been discussed from the view-point of solute-solvent and solvent-solvent interactions in pure solvents and their mixtures on the basis of thermodynamic and structural measurements. In water and dioxane-water mixtures, it was suggested that the solvation structure in the secondary shell of ionic species significantly changes by adding dioxane to water due to the formation dioxane-water associates in the bulk. It was found that 1,10-phenanthroline formed its stacked species, such as $[H(phen)_2]^+$ and $(phen)_2$, in water, but the species hydrophobically associated disappeared in dioxane-water mixtures due to breaking of the hydrogen-bonded structure of water. Complexation of Zn(II), Cd(II) and Hg(II) ions with SCN^- ions in water was discussed in relation to the structures of the complexes determined by X-ray diffraction, and NMR and Raman spectral measurements. The solvent effect on the complexation of Cu(II) with chloride ions in acetonitrile, *N,N*-dimethylformamide and their mixtures was found to be remarkable, which was well explained in terms of preferential solvation of *N,N*-dimethylformamide, i.e., the formation of $[Cu(dmf)_n]^{2+}$ (n = 1–6), in acetonitrile.

VI-A-2 Solvation Structure of Copper(II) Ion in *N,N*-Dimethylformamide and *N,N*-Dimethylformamide-Acetonitrile Mixtures Determined by the X-Ray Diffraction Method

Kazuhiko OZUTSUMI, Shin-ichi ISHIGURO and Hitoshi OHTAKI

[*Bull. Chem. Soc. Jpn.*, **61**, 945–951 (1988)]

The solvation structure of copper(II) ion in *N,N*-dimethylformamide (DMF) and *N,N*-dimethylformamide-acetonitrile (AN) mixtures has been investigated by means of X-ray diffraction at 25°C. The X-ray scattering data for the copper(II) perchlorate DMF solution were well-interpreted in terms of the presence of the axially elongated octahedral $[Cu(dmf)_6]^{2+}$ ion in DMF. Among the six DMF molecules, four of them are at the distance of 203(3) pm at the equatorial position and the other two are at 243(5) pm at the axial one. On the other hand, in copper(II) perchlorate DMF-AN solutions with the C_{dmf}/C_{Cu} mole ratios of 5.308 and 7.435, where C_i denotes the total concentrations of species i, the copper(II) ion is coordinated with four DMF molecules within the square-plane and with no solvent molecule along the axis of the plane. The equatorial Cu-O bond length is 200(1) pm and practically the same as that within the $[Cu(dmf)_6]^{2+}$ ion in DMF. In copper(II) nitrate DMF solutions (1.086 and 1.500 mol dm^{-3}), a nitrate ion binds to copper(II) ion at the equatorial position and the distorted octahedral $[CuNO_3(dmf)_5]^+$ complex is formed.

VI-A-3 EXAFS Study of Iron(III) Complexes of Sugar Type Ligands

Lazslo NAGY*, Toshio YAMAGUCHI, Masaharu NOMURA***, and Hitoshi OHTAKI** (**A. Jozsef Univ., Szeged, Hungary, **Fukuoka Univ., ***Natl. Lab. High Energy Phys.)*

[*Inorg. Chim. Acta*, in press]

Three kinds of iron(III) complexes formed with sugar type ligands, ketose, polyalcohol, and sugar acid, were prepared. The Fe *K*-edge absorption spectra of the complexes were measured both in aqueous solution and in the solid state to reveal the structure from the analysis of their EXAFS and XANES. It was concluded that the iron(III) sugar complexes have a distorted octahedral structure with a mean Fe-O distance of 195 pm irrespective of the sugar type ligands both in aqueous solution and in the solid state. In the case of iron(III) fructose complex the dimerization of the complex was evidenced and the most likely structure was proposed.

VI-A-4 EXAFS Study of Aqueous Rare Earth Perchlorate Solutions in Liquid and Glassy States

Toshio YAMAGUCHI*, Masaharu NOMURA, Hisanobu WAKITA*, and Hitoshi OHTAKI** (**Fukuoka Univ., **Natl. Lab. High Energy Phys.)*

[*J. Chem. Phys.*, in press]

Extended X-ray absorption fine structure (EXAFS) measurements were performed for concentrated aqueous rare earth perchlorate solutions ($R = 28$; R is the moles of water per mole of salt) in the liquid state at room temperature and in the glassy state at liquid nitrogen temperature. The quantitative analysis of the EXAFS data has revealed that the hydration number changes from about nine for light rare earth ions to about eight for heavy rare earth ions through the intermediate ions of $Sm^{3+} \sim Eu^{3+}$ in both liquid and glassy states. The average Ln^{3+}-OH_2 distances were determined and they are in agreement with previously reported values from X-ray and neutron diffraction. The ratio of the Debye-Waller factor of the average Ln^{3+}-OH_2 bonds for the intermediate rare earth ions in the two states is larger than that for the light and heavy ions, the result showing that the hydration shell of the intermediate rare earth ions is disordered, consisting of different Ln^{3+}-OH_2 bonds.

VI-A-5 Structural Studies on Superionic Glass AgI-Ag_2O-V_2O_5

Awantharaman RAJALAKSHMI*, Maha SESHASAYEE*, Toshio YAMAGUCHI, Masaharu NOMURA*** and Hitoshi OHTAKI** (**Indian Inst. Technology, Madras, India, **Fukuoka Univ., ***Natl. Lab. High Energy Phys.)*

An amorphous thin plate of mole percent 50% AgI-30% Ag_2O-20% V_2O_5 was prepared by rapid quenching from the melt. An EXAFS study at the Ag *K*-edge shows r_{Ag-I} = 2.87 Å, n_{Ag-I} = 1.4, where n_{i-j} is the coordination number, and the difference between two close Ag-O distances Δr_{Ag-O} = 0.37 Å. X-Ray studies yield similar values of r_{Ag-I} = 2.86 Å, n_{Ag-I} = 1.3, and Δr_{Ag-O} = 0.37 Å. On the other hand, X-ray RDF studies yield two V-O interactions with distances 1.78 and 2.39 Å and their coordination numbers are 3.6 and 1.7, respectively. From these results we proposed a model comprising of a three dimensional network of distorted VO_5 pyramids which are 5, 4, and 3 corner-shared leading to large channels in the structure. Silver(I) ions form bonds and secondary interactions with the network non-bridging and bridging oxygen atoms and I^- ions around the Ag^+ ions in the large voids created by the glass network. The results favor a model of dispersed Ag^+ and I^- ions in the glass rather than the presence of clusters or microdomains of AgI in the glass.

VI-A-6 Liquid Structure of *N,N*-Dimethylformamide, Acetonitrile and their 1:1 Molar Mixture

Tamas RADNAI*, Sumiko ITOH*, and Hitoshi OHTAKI *(*Tokyo Inst. Technol.)*

[*Bull. Chem. Soc. Jpn.*, in press]

Liquid structures of pure *N,N*-dimethylformamide (DMF) and acetonitrile (AN) as well as of their 1:1 molar mixture were investigated by X-ray diffraction at 25°C. The careful reinvestigation of pure DMF led to a good reproducibility of the previous result. Slight deviations in the structural parameters are discussed and a detailed parameter table is reported. A simple model in which each AN molecule has 2 neighbors at an average distance of 330 pm describes the more ordered first neighbor structure of pure AN. The main interaction forming the structure is of dipole-dipole type, in agreement with previous findings.

In the 1:1 molar mixture a dipole-dipole model also leads to a satisfactory description of the first neighbor structure. The preferred orientation is that with dipoles in the antiparallel position. A central DMF molecule has 1.75 neighboring AN molecules in average at a distance of 316 pm. The same stands for DMF around AN. No evidence for other kinds of interaction, e.g., weak H-bond type intermolecular interactions could be found in the mixture.

VI–B Molecular Dynamics Studies on the Structure and Microdynamic Behavior of Ions in Solution

Molecular dynamics simulations are employed to elucidate microscopic structure and behavior of ions in aqueous solutions. Dissolution and nucleation (deposition) processes are simulated, which are visualized on video.

VI-B-1 Dissolution Process of Sodium Chloride Crystal in Water

Hitoshi OHTAKI, Nobuhiro FUKUSHIMA*, Ei HAYAKAWA*, and Isao OKADA* *(*Tokyo Inst. Technol.)*

[*Pure Appl. Chem.*, **60**, 1321–1326 (1988)]

A molecular dynamics simulation has been employed in order to *observe* the dissolution process of an NaCl crystal in water at 25°C. The Tosi-Fumi, Popkie-Kistenmacher-Clementi and Matsuoka-Clementi-Yoshimine potentials have been used to describe ion-ion, ion-water and water-water interactions, respectively. The side length of a box assumed was 2000 pm, in which 216 water molecules, 32 Na^+ and 32 Cl^- ions were contained. The length of the edge of the cubic NaCl crystal having the (100) and the corresponding faces was 1120 pm. The process of dissolution of ions in the crystal was followed over the period of 7 ps from the beginning of the dissolution. It was *observed* that a chloride ion at a corner of the crystal first dissolved in water. Then another chloride ion at a different corner left the crystal surface. The third and fourth ions dissolving were also chloride ions at the other corners. The velocity of ions leaving from the

crystal was estimated from the displacement of the ions with time. For the first chloride ion, this velocity was about 4×10^2 ms^{-1}. The velocity of other chloride ions was less than that of the first one owing to electrostatic interactions between a leaving chloride ion and the crystal skeleton becoming successively positively charged.

VI-B-2 Dissolution of an NaCl Crystal with the (111) and (−1−1−1) Faces

Hitoshi OHTAKI, and Nobuhiro FUKUSHIMA* *(*Tokyo Inst. Technol.)*

[*Pure Appl. Chem.*, in press]

The dissolution process of an NaCl crystal with the (111) and (−1−1−1) faces, the former consisting of only chloride ions and the latter only sodium ions, as well as the {100} faces, in water has been demonstrated by means of molecular dynamics simulation. Ion-ion, ion-water and water-water interactions are assumed to be described in terms of the Tosi-Fumi, Popkie-Kistenmacher-Clementi and Matsuoka-Clementi-Yoshimine potentials, respectively. Twenty-eight sodium ions, twenty-eight chloride ions and 189 water molecules were placed in a box having the side-length of 2000 pm. Collision of water molecules with the walls of the box was assumed to be completely elastic. The temperature of the system was kept at 298 K during the simulation procedure, which was carried out for 7 ps (the time step $\Delta_t = 1.0 \times 10^{-15}$ s, the total steps performed were 7000) after starting dissolution of the NaCl crystal. The first, second and third ions dissolved are chloride ions at the corners of the crystal, as have been found in the previous work. The fourth one liberated was also a chloride ion on the (111) face. As we have seen in the previous simulation using another NaCl crystal with the {100} faces, no sodium ion was removed within 7 ps even from the (−1−1−1) face which was exposed to the bulk water phase. Repulsive forces arising between the chloride ions and water molecules which tend to hydrate sodium ions around the chloride ions are the force for separating the chloride ions from the crystal.

VI−C Thermodynamic Studies on Complex Formation of Metal Ions in Aqueous and Nonaqueous Solvents

Calorimetric and spectrophotometric investigations on complex formation reactions of metal ions with various ligands are carried out in aqueous and in nonaqueous solvents. Formation constants, enthalpies and entropies of the reactions are thus determined and these quantities are discussed in connection with structures of the complexes which are determined by the diffraction method and with structures and properties of the solvents, the former are also determined by the diffraction method.

VI-C-1 A Calorimetric Study of *N,N*-Dimethylformamide Complexes of Copper(II) in Acetonitrile

Shin-ich ISHIGURO, Bojana G. JELIAZKOVA*, and Hitoshi OHTAKI *(*Sofia Univ., Sofia, Bulgaria)*

[*J. Solution Chem.*, **16**, 1–10 (1987)]

Complex formation of copper(II) with *N,N*-dimethylformamide (DMF) has been investigated calorimetrically in acetonitrile at 25°C. Calorimetric titration curves obtained are explained in terms of formation of $[Cu(dmf)_n]^{2+}$ (n = 1 – 4, 6) and their formation constants, enthalpies and entropies were determined. Formation of $[Cu(dmf)_5]^{2+}$ is uncertain. The stepwise enthalpies ΔH_n° and entropies ΔS_n° at each consecutive step are all negative except for ΔS_3°. The overall enthalpies of formation of $[Cu(dmf)_6]^{2+}$ is −(77.8 ±5.4) kJ mol^{-1}, which is compared with the enthalpy of transfer of copper(II) ion, ΔH_t° = −79.7 kJ mol^{-1}, from acetonitrile to DMF.

VI–D Synthesis, Structure, and Properties of Novel Macrocyclic Polyamine Ligands and Their Complexes

Novel functions are attached to macrocyclic polyamines for further extension of useful polyamine chemistries. Thus synthesized new ligands have shown interesting chemical properties by themselves and as metal complexes. The first Pt^{II}-inclusion complex by macrocyclic ligands has also been studied by X-ray analysis.

VI-D-1 The First X-ray Crystal Structures of Ni^{II}-Monooxocyclam Complexes. The Effects of the Deprotonated Amide and of an Intramolecular Pendant Pyridine on Cyclam Ligand Field.

Eiichi KIMURA, Tohru KOIKE*, Hiroko NADA*, and Yoichi IITAKA** *(*Hiroshima Univ., **The Univ. of Tokyo)*

[*Inorg. Chem.*, **27**, 1036 (1988)]

Nickel(II) complex $Ni^{II}H_{-1}L$ **3b** of 14-membered macrocyclic tetraamines containing a deprotonated amide (monooxocyclam) attached with phenyl-pendant (**1b**) remains low-spin both in solid state and aqueous

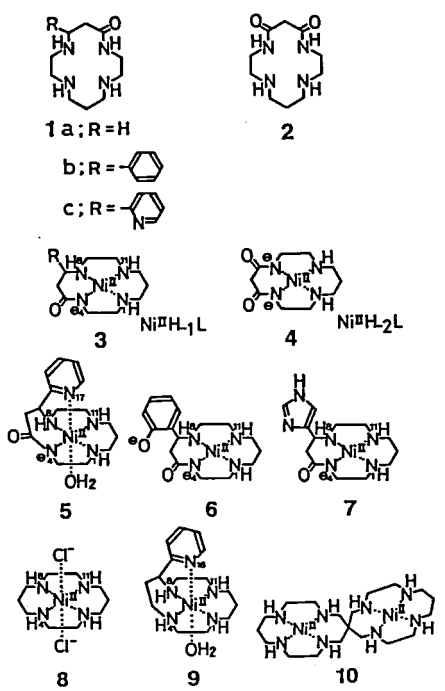

solution. On the other hand, nickel(II) complex $Ni^{II}H_{-1}L$ **5** of monooxocyclam with pyridyl-pendant (**1c**) is always high-spin. The X-ray crystal structures of **3b** and **5** have been determined to find effects of the deprotonated amide and of the pendant pyridine on cyclam ligand field. The crystal of **3b** (as monoperchlorate salt), $C_{16}H_{25}N_4ONiClO_4 \cdot H_2O$ are monoclinic, space group $P2_1$, with two molecules in the unit cell of dimensions a = 12.019(5) Å, b = 8.915(4) Å, c = 10.209(5) Å, and β = 110.95(5)°. Crystals of **5** (as monoperchlorate salt), $C_{15}H_{24}N_5ONiClO_4 \cdot 2H_2O$ are triclinic, space group $P\bar{1}$, with two molecules in the unit cell of dimensions a = 11.669(6) Å, b = 11.388(6) Å, c = 8.535(5) Å, α = 110.51(6)°, β = 90.44(5)°, and γ = 96.37(6)°. Those structures were solved by the heavy-atom method and refined by block-diagonal least-squares calculations: for **3b**, R = 0.044 for 2005 independent reflections and for **5** R = 0.060 for 4014 independent reflections.

VI-D-2 The First Fluorinated Cyclams

Eiichi KIMURA, Mitsuhiko SHIONOYA, Miho OKAMOTO*, and Hiroko NADA* *(*Hiroshima Univ.)*

[*J. Am. Chem. Soc.*, **110**, 3679 (1988)]

Synthesis and some of the novel chemical properties of the first cyclams and dioxocyclams containing CF and CF_2 moieties (**7–9** and **11–13**) are reported; the fluorine atoms dramatically reduce the basicity of distal amines and alter the redox potential of the metal complexes.

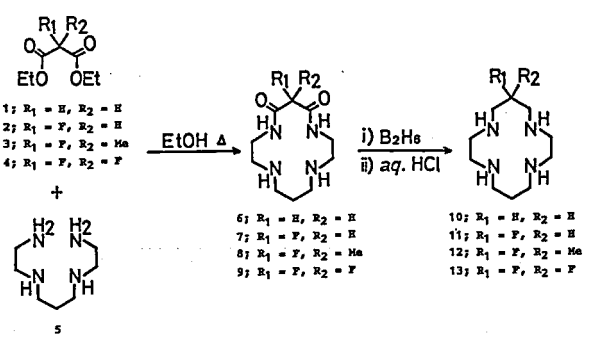

VI-D-3 The First X-Ray Crystal Structures of the Pt(II)-in and -out Complexes with Dioxocyclams

Eiichi KIMURA, Sachiko KORENARI*, Mitsuhiko SHIONOYA, and Motoo SHIRO** *(*Hiroshima Univ., **Shionogi & Co., Ltd.)*

[*J. Chem. Soc., Chem. Commun.*, 1166 (1988)]

X-ray studies of the two macrocyclic tetraamine complexes $[Pt(H_{-2}L')]^0 \cdot 5H_2O$ (**3b**) and $[PtLCl_2]^0 \cdot 2H_2O$ (**4a**), where L = dioxocyclam and L′ = 6-methyldioxocyclam, show the first Pt^{II}-in and -out structures, respectively.

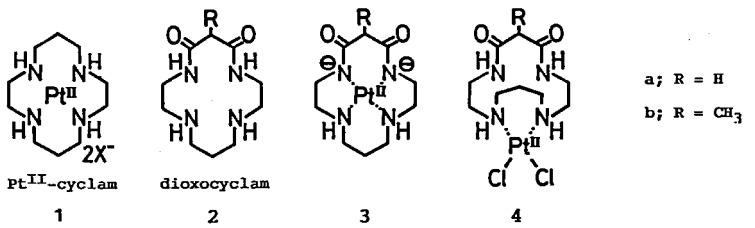

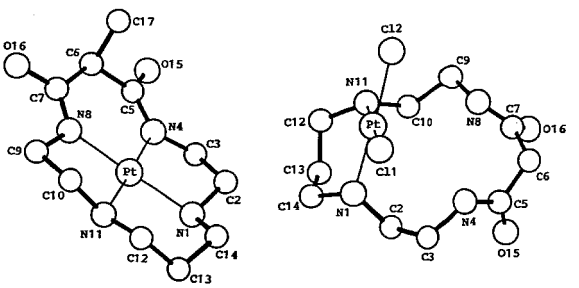

VI-D-4 Developments in Functionalization of Macrocyclic Polyamines.

Eiichi KIMURA

[*Pure & Applied Chemistry*, in press]

The classical structure of macrocyclic polyamines (*e.g.* cyclam **1**) have been renovated by means of (1) conversion of amines into amides (*i.e.* dioxocyclam); (2) replacement of N donors for S donors; (3) replacement of skeletonic C-H for C-F; and (4) attachment of intramolecular pendant donors. The characteristics of dioxocyclam **2** is best illustrated by its ability to incorporate Pt^{II}, while the oxo-free cyclam **1** fails to do so. A new version of dioxocyclam **3** containing two S donors in place of N donors of **2** was designed, which astonishingly selectively accommodates noble metal ions Pt^{II} and Pd^{II}, but not Cu^{II}, Ni^{II}, or Co^{II} as **2** does. Furthermore, **3** detracts Pt^{II} much more rapidly than **2** from *cis*-$[Pt^{II}(NH_3)_2Cl_2]$. The fluorinated polyamines show lower N basicities than nonfluorinated counterparts, and yet, the Cu^{II} complex of **11** ($CuH_{-2}L$) is more stable than that of **2**. The fluorinated polyamine complexes stabilize metal ions with lower oxidation states than nonfluorinated counterparts. Intramolecular pendant donors greatly affect the redox and other chemical properties of the central metal ions, as well as the complex properties.

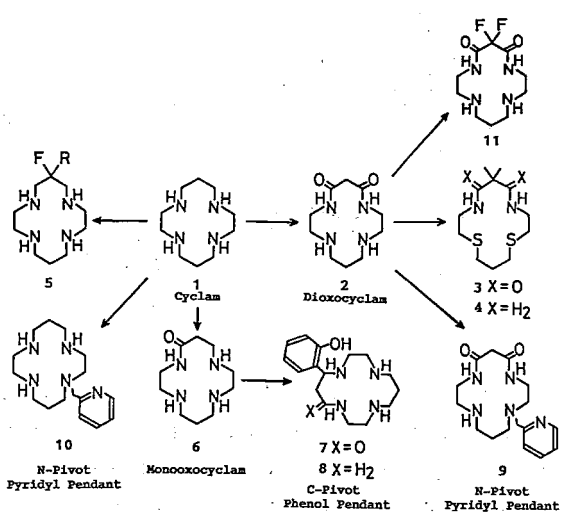

VI-E Biomimetic Studies Using Polyamine Complexes

Active sites of a metalloenzyme (*e.g.* Zi^{II}-containing carbonic anhydrase) and a metal-activated drug (bleomycin) have been mimicked by synthetic polyamine ligands.

VI-E-1 A Trigonal Bipyramidal Zn(II) Complex of Phenol-pendant Macrocyclic Triamine.

Eiichi KIMURA, Tohru KOIKE*, and Koshiro TORIUMI *(*Hiroshima Univ.)*

[Inorg. Chem., **27**, 3687 (1988)]

An *X*-ray crystal structure analysis of the zinc complex of a tetradentate phenol-pendant tri-aza macrocyclic ligand, 2-(2-hydroxyphenyl)-1, 5, 9-triazacyclododecane, **1**, has revealed a distinct trigonal bipyramidal structure **2** with an additional apical water molecule. Crystal data: $C_{15}H_{24}N_3OZnClO_4 \cdot H_2O$, *fw* = 445.2, monoclinic, space group $P2_1/a$, a = 16.673(2), b = 13.952(2), c = 8.826(1) Å, ß = 91.73(1) °, D_c =1.536 g cm^{-3}, V = 1926.5(5) Å^3, Z = 4, μ(MoKα) = 1.488 mm^{-1}. A block diagonal least-squares refinement yielded R = 0.044 and R_w = 0.056 for 2239 independent reflections.

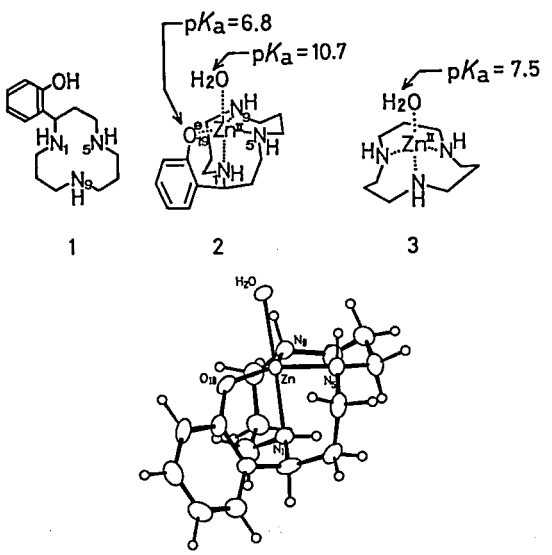

Figure 1. Perspective view of 2. The perchlorate is omitted for clarity.

VI-E-2 Chemistry and Functions of Recently Developed Macrocyclic Polyamines

Eiichi KIMURA

[*J. of Inclusion Phenomena*, (1988) in press]

New, functionalized macrocyclic polyamines, **1**, **2**, **3**, and **4** have been synthesized for investigation of their metal and molecular inclusion.

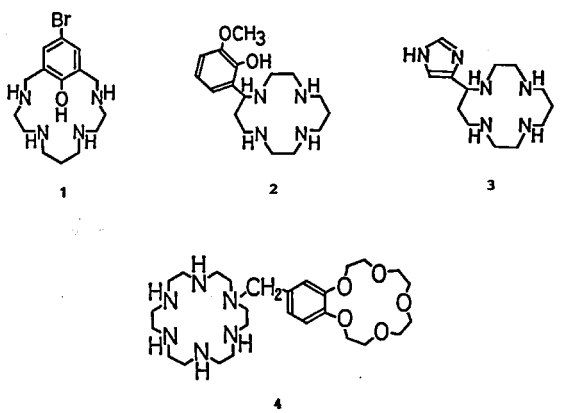

VI-E-3 Studies on Bleomycin Model Complexes

Hiromasa KUROSAKI, Hideki ANAN*, and Eiichi KIMURA *(*Hiroshima Univ.)*

[*Nippon Kagaku Kaishi* Special articles on "Coordination Chemistry of Biologically Important Substances", **No. 4**, 691 (1988)]

New bleomycin(BLM)-mimic pentaamine ligands L_1 and L_2 have been synthesized. Complexation behaviors of L_1 and L_2 with copper(II) and iron(II) were studied with pH-metric titrations. The amide-proton dissociated L_1 and L_2 complexes with Cu(II) (formulated as $CuH_{-1}L$) were isolated as monoperchlorate salts. Taken with other similarities in visible spectra, metal redox properties, or ESR spectra, L_1 and L_2 complexes are concluded to possess a similar complex structure to that of bleomycin. The role of the

carbamoyl group adjacent to the N-terminal NH_2 in BLM is deduced from comparison of L_1 and L_2 behaviors towards Fe(II). Fe(II)-L_2 complex is shown to activate O_2 to generate ·OH radical, which attacks and cleaves DNA, in an analogous manner as Fe(II)-BLM. However, its minimum effective concentration is 10^{-4} mol·dm^{-3}, as compared with 10^{-7} mol·dm^{-3} for BLM.

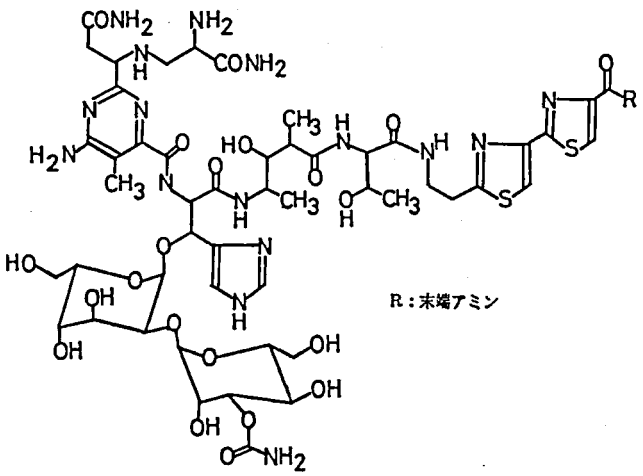

Bleomycin

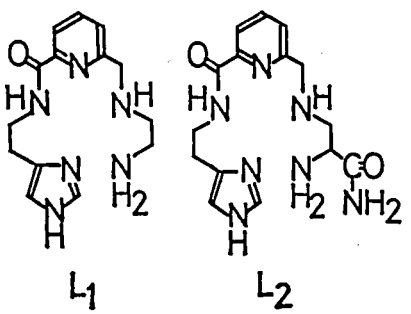

VI-F Lattice Dynamics and Phase Transitions in Solids

Dynamical behavior of molecules and ions in crystals and its relation with structural phase transitions are studied for hexa- and tetrahalogen metal complexes and a new group of ionic crystals named "ionic plastic crystals", for example, simple alkylammonium salts, which have a solid phase of intermediate properties between solid and liquid at high temperatures just below the melting point.

VI-F-1 Studies on Structure and Dynamics of Dimethylammonium Ions in Solids using ^{2}H FT Spectra Observed by Quadrupole Echo Technique.

Ryuichi IKEDA, Atsushi KUBO* and Charles A. McDOWELL* *(*Univ. of British Columbia)*

^{2}H NMR powder spectra obtained by Fourier transform of quadrupole echo signals were recorded for $[(CD_3)_2NH_2]_2MCl_6$ (M: Sn, Te) to elucidate motional effects on line shapes. Observed spectra were analyzed by comparing with line shapes calculated for various jump angles of the CD_3 group in the cation, its jump rates, and interpulse spacing times. Both complexes showed narrowing of spectra around room temperature due to a new motional process of cations. Spectra with

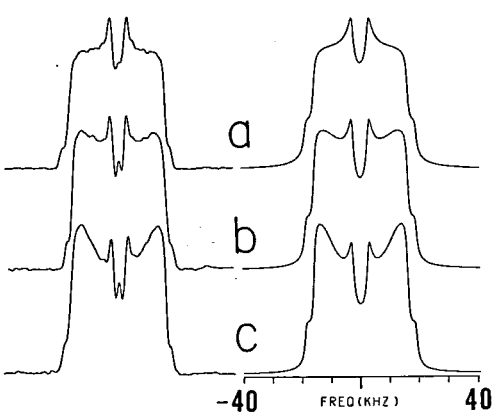

Figure 1. Comparison of observed (left) and simulated (right) line shapes of ^{2}H spectra for $[(CD_3)_2NH_2]_2SnCl_6$ at three echo delay times between two 90° pulses employed: (a) 25 μs, (b) 50 μs, (c) 100 μs. Spectra were observed at 350 K. Simulation was performed for two site jumps of CD_3 groups by an angle of 116.8° and its rate of 200 kHz.

large asymmetry of the electric field gradient tensors observed in the narrowing process were explained very well by the 180° flip of the cation about its C_2 axis. From line shape analysis, C-N-C bond angles in the tin and tellurium complexes are evaluated as 116.8° and 119.0°, respectively. The ND_2 bond angle was also determined to be 103.6° for $[(CH_3)_2ND_2]_2SnCl_6$. Activation energies and correlation times of the 180° flip of the cations were derived and compared with those of the fully protonated cations and those for 90° rotational jumps of the complex anions.

VI-F-2 ^{35}Cl Nuclear Quadrupole Relaxation in Pyridinium hexachlorostannate (IV)

Yutaka TAI*, Atsushi ISHIKAWA*, Keizo HORIUCHI*, Tetsuo ASAJI*, Ryuichi IKEDA, and Daiyu NAKAMURA* *(*Nagoya Univ.)*

[*Z. Naturforsch.*, 1988, in press]

The temperature dependence of ^{35}Cl quadrupole spin-lattice relaxation time T_{1Q} was observed for three resonance lines of pyridinium hexachlorostannate(IV) already reported. With increasing temperature, the sharp decrease of T_{1Q} was observed below the phase transition temperature of 331 K. This decrease can be explained through the reorientational motions of the complex anions. The activation energy for the motions was determined as 97 and 63 kJ mol^{-1} from the T_{1Q} data obtained from the highest-frequency resonance line and the remaining two lines, respectively. The two different barriers observed for the reorientations of a single anion suggests the existence of anisotropy of the anionic motion. An anomalous T_{1Q} vs. T^{-1} relation observed in an intermediate-temperature region is discussed by referring to the cationic motion.

VI-F-3 A New High-Temperature Solid Phase of Methylammonium Bromide Studied by ^1H NMR and Thermal Measurements

Masataka TANSHO*, Ryuichi IKEDA, and Daiyu NAKAMURA* *(*Nagoya Univ.)*

A new high-temperature solid phase of CH_3NH_3Br was found above 483 K up to the melting point (515 K) by measuring ^1H NMR and differential thermal analysis. The cations in this phase were revealed to perform rapid translational self-diffusion as well as overall rotation about their center of gravity. X-ray diffraction patterns taken in this phase were explained well by a bcc lattice. These results indicate that this phase is a kind of "ionic plastic crystals" analogous to the highest-temperature phases of methylammonium nitrate, perchlorate, and iodide. A characteristic feature of the bromide is that this phase is metastable and the crystals gradually melt in this phase on keeping a long time. The transition entropy and dynamical parameters of the cationic motions were experimentally derived and discussed by comparing with the results on other plastic crystals.

VI-G Bioinorganic Studies on Electronic and Molecular Structures of Copper Complexes as a Model for Active Site in Some Copper Proteins

Copper-containing proteins have been found to be widely distributed in both plants and animals and have been related to such metabolic processes as hydroxylation, oxygen transport, electron transfer and oxidative catalysis. In this project the electronic and molecular structures for several copper complexes are studied as a model of copper-proteins or copper-enzymes by some physico-chemical methods.

VI-G-1 Study on the Structure of a Ternary Cu(II)-Diamine-Amino Acid Complex Involving Intramolecular Aromatic Ring Stacking Interactions

Hideki MASUDA, Osamu MATSUMOTO *(Kyoto Univ.)*, **Akira ODANI** *(Nagoya Univ.)*, **and Osamu YAMAUCHI** *(Nagoya Univ.)*

Ternary metal complexes comprising an aromatic amino acid and an aromatic amine such as 1,10-phenanthroline(phen) and 2,2'-bipyridine have recently been shown to have the intramolecular aromatic ring stacking in dilute aqueous solution. With a view to understanding the precise binding mode of the stacking interaction, the crystal structure of [Cu(phen)(L-tryptophan)]$ClO_4 \cdot 2.5H_2O$ has been determined by the X-ray method. The geometry about the copper(II) ion is five-coordinate square-pyramidal, with the two nitrogen atoms of phen and the nitrogen and oxygen atoms of L-tryptophan (L-trp) coordinated at the equatorial position in an approximately planar form and one oxygen atom of the carboxyl group of the neighboring complex molecule at the axial position. The most interesting structural feature of the complex is the existence of the intramolecular stacking between the L-trp indole ring and the aromatic rings of phen with the average spacing of 3.51 Å from the vacant axial position. To understand the binding mode of the stacking interactions, we calculated the charge densities of a model system, protonated phen-L-trp, by the CNDO/2 MO method. The charge densities obtained from the MO calculation suggest that the intramolecular stacking interactions are dominated by the electrostatic interactions between the two aromatic rings.

VI-G-2 Structure of [Cu(L-tyrosyl-L-histidine)] Involving an Axial Cu(II)-Phenol OH Bonding. Implication for Substrate Binding at the Active Site of Tyrosinase

Hideki MASUDA, Akira ODANI* and Osamu YAMAUCHI* *(*Nagoya Univ.)*

[*Submitted to J. Am. Chem. Soc.*]

With a view to obtaining information on the mode of interactions between the tyrosine side chain and the binuclear copper site of tyrosinase in the hydroxylation reaction, a Cu(II) complex of L-tyrosyl-L-histidine (Tyr-His) has been prepared and characterized by the X-ray diffraction method. The geometry about the copper atom is square-pyramidal, with the three nitrogen atoms of Tyr-His and one carboxylate oxygen atom from the neighboring molecule at the equatorial positions in an approximately planar form. A remarkable feature of the complex is that the phenol oxygen of the tyrosyl residue apically coordinates to Cu(II) to complete the square pyramid with the Cu(II)-O bond length of 2.601 Å, which is greater than the values hitherto reported for other axial Cu(II)-O bonds. To our knowledge this is the first structural evidence for phenolic oxygen coordination to Cu(II) without deprotonation. The present finding raises the possibility of the coordination of a phenol OH group to the active site copper(II) of oxytyrosinase in its cresolase activity.

VI-G-3 Structure and Properties of a Pterin-containing Ternary Copper(II) Complex, [Cu(bpy) (PC) (H_2O)]·$3H_2O$ (bpy=2,2'-bipyridine; PC=pterin-6-carboxylate). First Chemical Model for the Active Site Copper-Cofactor Bonding in Chromobacterium Phenylalanine Hydroxylase

Takamitsu KOHZUMA, Hideki MASUDA and Osamu YAMAUCHI *(Nagoya Univ.)*

[*Submitted to J. Am. Chem. Soc*]

Phenylalanine hydroxylase and other aromatic amino acid hydroxylases are metalloenzymes that introduce a hydroxyl group into the side chain aromatic rings in the presence of a pterin cofactor biopterin. The hydroxylases usually require Fe and biopterin in its reduced form, and the phenylalanine hydroxylase from *Chromobacterium violaceum* has been reported to contain 1 mole of Cu per mole of enzyme in place of Fe. The copper atom has been infered to be coordinated through the N(5) atom of a reduced pterin ring and equatorially to two imidazole groups from the enzyme. With a view to obtaining the information regarding the metal ion-pterin coenzyme interactions, we now investigated the molecular structure and ESR spectral properties of the first active site Cu(II)-pterin model complex, [Cu(bpy)(PC)(H_2O)]. The molecular structure reveals that the Cu(II) ion is basically in a square-planar geometry with two nitrogens of bpy, one nitrogen (N(5)) of PC, and one water oxygen in the plane and two oxygens of the pterin moiety occupying remote axial positions. The ESR spectra for Cu(bpy)(PC) at neutral pH also indicated to be the same coordination sphere as the solid state. The ESR spectra for addition of one equivalent of imidazole to the above

solution suggested that imidazole displaces the coordinated water Cu(bpy) (PC) (Im), with increased planarity.

IV-H Synthesis of Optically Active Schiff Base-Oxovanadium (IV, V) Complexes and Their Application for the Asymmetric Oxidation of Sulfides.

Kiyohiko NAKAJIMA, Masaaki KOJIMA*, and Junnosuke FUJITA* *(*Nagoya Univ.)*

Optically active Schiff base-oxovanadium (IV) complexes, $V^{IV}O(SB)$ (SB; *N,N'*-disalicylidene-(*R,R*)-1,2-cyclohexanediamine, *N,N'*-disalicylidene-(*R*)-1,2-propanediamine, and their derivatives) catalyze the oxidation of sulfides with organic hydroperoxides to give optically active sulfoxides with an enantiomeric excess of 20~40%. In these reactions, $V^{IV}O(SB)$ catalysts are finally oxidised to $V^{V}O(SB)^{+}$. However, the corresponding oxovanadium(V) complexes, $V^{V}O(SB)X$ (X=Cl^{-}, ClO_4^{-}, etc.), which were prepared by oxidation of $V^{IV}O(SB)$ with Ce^{IV}, have less effective catalytic activities than those of $V^{IV}O(SB)$. Other catalytically active species than those of $V^{IV}O(SB)$ and $V^{V}O(SB)X$ are suggested by UV absorption spectroscopy.

VI–I Mechanism of Ligand Substitution Reactions of Transition Metal Complexes

Solvent exchange is the most fundamental substitution reaction of metal complexes, and is suitable for discussing the lability of relavant metal ions and the reaction mechanism. We have continued such kinetic studies by the isotope labelling method by use of acetylacetone[^{14}C].

VI-I-1 Ligand Isotopic Exchange of cis-Bis-(acetylacetonato)-dioxomolybdenum(VI) in Solution.

Akira NAGASAWA*, Hideaki K. TANAKA*, Masayuki MIYOSHI*, and Kazuo SAITO *(*Tohoku Univ.)*

[Inorg. Chem., **26**, 4035 (1987)]

The ligand exchange kinetics is expressed by Rate = $(k_1 + k_2[H_2O])$[complex], k_1 and k_2 being 1.05×10^{-3} s^{-1} and $8.27 \times 10^{-3}M^{-1}s^{-1}$, respectively at 25°C. The $\Delta H^{\ddagger}$, $\Delta S^{\ddagger}$ and $\Delta V^{\ddagger}$ values are 64±2 and 64±1 kJ mol^{-1}, −86±5 and −71±4 J $mol^{-1}K^{-1}$, and +0.2±0.4 and −0.4±0.4 cm^3mol^{-1} for k_1 and k_2, respectively. Dilution of the solvent with acetonitrile and deuteration of acidic hydrogen decreased the rate. A reaction intermediate containing unidentate acetylacetone and acetylacetonate seems to undergo rate-determining internal rearrangement. Water catalyses the reaction by accelerating the formation of the intermediate.

VI-I-2 Metal Ion Lability Constant Derived from a Linear Free Energy Relationship between Ligand-Substitution Rates of Tris(acetylacetonato) and Aqua Complexes of Various Tervalent Metal Ions

Horoaki KIDO* and Kazuo SAITO *(*Tohoku Univ.)*

[*J. Am. Chem. Soc.*, **110**, 3187 (1988)]

A linear relationship is found between the first order rate constants of the ligand exchange of tris-(acetylacetonato) complexes of tervalent metal ions $[M^{III}(acac)_3]$ (M = Sc, V, Cr, Mn, Fe, Ru, Co, Rh, Al, Ga and In) in acetylacetone and/or acetonitrile and those of substitution reactions of their aqua complexes in water. The gradient of log-log plot is very close to unity over the range 10^{14}. The former is shifted invariably by ca. $10^{-4.5}$ to the latter. It seems as if the nature of the central metal ion dominates the lability of ligand substitution of metal complexes over the great

differences in ligands and reaction environment around the ion. A metal ion lability constant σ is proposed and evaluated for each M^{III} as a measure of lability of octahedral complexes.

VI–J Synthesis and Properties of Mixed Capping Ligand Complexes of Hexamolybdenum Cluster

Hexamolybdenum cluster gives very stable luminescent dicrete complex ions with 8 capping halides, whilst solid state super-conducting Chevrel-type crystals are formed with 8 capping chalcogenide and counter rare earth ions. We have synthesized mixed capping ligand discrete complexes in which the capping halide is successively replaced by chalcogenide. Disubstituted species of the type $[(Mo_6Cl_6Se_2)Cl_6]^{12+\sim14+}$ have been obtained in crystalline state as cesium salt, their structure analyzed and their electrochemical properties disclosed as tetrabutylammonium salts in acetonitrile. Such results were shortly reported. [K. Saito, and Y. Sasaki, *Pure & Appld. Chem.*, **60**, 1123 (1988)]

XI-J-1 Synthesis and Properties of Monochalcogenide-substituted Hexamolybdenum Halide Clusters

Masahiro EBIHARA, Koshiro TORIUMI and Kazuo SAITO

[*Inorg. Chem.*, **27**, 13 (1988)]

The cesium salt $Cs_3[Mo_6Cl_6Se)Cl_6]\cdot H_2O$ and its analogue with capping sulfide crystallize in triclinic state, and the chalcogenide is disordered among the 8 capping sites. The difference in Mo-Mo, Mo-capping ligand and Mo-terminal Cl distance is very small among these and $[(Mo_6Cl_8)Cl_6]^{2-}$, whereas the electrode potential Mo_6^{12+}-Mo_6^{13+} decreases by 0.8 V on introducing one S or Se. Change in terminal ligand from Cl to Br brings about only modest change in $E_{1/2}$.

VI–K Pressure Effect on Equilibria and Rates of Metal Complex Formation in Solution

Reaction volumes and activation volumes for metal complex formation are very useful for elucidating mechanisms of the complexation in solution. Therefore we have measured reactions under high pressures and discussed the mechanisms on the basis of parameters of volumes.

VI-K-1 Dilatometric Studies of Reaction Volumes for the Formation of Metal Complexes in Several Solvents

Shigenobu FUNAHASHI *(Nagoya Univ. and IMS)*, **Kimiyo SENGOKU*, Toru AMARI*, and Motoharu TANAKA*** *(*Nagoya Univ.)*

[*J. Solution Chem.* **17**, 109 (1988)]

A convenient technique is described to determine reaction volumes by means of direct dilatometry. Reaction volumes were determined for the following complexation reactions: formation of monoammine-nickel(II) in water (-0.1 ± 0.5 cm^3 mol^{-1}); formation of the 1:1 nickel(II) complex with isoquinoline in methanol and ethanol (3.2 ± 0.1 and 1.1 ± 0.1 cm^3 mol^{-1}, respectively); formation of the 1:1 isothiocyanato-iron(III) complex in water, Me_2SO, and DMF (8.9 ± 0.2, 12.4 ± 0.7, and 25.1 ± 0.3 cm^3 mol^{-1}, respectively); formation of the 18-crown-6 potassium complex in water (10.9 ± 0.2 cm^3 mol^{-1}). We discussed these values in terms of electrostriction and molecular size.

VI-K-2 Dilatometric Studies on Reaction Volumes for the Formation of Nickel(II) Complexes in Aqueous Solution

Toru AMARI*, Shigenobu FUNAHASHI *(Nagoya Univ. and IMS)*, **and Motoharu TANAKA*** *(*Nagoya Univ.)*

[*Inorg. Chem.*, **27**, Sept. (1988)]

Reaction volumes for the formation of nickel(II) complexes with acetate (OAc^-), ethylenediamine (en), glycinate (gly^-), sarcosinate (sar^-), and ethylenediamine-N,N'-diacetate ($edda^{2-}$), and reaction volumes for proton dissociation of the conjugate acids of the ligands have been measured dilatometrically at 25.0°C and I = 0.10 mol dm^3 ($NaClO_4$) in aqueous solution; $\Delta V°/cm^3\ mol^{-1}$ for complex formation: 8.0±1.5 ($Ni(OAc)^+$), 11.2±0.2 ($Ni(gly)^+$), 12.0±0.5 ($Ni(gly)_2$), 11.7±0.5 ($Ni(sar)^+$), 9.9±0.8 ($Ni(sar)_2$), 5.2±0.5 ($Ni(en)^{2+}$), 5.6±0.9 ($Ni(en)_2^{2+}$), 28.6±0.2 (Ni(edda)), and $\Delta V°/cm^3\ mol^{-1}$ for proton dissociation: −10.6±0.2 (HOAc), 1.4±0.3 (Hgly), 0.7±0.2 (Hsar), 5.6±0.2 (Hen^+), 12.0±0.1 (H_2en^{2+}), −0.6±0.2 ($Hedda^-$), 4.9±0.3 (H_2edda). We discussed these reaction volumes in terms of electrostriction, contraction of donor atoms in ligands in the first coordination sphere, expansion of complexes by bond elongation due to bound ligands, and "volume chelate effect" resulting from different packing of multidentate ligands at the metal ion and in the bulk solvent.

VI-K-3 Kinetic Study of the Dissociation of Sodium Cryptate(2,2,1)

Koji ISHIHARA*, Hiroko MIURA*, Shigenobu FUNAHASHI *(Nagoya Univ. and IMS)*, **and Motoharu TANAKA*** *(*Nagoya Univ.)*

[*Inorg. Chem.* **27**, 1706 (1988)]

The rate of dissociation of sodium crypate(2,2,1)-($NaCry^+$) has been measured at various temperatures and pressures in Me_2SO, DMF, and acetonitrile by using a high-pressure stopped-flow apparatus with conductometric detection. There are two reaction paths: an acid-independent path (k_{d1}), $CryNa^+ \rightarrow Cry + Na^+$, and an acid-dependent path (k_{d2}), $CryNa^+ + Hdca \rightarrow CryH^+ + Na^+ + dca^-$, where Hdca is dichloroacetic acid. Activation volumes ($\Delta V^{\ddagger}/cm^3\ mol^{-1}$) are as follows: $\Delta V_{d1}^{\ddagger}$ = 2.1±0.7 in Me_2SO, $\Delta V_{d1}^{\ddagger}$ = 2.0±0.2 and $\Delta V_{d2}^{\ddagger}$ = −8.8±1.0 in DMF, and $\Delta V_{d2}^{\ddagger}$ = −16.0±0.8 in CH_3CN. The reaction mechanism is discussed on the basis of activation parameters of enthalpy, entropy, and volume.

VI-K-4 Variable-Pressure Oxygen-17 NMR Studies on Acetic Acid Exchange of Manganese(II) Perchlorate and Manganese(II) Acetate

Masao ISHII*, Shigenobu FUNAHASHI *(Nagoya Univ. and IMS)*, **and Motoharu TANAKA*** *(*Nagoya Univ.)*

[*Inorg. Chem.* **27**, Sept. (1988)]

Acetic acid exchange of manganese(II) perchlorate and manganese(II) acetate in acetic acid (HOAc) involving dichloromethane-d_2 as a diluent has been studied at various pressures up to 180 MPa by the variable-pressure ^{17}O FT-NMR line-broadening method. The activation volumes at 258 K are +0.4±0.7 $cm^3\ mol^{-1}$ for $Mn(ClO_4)_2$ and +6.7±0.6 $cm^3\ mol^{-1}$ for $Mn(OAc)_2$, respectively. These positive values are unusual for the solvent exchange on manganese(II) studied so far and are discussed in terms of the bulkiness of acetic acid molecules and the effect of the ligand bound to the manganese(II).

VI-L Studies on Dinuclear and Polynuclear Metal Complexes

New dinuclear and polynuclear metal complexes, including heteronuclear complexes, have been synthesized and characterized in the hope to examine new physicochemical properties and functions expected for such metal-condensed systems.

VI-L-1 Copper(II)-Lanthanoid(III) Complexes of Binucleating Ligands Derived from 3-Formylsalicylic Acid and Diamines

Masatomi SAKAMOTO*, Minoru TAKAGI*, Tomitaro ISHIMORI*, and Hisashi ŌKAWA *(Kyushu Univ. and IMS) (*Ehime Univ.)*

[*Bull. Chem. Soc. Jpn.*, **61**, 1613 (1988)]

Cu(II)-Ln(III) heterodinuclear complexes, $[CuLn(fsaen)(H_2O)_4]NO_3$ and $[CuLn(fsapn)(H_2O)_4]NO_3$ (Ln=lanthanoid ion), have been synthesized and characterized, where $fsaen^{2-}$ and $fsapn^{2-}$ denote *N,N′*-bis(3-carboxysalicylidene)ethylenediaminate ion and *N,N′*-bis(3-carboxysalicylidene)-1,2-propanediaminate ion, respectively. Electronic spectral investigations in various solvents reveals that the complexes show unique "solvation selectivity". That is, nitrogenous molecules solvate by coordination at the Cu center whereas oxygenous molecules at the Ln center. When oxygenous molecules such as DMF and DMSO solvate at the Ln center, then the hydrophobic part of the molecules block the apical sites of the Cu center and hence hinder the approach of other solvent molecules to the Cu center. Thus, the planar configuration around the Cu is maintained even in those highly donating solvents.

VI-L-2 New Dinucleating Ligand, *N,N′*-Ethylenebis(3-carboxysalicylamine), and Its Dinuclear Copper(II) and Nickel(II) Complexes

Hisashi ŌKAWA *(Kyushu Univ. and IMS)*, **Kazuhiko KOGAWA*, Makoto HANDA*, Naohide MATSUMOTO*, and Sigeo KIDA** *(*Kyushu Univ.)*

[*Chem. Lett.*, 1079 (1988)]

A new dinucleating ligand *N,N′*-ethylenebis(3-carboxysalicylamine) (H_4L) has been prepared, and its complexing behaviors are compared with its imine analogue, *N,N′*-ethylenebis(3-carboxysalicylideneamine)(H_4L'). Dinuclear copper(II) complex, $[Cu_2(L)]\cdot 2H_2O$, shows a strong antiferromagnetic spin-exchange ($J=-270\ cm^{-1}$) between a pair of copper(II) ions. H_4L forms a dinuclear nickel(II) complex, $[Ni_2(L)(H_2O)_4]$, comprised of two paramagnetic metal ions while H_4L' forms dinuclear complex comprised of a paramagnetic and a diamagnetic nickel ions.

IV-L-3 X-Ray Crystal Structure and Electrochemical Property of a Novel Monohydroxo-Bridged Binuclear Cobalt(II) Complex with *N,N′,N″,N‴*-Tetrakis(2-aminoethyl)-1,4,8,11-tetraazacyclotetradecane

Masahiro MIKURIYA *(Kwansei Gakuin Univ.)*, **Sigeo KIDA, and Ichiro MURASE** *(Kyushu Univ.)*

[*Bull. Chem. Soc. Jpn.* **61**, 2666–2668 (1988)]

The crystal structure of a binuclear cobalt(II) complex of *N,N′,N″,N‴*-tetrakis(2-aminoethyl)-1,4,8,11-tetraazacyclotetradecane(taec), $[Co_2(taec)(OH)](ClO_4)_3$ was determined by the single-crystal X-ray diffraction method. The two cobalt ions are bridged by a single hydroxide ion in the cavity of taec. The cyclic voltammogram showed an irreversible profile with two anodic peaks at ca. 1.4 and 1.8 V vs. SCE.

VI-L-4 Preparation and Structural Characterization of Binuclear Manganese(III) Complexes with 1,5-Bis(salicylideneamino)-3-pentanol and its derivatives

Masahiro MIKURIYA *(Kwansei Gakuin Univ.)*, **Sigeo KIDA, and Ichiro MURASE** *(Kyushu Univ.)*

[*Chem. Lett.*, 1988, 35–38]

Three binuclear manganese(III) complexes with the title Schiff base ligands have been prepared and characterized. X-Ray structure analysis of $[Mn_2(L_b)(CH_3O)(CH_3COO)(CH_3OH)(ClO_4)]$ (H_3L_b=1,5-bis(5-chlorosalicylideneamino)-3-pentanol) has revealed that the two manganese ions are bridged by the alkoxide oxygen atom of the Schiff base ligand, the methoxide oxygen atom, and the oxygen atoms of the acetate ion with the Mn–Mn separation of 2.921(2) Å.

VI-L-5 Completely Spin-coupled Trinuclear Copper(II) Complex, $[(Cu_2\{\mu\text{-dmg}\}_2)(bipy)_2(CH_3OH)_2](NO_3)_2$

Dominique LUNEAU, Hiroki OSHIO, Hisashi Ō-KAWA *(Kyushu Univ. and IMS)*, **and Sigeo KIDA**

[*Submitted to J. Chem. Soc. Chem. Commun.*]

A linear trinuclear copper(II) complex $[Cu_2\{\mu\text{-}Cu(dmg)_2\}(bipy)_2(CH_3OH)_2](NO_3)_2$ has been prepared and structurally characterized. The molecule consists of trinuclear cation and nitrate ions and has the inversion center at the central copper (see Figure). The bis(dimethylglyoxymato)copper(II) dianion $[Cu(dmg)_2]^{2-}$ functions as the bridge through its deprotonated oxime oxygens, with the Cu(1)-Cu(2) intermetal distance of 3.754(2) Å. The magnetic moment is practically constant (1.85 ± 0.01 μ_B per three copper atoms) in the temperature range 80–300K, demonstrating that the complete spin-coupling is attained even at room temperature.

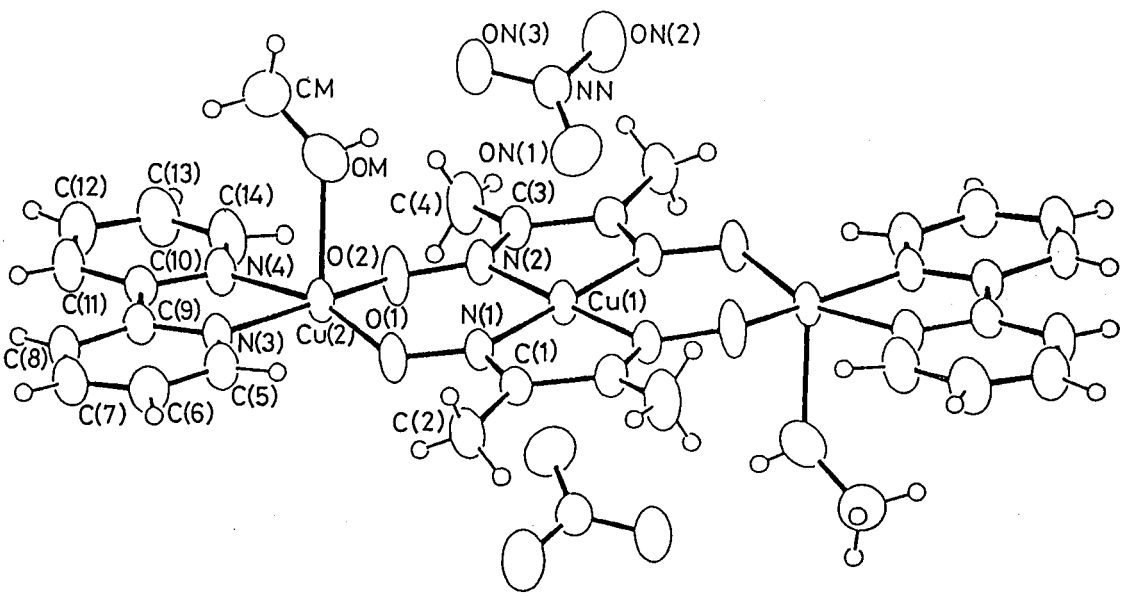

VI–M Studies on Noncovalent Interligand Interactions in Metal Complexes

In the previous studies of this series it is revealed that high stereoselectivity of metal complexes occurs if ligands used are designed so as to cause noncovalent interligand interactions when coordinated to a metal ion. Studies in this line are developed to the complexes of labile metal ions, in the hope to exploit new stereoselective reactions based on those sterically controlled metal complexes.

VI-M-1 Noncovalent Interactions in Metal Complexes. Part 16. Stereoselectivity of 1:3 Complexes of Sc, Y, La, Al, Ga, and In Ions with 1-(*l*-Menthyloxy)-4-phenyl-1,3-butanedione and 1-(*l*-Menthyloxy)-4-(p-tolyl)-1,3-butanedione

Hisashi ŌKAWA *(Kyushu Univ. and IMS)*, **Hirofumi TOKUNAGA*, Tsutomu KATSUKI*, Masayuki KOIKAWA*, and Sigeo KIDA** *(*Kyushu Univ.)*

[Inorg. Chem., in press]

1:3 Complexes of Sc, Y, La, Al, Ga, and In ions with 1-(*l*-menthyloxy)-4-phenyl-1,3-butanedione and 1-(*l*-menthyloxy)-4-(p-tolyl)-1,3-butanedione have been prepared and their stereoselectivities have been examined in view of noncovalent interligand interactions. The distributions of the diastereomers for the relatively inert Al and Ga complexes are determined by 400 MHz

^{1}H NMR spectra. The results indicate that the fac/mer ratio is larger than the statistical value (1/3) for all cases. Based on CD induced at the ligand π-π^* transition, the configuration of the preferred diastereomer in solution is determined as fac-*Λ*. The stereoselectivity to afford the fac-*Λ* isomer is enhanced when the size of the central ion becomes larger. All these facts add a support to the operation of noncovalent interligand interaction in the form of left-handed three-bladed propeller, comprising of three interligand *l*-menthyl/aryl contacts.

VI-M-2 Enantioselective Reduction of Ketones on Sterically-controlled Lanthanoid(III) Complex

Hisashi ŌKAWA *(Kyushu Univ. and IMS)*, **Tsutomu KATSUKI*, Michio NAKAMURA*, Naohisa KUMAGAI*, Yuko SHUIN*, Teruo SHINMYOZU*, and Sigeo KIDA** *(*Kyushu Univ.)*

[Submitted to *J. Chem. Soc. Chem Commun.*]

Sterically-controlled lanthanoid complexes, fac-*Λ*-tris{4-(*l*-menthyl)-1-(p-tolyl)-1,3-butanedionato}lanthanoid(III) (Ln=La, Pr, Gd, Er), have been used as chiral Lewis acid catalysts for enantioselective reduction of ketones (acetophenone, 2-octanone, 2-butanone) with $NaBH_4$ in cyclohexane. The preferred enantiomer is (S) for 1-phenylethanol (best result, 84 e.e.%) whereas (R) for 2-octanole (42 e.e.%) and 2-butanole (16 e.e.%). The reaction is stoichiometric but not catalytic. However, the host complex can be recovered in good yield (>90%) and used for another run after recrystallization from absolute ethanol. Thus, the reaction cycle given in the Scheme 1 has been proposed.

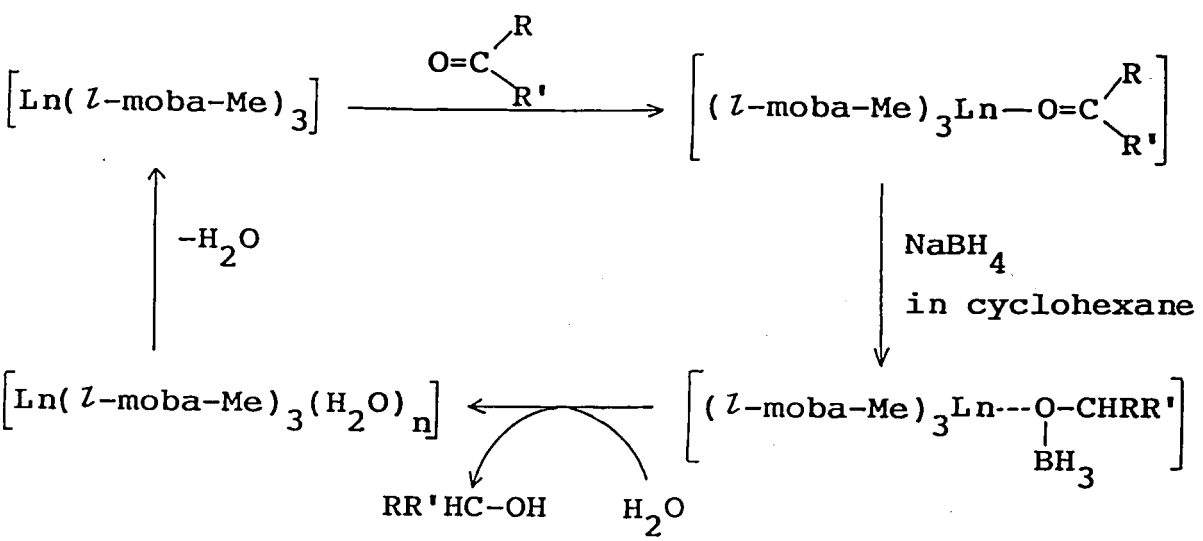

Scheme 1

VI–N Studies on High Oxidation State Metal Complexes

First transition metal chelates of higher oxidation states have attracted much interests for their unusual chemical and physico-chemical properties. In order to obtain such complexes chelating ligands with high donating ability were prepared. Metal complexes with these ligands are easily oxidized and are stable even in higher oxidation state.

VI-N-1 Manganese(IV) and Manganese(V) Complexes with *N*-(2-hydroxyphenyl)salicylamides

Masayuki KOIKAWA *(Kyushu Univ.)*, **Hisashi Ō-KAWA, and Sigeo KIDA**

N-(hydroxyphenyl)salicylamide(H_2L^1) and its homologues with a substituent on the 2-hydoxyphenyl moiety(5-Me, H_3L^2; 5-Cl, H_3L^3; 4-NO_2, H_3L^4; 5-NO_2, H_3L^5) form manganese(IV) complexes of general composition $K_2[MnL_2]$ (L=L^1—L^5) when treated with manganese(II) ion methanolic KOH solution in air. They were characterized by their magnetic monents at room temperature (μ_{eff}=3.67–4.06), molar conductances in methanol (150–170Ω^{-1} cm^2 mol^{-1}), and e.s.r. spectra of the complexes in frozen acetonitrile solution showed signals at g = ca. 2.0 and 4.0 which were assigned to the $g_{//}$ and $g_{\perp}$ components, respectively, of Kramer's doublets (M=+1/2 and −1/2) derived from a d^3 electronic configuration. Intense absorptions in the region 16000–20000 cm^{-1} were attributed to LMCT bands. Cyclic voltammograms of the complexes in CH_2Cl_2 (solubilized with 1,4,7,10,13,16-hexaoxacyclo-octadecane) showed three irreversible couples which were assigned to Mn^{VI}/Mn^{V}, Mn^{V}/Mn^{IV} and Mn^{IV}/Mn^{III} redox processes based on controlled-potential electrolyses. The redox potential of each process was significantly affected by the electronic nature of the substituents, and the higher oxidation states of manganese were stabilized when an electron-releasing group was attached to the ligand. Chemical oxidation of $K_2[Mn(L^2)_2]$ with Ce^{IV} in acetonitrile led to the isolation of a novel manganese(V) complex of composition $K[Mn(L^2)_2]$, which was characterized by its magnetic moment (μ_{eff}=2.83) corresponding to two unpaired electrons.

VI–O Crystal and Molecular Structure of ΔΛΔ(+)-[*N,N'*-1,2-Ethanediylbis[*N*-(carboxymethyl)glycyl-L-methionine] ethyl esterato]copper(II) Sesquihydrate. Asymmetric Induction in Synthesis and Amide Carbonyl Coordination to Copper

Robert A. BULMAN *(Univ. London)*, **Nirupa JOBANPUTRA** *(Univ. London)*, **Reiko KURODA** *(Inst. Cancer Research UK, Tokyo Univ. and IMS)*, **and Peter J. SADLER** *(Univ. London)*

The ligand *N,N'*-1,2-ethanediylbis[*N*-(carboxymethyl)glycyl-L-methionine]ethyl ester (H_2L) has been synthesized and its binding to Cu(II) in aqueous solution studied by a variety of methods including circular dichroism. These indicate that asymmetric induction at Cu(II) occurs. Crystals of the blue complex $C_{24}H_{40}O_{10}N_4S_2Cu.3/2H_2O$ were studied by X-ray diffraction: orthorhombic a=8.962(2) Å, b=11.595 Å, c=31.491(2) Å, Z=4, space group $P2_12_12_1$ R=0.038. The single Δ(+) enantiomer in the crystal contains tetragonally distorted N_2O_4 Cu(II) ions with trans N,O equatorial coordination from ethylenediamine nitrogens and -CH_2COO- oxygens. The ethylenediamine ring adopts a skewboat conformation. The axial ligands are amide carbonyl oxygens. The average axial Cu-O distance (2.39 Å) is 0.4 Å longer than the equatorial Cu-ligand bond length. The methionine sulfurs are not coordinated.

VI–P Novel Molybdenum(0) Dinitrogen Complex of Crown Thioether

Toshikatsu YOSHIDA *(Univ. Osaka Pref. and IMS)*, **Tomohiro ADACHI*, Manabu KAMINAKA*, Tatsuo UEDA***, *(*Univ. Osaka Pref.)*, **and Taiichi HIGUCHI** *(Osaka City Univ.)*

[*J. Am. Chem. Soc.*, **110**, 4872 (1988)]

The first example of a molybdenum(0) dinitrogen complex containing only sulfur coligands, trans-

$Mo(N_2)_2Me_8[16]aneS_4$ (**1**, $Me_8[16]aneS_4$=3,3,7,7,11,11,15,15-octamethyl-1,5,9,13-tetrathiacyclohexadecane), was prepared by reducing trans-$MoBr_2Me_8[16]aneS_4$ with 40% Na/Hg under N_2 (5 atm). The molecular structure of **1** shows a slightly distorted octahedral geometry around the Mo atom with two N_2 molecules in axial and four S atoms in equatorial sites. The coordinated $Me_8[16]aneS_4$ assumes an all-up conformation where four $MoSCH_2CMe_2CH_2S$ rings adopt a chair form. The Mo atom is displaced towards the ring C atoms by 0.101(1) Å from the strict plane defined by the four S atoms. On the basis of oxidation potential due to Mo(0/I) (−0.52 V vs. SCE), ν(N≡N) (1995, 1890 cm^{-1}), and Mo-N distances (1.991(5), 2.008(5) Å), **1** was deduced to be more electron-rich than the phosphine analogues, trans-$Mo(N_2)_2(diphos)_2$. Extended Hückel MO calculations on the hypothetical model compounds, MoL_4 and trans-$Mo(N_2)_2L_4$ (L=SH_2) of D_{4h} symmetry, indicated that p_π electrons are donated from the thioether to Mo atom through p_π-$d_{xz}(d_{yz})$ interactions. Further evidence for the electron richness of **1** was the facile dimethylation of the coordinated N_2 ligand with MeBr affording trans-$\{MoBr(N_2Me_2)Me_8[16]aneS_4\}Br$ (**2**) rather than a methyldiazenido complex.

VI−Q Syntheses and Characterization of Dinuclear High-Spin Iron(II,III) and (III,III) Complexes with 2,6-Bis[bis(2-benzimidazolylmethyl)aminomethyl]-4-methylphenolate(1−)

Masatatsu SUZUKI *(Kanazawa Univ.)*, **Hiroki OSHIO, Akira UEHARA** *(Kanazawa Univ. and IMS)*, **Kazutoyo ENDO** *(Tokyo Metropolitan Univ.)*, **Makoto YANAGA** *(Tokyo Metropolitan Univ.)*, **Sigeo KIDA** *(Kyushu Univ.)*, **and Kazuo SAITO** *(International Christian Univ.)*

[*Bull. Chem. Soc. Jpn.*, in press]

Two types of dinuclear high-spin mixed valence iron(II,III) complexes, $[Fe_2(L\text{-}Bzim)(RCOO)_2](BF_4)_2\cdot nH_2O$ (RCOO=CH_3COO (1) or C_6H_5COO (2)), and $[Fe_2(L\text{-}Bzim)(C_6H_5COO)_2(OH)]BF_4\cdot H_2O$ (3), and dinuclear high-spin iron(III,III) complexes $[Fe_2(L\text{-}Bzim)\text{-}(CH_3COO)_2](ClO_4)_3\cdot 3.5H_2O$ (4) and $[Fe_2(L\text{-}py)(C_6H_5COO)_2]\text{-}(ClO_4)_3\cdot CH_3CN\cdot H_2O$ (5) were prepared, where L-Bzim is 2,6-bis[bis(2-benzimidazolylmethyl)aminomethyl]-4-methylphenolate(1−) and L-py is 2,6-bis[bis(2-pyridylmethyl)aminomethyl]-4-methylphenolate(1−). Mössbauer spectra of the mixed valence complexes revealed that they involve high-spin iron(II) and (III) ions in equimolar amount. Their ESR spectra exhibited a signal at g_{av}=1.7 near liquid helium temperature characteristic of an antiferromagnetically spin coupled high-spin iron(II,III) dimer. Magnetic susceptibility measurements over the temperature range 80 – 300 K revealed that weak antiferromagnetic spin exchange interactions are present between iron(II) and iron(III) ions (J= −5 cm^{-1}). The complexes showed an intervalence absorption band in the near infrared region, indicating that they belong to class II mixed valence type on the classification of Robin and Day. Cyclic voltammogram of 3 in acetonitrile showed two sets of reversible redox couples a 0.00 and 0.66 V vs. SCE, which are assigned to the redox reactions of Fe(II,III)/Fe(II,II) and Fe(III,III)/Fe(II,III), respectively. The complexes 4 and 5 exhibited weak antiferromagnetic interaction (J= −9 ~ −12 cm^{-1}). ESR spectra of 4 and 5 showed a significant temperature dependence.

RESEARCH ACTIVITIES VII
Computer Center

VII–A Theoretical Investigations of Metalloporphyrins by the Ab Initio SCF MO Method

Metal complexes are interesting polyatomic systems because of their complicated electronic structure and their catalytic functions. Metalloporphyrins are prominently important as an active center of energy conversion processes in biological systems. In this project the electronic structure and the fundamental functions are studied for several complexes by using the *ab initio* SCF MO program JAMOL4 and a newly developed MCSCF program JASON2.

VII-A-1 Development of a program for MCSCF calculations with large basis sets

Shigeyoshi YAMAMOTO, Umpei NAGASHIMA, Tomoo AOYAMA *(Hitachi Computer Engineering Co., Ltd.)*, **and Hiroshi KASHIWAGI**

[*J. Comput. Chem.*, **9**, 627 (1988)]

In many transition-metal complexes, Hartree-Fock scheme is often a poor approximation and multi-configurational treatment is required. We have developed a new program named JASON2 for *ab initio* MCSCF (multiconfiguration self-consistent field) calculations with large basis sets. The program is constructed from about 50,000 FORTRAN statements. We designed the program to be able to handle large transition-metal complexes such as iron-porphyrins. The density-formulated super-CI CASSCF method proposed by Roos *et al.* was adopted in order to overcome difficult problems caused by large basis sets. The sparsity of integrals and vectorization on supercomputers were utilized as much as possible. We have proposed new algorithms to speed up the 4-index integral transformation, which was a bottleneck in MCSCF calculations. By vectorization, the integral transformation can be accelerated by 4~6 times on the supercomputer. As shown in Table 1 where timing data for iron-oxo-porphyrin FeP(py)O are listed, large basis sets can be treated practically with JASON2.

Table 1. CPU time (sec) for one interation of CASSCF-6 calculation of FeP(py)O on the supercomputer HITAC S-810/10.

Step	scalar (S)	vector (V)	ratio (S/V)
Integral transform	272	71	3.8
CAS-CI	27	19	1.4
Super-CI	83	60	1.4
Total	382	150	2.5

The total number of active orbitals is 6.
The total number of CGTFs is 232.

VII-A-2 CASSCF study on iron-oxo-porphyrin π cation radical

Shigeyoshi YAMAMOTO and Hiroshi KASHIWAGI

[*Chem. Phys. Lett.*, **145**, 111 (1988)]

We have performed *ab initio* CASSCF (complete active space self-consistent field) calculations on iron-oxo-porphyrin π cation radical $FeP^+(py)O$, which is a model for peroxidase compound I, to elucidate the electronic structure of its Fe-O bond. Its molecular geometry is given in Figure 1. The total number of CGTFs (contracted Gaussian-type functions) is 232. The Mössbauer spectrum parameters (quadrupole splitting, isomer shift, sign and direction of the principal axis of the electric field gradient tensor) are in good agreement with observed data. From the comparison with the previous result[1] on the neutral iron-oxo-

porphyrin, a model for peroxidase compound II, it was found that removing an electron from the porphine π orbital does not change the electronic structure of the Fe-O bond. This is consistent with experimental results. All calculations were carried out on the supercomputer HITAC S-820/80 with the program JASON2.

Reference

1) S. Yamamoto, J. Teraoka, and H. Kashiwagi, *J. Chem. Phys.*, **88**, 303 (1988).

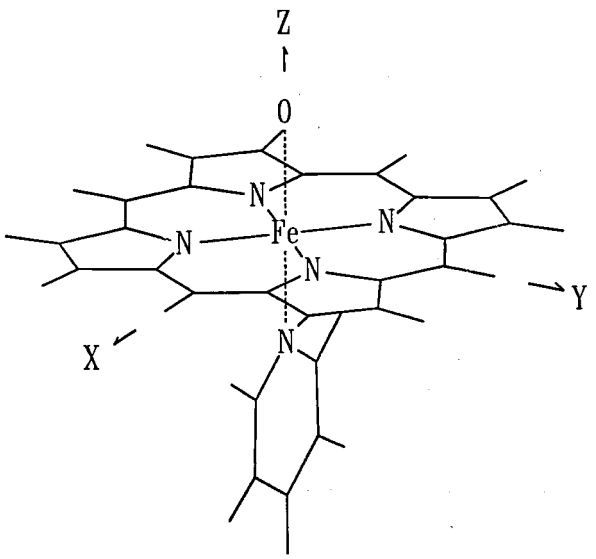

Figure 1. Geometry assumed for $FeP^+(py)O$. The pyridine molecule lies in the xz plane.

VII-A-3 The Ground State Wavefunction of Carbon Monoxide Far from Equilibrium

Umpei NAGASHIMA and Shigeyoshi YAMAMOTO

[*Chem. Phys. Lett.* **143**, 299 (1988)]

The ground state wave function of carbon monoxide at equilibrium correlates to the excited states of carbon and oxygen atoms (^{1}S (C)+^{1}S (O)). The ground states of carbon and oxygen atoms (^{3}S (C)+^{3}S (O)) correlate to the excited state of carbon monoxide. Since these two states are crossing in the intermediate nuclear distance around 5.0 au, the description of the dissociation of carbon monoxide is quite sensitive to the method of calculation.

CASSCF and CI calculations have been carried out on a geometry (Rco=5.5 au) by using almost ten kinds of basis sets and seven kinds of levels of the electron correlation. It is concluded from our calculations that the dissociation of carbon monoxide is best described as a four-electron excitation process from the Hartree-Fock configuration rather than a two-electron process. The dipole moment and the character of the wavefunction at large internuclear separation are sensitive to the calculational scheme employed. Accounting for the electron correlation effects induced by higher excitations and a well-balanced treatment of both the basis set and the electron correlation are essential to obtain a reliable picture of the ground state wavefunction of carbon monoxide far from equilibrium.

Well-balanced CASSCF and MRCI with CASSCF orbitals are useful methods for this purpose.

VII-A-4 Electronic and Geometric Structures of Oligothiophens

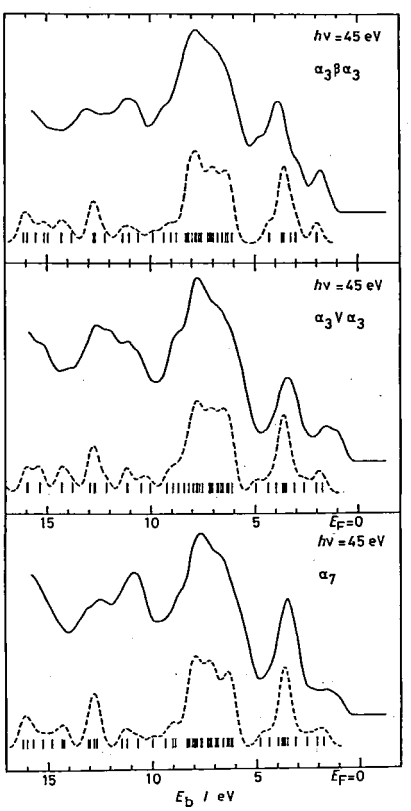

Figure 1. Observed[1)] and simulated UPS spectra of α_7, $\alpha_3\beta\alpha_3$ and $\alpha_3 V\alpha_3$. The broken lines indicate the simulated UPS spectra.

Umpei NAGASHIMA, Hitoshi FUJIMOTO, Kazuhiko SEKI *(Hiroshima Univ.)* **and Hiroo INOKUCHI**

Ultra violet photoelectron spectra (UPS) of some oligothiophenes were reported by using synchrotron radiation[1]: α_7 which is an α-linked septithiophene, $\alpha_3\beta\alpha_3$ in which the middle thiophene ring of septithiophene has β-linkages, and $\alpha_3V\alpha_3$ in which the forth thiophene ring of α_7 is replaced by a vinyl group. The shape of the UPS spectrum of $\alpha_3\beta\alpha_3$ is quite different from that of α_7, although the shape of the UPS spectrum of $\alpha_3V\alpha_3$ is very similar to α_7's.

To investigate the origin of this difference in detail, we carried out the semi-empirical MNDO-SCF-MO calculation. As shown in Figure 1, the observed UPS spectra were well reproduced by using the Koopmans' theorem ionization energies with a Gaussian function of δ=0.6.

The β-linkage and the vinyl group act as an impurity in the polythiophene system. It is shown from the MNDO optimized molecular geometry of $\alpha_3\beta\alpha_3$, that a β-linked thiophene ring is perpendicular to the plane of normal α-linked parts (α_3) and that the π-band spectrum of $\alpha_3\beta\alpha_3$ could be reproduced by the superposition of the spectra of two α_3s and thiophene. The β-linkage prohibits the delocalization of π-electrons and divides the polythiophene chain into short π-segments. On the other hand, the calculated molecular geometry of $\alpha_3V\alpha_3$ was almost planer and the UPS spectrum was almost the same as that of normal α_7.

Reference

1) H. Fujimoto, K. Seki, U. Nagashima, H. Nakahara, J. Nakayama, H. Hoshino, K. Fukuda, and H. Inokuchi, *J. Chem. Phys.* **89**, 1198 (1988)

Chemical Materials Center

VII-B Synthesis of New Chiral Diphosphine Ligands and Their Use in Homogeneous Asymmetric Catalysis

The molecular designing and synthesis of new effective chiral ligands are the most important requirements for developing synthetically useful asymmetric catalysis. Our attention has been focused on the subjects of developments of new effective homogeneous asymmetric catalysis, elucidation of the reaction mechanisms, and explication of the factors controlling the asymmetric induction.

VII-B-1 Studies on the Mechanism of Asymmetric Hydrogenation of Unsaturated Carboxylic Acids Catalyzed by BINAP–Ruthenium(II) Complexes

Tetsuo OHTA *(IMS)*, **Ryoji NOYORI** *(Nagoya Univ.)*, **and Hidemasa TAKAYA** *(IMS and Kyoto Univ.)*

We have reported homogeneous asymmetric hydrogenation of α,β- and β,γ-unsaturated carboxylic acids catalyzed by Ru(II) dicarboxylate complexes of (*R*)-2,2′-bis(diaryl- or dialkylphosphino)-1,1′-binaphthyl (aryl = phenyl, *p*-tolyl, *p*-anisyl; alkyl = cyclohexyl) and their enantiomers to give the corresponding saturated acids in high enantiomeric excesses and in quantitative yields.[1] It was found that the effect of hydrogen pressure on enantiomeric excesses of the products depends highly on the structures of the substrates and is not straightforward. For example, hydrogenation of tiglic acid in methanol using (*S*)-BINAP–Ru complex as catalyst at initial hydrogen pressure of 4 and 101 atm gave the product, (*S*)-2-methylbutanoic acid, in 91% and 50% ee, respectively. The opposite trend, however, was observed in the reaction of atropic acid with the same catalyst, producing (*S*)-methylphenylacetic acid in 48% ee at 4 atm and in 92% ee at 112 atm. Substituents at β-position of the olefins exerts important influence on the enantioselectivity, which suggests that there are several hydrogenation paths through the reaction.

Deuterium incorporation in the catalytic hydrogenation of α,β-unsaturated carboxylic acids has been

investigated using CH_3OH–D_2 or CH_3OD–H_2 system.

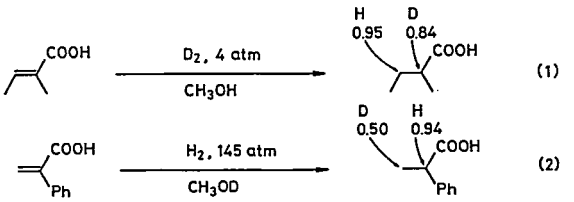

As shown in eqs (1) and (2), the hydrogen α to carboxylic function comes mainly from molecular hydrogen, while the hydrogen on β-position originates from the solvent molecules. These findings coupled with pressure effects on the enantioselectivity suggest that monohydridoruthenium complexes act as important intermediates. The catalytic reactions have also been studied by ^{31}P NMR spectroscopy.

Reference

1) T.Ohta, H. Takaya, M. Kitamura, K. Nagai, and R. Noyori, *J. Org. Chem.*, **52**, 3174 (1987).

VII-B-2 Synthesis and Characterization of [RuX(binap)(arene)]X, New Cationic BINAP–Ruthenium Complexes

Kazushi MASHIMA *(IMS and Kyoto Univ.)*, **Tetsuo OHTA** *(IMS)*, **Ryoji NOYORI** *(Nagoya Univ.)*, **and Hidemasa TAKAYA** *(IMS and Kyoto Univ.)*

We have been studying asymmetric hydrogenations of a variety of olefins and ketones using BINAP–Ruthenium(II) complexes as catalysts. The complexes with empirical formula RuX_2(binap),[1] which have been prepared by the addition of HX to $Ru(OCOCH_3)_2$(binap),[2] catalyzes the asymmetrtic hydrogenation of β-functionalized ketones in very high enantioselectivity. This time, we have prepared new cationic BINAP–ruthenium complexes **2** in very high

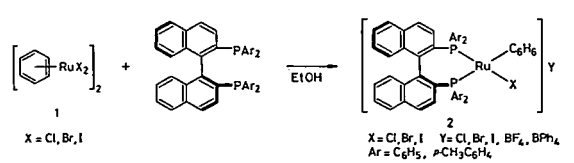

yields. Treatment of the complex **1** with (*S*)-BINAP in a mixture of ethanol and benzene at 50–55 °C afforded the cationic complexes **2** in 90–99% yields. The molecular structure of **2** (X=Cl; Y=BF_4) has been determined by single crystal *X*-ray analysis which is shown in Figure 1. Similarly, the complexes bearing *p*-cymene or methyl benzoate in place of benzene ligand have been prepared in high yields. These complexes are found to be highly efficient catalysts for asymmetric hydrogenations of β-functionalized ketones, allylic alcohols, α,β-unsaturated carboxylic acids, *etc.*

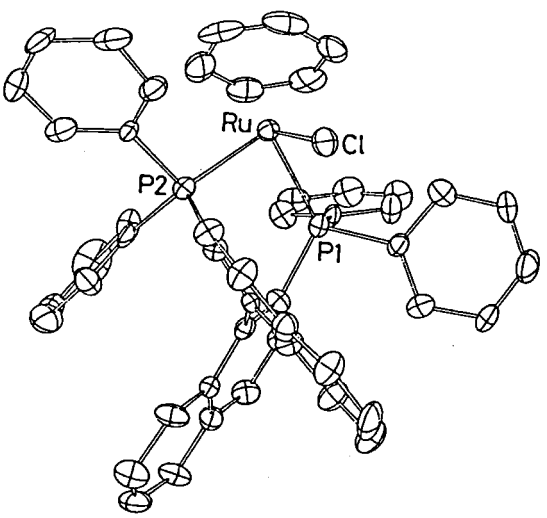

Figure 1. The ORTEP drawing of the complex **2** (X=Cl; Y=BF_4). All hydrogen atoms are omitted for simplicity.

References

1) R. Noyori, T. Ohkuma, M. Kitamura, H. Takaya, N. Sayo, H. Kumobayashi, and S. Akutagawa, *J. Am. Chem. Soc.*, **109**, 5856 (1987).
2) T. Ohta, H. Takaya, and R. Noyori, *Inorg. Chem.*, **27**, 556 (1988).

VII-B-3 Asymmetric Hydrogenation Catalyzed by Cationic [RuX(binap)(arene)]X Complexes

Tetsuo OHTA *(IMS)*, **Kazushi MASHIMA** *(IMS and Kyoto Univ.)*, **Ryoji NOYORI** *(Nagoya Univ.)*, **and Hidemasa TAKAYA** *(IMS and Kyoto Univ.)*

Homogeneous asymmetric hydrogenation of several unsaturated compounds using [RuX(binap)(arene)]X complexes has been studied. Methyl acetoacetate can be hydrogenated in the presence of [RuCl((*S*)-binap)(benzene)]Cl in methanol under hydrogen (100

atm) to methyl 3-hydroxybutanoate in 97–98% ee.

The effects of substituents on benzene ligand and the kinds of anions on the catalyst activity and selectivity have also been studied. The complexes are also effective for asymmetric hydrogenation of α,β-unsaturated carboxylic acids and allylic alcohols. For example, geraniol was hydrogenated in the presence of [RuCl((*S*)-binap)(benzene)]Cl to (*R*)-citronellol (H_2 100 atm, 18 °C, 4 h) in 96% ee. Dihydrocitronellol was produced in less than 3% yield. Hydrogenation of tiglic acid with the same catalyst afforded (*S*)-2-methylbutanoic acid in 89% ee.

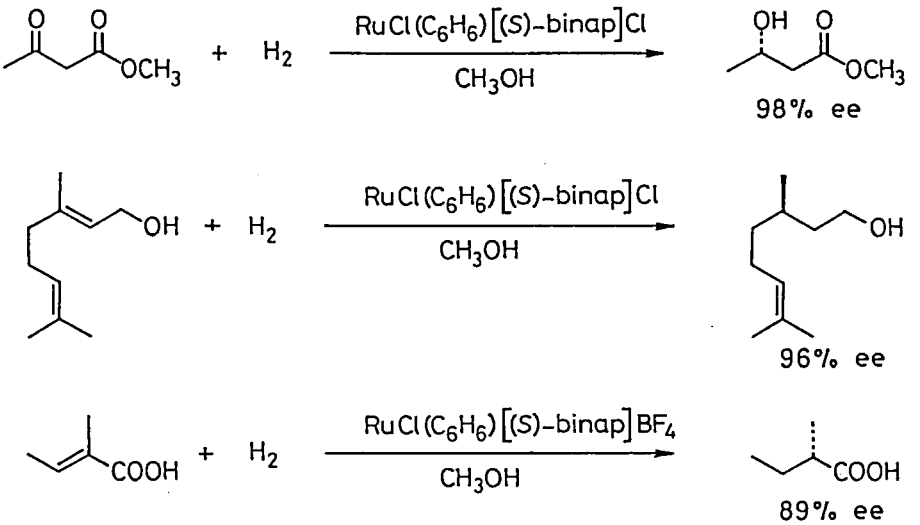

VII-B-4 Kinetic Resolution of Racemic Allylic Alcohols by BINAP–Ruthenium(II)-Catalyzed Hydrogenation

Masato KITAMURA*, Isamu KASAHARA*, Kenji MANABE*, Ryoji NOYORI*, and Hidemasa TAKAYA
*(IMS) (*Nagoya Univ.)*

[*J. Org. Chem.*, **53**, 708 (1988)]

In view of the extremely high enantioface-differentiating ability of our BINAP–Ru(II) dicarboxylate complexes in hydrogenation of prochiral unsaturated alcohols,[1] we examined kinetic resolution of chiral substrates using the double stereodifferentiation and found that appropriate substrate/catalyst chirality matching can achieve excellent enantiomer recognition. The asymmetric hydrogenation of racemic allylic alcohols was conducted with BINAP–Ru($OCOCH_3$)$_2$ (**1**) as catalyst in methanol at 0–30 °C with substrate/catalyst mole ratio of 200–1800. The catalytic reaction afforded a high level of kinetic enantiomer selection (k_{fast}/k_{slow}) for some acyclic substrates. This asymmetric catalysis is also applicable to the previously unexploited resolution of cyclic alcohols. The Ru-catalyzed hydrogenation of 3-methyl-2-cyclohexenol (**2**) afforded *trans*- and *cis*-3-methylcyclohexanol in a 300:1 ratio. In addition, hydrogenation of racemic **2** exhibited an extremely high enantiomer differentiation up to 76:1.

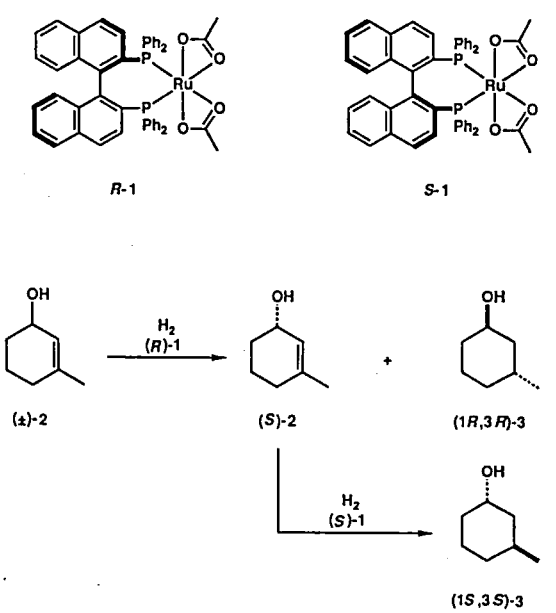

This method allows ready access to both antipodal unsaturated and saturated alcohols in high enantiometric purity. A significant application of the present method includes a practical resolution of 4-hydroxy-2-cyclopentenone which serves as an important building block for prostaglandin synthesis.

Reference

1) H. Takaya, T. Ohta, N. Sayo, H. Kumobayashi, S. Akutagawa, S. Inoue, I. Kasahara, and R. Noyori, *J. Am. Chem. Soc.*, **109**, 1596 (1987).

VII-B-5 A Practical Asymmetric Synthesis of Carnitine

Masato KITAMURA*, Takeshi OHKUMA*, Hidemasa TAKAYA *(IMS)*, **and Ryoji NOYORI*** *(*Nagoya Univ.)*

[*Tetrahedron Lett.* **29**, 1555 (1988)]

(*R*)-Carnitine (vitamin B_T) (**1**) is a physiologically and pharmacologically significant agent which is responsible for the human metabolism and transport of long-chain fatty acids through the mitochondrial membrane. We have accomplished the first efficient chemical synthesis of (*R*)-carnitine on the basis of homogeneous enantioselective hydrogenation of ethyl 4-chloro-3-oxobutanoate (**2**). The reaction of **2** catalyzed by $Ru(OCOCH_3)_2$[(*S*)-binap] or RuX_2[(*S*)-binap]

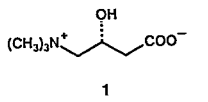

1

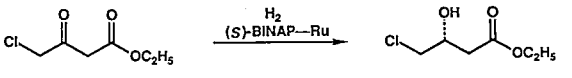

2 3

(X=Cl, Br) under the standard conditions (ethanol as solvent, room temperature, 100 atm, 25–40 h) afforded the desired (*R*)-alcohol **3** in only <70% ee. Fortunately, however, a surprising chiral efficiency was obtained by the high-temperature, short-period reaction. For example, when a 3.5 *M* ethanolic solution of **2** containing 0.05 mol% of $Ru(OCOCH_3)_2$[(*S*)-binap] was stirred under 100 atm of hydrogen at 100 °C, the hydrogenation was completed within 5 min, giving the (*R*)-alcohol **3** in 97% ee. The chloro alcohols can be converted to homochiral **1** by the standard functional group transformation followed by recrystallization. The present method is more convenient than the existing procedures in view of the excellent efficiency and simplicity.

References

1) T. Ohta, H. Takaya, and R. Noyori, *Inorg. Chem.*, **27**, 566 (1988).
2) R. Noyori, T. Ohkuma, M. Kitamura, H. Takaya, N. Sayo, H. Kumobayashi, and S. Akutagawa, *J. Am. Chem. Soc.*, **109**, 5856 (1987).

Instrument Center

VII–C Study of Ultrafine Particles Prepared by Gas Evaporation Technique

The physical properties of fine particles, the size of which is less than ten nm, are affected by the quantum size effect, by the surface effect and by a fluctuation of a thermodynamical property due to low dimensionality. These effects were studied as functions of particle species, supporting organic liquids and preparation techniques.

VII-C-1 Shape Effect and Quantum Size Effect on Small Metal Particles

Keisaku KIMURA

The electronic properties of small particles are expressed by the generalized formula that incorporates the effect of particle shape in addition to the quantum size effect in such a way as to connect the Poisson distribution and orthogonal distribution from random

matrix theory. The physical interpretation was made using the Poisson and orthogonal level distribution. The experiments on the static magnetic susceptibility of small magnesium particles recently obtained were analyzed by means of the proposed formula and were well explained assuming the regularity of particle shape. The observation by high resolution electron microscopy suggests that many particles are not rough in shape. This is inconsistent with commonly accepted assumptions made about small metal particles. "The degree of metallicity" is introduced to characterize the statistics of level spacing fluctuation of metal small particles and this divides the statistics into four regions: bulk metal with Fermi-Dirac statistics, metallic small particles with Poisson statistics, small particles with Wigner-Dyson statistics and insulating molecules.

VII-C-2 Electron Spin Relaxation Time of Ultrafine Zinc Particles Measured by Spin Probe Method

Shunji BANDOW and Keisaku KIMURA

[*J. Phys. Soc. Jpn.* **57**, 2807 (1988)]

A new method of observing the quantum size effect of ultrafine particles is proposed. In the method proposed, an ESR-active ion as a spin probe is added to ultrafine particles (UFP's). The electron state of conduction electron of UFP's is indirectly monitored via an observation of the ESR of this spin through the interaction between a spin probe and conduction electrons as in the case of d-electron spin resonance in metals. We measure the longitudinal electron spin relaxation time T_1 as functions of temperature and particle size. The observed T_1 is an exponential function of the inverse of temperature in the low temperature region ($T<10$ K). When the particle size becomes smaller, a phonon with a long wavelength no longer exists in a particle and the energy transfer from a spin system to a phonon system is prevented in a low temperature region. The quantum size effect on the phonon energy dispersion stated above is discussed in detail.

VII-C-3 Size Effect of the CESR Line Width in Ultrafine Magnesium Particles

Shunji BANDOW and Keisaku KIMURA

Size dependences of the ESR line width ΔH were studied in the ultrafine particles (UFP's) prepared by the gas evaporation method. When the surface of UFP is irregular, sharp ESR signal will be observed in the diameter less than 10 nm, which obeys the functional relation of $\Delta H=\hbar\omega_z/\delta\tau_{so}$ and is represented in Figure 1 by curve A. Here δ is the mean level spacing near the Fermi level and τ_{so} the spin relaxation time due to the spin-orbit interaction. When the surface of UFP is regular, *i.e.* have a very clear crystal habit, the line width will be represented by $1/\tau_{so}$ (curve B). Experimental results did not follow curve A, but seem to follow curve B. Electron microscopy revealed that the shape of UFP was not irregular when the UFP's were prepared by the gas evaporation method. The morphology of particles does not contradict to the ESR results.

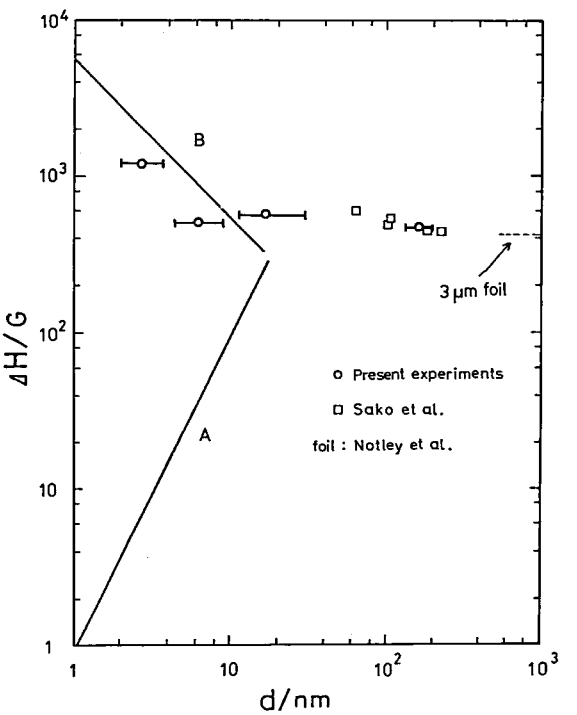

Figure 1. Size dependence of the ESR line width. Results of Sako and Kimura (Ref. 1) and Notley *et al.* (Ref. 2) are also included in the figure. Curves A and B are follow the functional relations of $\hbar\omega_z/\delta\tau_{so}$ and $1/\tau_{so}$ respectively. The value of τ_{so} is represented by the equation of $d/v_F\Delta g^2$ (d: diameter of a particle, v_F: Fermi velocity and Δg: g-shift from a free electron).

References
1) S. Sako and K. Kimura, *J. Phys. Soc. Jpn.*, **53**, 1495 (1984).
2) R.P. Notley, J.R. Sambles and J.E. Cousins, *Solid State Commun.*, **25**, 1125 (1978).

VII-C-4 Development of Apparatus for the Formation of Ultrafine Particles by Sputtering

Shunji BANDOW and Keisaku KIMURA

Ultrafine particles (UFP's) are generally prepared by the gas evaporation method with electro-resistance heating. By this method, however, it is difficult to produce the UFP's with high melting temperature. Sputtering is one of the useful technique to evaporate the metals with high melting temperature. This method was firstly applied to produce UFP's by Yatsuya *et al.*[1] We modified their technique and redesigned the preparation chamber appropriate for the gas flow method. The UFP's produced by the sputtering were carried by the gas stream to the collection chamber. Two plate-electrodes were set in parallel in the vacuum chamber (cathode is a target plate) with a distance of ca. 15 mm and the sputtering gas was flowed between the plate-electrodes with a pressure of a few Torr. DC high-voltage (400–1000 V) was applied to the electrodes through a series resistance of 500 Ω. Figure 1 is Fe UFP's produced by the present experiment. Other UFP's such as Cu, Si, Pt and Ag can be produced by the sputtering. The sputtering rate is in the order of a few hundreds $\mu g/min \cdot cm^2$. Reactive sputtering is also possible with changing the sputtering gas to the active one.

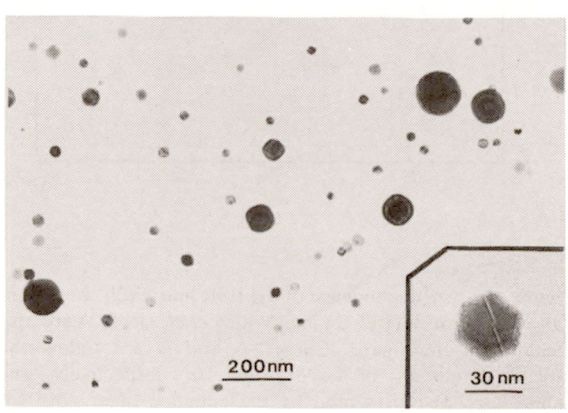

Figure 1. Ultrafine ion particles prepared by the gas flow sputtering method. Sputtering conditions are P_{Ar} = 6 Torr, V = 1000 V and I = 100 mA. Frequent diameter range is about 30 to 40 nm.

Reference
1) S. Yatsuya, T. Kamakura, K. Yamauchi and K. Mihama, *Jpn. J. Appl. Phys.*, **25**, L42 (1986).

VII-C-5 High Resolution Solid State NMR of Fine Particles in a Liquid.

Naoki SATOH *(Kao Corporation and IMS)* **and Keisaku KIMURA**

The effect of motional narrowing to get high resolution solid state NMR was tested. Fine particles moving vigorously and randomly in a liquid phase by thermal energy (Brownian motion) are expected to give a high resolution NMR signal because of motional narrowing. A merit of this method is that one can obtain informations about solid surfaces in a liquid phase such as reacting catalysts or growing crystals, etc. AlF_3 fine particles were dispersed in methanol by gas flow-cold trap method[1] using 20 torr Ar gas flow. TEM

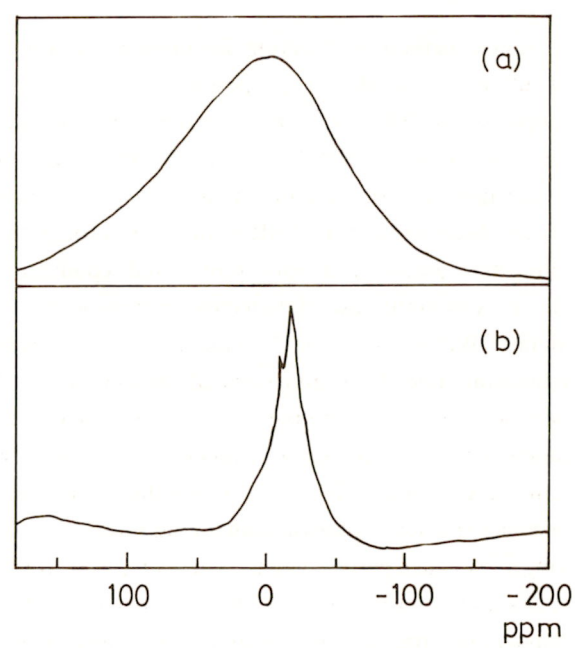

Figure 1. (a) ^{27}Al NMR MAS spectrum of powder AlF_3 measured by JEOL GX270 FT NMR equipped with a solid probe. The observation frequency was 70.3 MHz, spinning frequency about 3 kHz. (b) ^{27}Al NMR spectrum of AlF_3/methanol dispersion measured by JEOL GX400 NMR with a normal probe. The observation frequency was 104.2 MHz.

observation of deposited sample showed that the particle sizes were from several nm to several tens nm. Figure 1(a) shows that the resolution of ^{27}Al NMR could not be enhanced even by a conventional high resolution solid NMR using magic angle spinning (MAS). It is because that the strong local magnetic field by fluorine extremely shorten the spin-spin relaxation time of ^{27}Al nuclei. Figure 1(b) shows the ^{27}Al NMR signal from the dispersion of AlF_3 fine particles. Motional narrowing effect is clearly observed, and at the same time one can see the fine structures in the NMR line. Line width of figure 1(b)(1.2 kHz) are in good agreement with the calculated value for the spherical particles with diameter range from 10 nm to 50 nm using Stokes' theory about rotational diffusion of particles in a liquid.

Reference

1) K. Kimura and S. Bandow, *Bull. Chem. Soc. Jpn.*, **56**, 3578 (1983)

Low-Temperature Center

VII-D Development of an Automated Liquid Helium Supply System

Kiyonori KATO, Hisashi YOSHIDA, Mitsukazu SUZUI, and Keiichi HAYASAKA

An automated filling system for liquid helium in a closed circuit has been developed for simplified filling service. Figure 1 shows the system developed by our group. At the beginning of the liquid helium filling process a liquid helium vessel is put on the load cell which is fixed on a lift, and connected to the transfer tube from a liquid helium reservoir. If a user pushes some relevant keys, an NEC PC 9801 computer controls the valve mounted on the tube for transfer depending on helium gas pressure in the vessel, and on detecting the end of filling it closes the valve. An amount of consumed liquid helium can be printed out and loaded on a disk.

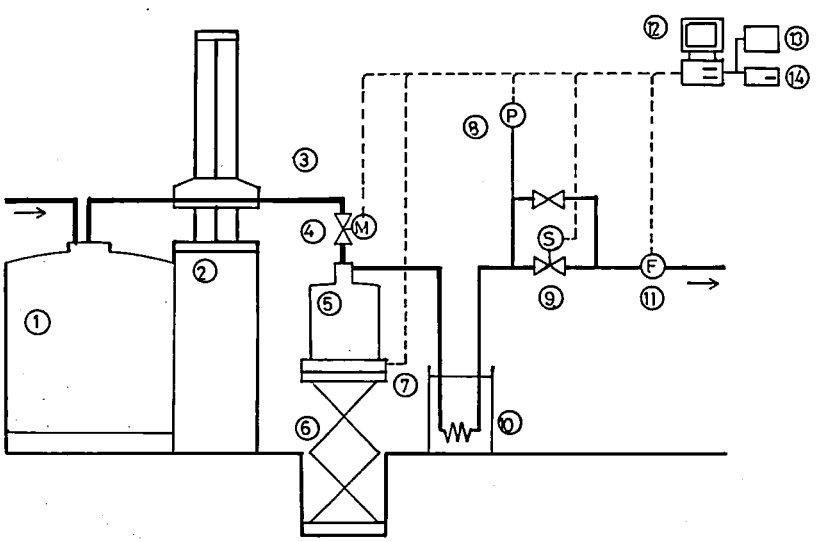

Figure 1. Automated liquid helium supply system: 1.Liq. helium reservoir, 2.transfer tube lift, 3.transfer tube, 4.transfer tube valve regulated by the pulse motor, 5.vessel, 6.lifter, 7.load cell, 8.digital pressure gauge, 9.solenoid valve, 10.heat exchanger, 12.PC-9801 computer, 13.printer, 14.16-key box and card reader.

VII-E Ferromagnetic Interaction in Molecular Crystal

There are only a few molecular crystals in which ferromagnetic interaction exists between neighboring radicals. The study of this interaction should bring us very important knowledge, not only to the establishment of molecular ferromagnet but also to the understanding about the chemical reaction of radicals.

In the present project, we investigate the ferromagnetic coupling by referring to the intramolecular spin-polarization effect. Our further attention is focused on the physical and chemical phenomena derived from intermolecular interaction of the spin-polarized electrons.

VII-E-1 Ferromagnetic Intermolecular Interaction of Organic Radical, Galvinoxyl

Kunio AWAGA, Tadashi SUGANO *(ISSP, Univ. of Tokyo)*, **and Minoru KINOSHITA** *(ISSP, Univ. of Tokyo)*

[*Synth. Metals*, in press]

The galvinoxyl radical is experimentally demonstrated to have ferromagnetic intermolecular interaction. This interaction is proved to extend one-dimensionally with the exchange energy of $2J_F \simeq 1.5$ meV. Furthermore, the ferromagnetic coupling in galvinoxyl is qualitatively interpreted by a combined effect of intramolecular spin polarization and intermolecular charge-transfer interaction.

Equipment Development Ceter

VII-F Optical Study of Electron and Proton Transfer in CT Complexes.

VII-F-1 Cooperative Phenomena Associated with Electron and Proton Transfer in Quinhydrone CT Crystal

Tadaoki MITANI, Gunji SAITO*, Hatsumi URAYAMA* *(*Univ. of Tokyo)*

[*Phys. Rev. Lett.*, **60**, 2299 (1988)]

Studies of the IR vibrational spectroscopy of single crystals of the H-bonded quinhydrone charge-transfer complexes show that a new phase transition occurs upon application of hydrostatic pressure, associated with the proton transfer in the 2D proton lattice. The temperature- and pressure-induced changes in the O-H vibrational spectra are accounted for in terms of the melting of the proton lattice due to the proton tunneling effect.

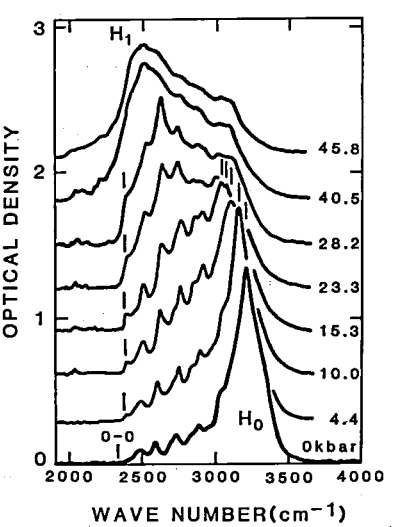

Figure 1. Pressure dependence of the unpolarized absorption spectra of the O-H stretching mode in monoclinic quinhydrone crystal at 300 K.

VII-F-2 Electron and proton transfer in naphthoquinhydrone CT crystals

Hiroshi OKAMOTO, Tadaoki MITANI, Kazuhiro NAKASUJI, Hiroshi YAMAMOTO*, and Ichiro MURATA* *(*Osaka Univ.)*

As an extension of our study of the cooperative phenomena of electron and proton transfer observed in quinhydrone CT crystals, naphthoquinhydrone composed of naphthohydroquinone as a donor and naphthoquinone as an acceptor has been newly synthesized. The excitation energy of the CT exciton is considerably reduced due to delocalization of the Π-electron system. The characteristic features of the vibrational spectra under hydrostatic pressure can be explained by modification of the model, which has been developed in the study of the phase transition observed in quinhydrone crystal associated with the proton transfer (VII-F-1). Further chemical modifications along this line are now in progress.

VII-F-3 Dynamical Aspect of Neutral-Ionic Phase Transition in Organic Charge-Transfer Complex Crystals

Hiroshi OKAMOTO, Tadaoki MITANI, Yoshinori TOKURA*, Takao KODA*, and Gunji SAITO* *(*Univ. of Tokyo)*

[*Synth. Metals* in press]

The phase diagram of the neutral-ionic (NI) phase transition in the TTF-CA crystal was obtained on the temperature-pressure plane from infrared molecular vibrational spectroscopy. From our recent investigations, it has been demonstrated that the NI domain walls (or equivalently the ionic domains embedded in the neutral lattice) and soliton-like defects are elementary excitations with relatively low energies in the TTF-CA crystal. The electric and dielectric properties of the TTF-CA crystal were investigated in detail. Anomalous field and pressure dependences of electric conductivities have been observed, which can be accounted for in terms of solitons and NI domain walls. The large dielectric response has been also observed, which is attributable to the ionic domain between the NI domain wall pair. The dynamics of the ionic domain is discussed on the basis of the results.

VII-F-4 Infrared Molecular-Vibration Spectra of Tetrathiafulvalene-p-Chloranil Crystal at Low Temperature and High Pressure

K. TAKAOKA*, Yoshio KANEKO*, Hiroshi OKAMOTO, Yoshinori TOKURA*, Takao KODA*, Tadaoki MITANI, and Gunji SAITO* *(*Univ. of Tokyo)*

[*Phys. Rev.* **B36**, 3884 (1987)]

Temperature (T) variations of the infrared molecular-vibration spectra on Tetrathiafulvalene (TTF)-p-chloranil crystalline powders have been measured at various pressure (P). From the observed behavior of the spectra as a function of T and P, it is concluded that both quasi-ionic and quasi-neutral molecules coexist in an intermediate range of T and P, until the crystal undergoes a phase transition to the dimerized ionic phase at T_c which depends on P. These results are discussed in terms of a P-T phase diagram of TTF-p-chloranil crystal.

VII-F-5 Nonlinear Electric Transport and Switching Phenomenon in the Mixed-Stack Charge-Transfer Crystal TTF-p-Chloranil

Yoshinori TOKURA*, Hiroshi OKAMOTO, Takao KODA*, T. Mitani, and Gunji SAITO* *(*Univ. of Tokyo)*

[*Phys. Rev.* **B38**, 2215 (1988)]

A remarkable nonlinearity and a switching effect have been observed for electric transport in a TTF-p-chloranil crystal. Experimental evidence indicates that these features are of an intrinsic origin associated with the neutral-ionic transition. A possible mechanism is discussed in terms of field-dependent low-energy excitations, such as solitons and neutral-ionic domain walls, which are inherent to the quasi-one-dimensional donor-acceptor stacks in the TTF-p-chloranil crystal.

VII-G Novel Optical Sampling Technique for Femtosecond Spectroscopy

VII-G-1 Two-Photon Absorption Sampling Spectroscpy for Fast Transient Luminescence Measurement

Yoshihiro TAKAGI and Keitaro YOSHIHARA

[*Ultrafast phenomena VI, Springer, in press*]

Two-photon absorption in atomic vapor has been applied to a sampling spectroscopy for fast transient luminescence measurement with extremely high time-resolution. A ultrashort light pulse excites a sample which emitts a short-lived fluorescence and the fluorescence beam and a part of the exciting light pulse are fed into an atomic vapor. Two-photon transition taking place using one photon from the fluorescence and one photon from the light pulse is monitored by either fluorescence from appropriate excited states of the atom or ionization successively following the two-photon transition. Decay profiles of fluorescence of a few organic dye solutions with life times of picosecond to nanosecond were obtained, This method is particularly useful in the transient fluorescence measurement in vacuum ultraviolet spectral region, where existing nonlinear techniques are not applicable.

VII-G-2 Autocorrelation Measurement of Ultrashort Light Pulse Using Two-Photon Absorption in Atomic Vapor

Yoshihiro TAKAGI

An autocorrelation profile of the output of a synchronously pumped mode-locked dye laser has been measured for the first time using two-photon absorption (TPA) in a sodium vapor. The output of the laser was tuned to 578.7nm giving rise to the two-photon transition between 3S ground state and 4D excited state. An ordinary Michelson interferometer-type arrangement was used for autocorrelation measurement except for replacement of the second harmonic crystal by an atomic vapor contained in a heat-pipe oven. The two-photon transition was monitored by the detection of ionization current due to further excitation by excess incident photons. Figure 1 shows a typical autocorrelation profile obtained by this method. The signal-to-noise ratio was very low because of inefficient collection of the photo-electron in our design of the ionization detection. This must be improved by the use of an electron multiplier. The shape of the autocorrelation profile was nearly the same as that obtained by the second harmonic generation except for a large offset due to TPA coming from uninteresting region where the two incident beams are not over-lapped. It should be noted that the autocorrelation using very narrow bandwidth TPA gives a time resolution as high as the second harmonic generation. The TPA linewidth of atomic vapor (Doppler width of the order of 0.1 cm^{-1}) is much narrower than our laser bandwidth (6 ps pulsewidth). Nevertheless, the autocorrelation width, which is shorter than the reciprocal of 0.1 cm^{-1}, indicates that a fraction in the laser bandwidth larger than the TPA linewidth can contribute to the transition.

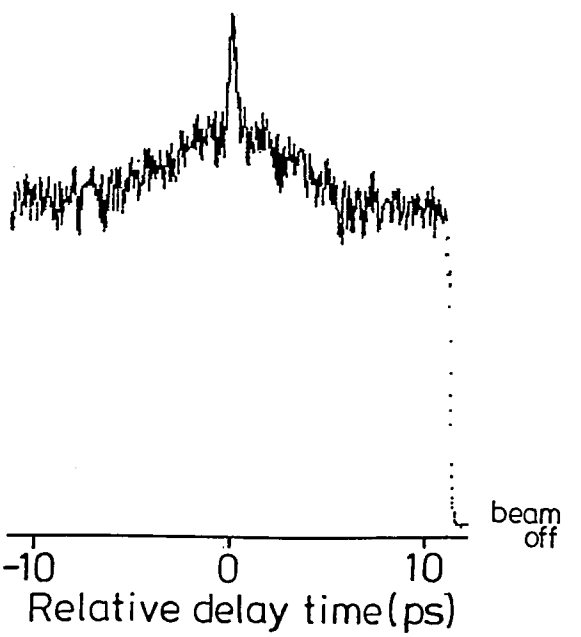

VII-H Development of Experimental Devices

VII-H-1 Delay-time Modulation Spectroscopy Using a CW Mode-locked Nd:YAG Laser Synchronized with the SR Light Pulses

Hiroshi OKAMOTO, Tadaoki MITANI, Yoshihiro TAKAGI, Makoto WATANABE, Kazutoshi FUKUI, Shinya KOSHIHARA *(Univ. of Tokyo)* **and Chihiro ITO** *(Nagoya Univ.)*

Picosecond light pulses (70 psec) synchronized with successive pulses of the synchrotron radiation (460 psec) at 90MHz have been generated using a CW mode-locked Nd:YAG laser. By improvement of the time-characteristics of the synchronized light pulses, transient absorption measurements have been made in a short time domain of 0.05-11nsec using a delay-time modulation technique. The experimental instrumentation of the transient spectroscopy is schematically illustrated in Figure 1. Using the tuning method of the laser pulses as shown in Figure 1, a delay time of the SR pulses measured from the peak position of the laser pulses can be modulated by applying an AC voltage (e.g.200Hz). A change of the transmitted SR light induced by the modulated irradiation of the laser beam on the sample material is detected by a phase-sensitive lock-in amplifier as a modulation signal of the absorption coefficient. This system opens a possibility of expanding a measurable region of transient spectroscopy to the infrared and far-infrared regions.

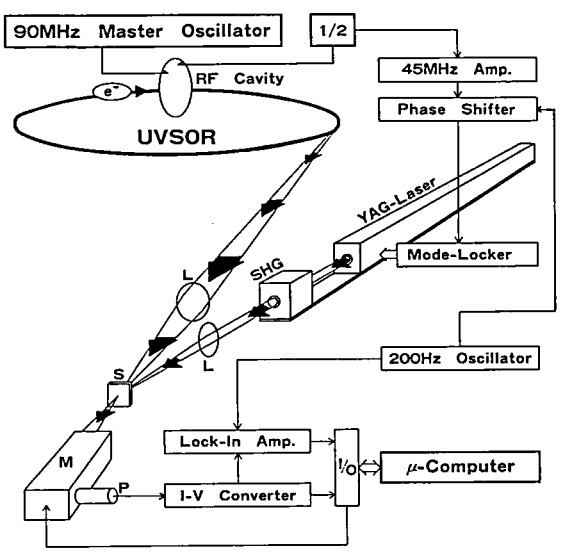

Figure 1. Schematic diagram of the experimental setup for the transient SR absorption measurements.

VII-H-2 IR-VUV Windows for Ultra-High Vacuum Instrumentations

Norio OKADA and Toshio HORIGOME

A newly designed window available for optical measurements under an ultra-high vacuum has been developed using several kinds of materials such as NaCl, CaF_2, and SiO_2 plates, which allow to expand a measurable region to the far IR or the VUV region. As shown in Figure 1, the optical window is attached to a ultra-high vacuum flange free from thermal or mechanical stress through vacuum-shield substances (Ag ring, AgCl, and Au spattered film). Since this window is bakable at 250°C, an ultra-high vacuum is obtained to be less than 10^{-10} Torr. Furthermore, it can be used as an optical window for instrumentations at low temperatures down to a liquid helium temperature.

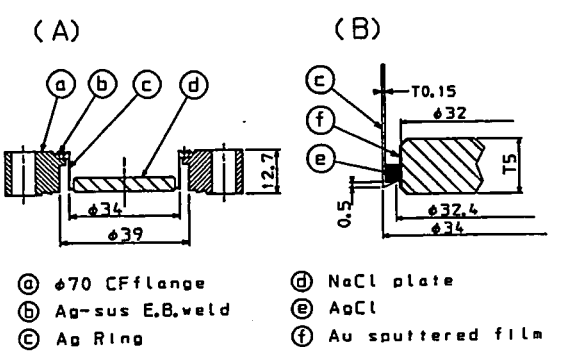

Figure 1. Cross sections of the ultra-high vacuum window.

Ultraviolet Synchrotron Orbital Radiation Facility

VII-I Construction of UVSOR Light Source

VII-I-1 Suppression of Longitudinal Coupled-Bunch Instability by Decoupling Method

Toshio KASUGA, Hiroto YONEHARA, Masami HASUMOTO and Toshio KINOSHITA

A longitudinal coupled-bunch instability in the UVSOR electron storage ring for synchrotron radiation research had been observed when routine operation of the ring was started. It was successfully damped with a longitudinal active damping system, which consists of sixteen independent feedback loops; each of them corrects the energy deviation of any one of sixteen bunches individually. We also tested a passive damper. Two kinds of passive damping systems have been reported: Landau cavity or harmonic cavity method and a decoupling method. The former makes use of the Landau damping by the synchrotron frequency spread due to the strong nonlinearity which is introduced into the effective acceleration voltage around the stable phase angle. In the latter method, the phase oscillation of individual bunches are decoupled by a spread in their synchrotron frequencies, which is induced externally by modulation of the acceleration voltage. We adopted the latter because the required RF voltage is much smaller than that of the former. The coupled-bunch instability was damped with this mthod when the beam current was less than 80mA and the growth rate of the instability is not very fast. The limitation of this method is not in principle but in the maximum applicable voltage across the acceleration gap.

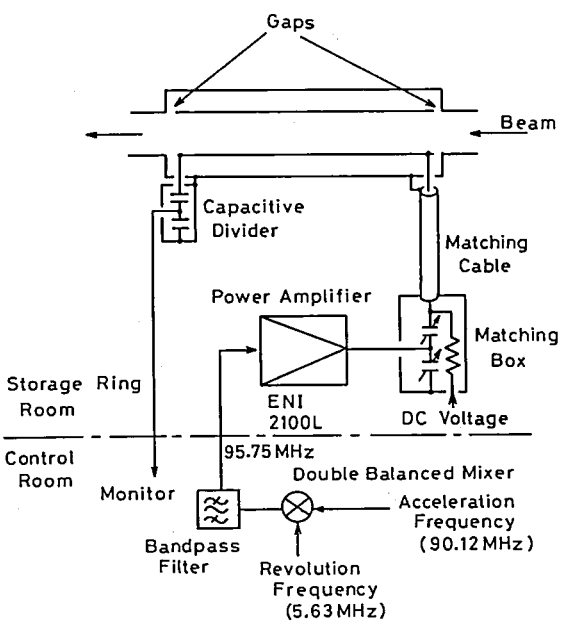

VII-I-2 Bunch Lengthening in Single Bunch Mode of UVSOR Storage Ring

Hiroto YONEHARA, Toshio KASUGA, Masami HASUMOTO and Toshio KINOSHITA

It is well known that a bunch lengthening occurs above a certain threshold current in an usual electron storage ring. We measured the beam current dependence of the bunch length in the single bunch mode at the beam energy of 500, 600 and 750 MeV in order to estimate the density of the beam. Certain thresholds are appreciated in the bunch lengthening data, and it is well explained by the microwave instability. The measured bunch length at zero-current is about 1.5 times as large as the natural bunch length, which is determine by the equilibrium condition between the radiation damping and the quantum excitation. The longitudinal coupling impedance of the UVSOR ring was estimated with the threshold current and this value is about twice as large as the expected one of 2Ω. The horizontal bunch widening of the beam was also observed above the threshold current.

VII–J Development of Equipments for UVSOR

VII-J-1 2.2 m Constant-Deviation Grazing-Incidence Monochromator at BL3A2

M. SUZUI, J. YAMAZAKI, E. NAKAMURA, K. SAKAI, O. MATSUDO, K. FUKUI, N. MIZUTANI, E. ISHIGURO *(Osaka City Univ.)* and M. WATANABE

A 2.2 m constant-deviation grazing-incidence monochromator can utilize the undulator radiation and the synchrotron radiation from B_3 bending section. It covers the wavelength region of 1000–100 Å using three gratings, the groove densities of which are 600/mm, 1200/mm and 2400/mm and their radii of which are 2217.6 mm. Figure 1 shows the side view of the monochromator. The positions of the entrance and the exit slits, and the directions of incident and monochromatized lights are fixed. The wavelength is scanned by the rotation of the grating with the translation of the combination of the grating and the plane mirror along the incident light direction. The relative position of the grating and the mirror is unchanged. The distance between the M_3 pre-mirror and the M_5 post-mirror is about 2.9 m. The height of the output beam is about 1.9 m. The grating chamber accommodating the plane mirror moves on a bed inclined by 14°. The entrance and exit slits are connected to the grating chamber with the bellows. The intensity of the first harmonic of the undulator radiation around 250 Å through the monochromator with the 100 μm slits was 10^{12} photons/s.

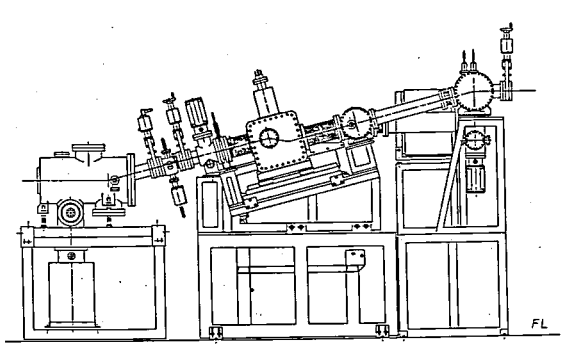

Figure 1. Side view of 2.2 m constant-deviation grazing-incidence monochromator.

VII-J-2 2.2 m Rowland Circle Grazing Incidence Monochromator at BL8B1

K. SAKAI, E. NAKAMURA, J. YAMAZAKI, O. MATSUDO, K. FUKUI, E. ISHIGURO *(Osaka City Univ.)*, S. MITANI *(Osaka City Univ.)* and M. WATANABE

The beam line BL8B1 has been equipped with a Rowland circle grazing incidence monochromator. The radius of the grating is 2217.6 mm. Figure 1 shows the side view of the monochromator. Synchrotron radiation is focused on to the entrance slit by the pre-mirrors M_1 and M_2 (not shown in Figure 1). The entrance slit and the grating is fixed. The exit slit moves along the Rowland circle. The direction of the monochromatized light is fixed on horizontal plane by the two-post mirrors (M_3 and M_4). One of two gratings can be chosen with keeping the vacuum, the groove densities of which are 1200/mm and 2400/mm. The useful range is 200–20 Å with the 2400/mm grating. Three M_4 mirrors are provided. One of them is chosen, the monochromator chamber being opened. By the use of the 2400/mm grating, the resoution $\lambda/\Delta\lambda$ of 10^3 was achieved and the photon number behind the exit was 10^8/s with 10 μm slits.

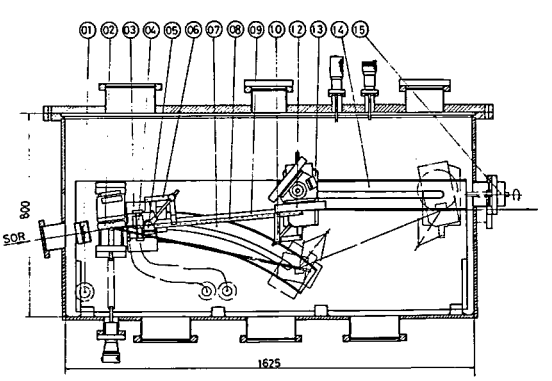

Figure 1. Side view of the 2.2 m Rowland circle grazing incidence monochromator. 01: entrance slit, 02: grating, 04: exit slit, 05: M_3 mirror, and 12: M_4 mirror.

VII-K Researches by the Use of UVSOR

Researches of IMS staff other than UVSOR staff are reported at some other places in this issue. Details of all researches preformed by inside and outside users will be reported in UVSOR Activity Report 1988.

VII-K-1 Molecular Center in KCl Created by Undulator Light Irradiation

Hideyuki NAKAGAWA[a)], Toshiki DEGUCHI[a)], Hiroaki MATSUMOTO[a)], Takeshi MIYANAGA[b)], Kazutoshi FUKUI, and Makoto WATANABE *(a) Fukui Univ., b) Wakayama Univ.)*

Luminescence and optical absorption measurements were performed on the KCl single crystals irradiated with VUV-light from the undulator at BL3A1. The fundamental harmonic peak of undulator radiation (UR) is at 31.5 nm and its spectral width is about 1.7 nm. The photon number at the sample position (1 mm dia.) is about 10^{14} /s.

Molecular emission bands were observed in the 4 – 6 eV region. A typical example is shown in Figure 1. Measurements were made at 330 K under the UR excitation after the same UR irradiation of about 500 mA·h dose at RT. The emission spectrum consists of well-defined structures. The values of the separation energy in the emission spectrum (0.24 – 0.30 eV) are much larger than the typical lattice phonon energies of KCl (< 30 meV). No discernible luminescence was observed at RT in the non-irradiated KCl crystals. The intensities of luminescence increase in proportion to the irradiation dose. These structures are similar to the luminescence bands induced by ion and electron bombardments which are attributed to the CN^- ions created on the surface or in the bulk near surface by the bombardment. If the crystal contains the CN^- impurity, the luminescence should be observed even in non-irradiated samples. Thus, it is supposed that some photo-induced chemical reaction occurs to create the CN^--ions from the species adsorbed on the crystal surface.

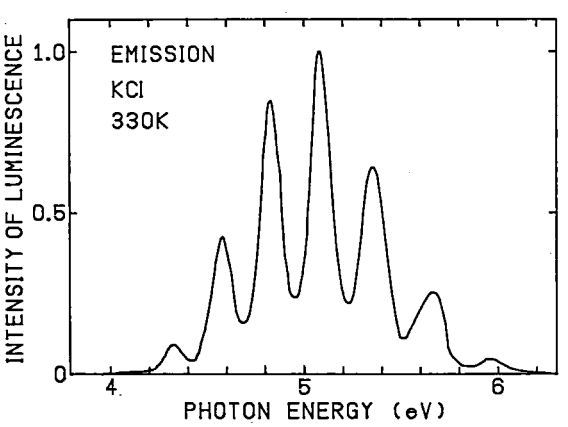

Figure 1. Emission spectrum obtained at 330 K under the undulator light (31.5 nm) excitation in the KCl crystal after irradiation at RT with the same undulator light by the dose of about 500 mA·h.

VII-K-2 The Fast Recombination Luminescence in Alkali Chlorides Excited by Undulator Radiation

Kazutoshi FUKUI, Makoto WATANABE, Hideyuki NAKAGAWA[a)], Toshiki DEGUCHI[a)], Hiroaki MATSUMOTO[a)], and Takeshi MIYANAGA[b)] *(a) Fukui Univ., b) Wakayama Univ.)*

Emission spectra were measured with the lifetime on the alkali chloride single crystals (NaCl, KCl, RbCl) excited by the undulator radiation (UR) at BL3A1. UR was about 31.5 nm quasimonochromatic VUV light and its density was about 10^{14} photons/s in the spot of 1 mm diameter at the sample position.

New emission bands were found around 5 eV in KCl and RbCl at low temperature. Figure 1 shows decay curves at 7.3 K in each crystal at the peak of the emission bands including that of NaCl crystal. These data were measured under the single bunch operation of UVSOR (pulse intervals was 178 ns and pulse width was 0.4 ns). The 5 eV emission band of NaCl was known as σ-emission and its lifetime was 2.8 ns.[1)] Lifetime calculated from present data was in good agreement with this value. However, baseline increases due to the presence of another decay component which was longer than pulse intervals was found. Same phenomena also could be seen in RbCl. Dependence of decay curve on emission energy were measured in both

KCl and RbCl. Thus 5 eV emission band of these crystals may consist of more than two emission bands. At present, it is not clear that the fast recombination luminescence in both KCl and RbCl is σ-emission.

Reference

1) I. M. Blair et al., *J. Phys. C*, 5, 1537 (1972).

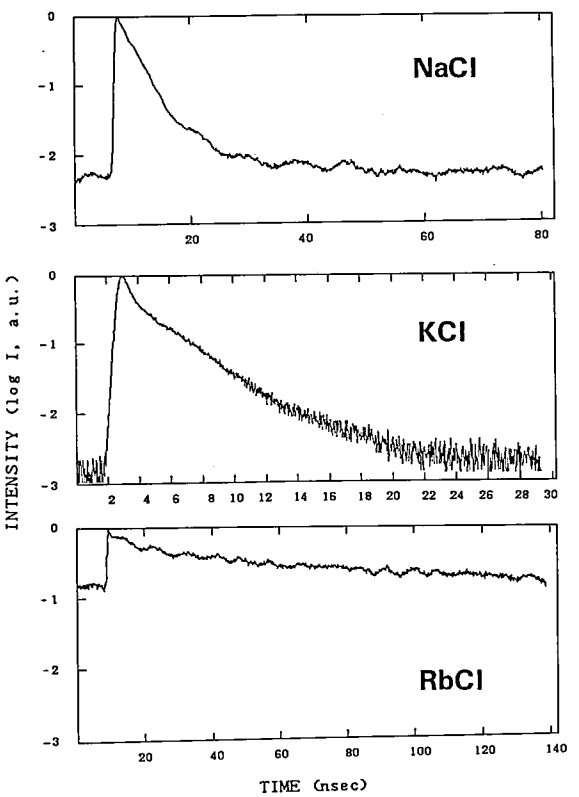

Figure 1. Luminescence decay curves of NaCl, KCl and RbCl, excited at the peak of the luminescence of 5.2, 5.2 and 4.9 eV, respectively. They were measured under single bunch operation by the TAC method. Temperature was 7.3 K.

VII-K-3 The Measurement of the Total Photoelectron Yield in the Soft X-Ray Region at BL7A

Shun-ichi NAOÉ*, Tokuo MATSUKAWA and Takatoshi MURATA***** *(*Kanazawa Univ. and IMS, **Osaka Univ., ***Kyoto Univ. of Education)*

We have made absorption measurements on solids in the soft X-Ray region. The samples were constrained so far to be thin films which were usually prepared by the evaporation technique. However, an another experimental technique was desired to make the measurements on single crystals or bulk samples. In the X-Ray region, the excitation spectra of the photoelectron obtained by gathering all the electrons regardless of their kinetic energy, so called total yield spectra, are known to reflect to their absorption spectra fairly accurately. The convenient DC measurement of the electron yield was done by the use of an electron multiplier as a detector. Figure 1 shows the yield spectrum of the Ge-$L_{3,2}$ edge of a single crystal with the absorption spectrum of the evaporated thin film which is amorphous. The base pressure of the sample chamber is the order of 10^{-10} Torr and a cryostat for the measurement at the low temperature (L.N.T.) are prepared. By the measurement of this electron yield, the field of a research will be further extended.

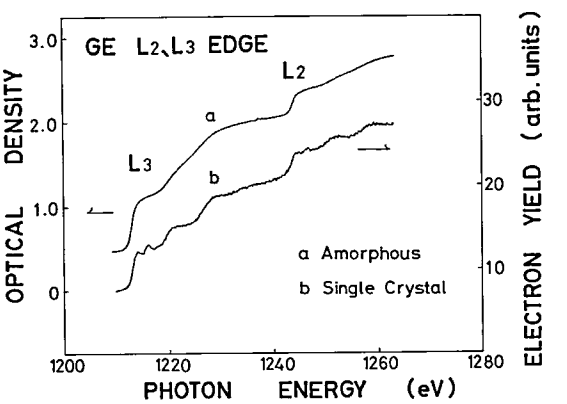

Figure 1. a) an absorption spectrum of a thin film, b) a total yield spectrum of a single crystal. Both spectra were measured at RT (their spectral profiles did not change at low temperature).

VII-K-4 Near-edge and EXAFS Spectroscopy of Light Elements

I.H. MUNRO*, T. MATSUKAWA^{+}, T. MURATA $^{++}$, S. NAOE^{+++}, M. HENDERSON, S. MARSHALL*, G.N. GREAVES*, S. GURMAN***, J. CHARNOCK***
*($^{+}$College of Education, Osaka University, $^{++}$Kyoto University of Education, $^{+++}$College of Arts & Science, Kanazawa University, *Daresbury Laboratory, Warrington WA4 4AD, UK, **Geology Department, Manchester University, UK, ***Physics Department, Leicester University, UK)*

A new double crystal, soft x-ray monochromator on BL7A has been used to study a wide range of materials

close to the K-edges of Na, Mg, Si, S, Cl. Figure 1 is an example of the EXAFS spectrum of Mg in MgO crystal, which was used as reference in the study of a range of 15 different crystalline and glassy samples of Magnesium/Aluminium silicate glasses. The results reveal a variety of Mg and Al coordination conditions in different materials based on Mg and Na edge measurements.

A study was made at the S-edge for NiS and the Cl edge for Fe $(OC_2H_2OCH_2CO_2)(H_2O)_2Cl$. Measurements were made at the Si-edge for a variety of thin film (~2 μm) samples of Cd/Si/As mixtures, which had the general composition $(CdAs_2)_xSi_{1-x}$, where x was varied from 0.2 to 0.5. The samples were supported on a 70% transmitting, 30 μm thick Be film.

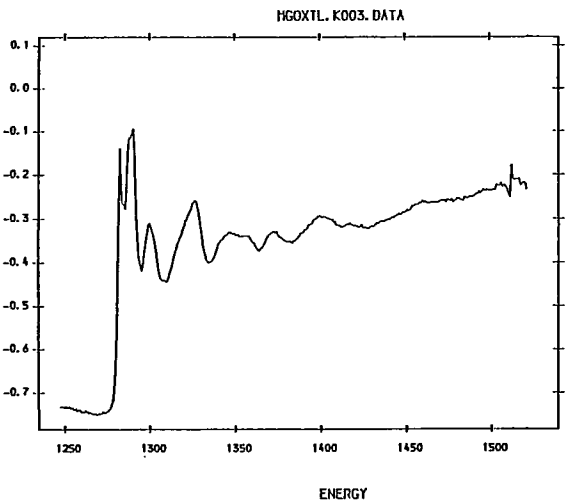

Figure 1. Normalised MgO EXAFS.

RESEARCH FACILITIES

For the sake of brevity the present issue includes only the newly installed facilities and the activities since September 1987. Concerning the activities and facilities before September 1987, please refer to older IMS Annual Review issues (1978～1987).

Computer Center

In February 1988 a supercomputer HITAC S-820/80 was introduced replacing S-810/10 and was coupled with an M-680H. The maximum speed of S-820 is 2 GFLOPS. This is the fastest single processor in the world. S-820 has 128 mega byte main memory and 1 giga byte extended storage. The CPU speed of M-680H is about 14 MFLOPS and it has a 64 mega byte main memory. Both computers can access an 85 giga byte disk memory and an optical disk memory whose maximum content is 86 giga bytes. Two kinds of high speed IO facilities are available. Although the extended storage (2GB) is used only for working files, its access speed is 1.6 GB/sec. The other is a parallel IO disk set which consists of 16 channels for each computer and a 40 giga byte disk memory. Its I/O speed is about 40 times as fast as the normal usual disk. The computer system can be accessed from any place in Japan through telephone lines and the package exchange network. On the campus of IMS, an optical fiber local area network supports high speed data transfer.

The computers are used not only by the research staff at IMS but also by the staff at nearby National Institutes as well as by scientists outside the Institutes in the related fields. The number of project groups was 213 consisting of 663 users in March 1988. In the twelve month period ending March 1988, 278956 jobs were processed with 6624 hours of CPU time on both processors in the unit of M-680H speed.

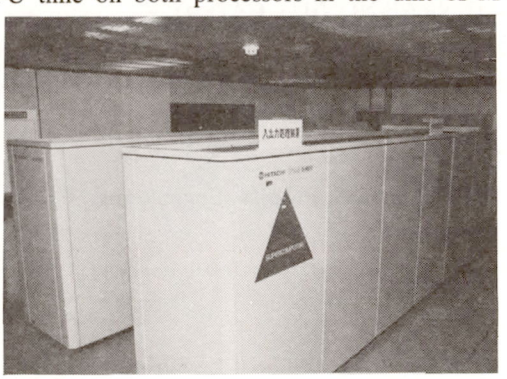

Supercomputer HITAC S-820/80

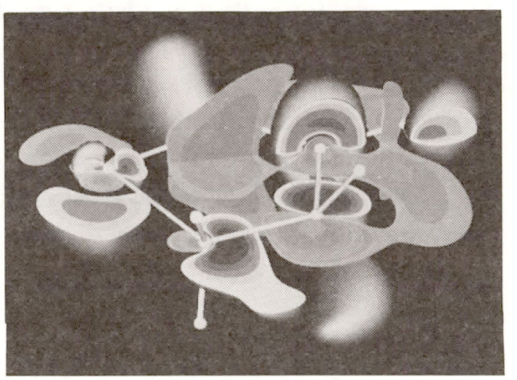

S-820/80 Computer graphics

Chemical Materials Center

The Chemical Materials Center plays an important role in the synthesis and purification of chemical substances in IMS. The scientists and technical associates of this facility support other people in IMS to carry out the above works. Upon request, technicians carry out elemental and mass spectrometric analyses of new compounds prepared at IMS. They also carry out their own researches on synthesis of new interesting compounds, developments of new selective chemical transformations, elucidation of reaction mechanisms, and application of new methodologies developed in IMS to the analysis of chemical substances and reactions. Parts of the scientific activities are presented in the Section

VII.

Associate Professor Hidemasa Takaya moved to Department of Industrial Chemistry, Faculty of Engineering, Kyoto University on April 1st, 1988. In June, 1988, research associate Kazushi Mashima also moved to Department of Industrial Chemistry, Faculty of Engineering, Kyoto University.

Instrument Center

For the efficient use of instruments, the Center is equipped with various types of instruments for general use.[1] Three instruments have been newly installed in 1988.

1) **Mode-Locked cw Nd:YAG laser** (Coherent 76-s Antares)
N:YAG laser generates a continuous wave light at a wavelength of 1064 nm, producing 25 W of power in TEM_{00} mode. Using a mode-locker driver, 100 ps pulses at 1064 nm and 70 ps pulses at 532 nm with a energy of 2 W using a KTP crystal are obtained at a repetition rate of approximately 76 MHz. This laser system is used as the synchronous pumping of dye laser for the application of time-correlated single-photon counting.

2) **Fourier Transformed Interferometric Spectrophotometer** (Bomem DA3.36)
Using a dynamic alignment technique for a Michelson interferometer with a path difference of 250 cm, absorption spectra can be obtained for wavelength regions from 5 cm^{-1} to 50000 cm^{-1}. Unapodized maximum resolution is 0.0026 cm^{-1} in a infrared region. Fourier transformed raman, photoacoustic, and time-resolved infrared spectroscopies are also possible with this interferometric spectrophotometer.

3) **Single Crystal Automatic Four Circle X-ray Diffractometer** (ENRAF-NONIUS CAD 4)
This single crystal diffractometer includes the unique CAD4 kappa cirlce axis X-ray diffraction equipment which enables the wide angle reflection search and high X-ray intensity operation. The measurement temperature covers the range from 350 to 90 K. High pressure measurement is also available.

Associate Professor Iwao Ymazaki moved to Department of Chemical Process Engineering, Faculty of Engineering, Hokkaido University on April 1st, 1988.

Reference

1) *List of Instruments*, No.6, IMS Instrument Center (1986).

Low Temperature Center

The noticeable technical service activities of the center in 1987–1988 are the followings:

1. Dr. Kunio Awaga was appointed a research associate as a new staff member of the center at March, 1988.
2. The amount of liquid helium supplied in 1987 was about 18,000 l with the increase by 3,000 l compared with the last year.
3. The equipments newly installed in 1987 fiscal year are:
   a) Helium liquefier with internal purification system (150 l/h, Model HE-150, KOBE STEEL, LTD.),
   b) Liquid nitrogen storage tank (10,000 l, Model CE-S-10, KOBE STEEL, LTD.),
   c) Helium gas holder (50 m^3, Model GH-50, KOBE STEEL, LTD.),
   d) Mass spectrometer (Model MS-18AB, Veeco Instruments Inc.).
4. New service activities started in 1987 and 1988 are:

a) The new billing-system for liquid nitrogen users by the unit of each research group (from Dec. in 1987),
b) The automated liquid helium supplying system (from the April in 1988),
c) Opening of the stock-room service in the center (from the April in 1988).

Equipment Development Center

A number of research instruments have been designed and constructed by making use of the mechanical, electric and glass-blowing technologies at this Facility. Representative instruments developed during this fiscal year of 1987 are listed below.

Preparation Chambers of Small Particles
1: Spattering Type.
2: Jet-Flow Type.

- VUV Heat Pipe Oven.
- Optical Chamber for Afterglow and Laser-Induced Fluorescence.
- Electrostatic Ion Lens System for a Tandem Mass Spectrometer.
- Driving System of a Post-Mirror in UVSOR BL3B.
- Specific Heat Apparatus.
- Double Resonance MPI Cell.
- Temperature-Variable Pulsed Supersonic Free Jet Nozzle.
- Fine-Tunable 2nd Harmonic Generator.
- Xe Gas Cell for Higher Order Harmonic Generation.
- Time-Delay Threshold-Electron Analyzer.
- Molecular Beam Valve Controller.
- High Voltage Pulse Generator.
- Pockels Cell Driver.
- Floating Pulse Generator.
- 30-Channel floating power supply.
- 3-Channel Peak holder & A/D Converter circuit.
- Automated Liquid Helium Supply System.
- Correction System of the UVSOR Undulator & Wiggler.
- Vidal-Type Hg Vapor Cell.
- Quartz Cells for X-Ray diffraction.
- Discharge flow line.

Ultraviolet Synchrotron Orbital Radiation Facility

The UVSOR light source is usually operated at an electron energy of 750 MeV with an initial current of 100 mA. Single bunch operation has been performed with a frequency of 1 week per 2 months. Two beam lines have been opened to users. They are BL2B1 equipped with a 2 m Grasshopper monochromator and BL3A2 equipped with a 2.2 m constant-deviation grazing-incidence monochromator. The Activity Report 1987 has been published in this April.

SPECIAL RESEARCH PROJECTS

IMS has special research projects supported by national funds. Three projects presently in progress are:

(1) Development and evaluation of molecular synergistic systems and their application to chemical energy conversion (1985–1990).

(2) Fundamental research of molecular devices (1985–1990).

(3) Molecular science of primordial chemical evolution and selforganization (1987–1991).

These projects are being carried out with close collaboration between research divisions and facilities. Collaborators from outside also make important contributions. Research fellows join these projects. The results in 1987 are reviewed in this report.

(1) Development and Evaluation of Molecular Synergistic Systems and their Application to Chemical Energy Conversion

Dynamical Molecular Structure and Control of Reactive Molecules

Eizi HIROTA*, Chikashi YAMADA, Yasuki ENDO, Kentarou KAWAGUCHI, Hideto KANAMORI, Masatoshi KAJITA, Masaharu FUJITAKE, Haruhiko ITO, Eberhard TIEMANN *(Univ. Hannover and IMS)*, **and Sean C. O'BRIEN** *(Rice Univ. and IMS)*.

Infrared diode laser kinetic spectroscopy combined with excimer laser photolysis has been applied to the acetylene and acetylene-d_2 photolysis at 193 nm (II-A-3, II-A-12, II-A-13, II-A-15), to the 248 nm photolysis of methyl iodide (II-A-9), and also to the photolysis of either diacetylene or allene to generate C_3 (II-A-16). A similar technique has been employed to clarify the photodecomposition process of phenylsilane (II-A-17, II-A-20), Cl_2SO (II-A-21), and S_2Cl_2/SCl_2 (II-A-22).

In order to understand photochemical reactions unique to organosilicon compounds, attention has been focused on important intermediates in these processes, namely silylenes. Two halogen derivatives have so far been investigated in detail (II-A-4, II-A-5, II-A-11).

Laser Spectroscopic Studies of Highly Excited Atoms and Molecules in the Vacuum Ultraviolet Region

Norio MORITA and Toshifumi SUZUKI

For the purpose of studying the electron correlation effect of high-lying doubly excited states of atoms, those states of Ca atoms have been investigated with three-step four-photon excitation by pulsed dye lasers (II-D-1, 2, and 3). We have so far observed more than 100 of doubly excited *mlns* states (m=6 to 10 for l=s and m=5 to 9 for l=d; $m \leq n \leq 20$), which lie in the extreme vacuum ultraviolet region (700–1000Å) from the ground state. In particular, we have successfully observed some $m \approx n$ states, for the first time, which have been theoretically expected to have the strongest correlation effect but have never been observed with laser spectroscopic methods. In addition, remarkable splitting and narrowing of the resonance lines have been seen, and they have been analyzed and attributed to interferences among direct and indirect autoionization paths through some other autoionizing Rydberg states. A dependence of the outer electron's quantum defect on the inner electron's state has also been obtained and analyzed. The behavior of the $m \approx n$ states is quite complicated and the analysis of those states is in progress.

We have also been preparing a very narrow band coherent vacuum ultraviolet light source for the purpose of studying highly excited states of molecules with high spectral resolution (II-E).

Laboratory EXAFS System

Kazuyuki TOHJI, Takanori MIZUSHIMA, and Yasuo UDAGAWA

In the past years a continued effort was made to construct laboratory EXAFS system and the system is now almost in completion. The system consists of two spectrometers; a single crystal monochromator for low energy region (<15 keV) and a double crystal monochromator for high energy region (>15 keV). The characteristics of the former has already been described in ref. 1, and the latter, whose schematic picture is shown in Figure 1, is also reported in ref. 2. Now it is possible to obtain EXAFS spectra of materials whose K absorption edge lie between 5 keV to 25 keV, that is, from Cr to Ag. By the use of L absorption, subject materials can be extended to rare earth metals and heavier elements.

It takes from few hours to a day to obtain one spectrum and immediately after the measurement the analysis by Fourier transform and least squares fits can be done by the use of the softwares developed by this group. The system is now routinely used for the structural study of supported catalysts, glasses and other amorphous materials. Some of the applications of this system can be found in II-G of this volume and the previous Annual Reviews.

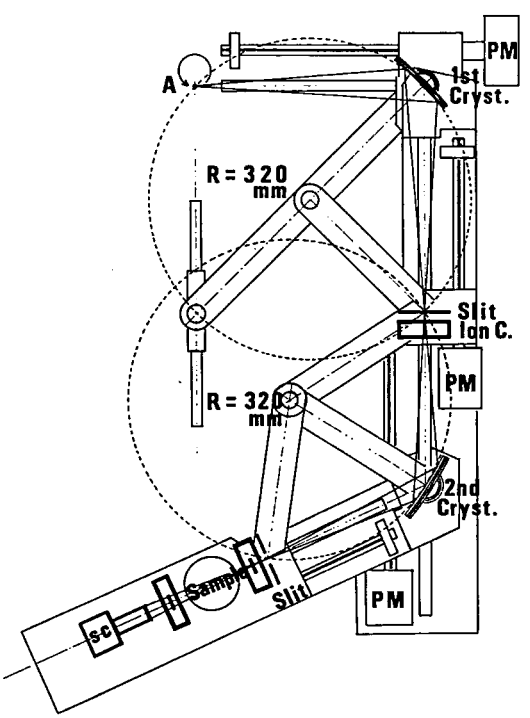

Figure 1. A schematic diagram of the double crystal EXAFS monochromator. A: rotating anode x-ray generator; I: ionization chamber for I_0 detection; Ion C: ionization chamber for the alignment of the first monochromator; SC: scintillation counter or solid state detector; PM: pulse motor. Dots represents two Rowland cirlces.

References

1) K. Tohji, Y. Udagawa, T. Kawasaki, and K. Masuda, *Rev. Sci. Instrum.* **54**, 1482 (1983).
2) K. Tohji, Y. Udagawa, T. Kawasaki, and K. Mieno, *Rev. Sci. Instrum.* **59**, 1127 (1988).

Construction of a Femtosecond Laser Spectroscopy System for the Research of Ultrafast Molecular Processes

Hiromi OKAMOTO, Yoshihiro TAKAGI and Keitaro YOSHIHARA

Recent development in laser technique enables us to obtain coherent light pulses in the femtosecond time domain. The time scale corresponds to the period of a molecular vibration (100 fs = 333 cm^{-1}, for example). Vibrational relaxation processes therefore occurs in a time scale longer than that. We are constructing a femtosecond laser spectroscopy system for the research of vibrational relaxation. The second harmonic of a home-made CW mode-locked Nd:YAG laser (wavelength 532 nm, average power >1 W, pulse width 70 ps, repetition rate 83 MHz) excites two dye lasers. We adopt a linear-cavity hybridly mode-locked dye laser, which produces frequency tunable ultrashort pulses without an extra-cavity dispersion-compensation element.[1] In the present stage the pulse width of less than 0.5 ps is achieved. Another synchronously pumped dye laser which oscillates at a longer wavelength is excited at the same time. The pulse width of the second dye laser is elongated to about 15 ps by inserting an etalon. Several devices are developed to stabilize the laser output energy and pulse width. The detection system (time-resolved CARS or CSRS) using these two dye lasers is now under construction.

Reference

1) M.D. Dawson, T.F. Boggess, D.W. Garvey and A.L. Smirl, *Opt. Commun.*, **60**, 79 (1986).

Photoinduced Electron Transfer on Semiconductor Surfaces

Kazuhito HASHIMOTO, Masahiro HIRAMOTO, Masashi AZUMA and Tadayoshi SAKATA

The electon transfer (ET) on the solid surfaces is essentially important as an elemental process in various fields such as electrochemistry, catalysis and photography. In order to understand the dynamical aspects of ET on the semiconductor surfaces, we have measured transient photovoltage and time resolved luminescence spectra for photoexcited semiconductors and dye sensitized semiconductors.

In the investigation of the dynamical ET processes in the dye sensitized semiconductor system, we have found a new type of energy gap dependence of ET rate: The ET rate increases monotonically with increasing the energy gap. This energy gap dependence is quite different from that for ET between molecules, where an inverted region is observed. This anomolous behavior is found to be explained well by ET from the excited dye to the conduction band of the semiconductors. We propose a new model of ET on semiconductor surfaces. This theory predicts the existence of temperature independent electron transfer. Experimentally such temperature independent ET processes were discovered in several systems such as TiO_2/RhB and ZrO_2/RhB. On the other hand, in the cases of Ru complexes on semiconductors, ET process with a very small activation energy was observed. A simple model in which temperature dependence of the exchange energy is a new origin of the activation energy is proposed. Related studies are reported in III-E.

External Magnetic Field Effects upon Chemical Reactions

Haruo ABE *(Inst. of Phys. and Chem. Res. and IMS)*, **Ryoichi NAKAGAKI, Minoru SUMITANI, and Saburo NAGAKURA**

In the present research project, we have studied magnetic field effects on photoredox reactions involving biradical reaction intermediates for a series of bichromophoric chain molecules. The relative yield between the escape and cage products, Φ(escape)/Φ(cage) is appreciably changed by an external magnetic field. We have shown that the magnetic field effects have some potential for application, *e.g.* control of reaction yields or selection of reaction pathways.

We have also found a conspicuous magnetic field effects on the emission intensity of NO in the $B^2\Pi_r$ excited state, which is populated through collisions between N and O atoms produced on microwave discharge. The detailed study on reaction mechanism for excited NO formation is currently in progress in our laboratory.

Excited-State Photoelectron Spectroscopy for Studying Photophysical and Photochemical Behaviors of Molecules and van der Waals Complexes

Katsumi KIMURA, Katsuhiko OKUYAMA, and Masahiko TAKAHASHI

Excited-state photoelectron spectroscopy combining a UV/visible pulse laser technique and a supersonic molecular beam technique has been developed in this Institute since 1980 (IMS Annual Review, 1980–87). The method which is often called "MPI photoelectron spectroscopy" has made it possible to study dynamic behavior of excited-state species which include nonradiative electronic states. Photoelectron spectra originating from various molecular excited states have been investigated from photophysical and photochemical points of view. The information deduced from excited-state photoelectron spectra have been found to be unique and important.

In this project, with this technique we have being studying not only single molecules but also van der Waals molecules (or molecular clusters) produced in supersonic jet, and we have demonstrated some typical applications in the following several subjects: (1) ionization selectivity, (2) autoionization, (3) intramolecular vibrational redistribution, (4) photodissociation, and (5) excited states of van der Waals molecules (see IV-E).

Synthesis and Properties of a New Type of Organometallic Compounds Containing Polyoxometalates as a Ligand

Kiyoshi ISOBE, Yoshihito HAYASHI, and Yoshiki OZAWA

Molecular design of mixed metal- and mixed valence-clusters have been carried out with the intention of getting cooperative effects on reactivities, physicochemical properties and catalytic actions which can not be obtained from mono and binuclear complexes. We have recently succeeded in preparing a new type of organometallic oxide clusters $[MCp^*MoO_4]_4$ and $[(MCp^*)_4V_6O_{19}]$ (M=Rh, Ir, $Cp^*=C_5Me_5$). The former has a triple cubane-type framework which is smilar to the fragment structure of MoO_3 and the later has a quadruple cubane-type framework containing V_6O_{19} cage which is the first hexavanadate. These clusters show multi-electron transfer in solution and catalysis for the oxidation of hydrocarbons.

We are now trying to elucidate the relationship between the structure of cluster and the following factors; charges of the organometallic group and the oxometalate, steric factors of the organometallic group, and the number of the available coordination site on the organometallic group.

Synthesis of Highly Functional Transition Metal Complexes and Their Use in Catalytic Reactions

Hidemasa TAKAYA*, Tetsuo OHTA and Kazushi MASHIMA

We have prepared mononuclear chiral Ru(II) complexes bearing axially dissymmetric (*R*)- or (*S*)-2,2′-bis(diphenylphosphino)-1,1′-binaphthyl [(*R*)- or (*S*)-BINAP] and its derivatives and showed that these complexes are highly efficient catalysts for asymmetric hydrogenation of a variety of substrates such as enamides, α-acylaminoacrylic acids, alkyl- and aryl-substituted acrylic acids, allylic and homoallylic alcohols, α-amino ketones, *etc.* This time, we synthesized new cationic complexes, [RuX(binap)(arene)]X in pure forms and in high yields, and elucidated their molecular structures by single crystal *X*-ray analysis. We found that these complexes are also excellent catalysts for above described substrates. Extensive studies on the mechanism of asymmetric hydrogenation catalyzed by BINAP–Ru(II) complexes have also been carried out. Parts of these results are presented in the Section VII-B.

Molecular Beam Study of Dynamics of Molecule-Molecule Reactions

Kosuke SHOBATAKE, Kiyohiko TABAYASHI, and Ye WEN

Dynamics of chemical reactions involving atoms or radicals has been studied very extensively for the last 25 years. In contrast dynamics of molecule-molecule reactions has not been interogated as extensively as atom-molecule reactions. In the present project we seek to clarify the dynamics of molecule-molecule reactions from the viewpoint of molecular interactions on van der Waals potential surfaces.

The reaction of F_2 with C_6D_6 has been studied on a Molecular Beam Chemistry Apparatus-I (MBC-I) using a crossed molecular beam technique. During the past year we have measured the angular and TOF velocity distributions of the C_6D_6F product molecules and the product contour diagrams have been obtained (see IV-H-1). An excimer laser was purchased for the study of electronically excited molecule-molecule reactions.

(2) Fundamental Research of Molecular Devices

Resonance Raman Study on Vectorial Proton Transfer by Bacteriorhodopsin

Teizo KITAGAWA

Bacteriorhodopsin (bR) is a retinoid-containing protein found in the purple membrane of a light-harvesting bacterium, *H. halobium*. This protein transforms light energy into electrochemical energy by transporting protons across the membrane. The proton transfer is vectorial. Light-adapted bR_{570} has all-trans retinal bound to Lys-216 via a protonated Schiff base and upon absorbing light it undergoes a cyclic reaction involving the trans to cis isomerization at $C_{13}=C_{14}$ bond, followed by deprotonation of the Schiff base; $bR_{570} \rightarrow K_{590} \rightarrow L_{550} \rightarrow M_{412} \rightarrow N \rightarrow O_{640} \rightarrow bR_{570}$. Ejection of protons from the membrane to the outside takes place at a rate comparable to that for the formation of M_{412} and the uptake of protons occurs in the decaying process of M_{412}. In order to elucidate the pumping mechanism of protons, we have investigated transient resonance Raman spectra of L_{550} and M_{412} in a time range of 15 to 1200 μsec by using a double-beam flow apparatus. We noticed the presence of a very fast decaying M_{412} at alkaline pH, in addition to the reported msec decaying component. This species with a decay constant of 0.39 msec did not give the N intermediate, although the other M_{412} is believed to give the N intermediate. The efficiency for the practical photoreaction appeared 1.6 times higher at pH 10.5 than at pH 7.0 and the increment was ascribable to generation of the very fast M_{412}. Details are described in II-F-5 and II-F-6.

Fabrication of Novel Organic Molecular Assemblies with the Use of the Molecular Beam Epitaxy Technique

Yusei MARUYAMA, Hajime HOSHI, Anthony John DANN *(Univ. of Nottingham and IMS)*, and Tamotsu INABE

In order to prepare new materials which could be useful for molecular devices elements, we have started to design and fabricate ultra-thin organic multi-layered systems. After the trial for TCNQ and TTF-TCNQ films, we are now preparing ultra-thin μ-bridged (-F-) metallo (Al) phthalocyanine polymer mono-films on several kinds of substrate. Fairly well oriented crystalline films are obtainable on the alkali halide substrates. Based on this kind of mono-film, we are going to fabricate a multi-layered system.

Besides the conventional MBE evaporation, highly-regulated deposition with the use of a high power laser and high electric field will be challenged to fabricate more highly-oriented thin films.

Coupled Proton and Electron Transfer in the Crystals of Salicylideneaniline Derivatives and their Complexes

Tamotsu INABE, Naomi HOSHINO *(Hokkaido Univ.)*, Hiroshi OKAMOTO, Tadaoki MITANI, and Yusei MARUYAMA

Our interest in this particular area of research on molecular devices lies in the possibility of furnishing molecular assemblies with novel physical properties through an appropriate modification of the costituent molecules. Proton-transfer process was chosen as the molecule-based function, and its coupling to the assembly-based properties has been investigated. A framework of salicylideneanilines has such a function of intramolecular proton transfer. The thermochromic behavior observed in many of the derivatives gives a clue for changes in the π-electron state accompanying the proton transfer. Thus, the work has been devoted to the crystal structure determination at varied temperature and elucidation of possible cooperation in proton- and electron-transfer processes in the crystals of these compounds by means of optical measurements. Since the assembly-based property is expected to be influenced by a stronger intermolecular interaction, some derivatives are employed as a donor component of charge-transfer complexes with various acceptors. Details of the work are given in Section IV-O.

High Temperature Oxide Superconductors

Masatoshi SATO, Masashige ONODA, Masafumi SERA, Shin-ichi SHAMOTO, Kenji FUKUDA, Shinji KONDOH and Yoshiyasu ANDO

Based on our experimental results taken at the very beginning of the study on high-T_c oxides, we had an idea that the BCS's mean field theory would still be valid to describe the high temperature superconductivity and it seemed to be quite tough task to get the key information to extract the essential distinction of the properties between usual superconductors and the high-T_c oxides. Therefore, continuous effort has been made to accumulate various kinds of experimental results on the detailed properties of the high-T_c oxides by applying various experimental methods such as transport, thermal, magnetic and optical measurements and neutron scattering. Large single crystals were prepared and used in these experiments as well as sintered specimens. We have also made much effort to search for new oxide superconductors to see what kinds of oxides exhibit high-T_c superconductivity, where we have discovered the high-T_c superconductivity in Tl-Ba-Cu-O first. No distinction can be made between our usual activities and the special research project. Therefore please refer Research Activities IV-U.

Research of Cooperative Phenomena of Electron and Proton Transfer in Charge-Transfer Crystals

Tadaoki MITANI and Hiroshi OKAMOTO

The nature of the hydrogen bonding (H-bonding) is sensitively altered by changing the charge distribution in the surrounding molecular system. It is particularly interesting that there is always a finite probability of the quantum-mechanical proton-transfer between the H-bonding double-well potential, i.e. proton tunneling. Thus, it is possible to design a new molecular function based on the proton tunneling in the H-bonded charge-transfer (CT) complexes by controlling the degree of the electron-transfer by chemical modification or by external perturbations.

By recent study of a most typical H-bonded CT complex, quinhydrone crystal, a new phase transition was discovered by an application of hydrostatic pressure. From optical and vibrational spectroscopies, it was found that the proton transfer is cooperative with the electron transfer through the CT interaction and the proton tunneling plays an essential role in the dynamic properties of the phase transition. Near the phase transition, the presence of new types of the elementary electronic excitation has been confirmed; the first is the proton-linked super-CT transition enhanced by increase of the proton tunneling, and the second is due to the formation of topological defects associated with the phase mismatching of the proton transfer. These low-energy excitations in the CT complexes imply a unique possibility for generation of a new type of organic condutor. For the advanced study of the H-bonded CT complexes, new derivatives of naphthoquinhydrone complex have been synthesized, whose electric and optical properties are now in investigation.

Study of Ultrafine Particles

Keisaku KIMURA

Small particles are produced by the gas evaporation method and dispersed in organic liquids. The ratio of the number of atoms at surface to the total atoms in nm particles exceeds 50 % resulting in the enhanced surface effects. We have observed that the relaxation time of the ESR of Zn particles depends on the size of particles and can be related to the phonon cut off frequency of the particles. We have observed for the first time the zero-dimensional magnetism in the Mg small particles via the magnetic susceptibility measurement. The Pauli paramagnetism of small Mg particles gradually decreased with decreasing temperature suggesting the deviation of metallicity of the particles at low temperature.

(3) Molecular Science of Primordial Chemical Evolution

Study of Polymerization Reactions in Aqueous Environment: [1] Formaldehyde and Hydrazine; a preliminary report

Nobuyuki NISHI and Kazunori YAMAMOTO

Formaldehyde is one of popular interstellar molecules, that condenses producing white polymers on low temperature solid surface. This polymer, however, is dissoluble in hot water at temperatures higher than 80°C. Mass spectrometric analysis of this solution showed that the solute takes two forms: methylene diol ($H_2C(OH)_2$) and free aldehyde (H_2CO). These species are in equilibrium. Hydrazine (N_2H_4) is a photoproduct in solid ammonia photochemistry at low temperatures and expected to exist in interstellar icy dusts. A drop of hydrazine was added in the aldehyde solution (100 ml with 2% solute). Then the mixture was immediately analyzed mass-spectrometrically by the direct conversion of the solution to cluster beams. After 30 minutes, it changed to milky solution that contained fine particles. The solution was injected into vacuum and the hydrate clusters of the products were dehydrated by the collision with argon gas. Then the product beams were analyzed by a mass spectrometer at an ionization energy of 12 eV. The primary products were $H_2C{=}N{-}N{=}CH_2$ ($H_4C_2N_2$) and its dimer ($H_8C_4N_4$). Each of them produced addition compounds with formaldehyde such as $(H_4C_2N_2)_m(H_2CO)_n(H_2O)_l$, where l=0 or 1 and the ratio of m to n was dependent on the concentration of hydrazine. Although the structure of the products is not known yet, it is found that formaldehyde polymers are converted to nitrogen-containing new polymers ($H_{4m+2(n+1)}C_{2(m+n)}N_{2m}O_{n+1}$). Acid hydrolysis of this compound may produce various amino acids.

OKAZAKI CONFERENCES

"Okazaki Conferences" are principal symposia at IMS, which are held on the subjects related to the "Special Research Projects". They are held two or three times a year, with a moderate number of participants around 50, including several invited foreign speakers. The formal language for the conference is English. Outlines of the thirtieth to thirty-first conferences are as follows.

The Thirtieth Okazaki Conference

Electron Dynamics in Chemical Processes
(October 28–30, 1987)

Organizers: J. TANAKA *(Nagoya Univ.)* **and K. YOSHIHARA** *(IMS)*
Invited Speakers: R.A. MARCUS *(Calif. Inst. Tech.)*, **S. NAGAKURA** *(Okazaki National Res. Insts.)*, **P.G. WOLYNES** *(Univ. Ill. and IMS)*, **J.R. MILLER** *(Argonne National Lab.)*, **G.W. ROBINSON** *(Texas Tech. Univ.)*, **A.J. HOFF** *(Univ. Leiden)*, **and S.R. OVSHINSKY** *(Energy Conversion Devices)*.

The topic of the conference was the role of electron in fundamental chemical processes. Charge-transfer interaction, electron transfer, charge-resonance interaction, and spin-spin interaction were discussed in relation to chemical reaction dynamics, excited-state chemistry, solvation dynamics, magnetic chemistry, photosynthesis, enzymatic reactions, and super conductivity. The number of presentations, including two plenary lectures and five invited talks, was 22; about 100 scientists participated.

The Thirty-first Okazaki Conference

Ionization Processes of Gas-Phase Clusters
(Feb. 10–12, 1988)

Organizers: K. KUCHITSU *(Univ. Tokyo)*, **T. KONDOW** *(Univ. Tokyo)*, **E. HIROTA** *(IMS)*, **and N. NISHI** *(IMS)*
Invited Speakers: E. RECKNAGEL *(Univ. Konstanz)*, **A.W. CASTLEMAN, Jr.** *(Pennsylvania State Univ.)*, **H. HABERLAND** *(Univ. Freiburg)*, **K.D. JORDAN** *(Univ. Pittsburg)*, **W.C. LINEBURGER** *(Univ. Colorado)*, **and L. WÖSTE** *(Ecole Polytech., Lausanne)*

Cluster science is an interdisciplinary field of active research in physics and chemistry. The conference was organized to provide insight into the two questions: "How static and dynamic properties of clusters are related to constituent molecule(s)," and "What is the cluster response to interaction with photons and electrons". All 16 oral and 16 poster presentations were quite actively discussed by the participants with the six guests from overseas. The main subjects were: (1) Structure and dynamics of atomic (metal and nonmetal) clusters, (2) Attachment of low energy electrons to clusters, (3) Structure and reactivity of molecular clusters, (4) Spectroscopy and photochemistry of molecular complexes, and (5) Photoionization of clusters and photodissociation of cluster ions.

JOINT STUDIES PROGRAMS

As one of the important functions of an inter-university research institution, IMS undertakes joint studies programs for which funds are available to cover research expenses as well as travel and living expenses of individuals. The proposals from domestic scientists are reviewed and controlled by the inter-university committee. The programs are carried out under one of five categories:

1) Joint Studies on special projects (a special project of significant relevance to the advancement of molecular science can be carried out by a team of several groups of scientists).
2) Research Symposia (on timely topics in collaboration with both outside and IMS scientists).
3) Cooperative Research (carried out in collaboration with both outside and IMS scientists).
4) Use of Facility (the Computer Center, Instrument Center and other research facilities at IMS are open to all researchers throughout the country).
5) Joint studies programs using UVSOR facilities.
   a) Special Project, b) Cooperative Research, c) Use of UVSOR Facility.

In the fiscal year 1987, numbers of joint studies programs accepted amounted to 4, 10, 145 and 239 for categories 1)–4), respectively and 5, 19 and 75 for 5a)–5c), respectively.

1) Special Projects

Studies of Elementary Chemical Reaction Processes by Development of New Spectroscopic Methods

Coordinators: **Soji TSUCHIYA** *(Univ. Tokyo)*, **Seiichiro KODA** *(Univ. Tokyo)*, **Okitsugu KAJIMOTO** *(Univ. Tokyo)*, **Yasuki ENDO** *(Univ. Tokyo and IMS)*, **Kaoru YAMANOUCHI** *(Univ. Tokyo)*, **Hiroki NAKAMURA, and Eizi HIROTA**

The present research project aims at clarifying basic aspects of chemical reactions such as how the intermolecular forces affect reactions, how activation energy is distributed over the freedom of motions of activated complexes, and how the potential energy surface is related to the distributions of products over quantum states. It will start with setting up a tunable vacuum UV source in wavelength region shorter than 200 nm, which will allow us to unveil hitherto unknown dynamical behaviors of atoms and molecules. As an example of elementary reactions, the role of O atoms will be explored. An attempt will be made to select one of the three spin sublevels J=0,1, and 2 of O in the ground ^3P_J state and to examine their differences in reactions, if any. Another important example of reactions involving O, O+C_2H_4 and O+C_2D_4, will also be investigated in detail. Finally high resolution spectroscopic techniques will be extended to vacuum UV region to study various dynamical processes of fundamental importance.

Molecular Mechanism of the Electron and Proton Transfers by Proteins and Their Coupling

Teizo KITAGAWA and Takashi OGURA *(Department of Molecular Dynamics)*, **Akio MAEDA** *(Kyoto University)*, **Nobuhito SONE** *(Jichi Medical School)*, **Yutaka ORII** *(Kyoto University)*, **Kohki OHNO** *(Jichi Medical School)*, **Hideo AKUTSU** *(Yokohama National University)*, **Shin'ya YOSHIKAWA** *(Himeji Institute of Technology)*, **and Masamitsu FUTAI** *(Osaka University)*

The vectoral proton translocation across the energy transducing membrane against the concentration gradient is known to be essential to produce biological energy, but its molecular mechamism remains to be explored. This project aims to elucidate a mechanism of the proton translocation by proteins for three representative cases; 1) the light-driven proton pump, 2) the electron-driven proton pump, 3) a passive proton translocation. The first system is seen in light-harvesting bacteria and we selected bacteriorhodopsin which involves cis-trans isomerization of the retinal Schiff base and the subsequent deprotonation of the Schiff base. Drs. Maeda, Ogura and Ohno are involved

in this subject and our group at IMS has observed transient resonance Raman spectra by using the pump-probe flow-cell apparatus. The second system is seen in the respiratory chain of aerobic organisms, and out of three pumping sites we have picked up Site III, where cytochrome *c* oxidase pumps protons when electrons are transferred from cytochromes *c* to molecular oxygen. The Raman group at IMS and Dr. Yoshikawa have explored transient states for reduction of dioxygen by constructing a device for measuring Raman and absorption spectra simultaneously and an artificial cardiovascular system which enables us to regenerate the enzyme during the sample circulation through the cell and thus to accumulate the data for a long time with a small amount of sample. The timing of the proton ejection induced by the electron transfer will be determined with the time-resolved fluorescence spectra and a pH indicating fluoro-dye. Drs. Ogura, Sone, and Orii are involved in this project. The electron transfer through proteins is investigated with a multiheme cytochrome *c*, that is, cytochrome c_3. Drs. Akutsu and Kitagawa have been studying it with NMR and resonance Raman techniques, respectively. The third system intends to study a molecular mechanisms of the H^+ ATPase, which catalyzes the formation of ATP from ADP and P_i upon passive proton translocation. Drs. Futai, Sone and Ohno are involved in this project.

2) Research Symposia

1. Design of Organic Molecular Assemblies and Control of Their Properties
   (January 28th – 30th, 1988)
   Organizer: T. Mitani (IMS)
2. Dynamical Behavior of Photochemical Reactions
   (February 1st – 2nd, 1988)
   Organizer: K. Obi (Tokyo Inst. of Tech.)
3. Electric Structure Theory and Applications
   (February 24th – 25th, 1988)
   Organizer: K. Morokuma
4. MPI Spectroscopy
   (March 15th – 16th, 1988)
   Organizer: K. Kimura (IMS)
5. Mini-Symposium with Professor J.N. Murrell
   (March 17th – 18th, 1988)
   Organizer: K. Morokuma (IMS)
6. Organo-Transition Metal Complexes: Highly Selective Reagents and Catalysts
   (March 22nd – 23rd, 1988)
   Organizer: H. Takaya (IMS)
7. Structures, Reactivities and Properties of Metalloporphyrins with Unusual Electronic States
   (March 25th – 26th, 1988)
   Organizer: T. Kitagawa
8. New Techniques of Laser Raman Spectroscopy
   (May 9th – 10th, 1988)
   Organizer: M. Kobayashi (Osaka Univ.)
9. The Third Japan-Korea Joint Symposium on Molecular Science
   (June 7th – 9th, 1988)
   Organizer: I. Hanazaki (IMS)
10. Control of Coordination Environment and Appearance of Cooperative Effect
    (July 2nd – 3rd, 1988)
    Organizer: T. Yamamura (Science Univ. of Tokyo)

3) Cooperative Research

This is one of the most important programs IMS undertakes for conducting its own research of the common interest to both outside and IMS scientists by using the facilities at IMS. During the first half of fiscal year of 1987 ending on September 30, 72 outside scientists including 4 invited collaborated with IMS scientists; and during the second half of the fiscal year, 73 outside scientists including 4 invited worked in collaboration with IMS scientists, the names and the affiliations of these collaborators are found in the Research Activities.

4) Use of Facility

The number of projects accepted for the Use of Facility Program of the Computer Center during the fiscal year of 1987 amounted to 146 (494 users), and the computer time spent for these projects is 3648 hours (converted to the HITAC M-680 time), and amounts to 52% of the total annual CPU time used.

Sixty eight projects (140 users) were accepted for the Use of Facility Program of the Instrument Center during the fiscal year of 1987.

5) UVSOR

Joint studies programs using UVSOR facilities are carried out under one of three categories: 5-a) UVSOR Special Project, 5-b) UVSOR Cooperative Research, and 5-c) Use of UVSOR Facility.

The 9th UVSOR Research Symposium, organized by K. Kimura (IMS), was held during November 27th – 28th, 1987.

5-a) UVSOR Special Project

Analysis of the Electronic Structures of Molecular Assemblies with Photoelectron Spectroscopy Using Synchrotron Radiation

Coordinators: **Kazuhiko SEKI** *(Hiroshima Univ.)*
Makoto WATANABE *(UVSOR Facility)*

Angle-resolved photoemission system at BL8B2 has become in full operation, owing to the effects of H. Fujimoto. Using this apparatus, electronic structures of various molecular solids have been studied.

In particular, a detailed study was performed on oligothiophenes, which are model compounds of A-linked polythiophene, a typical conducting polymer. Pursuit of the change of the electronic structure from A-linked dimer to octamer showed how electronic structure of a polymer chain evolves. Further, studies of compounds with irregurality (insertion of ethenyl group or B-linkage) clearly demonstrated the effect of such irregularity on the electronic structure. These results are consistent with the electric and optical properties of polymers with similar defects.

The effect of defect on polymer electronic structure was also studied with $(C_{16}H_{33})_2CO$ as a model of defect-containing polyethylene. In this case, the angle-resolved spectra showed that the effect of the defect on the energy-dispersion relation E = E(k) is rather small.

Studies were also carried out on the electronic structures of poly(p-phenylene sulfide), naphthacene, and various quinones.

Far Infrared Spectroscopy under High Pressure Using Synchrotron Radiation

Coordinator: **Takao NANBA** *(Tohoku Univ.)*
Makoto WATANABE *(UVSOR Facility)*

The construction of the transmission measurement system in the far infrared region under high pressure up to 5 GPa using a diamond anvil cell was completed at the beam line BL6A1 of UVSOR. Using the system, the change in the phonon spectrum of KI with the pressure was observed.

It is well known from the X-ray diffraction method that KI shows a phase transition from a NaCl structure (B1) to a cesium chloride one (B2) under the pressure of 1.8 GPa. However, the measurement of the change in the phonon spectrum of alkali halide crystal, which possesses the inversion crystal symmetry, under the pressure has not been reported because of its Raman inactive character. From the measuremet of the shift of the TO phonon energy of KI with the pressure, the mode gruneisen parameter at room temperature was first determined to be 1.66 in the B1 structure and 1.20 in the B2 structure. In the B2 structure the TO phonon energy was also found to be 106 cm^{-1}.

Study of Transient Photo-Induced Phenomena in Organic Crystals

Tadaoki MITANI *(Equipment Development Center)*

The synchrotron radiation (SR) from the UVSOR electron storage-ring is composed of successive pulse trains with a pulse width of 460 ps, whose frequency is 90 MHz in a multi-bunch mode operation. The stable pulse structure of the SR makes it possible to synchronize the SR pulses with a CW mode-locked picosecond Nd:YAG laser. Using the SR as probe light pulses and the laser as excitation light pulses, a new system for photoinduced absorption measurements has been constructed for the first time by using the delay-time modulation technique (see VII-H-1). Taking acconut of a wide spectral region of the SR pulses from the far infrared to the soft X-ray, this system opens a unique possibility of expanding a measurable energy region, which has been limited to the region covered by laser techniques.

Compared with the SR-laser combination systems previously developed[1,2], in which the lasers were operated at a low frequency (30 – 50 Hz) with the pulse

widths of around 10 ns, the specific point of our system is that all the SR pulses are synchronized with the laser pulses at 90 MHz, whose pulse width is 70 ps. Thus, this system is suitable to perform the photoinduced absorption measurements with a short time resolution of ca. 100 ps. By an application of the delay-time modulation technique, it is possible to measure the transient spectra in a time period from 0.05 to 11 ns. Furthermore, a spurious signal due to a thermal change of the sample by a shot of intense laser pulse, which occasionally causes a serious problem in low frequency modulation spectroscopy in solids, might be automatically removed, since it would not follow the high repetition rate of pulses. As an experimental test of the ability of this system, the photoinduced absorption spectra of R6G in an aqueous solution has been successfully made in the visible region. The experiments on organic materials, such as polyacetylene and some CT complexes, are now under investigation in the infrared and UV regions. In parallel, an application of the delay-time modulation technique to a time-resolved photoelectron spectroscopy is undertaken.

Reference

1) V. Saile, *Appl. Opt.*, **19**, 4115 (1980).
2) R. Pizzoferrato et al., *Europhys. Lett.* **2**, 571 (1986).

5-b) UVSOR Cooperative Research

During the first half of fiscal year of 1987, 9 outside scientists including 4 invited collaborated with IMS scientists; and during the second half of the fiscal year, 10 outside scientists including 3 invited worked in collaboration with IMS scientists.

5-c) Use of UVSOR Facility

The number of projects accepted for the Use of UVSOR Facility Program during the fiscal year of 1987 amounted to 75.

FOREIGN SCHOLARS

Visitors from abroad play an important role in research activities and are always welcome at IMS. The following is the list of foreign scientists who visited IMS in the past year (Aug. 1987 – July 1988). The sign *1 indicates an attendant to an Okazaki Conference, *2 an IMS or Japan Society for the Promotion of Science Invited Foreign Scholar (period of stay is from 3 to 6 months), *3 an IMS councillor, *4 an IMS visiting scientist and *5 an IMS adjunct professor or associate professor from abroad (period of stay is from 9 to 12 months). Scientists who wish to visit IMS under programs 2 and 5 are invited to make contact with an IMS faculty in a related field.

Prof. J. Dou-Man	Inst. Chem., Acad. Sin. Henan	(China)	Aug. 1987
Prof. H. Ishida	Cape Western Reserve Univ.	(USA)	Aug. 1987
Prof. E.W.J. Mitchel	Sci. Eng. Res. Council	(UK)	Aug. 1987
Prof. T. Yonetani	Univ. of Pennsylvania	(USA)	Aug. 1987
Dr. E. Anni	Univ. of Pennsylvania	(USA)	Aug. 1987
Prof. H.C. Wolf	Univ. of Stuttgart	(FRG)	Aug. – Sep. 1987
Xie Ying	Fudan Univ.	(China)	Aug. – Dec. 1987
Prof. S.-J. Zheng*4	Dep. Chem., Hebei Teachers' Coll.	(China)	Sep. – Dec. 1987
Mr. H. Senhorst	Dep. Phys. Eingdhoven Univ. Tech.	(Netherlands)	Sep. 1987
Prof. Y. Liu	Tsinghua Univ.	(Taiwan)	Sep. 1987
R.R. Arunt		(South Africa)	Sep. 1987
Dr. A. Dorigo	Dep. Chem., Univ. of California, Los Angeles	(USA)	Sep. 1987 Feb. 1988 – Jul. 1989
Dr. A.J. Rest	Univ. of Southampton	(UK)	Sep. 1987
Prof. V. Helbig	Inst. Experimentalphys., Univ. Kiel	(FRG)	Sep. 1987
J.C. Hurt	NSF	(USA)	Sep. 1987
Prof. J.G. Snijiders	Vrije Univ.	(Netherlands)	Sep. 1987
Prof. M.O. Delcourt	Lab. Phys.-Chim. Rayonnem., Univ. Paris-Sud	(France)	Sep. 1987
Prof. I. Sutherland	Dep. Org. Chem., Univ. Liverpool	(UK)	Sep. 1987
Prof. N.G. Basov	Lebedev, P.N., Phys. Inst.	(USSR)	Sep. 1987
Prof. H.A. Staab	Max-Planck-Ges.	(FRG)	Sep. 1987 Mar. 1988
Dr. W.H. Diercksen	Max-Planck-Ges.	(FRG)	Sep. 1987
B. Cearlok	Battelle Memorial Inst.	(USA)	Oct. 1987
Prof. H. Hopf*2	Dep. Chem., Univ. of Braunschweig	(FRG)	Oct. 1987
Prof. V.P. Spiridonov	Dep. Chem., Moscow State Univ.	(USSR)	Oct. 1987
Dr. S.R. Meech	Heriot-Watt Univ.	(UK)	Oct. 1987 – Jan. 1989
Prof. S.R. Ovshinsky*1	EDC	(USA)	Oct. 1987
J.R. Miller*1	Argonne Natl. Lab.	(USA)	Oct. 1987
Prof. A.J. Hoff*1	Leiden Univ.	(Netherlands)	Oct. – Nov. 1987
Prof. G.W. Robinson*1	Texas Tech. Univ.	(USA)	Oct. – Nov. 1987

Prof. R.A. Marcus*[1]	California Inst. Technol.	(USA)	Oct. – Nov. 1987
J.T. Hougen*[4]	Natl. Bur. of Stand.	(USA)	Oct. – Nov. 1987
Prof. B. Holmström	Univ. of Göteborg	(Sweden)	Nov. 1987
Mr. K.B. Jensen*[4]	Univ. Odense	(Denmark)	Nov. – Dec. 1987
Prof. J.A. Koningstein	Carlton Univ.	(Canada)	Nov. – Dec. 1987
Dr. S.Y. Lee*[2]	Dep. Chem., Natl. Univ. Singapore	(Singapore)	Nov. 1987
Dr. P. Lagarde	LURE, Univ. Paris-Sud	(France)	Nov. 1987
Prof. M. Almgrem	Uppsala Univ.	(Sweden)	Nov. 1987
Dr. M.D. Newton*[2]	Brookhaven Natl. Lab.	(USA)	Nov. 1987 – Mar. 1988
Prof. L. Zhang*[2]	Inst. Chem., Acad. Sin.	(China)	Nov. 1987 – Nov. 1988
Ms. H. Wang	Inst. Photographic Chemistry	(China)	Nov. 1987 – Mar. 1988
Prof. He Duohui	Univ. of Sci. and Technol. of China	(China)	Nov. 1987
P.R. Herman	Univ. of Toronto	(Canada)	Dec. 1987
Prof. Z.R. Grabowski*[2]	Inst. Phys. Chem., Pol. Acad. Sci.	(Poland)	Dec. 1987 – Mar. 1988
Dr. A. Grabowska	Inst. Phys. Chem., Pol. Acad. Sci.	(Poland)	Dec. 1987 – Mar. 1988
Prof. S.C. Park	Dep. Chem., Kangweon Natl. Univ.	(Korea)	Dec. 1987 – Feb. 1988 Jun. 1988
Prof. R. Lü	Dalian Inst. Chem. Phys. Acad. Sin.	(China)	Dec. 1987
Dr. D. Kim*[2]	Korea Stand. Res. Inst.	(Korea)	Jan. – Mar. 1988 Jun. – Jul. 1988
Dr. E.D. Jemmis	Univ. of Hyderabad	(India)	Jan. 1988
Prof. B.J. Yoon*[4]	Kangreung Natl. Univ.	(Korea)	Jan. – Feb. 1988 Jun. 1988
Prof. H. Kim	Seoul Natl. Univ.	(Korea)	Jan. – Mar. 1988
Ms. B.A. Ruf	Univ. of California	(USA)	Jan. 1988
Prof. D.N.B. Ariffin	Malaysia, Univ. of Agriculture	(Malaysia)	Jan. 1988
Prof. T.S.A.B.A. Wahid	Malaysia, Inst. of Technol.	(Malaysia)	Jan. 1988
Prof. D.A.N.H. Ayob	Univ. of Malaya	(Malaysia)	Jan. 1988
Prof. J. Sukaimi	Malaysia, Natl. Univ.	(Malaysia)	Jan. 1988
Prof. K.J. Ratnam	Malaysia, Univ. of Science	(Malaysia)	Jan. 1988
Dr. M.R. Wasielewski*[2]	Argonne Natl. Lab.	(USA)	Jan. 1988
Dr. D. Luneau*[2]	CNRS, Toulouse	(France)	Jan. 1988 – Jan. 1990
Prof. M. Portara	Univ. of Alabama	(USA)	Jan. 1988
D. Cole	Univ. of Alabama	(USA)	Jan. 1988
Prof. H.-N. Kim	Ajou Univ.	(Korea)	Jan. 1988
Prof. Zhang Chunhao	Dalian Inst. Chem. Phys.	(China)	Jan. 1988
Prof. I. Miyagawa	Univ. of Alabama	(USA)	Jan. 1988 Mar. – Apr. 1988
Prof. J.M. Riveros*[2]	Univ. of São Paulo	(Brazil)	Feb. 1988
Prof. M.A. Bennett	Australian Natl. Univ.	(Australia)	Feb. – May 1988
Prof. G. Black*[5]	SRI Int.	(USA)	Feb. – May 1988
Prof. K.D. Jordan*[1]	Univ. of Pittsburgh	(USA)	Feb. 1988

Prof. W. Lineberger*[1]	Univ. of Colorado	(USA)	Feb. 1988
Prof. L. Wöste*[1]	Ecole Polytech. Fed. Lausanne	(Switzerland)	Feb. 1988
Prof. A.W. Castleman*[1]	Pennsylvania State Univ.	(USA)	Feb. 1988
Prof. E. Recknagel*[1]	Fak. Phys., Univ. Konstanz	(FRG)	Feb. 1988
Prof. H. Haberland*[1]	Fak. Phys., Univ. Freiburg	(FRG)	Feb. 1988
Prof. J.P. Reilly	Univ. of Indiana	(USA)	Feb. 1988
Prof. S. Chung	Pohang Inst. for Sci. and Technol.	(Korea)	Feb. 1988
J.W. Lee	Pohang Inst. for Sci. and Technol.	(Korea)	Feb. 1988
K.H. Nam	Pohang Inst. for Sci. and Technol.	(Korea)	Feb. 1988
Y.M. Koo	Pohang Inst. for Sci. and Technol.	(Korea)	Feb. 1988
Y.S. Kim	Pohang Inst. for Sci. and Technol.	(Korea)	Feb. 1988
S.C. Won	Pohang Inst. for Sci. and Technol.	(Korea)	Feb. 1988
K.B. Lee	Pohang Inst. for Sci. and Technol.	(Korea)	Feb. 1988
Prof. R.K. Mishra	North-Eastern Hill Univ.	(India)	Feb. 1988
Prof. R.G. Parr*[3]	Univ. of North Carolina	(USA)	Feb. 1988
Prof. K. Lu	Inst. Phys., Acad. Sin.	(China)	Feb. – Mar. 1988
Dr. J. Galayda	Brookhaven Natl. Lab.	(USA)	Mar. 1988
Prof. Byung Ha Cho	Korea Adv. Inst. Sci. Tech.	(Korea)	Mar. 1988
Dr. P.M. Martineau	Univ. of Cambridge	(UK)	Mar. – Apr. 1988
Prof. Yadong Hu	Inst. of Chem., Acad. of Sin.	(China)	Mar. 1988
Tong Lijuan	Beijing Inst. of Chemical Engineering	(China)	Mar. – May 1988
J.D. Grote	British Council	(UK)	Mar. 1988
Prof. J.N. Murrell*[2]	Univ. of Sussex	(UK)	Mar. 1988
Prof. P.M. Johnson	State Univ. New York	(USA)	Mar. 1988
Prof. I. Ojima	State Univ. New York	(USA)	Mar. 1988
Prof. Jian-Gao Zhao	Inst. of Phys., Acad. of Sin.	(China)	Mar. 1988
Prof. P. Batail	Univ. Paris-Sud	(France)	Mar. 1988
Prof. D. Jerome	Univ. Paris-Sud	(France)	Mar. 1988
J.H.D. Eland	Oxford Univ.	(UK)	Mar. 1988
Prof. P.N. Skancke	Univ. Tromsö	(Norway)	Mar. – May 1988
B. Bauld	Australian Acad. of Science	(Australia)	Mar. 1988
Dr. T. Amano	NRC	(Canada)	Mar. 1988
Dr. W. Siebrand	Natl. Res. Council	(Canada)	Apr. 1988
P.R. Bunker	Natl. Res. Council	(Canada)	Apr. – Jun. 1988
Prof. K. Siegbahn	Uppsala Univ.	(Sweden)	Apr. 1988
Prof. D. Haarer	Univ. Bayreuth	(FRG)	Apr. 1988
Dr. A. Bakac	Iowa State Univ.	(USA)	Apr. 1988
Dr. A. Aruchamy	Indian Inst. of Tech.	(India)	Apr. 1988
Prof. H.H. Huang	Natl. Univ. Singapore	(Singapore)	Apr. 1988

Prof. D.W. Pratt	Univ. of Pittsburgh	(USA)	Apr. 1988
Prof. D.A. Brown	Dep. Chem., Univ. Coll., Dublin	(Ireland)	Apr. 1988
Prof. H.A. Morrison	Dep. Chem., Purdue Univ.	(USA)	Apr. 1988
Lin He*[4]	General Inst. of Non-Ferrous Metals	(China)	Apr. – Sep. 1988
Dr. S.C. O Brien	Rice Univ.	(USA)	May – Jun. 1988
Prof. B.H. Bransden	Dep. Phys., Univ. of Durham	(UK)	May 1988
Prof. B. Kohler	Univ. of California, Riverside	(USA)	May 1988
Dr. B. Soep	CNRS	(France)	May 1988
Dr. J.E. Butler	Naval Res. Lab.	(USA)	May 1988
Prof. J. Reedijk	Dep. Chem., Leiden Univ.	(Netherlands)	May – Jun. 1988
Prof. J. Lee	Seoul Natl. Univ.	(Korea)	Jun. 1988
Prof. S.C. Shim	Korea Adv. Inst. Sci. Tech.	(Korea)	Jun. 1988
Prof. U.R. Kim	Keimyung Univ.	(Korea)	Jun. 1988
Prof. D.J. Lee	Natl. Fisheries Univ. Pusan	(Korea)	Jun. 1988
Prof. Y.S. Lee	Korea Adv. Inst. Sci. Tech.	(Korea)	Jun. 1988
Prof. Y.K. Kang	Chungbuk Natl. Univ.	(Korea)	Jun. 1988
Prof. Y.S. Kong*[2]	Jeon-Buk Natl. Univ.	(Korea)	Jun. 1988 Jul. 1988 – Mar. 1989
Prof. J.-J. Kim	Korea Adv. Inst. Sci. Tech.	(Korea)	Jun. 1988
Prof. K.H. Kim	Yonsei Univ.	(Korea)	Jun. 1988
Prof. H. Sun	Pusan Natl. Univ.	(Korea)	Jun. 1988 Aug. 1988
Prof. M.S. Jhon	Korea Adv. Inst. Sci. Tech.	(Korea)	Jun. 1988
Prof. H. Pak	Seoul Natl. Univ.	(Korea)	Jun. 1988
Prof. M. Boudart	Stanford Univ.	(USA)	Jun. 1988
Prof. F. Siebert	Albert-Ludwigs Univ.	(FRG)	Jun. 1988
Dr. P.K. Mukherjee*[2]	Dep. of Spectroscopy, Indian Assoc. for the Cultivation	(India)	Jun. 1988
Prof. B.Y. Lee	Gyeongsang Univ.	(Korea)	Jun. – Aug. 1988
R.B. Pansu	CNRS	(France)	Jul. 1988 – Aug. 1989
Prof. Y.-T. Chen	Inst. of Coordination Chemistry, Nankai Univ.	(China)	Jul. 1988
Prof. E. Tiemann*[4]	Univ. Hannover	(FRG)	Jul. 1988
Dr. M.R. Fahy*[2]	Univ. of Nottingham	(UK)	Jul. 1988 – Jul. 1989
Dr. Cuiji Zhang	Inst. Chem., Acad. Sin.	(China)	Jul. 1988
Prof. H. Port	Univ. of Stuttgart	(FRG)	Jul. 1988
Prof. R. Tipping*[4]	Univ. of Alabama	(USA)	Jul. – Aug. 1988
Prof. B.J. Orr	Macquarie Univ.	(Australia)	Jul. 1988
Prof. A. Piskarskas	Vilnius Univ.	(USSR)	Jul. 1988
Dr. D. Miller	Skrips Inst.	(USA)	Jul. 1988
Prof. G.R. Fleming	Univ. of Chicago	(USA)	Jul. 1988
Prof. T. Gillbro	Umea Univ.	(Sweden)	Jul. 1988
Dr. A.R. Holtzwarth	Max-Planck-Institute fur Strahlenchemie	(FRG)	Jul. 1988
Prof. D.J. Nesbitt	Univ. of Colorado	(USA)	Jul. 1988

Prof. Q.-Z. Qin	Fudan Univ.	(China)	Jul. 1988
Dr. M.M. Martin	CNRS	(France)	Jul. 1988
Prof. Sa Guohe	Dalian Inst. Chem. Phys.	(China)	Jul. 1988
Dr. P.J. Knowles	Univ. of Cambridge	(UK)	Jul. – Aug. 1988
Dr. C.B. Dane	Rice Univ.	(USA)	Jul. 1988
Dr. R. Blake	Battelle Memorial Inst.	(USA)	Jul. 1988

AWARD

Prof. Kitagawa's Scientific Achievement

Prof. Teizo Kitagawa received the Divisional (Interdiciplinary Chemistry) Award of the Chemical Society of Japan in 1988 for his contribution to "Resonance Raman study of microstructure of active sites in hemoproteins".

Since his graduation from Osaka University, Prof. Kitagawa continued his effort for the structural study by vibrational spectroscopy, especially for the study of active sites of biologically important molecules. First at Protein Research Institute and then at Medical School of Osaka University, he applied the resonance Raman effect for the study of biomolecules and established basic concepts about how to make use of resonance Raman sepctroscopy for the study of environmental change around iron and other atoms in protein. Consequenctly he moved to IMS in 1983 and here he extended excitation wavelength to uv region in order to study the structure of aminoacid residues. He also started time resolved Raman spectroscopy by using pulsed lasers or by combining cw laser with flow cell which was developed by his group.

Among various kinds of studies the following 5 topics are especially important and frequency cited in the literatures.

1. Establishment of the assignment of resonance Raman spectra from metal porphyrins by combining isotopic substitution experiment and molecular force field calculations.
2. Discovery of the relationship between iron-histidine stretching vibration frequency and oxygen affinity of hemoglobin.
3. Difference in the environment around iron atoms in the peroxidase and hemoglobin and its relation with catalytic activity.
4. Study on the proton pumping mechanism of cytochrome oxidase.
5. Structure of reaction intermediate between peroxidase and hydrogen peroxide by transient Raman spectroscopy.

LIST OF PUBLICATIONS

K. YAMASHITA and K. MOROKUMA, "*Ab Initio* Calculations of the Dipole Moments in Low-Lying Electronic States of the CCN Radical", *Chem. Phys. Lett.* **140**, 345 (1987).

I. RÖEGGEN, K. MOROKUMA, and K. YAMASHITA, "On the Binding Energy of the Ground State of Be_2", *Chem. Phys. Lett.* **140**, 349 (1987).

N. KOGA and K. MOROKUMA, "SiC Agostic Interaction with Ti: Origin of Alkenyl Group Distortion in $Ti(C(SiH_2CH_3)=CH_2)X_2^+$. An *Ab Initio* MO Study", *J. Am. Chem. Soc.* **110**, 108 (1988).

H. SHIRAISHI, K. ISHIGURE, and K. MOROKUMA, "An ESR Study on Solvated Electrons in Water and Alcohols: Difference in the g Factor and Related Analysis of the Electronic State by MO Calculation", *J. Chem. Phys.* **88**, 4637 (1988).

N. KOGA, S.Q. JIN, and K. MOROKUMA, "Rearrangement through Berry Pseudorotation and Olefin Insertion of d^8 Five-Coordinate $Rh(H)(C_2H_4)(CO)_2(PH_3)$. An *Ab Initio* MO Study", *J. Am. Chem. Soc.* **110**, 3417 (1988).

C. DANIEL, N. KOGA, J. HAN, X.Y. FU, and K. MOROKUMA, "*Ab Initio* MO Study of the Full Catalytic Cycle of Olefin Hydrogenation by the Wilkinson Catalyst $RhCl(PR_3)_3$", *J. Am. Chem. Soc.* **110**, 3773 (1988).

K. YAMASHITA and K. MOROKUMA, "Theoretical Study of Absorption Process during Chemical Reactions: Potential Surface and Classical Trajectory Study on K + NaCl", *J. Phys. Chem.* **92**, 3109 (1988).

K. MOROKUMA, W.T. BORDEN, and D.A. HORVAT, "Chair and Boat Transition States for the Cope Rearrangement. A CASSCF Study", *J. Am. Chem. Soc.* **110**, 4474 (1988).

Y. AOKI, A. IMAMURA, and K. MOROKUMA, "Self-Consistent-Field Iterative Transfer Perturbation Method and its Application to the Interaction between a Polymer and a Small Molecule", *J. Chem. Phys.* **89**, 1147 (1988).

H. TANAKA and I. OHMINE, "Large Local Energy Fluctuations in Water", *J. Chem. Phys.* **87**, 6128 (1988).

M. SASAI and H. FUKUTOME, "Zwitterionic and Diradical Breathers in Trans-Polyacetylene", *Prog. Theor. Phys.* **79**, 61 (1988).

H. NAKAMURA, "Resonance in Collinear Chemical Reactions Caused by Barrier Penetration and Non-Adiabatic Coupling", *Chem. Phys. Lett.* **141**, 77 (1987).

H. NAKAMURA, "Semiclassical Treatment of Nonadiabatic Transitions: Multilevel Curve Crossing and Nonadiabatic Tunneling Problems", *J. Chem. Phys.* **87**, 4031 (1987).

A. OHSAKI and H. NAKAMURA, "Approximate Quantum Mechanical Treatment of Light-Atom Transfer Reactions", *Chem. Phys. Lett.* **142**, 37 (1987).

M. BAER and H. NAKAMURA, "A Three-Dimensional, Quantum Mechanical Study of Exchange and Charge Transfer Processes in the $(Ar + H_2)^+$ System", *J. Chem. Phys.* **87**, 4651 (1987).

T. SHIRAI and H. NAKAMURA, "Ionization of Rydberg Atoms in Thermal Collisions with Polar Molecules", *Phys. Rev.* **A36**, 4290 (1987).

H. TAKAGI and H. NAKAMURA, "Theoretical Study of Associative Ionization of Hydrogen Atoms", *J. Chem. Phys.* **88**, 4552 (1988).

H. NAKAMURA, "Semiclassical Theory of Nonadiabatic Transitions", Invited Papers of the XV-International Conference on the Physics of Electronic and Atomic Collisions, Brighton, United Kingdom, 1987, H.B. Gilbody, W.R. Newell, F.H. Read and A.C.H. Smith Eds., North Holland, pp.413 (1988).

C. WU, X. SUN, and K. NASU, "Electron Correlation and Bond Alternation in Polymers", *Phys. Rev. Lett.* **59**, 831 (1987).

K. NASU, "Dynamics of Free Exciton Self-Localization", in "Optical Properties of Solids and Electron-Lattice Interaction", K. Nasu Ed., Special Volume of **Solid State Physics** (March, 1987, Tokyo, AGNE GIJUTSU CENTER, in Japanese) p.95.

K. NASU, "Contemporary Problems in the Theory for Tunneling", in "*Physics and Application of Tunneling Phenomena*", Y. Takeuchi and N. Mikoshiba Eds., (November 1987, Bifukan, Tokyo, in Japanese) p.95.

A. MISHIMA and K. NASU, "Ferromagnetism in a New Type of Organic Polymer Based on Benzene Rings Bridged by Carbons", *Synthetic Metals* **22**, 23 (1987).

K. NASU and A. YANASE, "Many-Polaron Theory for Superconducting Transition Temperatures, —Self-Consistent Method for Fluctuation from BCS Limit to Bipolaronic Limit—", *Jpn. J. Appl. Phys. 1* **26**, 1095 (1987).

K. NASU, "Tunneling and Relaxation from Free State to Self-Localized State of Exciton —Nonadiabatic Multi-Step Theory—", *J. Luminescence* **38**, 90 (1987).

K. YAMAGUCHI, Y. TAKAHARA, T. FUENO, and K. NASU, "*Ab Initio* MO Calculations of Effective Exchange Integrals between Transition-Metal Ions via Oxygen Dianions: Nature of the Copper-Oxygen Bond and Superconductivity", *Jpn. J. Appl. Phys.* **26**, L1362 (1987).

K. YAMAGUCHI, Y. TAKAHARA, T. FUENO, and K. NASU, "*Ab Initio* MO Studies on the Correlation and Spin Correlation Effects for Copper-Oxygen and Copper-Halogen Bonds in the High T_c Copper Oxide Superconductors", *Jpn. J. Appl. Phys.* **26**, L2037 (1987).

K. NASU, "Superconducting Transition Temperatures of Strongly Coupled Electron-Boson Systems; —A Self-Consistent Method for Fluctuation from BCS Limit to Bipolaronic Limit—", *Phys. Rev. B* **37**, 5075 (1988).

S. MURAMATSU, M. AIHARA, and K. NASU, "Hot Luminescence in F Center under One- and Two-Photon Excitations", *J. Luminescence* **40 & 41**, 603 (1988).

K. NASU, "Many-Polaron Theory for Superconductivity in Quasi Two-Dimensional Strongly Coupled Electron-Phonon Systems", *Physica* **148B**, 378 (1988).

K. NASU, "Superconducting States in a Quasi Two-Dimensional Peierls-Hubbard Systems", *Jpn. J. Appl. Phys.* (1988) Series 1 "*Superconducting Materials*" ed. by S. Nakajima and H. Fukuyama, (1988) p.242.

Y. AOKI, A. IMAMURA, and T. SASAKI, "Through Space/Bond Interaction Analysis of the Shape of the Band Structure of Polyacetylene", *Bull. Chem. Soc. Jpn.* **61**, 1063 (1988).

K. SAITO, K. MAKISHITA, T. KAKUMOTO, T. SASAKI, and A. IMAMURA, "Unimolecular Thermal Reaction of Formaldoxime at High Temperature: Experiments and Calculations", *J. Phys. Chem.* **92**, 4371 (1988).

K.W. KEHR and K. KITAHARA, "Spin Depolarization of a Quantum Particle on a Linear Chain with Alternating Larmor Frequencies", *J. Phys. Soc. Jpn.* **57**, 2819 (1988).

K. KITAHARA, Y. OONO, and D. JASNOW, "Phase Separation Dynamics and External Force Field", *Modern Physics Letters B2*, 765 (1988).

H. KANAMORI and E. HIROTA, "Infrared Diode Laser Kinetic Spectroscopy of the CCH Radical ν_3 Band", *J. Chem. Phys.* **87**, 73 (1987).

M. KAJITA, Y. ENDO, and E. HIRTOA, "The Microwave Spectrum of the PH_2 Radical", *J. Mol. Spectrosc.* **124**, 66 (1987).

Y. KAWASHIMA, K. KAWAGUCHI, Y. ENDO, and E. HIROTA, "Infrared Diode Laser and Microwave Spectra and Molecular Structure of an Unstable Molecule, FBO", *J. Chem. Phys.* **87**, 2006 (1987).

Y. ENDO, H. KANAMORI, and E. HIROTA, "Submillimeter-Wave Spectroscopy of $a^1\Delta$ SO in Excited Vibrational States Produced by 193 nm Photolysis of Cl_2SO", *Chem. Phys. Lett.* **141**, 129 (1987).

K. KAWAGUCHI, J.E. BUTLER, C. YAMADA, S.H. BAUER, T. MINOWA, H. KANAMORI, and E. HIROTA, "Observation of the Gas-Phase Infrared Spectrum of BH_3", *J. Chem. Phys.* **87**, 2438 (1987).

S. KODA, Y. ENDO, E. HIROTA, and S. TSUCHIYA, "Deuterium Isotope Effect on the Branching Ratio in $O(^3P)$+Ethylene Reaction", *J. Phys. Chem.* **91**, 5840 (1987).

T. AMANO, K. KAWAGUCHI, and E. HIROTA, "Infrared Diode Laser Spectroscopy of the ν_2 Fundamental Band of SH_3^+", *J. Mol. Spectrosc.* **126**, 177 (1987).

Y. ENDO, M.C. CHANG, and E. HIROTA, "The Microwave Spectrum of Cyclopropane-1,1-d_2. Molecular Structure of Cyclopropane", *J. Mol. Spectrosc.* **126**, 63 (1987).

Y. MATSUO, Y. ENDO, E. HIROTA, and T. SHIMIZU, "Direct Observation of Inversion Transitions in the ν=5 State of NH_3 by Millimeter Wave-Optical Double Resonance", *J. Chem. Phys.* **87**, 4395 (1987).

Y. KAWASHIMA, K. KAWAGUCHI, and E. HIROTA, "Detection of HBNH by Infrared Diode Laser Spectroscopy", *J. Chem. Phys.* **87**, 6331 (1987).

C. YAMADA and E. HIROTA, "Infrared Diode Laser Spectroscopic Study of the Active Nitrogen. The Electronic Transition between the Lowest Singlet Metastable States $a^1\Pi_g$-$a'^1\Sigma_u^-$ 0-0 Band", *J. Chem. Phys.* **87**, 6434 (1987).

K. KAWAGUCHI and E. HIROTA, "Diode Laser Spectroscopy of the ν_3 and ν_2 Bands of FHF^- in 1300 cm^{-1} Region", *J. Chem. Phys.* **87**, 6838 (1987).

M. KAJITA, K. KAWAGUCHI, and E. HIROTA, "Diode Laser Spectroscopy of the ν_3 (CN Stretch) Band of $HCNH^+$", *J. Mol. Spectrosc.* **127**, 275 (1988).

E. HIROTA, "Infrared Diode Laser and Microwave Spectroscopy of Molecular Ions", *Phil. Trans. R. Soc. Lond.* A **324**, 131 (1988).

K. TANAKA, Y. ENDO, and E. HIROTA, "Submillimeter-Wave Spectrum of $k=\pm1 \leftarrow \mp2$ Transitions of NH_3", *Chem. Phys. Lett.* **146**, 165 (1988).

N. OHASHI, S. SAITO, T. SUZUKI, and E. HIROTA, "Dye Laser Excitation Spectroscopy of Two New Bands of the DSO Radical in 6100-Å Region", *J. Mol. Spectrosc.* **127**, 481 (1988).

E. HIROTA and Y. ENDO, "Microwave Spectroscopy of HCO^+ and DCO^+ in Excited Vibrational States", *J. Mol. Spectrosc.* **127**, 527 (1988).

Y. ENDO and E. HIROTA, "The Submillimeter-Wave Spectrum of the Deuterated Vinoxy Radical, CD_2CDO", *J. Mol. Spectrosc.* **127**, 535 (1988).

Y. ENDO and E. HIROTA, "The Millimeter- and Submillimeter-Wave Spectrum of the DCO Radical", *J. Mol. Spectrosc.* **127**, 540 (1988).

C. YAMADA, E. HIROTA, S. YAMAMOTO, and S. SAITO, "The Vibrational Assignment for the $A^2\Pi$-$X^2\Sigma^+$ Band System of the SiN Radical: The 0-0 Bands of ^{29}SiN and ^{30}SiN", *J. Chem. Phys.* **88**, 46 (1988).

E. TIEMANN, H. KANAMORI, and E. HIROTA, "Diode Laser Spectroscopy for Monitoring the Yield of Metastable Cl from Photodissociation of Simple Molecules", *J. Chem. Phys.* **88**, 2457 (1988).

Y. MATSUO, Y. ENDO, E. HIROTA, and T. SHIMIZU, "Inversion Transition Frequencies in the ν=5 State of NH_3 Measured by Millimeter Wave-Optical Double Resonance", *J. Chem. Phys.* **88**, 2852 (1988).

T. MOMOSE, Y. ENDO, E. HIROTA, and T. SHIDA, "The Submillimeter-Wave Spectrum of the $^{13}CH_3O$ Radical", *J. Chem. Phys.* **88**, 5338 (1988).

S. SAITO, S. YAMAMOTO, and K. KAWAGUCHI, "The Microwave Spectrum of H_2Cl^+ Ion", *J. Chem. Phys.* **88**, 2281 (1988).

K. KAWAGUCHI, "Gas-Phase Infrared Spectroscopy of $ClHCl^-$", *J. Chem. Phys.* **88**, 4186 (1988).

K. KAWAGUCHI and T. AMANO, "Infrared Spectroscopy of NH^+: An Analysis of the Perturbation between the $X^2\Pi$ and $a^4\Sigma^-$ States", *J. Chem. Phys.* **88**, 4584 (1988).

M. OHISHI, S. YAMAMOTO, S. SAITO, K. KAWAGUCHI, H. SUZUKI, N. KAIFU, S. ISHIKAWA, S. TAKANO, T. TSUJI, and W. UNNO, "The Laboratory Spectrum of the PS Radical and Related Astronomical Search", *Astrophys. J.* **329**, 511 (1988).

S.K. LEE, T. AMANO, K. KAWAGUHI, and M. OLDANI, "Difference-Frequency Laser Spectroscopy of the ν_1 and ν_3 Fundamental Bands of H_2Cl^+: Determination of the Equilibrium Molecular Structure", *J. Mol. Spectrosc.* **130**, 1 (1988).

K. KAWAGUCHI, E. HIROTA, M. OHISHI, H. SUZUKI, S. TAKANO, S. YAMAMOTO, and S. SAITO, "Infrared Diode Laser Spectroscopy of the PS Radical", *J. Mol. Spectrosc.* **130**, 81 (1988).

N. MORITA, T. SUZUKI, and K. SATO, "Laser Spectroscopy of Doubly Excited 9*sns* ($11 \leq n \leq 20$) and 8*dns* ($10 \leq n \leq 20$) States of Ca", *Phys. Rev. A*, **38**, 551 (1988).

N. MORITA and T. SUZUKI, "Spectroscopic Observation of Doubly Excited 8*sns* and 7*dns* States of Ca with Multistep Laser Excitation", *J. Phys. B*, **21**, L439 (1988).

N. KITAJIMA, T. KODA, S. HASHIMOTO, T. KITAGAWA, and Y. MOROOKA, "An Accurate Synthetic Model of Oxyhemocyanin" *J. Chem. Soc. Chem. Commun.* 151 (1988).

K. KAMOGAWA, T. FUJII, and T. KITAGAWA, "Improved Fluorescence Rejection in Measurements of Raman Spectra of Fluorescent Compounds" *Appl. Spectrosc.* **42**, 248 (1988).

S. HASHIMOTO, Y. TATSUNO, and T. KITAGAWA, "Observation of the Fe^{IV}=0 Stretching Raman Band for a Ferryl Porphyrin π Cation Radical" *J. Am. Chem. Soc.* **109**, 8096 (1987).

S. FUJII, K. KAMOGAWA, and T. KITAGAWA, "Observation of Resonance Raman Spectra of S_1-, T_1-, and S_0-Pyrene in Solution: Application of a Fluorescent Rejection Technique" *Chem. Phys. Lett.* **148**, 17 (1988).

T. OGURA and T. KITAGAWA, "A Novel Optical Device for Simultaneous Measurements of Raman and Absorption Spectra: Application to Photolabile Reaction Intermediates of Hemoproteins" *Rev. Sci. Instr.* **59**, 1316 (1988).

K. TOHJI and Y. UDAGAWA, "Novel Approach for Structural Analysis by X-ray Raman Scattering", *Phys. Rev.*, **B36**, 9410 (1987).

T. IDA, H. TSUIKI, A. UENO, K. TOHJI, Y. UDAGAWA, K. IWAI, and H. SANO, "Characterization of Iron Oxide in Fe_2O_3/SiO_2 Catalyst", *J. Catal.*, **106**, 428 (1987).

H. MORIKAWA, Y. SHIMIZUGAWA, F. MARUMO, T. HARASAWA, K. TOHJI, and Y. UDAGAWA, "Local Structure around Y Atoms in Y_2O_3 Stabilized Tetragonal ZrO_2", *J. Jpn. Ceramic Soc.*, **96**, 253 (1988).

K. TOHJI, Y. UDAGAWA, T. KAWASAKI, and A. MIENO, "A Double Crystal Spectrometer for Laboratory EXAFS Spectroscopy", *Rev. Sci. Instrum.* **59**, 1127 (1988).

N. KAKUTA, K. TOHJI, and Y. UDAGAWA, "Characterization of Silica Supported Mo Catalyst by EXAFS and Raman Spectroscopy", *J. Phys. Chem.*, **92**, 2587 (1988).

T. MIZUSHIMA, K. TOHJI, and Y. UDAGAWA, "An EXAFS Study on the Morphology Change of Ru Catalyst by CO Adsorption", *J. Am. Chem. Soc.*, **110**, 4459 (1988).

Y. UDAGAWA and K. TOHJI, "Observation of X-ray Resonant Raman Spectra and Transition to Resonant Fluorescence", *Chem. Phys. Lett.*, **148**, 101 (1988).

T. OSUKA, H. MORIKAWA, F. MARUMO, N. DAIMON, Y. UDAGAWA, and K. TOHJI, "An EXAFS Study of Local Structures around Co Atoms in Synthetic Fluoromicas", *Rept. Res. Lab. of Engineering Materials*, **13**, 1 (1988).

B.X. YANG, D.M. HANSON, and K. TOHJI, "Optical Luminescence Excitation Spectra of Molecular Oxygen in the Soft X-ray Region", *J. Chem. Phys.* **89**, 1215 (1988).

N. NAKASHIMA, N. IKEDA, N. SHIMO, and K. YOSHIHARA, "Direct Measurements of Formation Rate Constants of Allylic Radical from Hot Olefins Formed by Internal Conversion. I", *J. Chem. Phys.* **87**, 3471 (1987).

N. IKEDA, K. IMAGI, H. MASUHARA, N. NAKASHIMA, and K. YOSHIHARA, "Picosecond Transient Absorption Spectral and Kinetic Study on Benzophenone Microcrystals by Diffuse Reflectance Laser Photolysis Method", *Chem. Phys. Lett.*, **140**, 281 (1987).

M. SUMITANI, Y. TAKAGI, and K. YOSHIHARA, "Direct Observation of Radiationless Transitions from the Excited to Ground Electronic State under Collision-Free Conditions", *Chem. Phys. Lett.*, **140**, 468 (1987).

Y. KAJII, K. OBI, N. NAKASHIMA, and K. YOSHIHARA, "ArF Laser Flash Photolysis of Phenol and Anisole", *J. Chem. Phys.*, **87**, 5059 (1987).

K. KEMNITZ, N. NAKASHIMA, and K. YOSHIHARA, "Electron Transfer by Isolated Rhodamine B Molecules Adsorbed on Organic Single Crystals. A Solvent-Free Model System", *J. Phys. Chem.*, **92**, 3915 (1987).

N. NAKASHIMA, N. IKEDA, and K. YOSHIHARA, "Hot Toluene as an Intermediate of UV Multiphoton Dissociation", *J. Phys. Chem.* **92**, 4389 (1987).

M. HIRAMOTO, K. HASHIMOTO, and T. SAKATA, "Ultramicrostructured Electrode System Prepared from the Multilayered Thin Film and its New Electrochemical Properties", Proceedings of a symposium on photoelectrochemistry and electro-synthesis on semiconducting materials, *Electrochem. Soc.*, p.304.

H. HARADA, T. SAKATA, and T. UEDA, "Photoanodic Reaction of Lactic Acid; Semiconductor and pH Effect", Proceeding of a symposium on photoelectrochemistry and electro-synthesis on semiconducting materials, *Electrochem. Soc.* p.144.

T. SAKATA, M. HIRAMOTO, and K. HASHIMOTO, "Dynamics of Charge Transfer Processes at Semiconductor-Electrolyte (or Gas) Interfaces", Proceedings of a symposium on photoelectrochemistry and electro-synthesis on semiconducting materials, *Electrochem. Soc.*, p.428.

K. HASHIMOTO, M. HIRAMOTO, and T. SAKATA, "Photoluminescence of TiO_2 Powder and its Relation with Photocatalytic Reactions", Proceedings of a symposium on photoelectrochemistry and electro-synthesis on semiconducting materials, *Electrochem. Soc.*, p.395.

K. HASHIMOTO, M. HIRAMOTO, and T. SAKATA, "Photo-Induced Electron Transfer from Adsorbed Rhodamine B to Oxide Semiconductor Substrates *in vacuo*: Semiconductor Dependence" *Chem. Phys. Lett.*, **148**, 215 (1988).

K. HASHIMOTO, M. HIRAMOTO, A.B.P. LEVER, and T. SAKATA, "Luminescence Decay of Ru(II) Complexes Adsorbed on Metal Oxide Powders *in vacuo*: Energy Gap Dependence of the Electron Transfer Rate", *J. Phys. Chem.*, **92**, 1016 (1988).

K. HASHIMOTO, M. HIRAMOTO, T. KAJIWARA, and T. SAKATA, "Luminescence Decays and Spectra of $Ru(bpy)_3^{2+}$ Adsorbed on TiO_2 *in vacuo* and in the Presence of Water Vapor" *J. Phys. Chem.*, **92**, 4636 (1988).

K. HASHIMOTO, M. HIRAMOTO, and T. SAKATA, "Temperature Independent Electron-Transfer: Rhodamine B/oxide Semiconductor Dye-Sensitization System" *J. Phys. Chem.*, **92**, 4272 (1988).

G. BLACK, T. NISHIYA, H. SHINOHARA, N. NISHI, and I. HANAZAKI, "REMPI Studies in The Lewis-Rayleigh Afterglow of Nitrogen", *Chem. Phys. Lett.* **142**, 409 (1987).

H.D. BIST, T. NISHIYA, M. BABA, and I. HANAZAKI, "Temperature-Induced Spontaneous Emission of Uranyl Nitrate Hexahydrate" *J. Am. Chem. Soc.* **110**, 3043 (1988).

N. NISHI and K. YAMAMOTO, "Conversion of Liquids to Cluster Beams by Adiabatic Expansion of Liquid Jets: Mass Spectrometric Analysis of Molecular Association in Aqueous Solution Systems", *J. Am. Chem. Soc.* **109**, 7353 (1987).

H. SHINOHARA and N. NISHI, "Resonance Enhanced 2PI Detection of Ammonia Clusters via a Linear Reflectron TOF Mass Spetrometer" *Chem. Phys. Lett.* **141**, 292 (1987).

T. ICHIMURA, H. SHINIOHARA, and N. NISHI, "Resonance Enhanced Two-Photon Ionization Spectra of Benzene in the Third Channel Region", *Chem. Phys. Lett.* **146**, 83 (1988).

N. NISHI, K. KOGA, C. OHSHIMA, K. YAMAMOTO, U. NAGASHIMA, and K. NAGAMI, "Molecular Association in Ethanol-Water Mixtures Studied by Mass Spectrometric Analysis of Clusters Generated through Adiabatic Expansion of Liquid Jets" *J. Am. Chem. Soc.* **110**, 5246 (1988).

K.MUTAI and R. NAKAGAKI, "Magnetic Field Effect as a Probe for Radical Pair Intermediates in the Photoreactions of Nitroaromatic Ethers", *Chemistry Lett.*, 2261 (1987).

T. WATANABE, Y. TANIMOTO, R. NAKAGAKI, M. HIRAMATSU, T. SAKATA, and S. NAGAKURA, "The Magnetic Field Effects on Electrolysis. II. The Anodic Surface Oxidation of Gold", *Bull. Chem. Soc. Jpn.* **60**, 4163 (1987).

T. WATANABE, Y. TANIMOTO, R. NAKAGAKI, M. HIRAMATSU, and S. NAGAKURA, "The Magnetic Field Effects on Electrolysis. III. The Anodic Oxidation of Phenylacetate Ion", *Bull. Chem. Soc. Jpn.* **60**, 4166 (1987).

M. HIRAMATSU, R. NAKAGAKI, Y. TANIMOTO, K. MUTAI, H. TUKADA, and S. NAKAKURA, "Intermolecular Photo-oxidation of Triphenyphosphine and 10-Alkylphenothiazine by Nitro-aromatic Moieties: Magnetic Field Effects and Long-range Oxygen Transfer", *Chem. Phys. Lett.* **142**, 413 (1987).

T. IMAMURA, K. TAMAI, Y. FUKUDA, I. YAMAZAKI, S. NAGAKURA, H. ABE, and H. HAYASHI, "External Magnetic Field Effect on the Fluorescence of CS_2 Excited to the V $^1B_2$ State with Nanosecond and Picosecond Dye Lasers." *Chem. Phys. Lett.* **135**, 208 (1987).

Y. FUKUDA, "Magnetic Field Effects on Atomic and Molecular Collisions", *Chem. Phys.* **118**, 199 (1987).

H. OKAMOTO, "Perturbation Theoretical Study of Resonance Raman Intensities: Contribution of Forbidden Electronic States", *J. Raman Spectroc.* **19**, 255 (1988).

K. TAKEDA, M. FUJINO, K. SEKI, and H. INOKUCHI, "Skelton-Side Group Interaction in Organopolysilanes", *Phys. Rev.* **B 15**, 8129 (1987).

H. FUJIMOTO, T. MORI, H. INOKUCHI, N. UENO, K. SUGITA, and K. SEKI, "Intermolecular Band Mapping of n-$CH_3(CH_2)_{45}CH_3$ over the Whole Brillouin Zone by Angle-Resolved Photoemission", *Chem. Phys. Lett.* **141**, 485 (1987).

H. NAKAHARA, H. FUKUDA, K. SEKI, S. ASADA, and H. INOKUCHI, "UV Photoelectron Spectroscopic Study of the Photopolymerizatin of Long-Chain Diacetylene Monocarboxylic Acid in the Langmuir-Blodgett Films", *Chem. Phys.* **118**, 1234 (1987).

K. SEKI, T. MORI, H. INOKUCHI, and K.MURANO, "Electronic Structure of Poly (dimethylsilane) and Polysilane Studied by XPS, UPS, and Band Calculation", *Bull. Chem. Soc. Jpn.* **61**, 351 (1988).

H. MITSUYA, H. OZAKI, Y. HARADA, K. SEKI, and H. INOKUCHI, "Characterization of Vacuum-Deposited Perfluorocarboxylic Acid Monomolecular Film by Penning Ionization Electron Spectroscopy", *Langmuir* **4**, 569 (1988).

H. FUJIMOTO, U. NAGASHIMA, H. INOKUCHI, K. SEKI, H. NAKAHARA, J. NAKAYAMA, M. HOSHINO, and K. FUKUDA, "Ultraviolet Photoemission Study of Oligothiophenes: The Effect of Irregularity on π-Electron System", *J. Chem. Phys.* **89**, 1198 (1988).

T. TAKAHASHI, H. MATSUYAMA, H. KATAYAMA-YOSHIDA, Y. OKABE, S. HOSOYA, K. SEKI, H. FUJIMOTO, M. SATO, and H. INOKUCHI, "Evidence from Angle-Resolved Resonant Photoemission for Oxygen-2p Nature of Fermi-Liquid States in $Bi_2CaSr_2Cu_2O_8$", *Nature* **334**, 691 (1988).

H. YAMAMOTO, K. SEKI, H. INOKUCHI, and G. SAITO, "Changes in the Electronic Structures of Tetrakis (alkylthio)-tetrathiafulvalenes (TTC_n-TTFs) during the Solid-Melt Transition", *J. Chem. Soc., Faraday Trans. 2* **83**, 2151 (1987).

J.K. JESKA, K. KIMURA, A. TRACZ, H. INOKUCHI, and M. KRYSZEWSKI, "X-Ray Photoelectron Spectroscopy of Tetrathiofulvalene- and Tetrathiotetracene- Tetracyanoquinodimethane Charge- Transfer Complexes in Reticulate Doped Polymers", *J. Mol. Elect.* **3**, 157 (1987).

G. SAITO, H. KUMAGAI, C. KATAYAMA, C. TANAKA, J. TANAKA, P. WU, T. MORI, K. IMAEDA, T. ENOKI, H. INOKUCHI, Y. HIGUCHI, and N. YASUOKA, "Chemical and Physical Properties of Capped and Uncapped Alkylthio Substituted Tetrathiafulvalenes and their Charge Transfer Complexes", *Israel J. Chem.* **27**, 319 (1986).

S. MIYAJIMA, T. CHIBA, T. ENOKI, H. INOKUCHI, and M. SANO, "Structural and Electronic Properties of Hydrogen in the Potassium-Hydrogen-Graphite Ternary Intercalation Compound $C_8KH_{0.55}$: A Nuclear-Magnetic Resonance Study.", *Phys. Rev.* **B37**, 3246 (1988).

T. ENOKI, H. INOKUCHI, and M. SANO, "ESR Study of the Hydrogen-Potassium-Graphite Ternary Intercalation Compounds.", *Phys. Rev.* **B37**, 9163 (1988).

I. KANAZAWA, S. TANIGAWA, R. SUZUKI, Y. MIZUHARA, M. SANO, and H. INOKUCHI, "Two-Dimensional Electron Momentum Distribution in Graphite Revealed by Means of Angular Correlation of Positron Annihilation.", *J. Phys. Chem. Solids* **48**, 701 (1987).

H. MURAKAMI, I. KANAZAWA, M. SANO, T. ENOKI, and H. INOKUCHI, "Hydrogen in a Graphite-Rubidium Intercalation Compound RbC_8 Studied by Positron Annihilation", *J. Phys. Chem. Solids* **49**, 457 (1988).

K. IMAEDA, T. ENOKI, G. SAITO, and H. INOKUCHI, "Electrical Properties of the Organic Conductor, $(BEDT\text{-}TTF)_3(ClO_4)_2$.", *Bull. Chem. Soc. Jpn.* **61**, 3332 (1988).

T. MORI and H. INOKUCHI, "Superconductivity in $(BEDT\text{-}TTF)_3Cl_2H_2O$.", *Solid State Commun.* **64**, 335 (1987).

T. MORI, P. WANG, K. IMAEDA, T. ENOKI, and H. INOKUCHI, "Structural and Electrical Properties of $(BEDT\text{-}TTF)_5Hg_3Br_{11}$.", *Solid State Commun.* **64**, 733 (1987).

T. MORI, K. IMAEDA, R. KATO, A. KOBAYASHI, H. KOBAYASHI, and H. INOKUCHI, "Pressure-Induced One-Dimensional Instability in $(DMDCNQI)_2Cu$.", *J. Phys. Soc. Jpn.* **56**, 3429 (1987).

N. IWASAWA, F. SHINOZAKI, G. SAITO, K. OSHIMA, T. MORI, and H. INOKUCHI, "Quasi Three-Dimensional Electrical Conductor Having Alternating Mixed Stacks: Tetrakis(methyltellulo)-tetrathiafulvalene ($TTeC_1$-TTF)(TCNQ) Complex.", *Chem. Lett.* **1988**, 215.

H. KOBAYASHI, R. KATO, A. KOBAYASHI, T. MORI, and H. INOKUCHI, "The First Molecular Metals With Ordered Spin Structures, R_1R_2-DCNQI$_2$Cu (R_1, R_2=CH_3, CH_3O, Cl, Br) – Jahn-Teller Distortion, CDW Instability and Antiferromagnetic Spin Ordering.", *Solid State Commun.* **65**, 1351 (1988).

T. MORI and H. INOKUCHI, "A BEDT-TTF Complex Including a Magnetic Anion.", *Bull. Chem. Soc. Jpn.* **61**, 591 (1988).

R. KATO, H. KOBAYASHI, H. KIM, A. KOBAYASHI, Y. SASAKI, T. MORI, and H. INOKUCHI, "Crystal and Electronic Structures of a New Two-Dimensional Molecular Metal, *a*-$Et_2Me_2N[Ni(dmit)_2]_2$.", *Chem. Lett.* **1988**, 865.

M.R. WILLIS, T. MORI, and H. INOKUCHI, "Band Structure of DEBP$(TCNQ)_4$.", *Bull. Chem. Soc. Jpn.* **61**, 2211 (1988).

T. MORI, H. INOKUCHI, A. KOBAYASHI, R. KATO, and H. KOBAYASHI, "Electrical Conductivity, Thermoelectric Power, and ESR of a New Family of Molecular Conductors, Dicyanoquinonediimine-Metal [$(DCNQI)_2M$] Compounds.", *Phys. Rev.* **B 38**, 5913 (1988).

T. MORI, S. BANDOW, H. INOKUCHI, A. KOBAYASHI, R. KATO, and H. INOKUCHI, "Anomalous Magnetic Properties of $(DMDCNQI)_2Cu$.", *Solid State Commun.* **67**, 565 (1988).

S. NAGAOKA, S. SUZUKI, and I. KOYANO, "Production of Pb^+ Ions Following 5d Core Photoionization of Tetramethyllead as Revealed by a Coincidence Experiment." *Phys. Rev. Lett.* **58**, 1524 (1987).

S. SUZUKI and I. KOYANO, "State-Selected Ion/Molecule Reactions by the TESICO Technique. XIV. Separation of Two Microscopic Reaction Mechanisms in the Reaction $CH_3Cl^+ + CH_3Cl \rightarrow CH_4Cl^+ + CH_2Cl$." *Int. J. Mass Spectrom. Ion Proc.* **80**, 187 (1987).

S. SUZUKI and I. KOYANO, "Dynamics of the Reaction $MH^+ + MH \rightarrow MH_2^+ + M$. Separation of Two Microscopic Reaction Mechanisms by TOF Coincidence." *Radiochimica Acta* **42**, 115 (1988).

I. KOYANO, K. TANAKA, T. KATO, and S. SUZUKI, "State-Selected Charge Transfer and Rearrrangement Reactions in Four-Atom Ion-Molecule Systems." *Faraday Disc. Chem. Soc.* **84**, 265 (1987).

S. NAGAOKA, S. SUZUKI, and I. KOYANO, "Investigation of Fragmentation Processes Following Core Photoionization of Organometallic Molecules in the Vapor Phase.", *Nucl. Instrum. Methods*, **A266**, 699 (1988).

S. NAGAOKA, "Simple Relation between Arrhenius Activation Parameters for Non-Radiative Processes from Proton-Transferred Forms of Intramolecularly Hydrogen-Bonded Molecules.", *J. Photochem. Photobiol.* **40**, 185 (1987).

S. NAGAOKA, U. NAGASHIMA, N. OHTA, M. FUJITA, and T. TAKEMURA, "Electronic-State Dependence of Intramolecular Proton Transfer of o-Hydroxybenzaldehyde.", *J. Phys. Chem.* **92**, 166 (1988).

H. SHIROMARU, H. SHINOHARA, N. WASHIDA, H.-S. YOO, and K. KIMURA, "Synchrotron Radiation Measurements of Appearance Potentials for $(H_2O)_2^+$, $(H_2O)_3^+$, $(H_2O)_2H^+$, $(H_2O)_3H^+$ in Supersonic Jets", *Chem. Phys. Lett.* **141**, 7 (1987).

M. FUJII, K. SATO, and K. KIMURA, "Selection Rule and Efficiency for Autoionization of Diazabicyclooctane as Studied by Two-Color Double-Resonance Spectroscopy", *J. Phys. Chem.* **91**, 6507 (1987).

I. TOKUE, A. HIRAYA, and K. SHOBATAKE, "Photoexcitation of CH_3NCO, CH_3NCS and CH_3SCN in the Vacuum Ultraviolet: Rydberg States and Photofragment Emission", *Chem. Phys.* **117**, 315 (1987).

K. TABAYASHI and K. SHOBATAKE, "Chemiluminescence of NB($B^2\Pi$) Produced by the Reaction of N(^2D, ^2P) with COS and CS_2, in Crossed Molecular Beam", *J. Chem. Phys.* **87**, 7344 (1987).

A. HIRAYA, K. SHOBATAKE, R.J. DONOVAN, and A. HOPKIRK, "Vacuum Ultraviolet Fluorescence Excitation Spectrum of I_2", *J. Chem. Phys.* **88**, 52 (1988).

K. TABAYASHI and K. SHOBATAKE, "Dissociative Excitation Processes of Water Molecule by Metastable Rare Gas Atoms: $H_2O + Rg(^3P_{0,2}) \rightarrow OH(A^2\Sigma^+) + H + Rg$, (Rg = Ar, Kr)," *J. Chem. Phys.* **88**, 835 (1988).

J.R. GROVER, Y. WEN, Y.T. LEE, and K. SHOBATAKE, "Reactive Scattering of F_2 Plus C_6H_6 in Crossed Molecular Beams", *J. Chem. Phys.* **89**, 938 (1988).

K. TABAYASHI and K. SHOBATAKE, "Production of Atomic Beams by Dissociation of Molecules Mixed in Hot Plasma Flow. — Characterization of Atomic Carbon Beam by TOF Analysis —", *J. Spectroscop. Soc. Jpn.* (in Japanese), **37**, 201 (1988).

T. MITSUHASHI, M. GOTO, K. HONDA, Y. MARUYAMA, T. INABE, T. SUGAWARA, and T. WATANABE, "A Twin-TCNQ-Type Acceptor. Synthesis of 11,11,12,12,13,13,14,14-Octacyano-1,4:5,8-anthradiquinotetramethane and Structures of the Tetraethylammonium Salts of Its Mono- and Dianion", *Bull. Chem. Soc. Jpn.* **61**, 261 (1988).

T. INABE, T. MITSUHASHI, and Y. MARUYAMA, "New Organic Conductor $(TTT)_2OCNAQ(DMF)$. Transverse Interaction through the OCNAQ Molecules", *Chem. Lett.*, **1988**, 429.

H. URAYAMA, H. YAMOCHI, G. SAITO, S. SATO, A. KAWAMOTO, J. TANAKA, T. MORI, Y. MARUYAMA, and H. INOKUCHI, "Crystal Structures of Organic Superconductor, $(BEDT\text{-}TTF)_2Cu(NCS)_2$, at 298K and 104K" *Chem. Lett.*, **1988**, 463.

H. URAYAMA, H. YAMOCHI, G. SAITO, T. SUGANO, M. KINOSHITA, T. INABE, T. MORI, Y. MARUYAMA, and H. INOKUCHI, "Valence State of Copper Atoms and Transport Property of an Organic Superconductor, $(BEDT\text{-}TTF)_2Cu(NCS)_2$, Measured by ESCA, ESR, and Thermoelectric Power", *Chem. Lett.*, **1988**, 1057.

Y. MARUYAMA, T. INABE, H. URAYAMA, H. YAMOCHI, and G. SAITO, "Tunneling Spectroscopic Study on the Superconducting Gap of $(BEDT\text{-}TTF)_2Cu(NCS)_2$ Crystals", *Solid State Commun.* **67**, 35 (1988).

H. URAYAMA, T. INABE, T. MORI, Y. MARUYAMA, and G. SAITO, "Crystal Structures and Electronic Properties of Organic Conductors Based on AzaTCNQ" *Bull. Chem. Soc. Jpn.* **61**, 1831 (1988).

M. SAKURAI, M. KITAGAWA, H. HOSHI, Y. INOUE, and R. CHUJO, "CNDO-Electrostatic Potential Maps for α-Cyclodextrin", *Chem. Lett.*, **1988**, 895.

S. SHAMOTO, M. ONODA, M. SATO, and S. HOSOYA, "High-T_c Superconductivity in New Oxide Systems and Their X-Ray Diffraction Study.", *Jpn. J. Appl. Phys.* **26**, L642 (1987).

M. SATO, S. HOSOYA, K. FUKUDA, M. SERA, M. ONODA, S. SHAMOTO, K. OKA, and H. UNOKI, "Studies of High-T_c Oxide Superconductors.", *Physica*, **148B**, 363 (1987).

T. TAKAHASHI, F. MAEDA, H. ARAI, H. KATAYAMA-YOSHIDA, Y. OKABE, T. SUZUKI, S. HOSOYA, A. FUJIMORI, T. SHIDARA, T. KOIDE, T. MIYAHARA, M. ONODA, S. SHAMOTO, and M. SATO, "Synchrotron Radiation Photoemission Study of High-T_c Superconductor $YBa_2Cu_3O_{7-\delta}$.", *Phys. Rev.* **B36**, 5686 (1987).

M. SATO, S. SHAMOTO, M. ONODA, M. SERA, K. FUKUDA, S. HOSOYA, J. AKIMITSU, T. EKINO, and K. IMAEDA, "Single Crystal Studies and Electron Tunneling of $(La_{1-x}M_x)_2CuO_{4-\delta}$ (M=Ba and Sr).", *Novel Superconductivity* Plenum Press, 1987, p927.

S. HOSOYA, S. SHAMOTO, M. ONODA, and M. SATO, "Crystal Preparation of $(La_{1-x}M_x)_2CuO_{4-\delta}$ (M=Sr and Ba) and Discovery of Magnetic Superconductors Ln-Ba-Cu-O Systems (Ln=Lanthanide Atoms).", *Novel Superconductivity* Plenum Press, 1987, p909.

M. ONODA, S. SHAMOTO, M. SATO, and S. HOSOYA, "Single Crystal X-Ray Diffraction Study of $(La_{1-x}M_x)_2CuO_{4-\delta}$ (M=Sr and Ba), $La_2CuO_{4-\delta}$ and $LnBa_2Cu_3O_{4-\delta}$ (Ln=Y, Dy and Ho) Systems.", *Novel Superconductivity* Plenum Press, 1987, p919.

T. KOIDE, H. FUKUTANI, A. FUJIMORI, R. SUZUKI, T. SHIDARA, T. TAKAHASHI, S. HOSOYA, and M. SATO, "Optical-Reflectance Study of the Single Crystal Superconductor $(La_{1-x}Sr_x)_2CuO_4$.", *Novel Superconductivity* Plenum Press, 1987, p915.

T. TAKAHASHI, F. MAEDA, T. MIYAHARA, S. HOSOYA, and M. SATO, "Photoelectron Spectroscopy of High-T_c Superconductor $(La_{1-x}Sr_x)_2CuO_{4-\delta}$.", *Jpn. J. Appl. Phys.* **S26-3**, 1013 (1987).

M. ONODA, K. FUKUDA, M. SERA, and M. SATO, "Superconducting Phase in $La_{3-x}Ba_{3+x}Cu_6O_y$ System.", *Solid State Commun.* **64**, 1225 (1987).

S. SUGAI, S. UCHIDA, H. TAKAGI, K. KITAZAWA, S. TANAKA, M. SATO, and S. HOSOYA, "Optical Studies of High-T_c Oxide Superconductors.", *Physica*, **148B**, 282 (1987).

T. TAKAHASHI, F. MAEDA, H. ARAI, H. KATAYAMA-YOSHIDA, Y. OKABE, T. SUZUKI, Y. TAKAKUWA, S. HOSOYA, A. FUJIMORI, T. MIYAHARA, T. KOIDE, T. SHIDARA, M. SATO, S. SHAMOTO, and M. ONODA, "Photoelectron Spectroscopy of $LnBa_2Cu_3O_{7-\delta}$ (Ln=Y and Sm).", *Physica*, **148B**, 476 (1987).

M. SERA, S. SHAMOTO, and M. SATO, "Electron Tunneling Studies of High-T_c Superconductors $YBa_2Cu_3O_{7-\delta}$.", *Solid State Commun.* **65**, 997 (1988).

M. ONODA, M. SERA, K. FUKUDA, S. KONDOH, M. SATO, T. DEN, H. SAWA, and J. AKIMITSU, "Superconducting and Electronic Properties of $Bi_{1-x}La_xSrCuO_y$ System.", Solid State Commun. **66**, 189 (1987).

K. FUKUDA, S. SHAMOTO, M. SATO, and K. OKA, "Anisotropy of Magnetic Behavior of High-T_c Oxides.", *Solid State Commun.* **65**, 1323 (1988).

K. FUKUDA, M. SERA, and M. SATO, "Doping Effect on Magnetic Behaviors of La_2CuO_4.", *Solid State Commun.* **65**, 1157 (1988).

S. KONDOH, K. FUKUDA, and M. SATO, "Magnetic Susceptibility of Ca_2CuO_3.", *Solid State Commun.* **65**, 1329 (1988).

S. KONDOH, Y. ANDO, M. ONODA, M. SATO, and J. AKIMITSU, "Superconductivity in Tl-Ba-Cu-O System.", *Solid State Commun.* **66**, 195 (1988).

S. SHAMOTO, S. HOSOYA, and M. SATO, "Single Crystal Growth of High-T_c Superconductors." *Solid State Commun.* **66**, 195 (1988).

M. SATO, "Growth and Properties of Single Crystals of High-T_c Oxides.", *Physica C*, **153–155**, 38 (1988).

M. SERA, S. KONDOH, Y. ANDO, K. FUKUDA, S. SHAMOTO, M. ONODA, and M. SATO, "On the Structure of High-T_c Oxide System Tl-Ba-Cu-O.", *Solid State Commun.* **66**, 707 (1988).

H. KATAYAMA-YOSHIDA, T. YONEZAWA, H. HIROOKA, Y. OKABE, T. TAKAHASHI, T. SASAKI, M. HONGOH, K. YAMADA, T. SUZUKI, S. HOSOYA, M. SATO, T. CISZEK, and S.K. DEB, "Growth and Characterization of $YBa_2Cu_3O_{7-\delta}$ Single Crystals.", *Physica C* **153–155**, 425 (1988).

T. TAKAHASHI, F. MAEDA, H. KATAYAMA-YOSHIDA, Y. OKABE, T. SUZUKI, A. FUJIMORI, S. HOSOYA, S. SHAMOTO, and M. SATO, "Photoemission Study of Single-Crystalline $(La_{1-x}Sr_x)_2CuO_4$.", *Phys. Rev.* **37B**, 9788 (1988).

M. SERA, S. KONDOH, K. FUKUDA, and M. SATO, "Absence of the T-Linear Term in Low Temperature Specific Heat of High-T_c Oxide, Bi-Sr-Ca-Cu-O System.", *Solid State Commun.* **66**, 1101 (1988).

M. ONODA and M. SATO, "Superlattice Structure of Superconducting Bi-Sr-Cu-O System.", *Solid State Commun.* **67**, 799 (1988).

Y. ANDO, K. FUKUDA, S. KONDOH, M. SERA, M. ONODA, and M. SATO, "Study on Normal and Superconducting Properties of $Bi_4Sr_3(Ca_{1-x}Y_x)_3O_y$.", *Solid State Commun.* **67**, 815 (1988).

S. SHAMOTO, "Growth and Annealing Effect of Single Crystals of High-T_c Superconductors", *Solid State Commun.* **66**, 1151 (1988).

S. KONDOH, M. SERA, K. FUKUDA, Y. ANDO, and M. SATO, "Synthesis of Superconducting Ba-K-Bi-O System with Perovskite Structure.", *Solid State Commun.* **67**, 879 (1988).

H. KIKUCHI, Y. AJIRO, Y. UEDA, K. KOSUGE, M. KAKANO, and M. SATO, "Gd^{3+} EPR of High Temperature Superconductor $GdBa_2Cu_3O_x$.", *J. Phys. Soc. Jpn. Letter* **57**, 1887 (1988).

M. ONODA, S. KONDOH, K. FUKUDA, and M. SATO, "Structural Study of Superconducting Tl-Ba-Cu-O System.", *Jpn. J. Appl. Phys.* **27**, L1234 (1988).

M. SATO, S. SHAMOTO, J.M. TRANQUADA, G. SHIRANE, and B. KEIMER, "Two Dimensional Antiferromagnetic Excitations from a Large Single Crystal of $YBa_2Cu_3O_{6.2}$", *Phys. Rev. Letters* **61**, 1317 (1988).

K. ISOBE, S. KIMURA, and Y. NAKAMURA, "Comparative Studies of the Molybdenum-Molybdenum Single Bond in $[Mo_2(\eta^5\text{-}C_5H_5)_2(CO)_6]$ and Triple Bond in $[Mo_2(\eta^5\text{-}C_5H_5)_2(CO)_4]$ towards Nitrite and Nitrate.", *J. Organometal. Chem.* **331**, 221 (1987).

Y. HAYASHI, Y. NAKAMURA, and K. ISOBE, "Thermolysis of $[\eta^3$-allyl)PdMe$(PPh_3)]$: An Unexpected Evolution of Ethane Gas as a Main Product.", *J. Chem. Soc., Chem. Commun.* 403 **(1988)**.

S. KIYOOKA, T. ATAGI, R. FUJIYAMA, and K. ISOBE, "Reactivity of Cumulene Compelxes. Two Competing Pathways in Oxidative Solvolysis of Tetramethylbutatriene(hexacarbonyl)diiron.", *Chem. Lett.* 891 (**1988**).

Y. HAYASHI, K. TORIUMI, and K. ISOBE, "Novel Triple Cubane-Type Organometallic Oxide Clusters: $[MCp^*MoO_4]_4 \cdot nH_2O$ (M=Rh and Ir; $Cp^*=C_5Me_5$; n=2 for Rh and 0 for Ir).", *J. Am. Chem. Soc.* **110**, 3666 (1988).

K. OGAWA, H. SUZUKI, T. SAKURAI, K. KOBAYASHI, A. KIRA, and K. TORIUMI, "Low- and High-Temperature Structure of (E)-2,2′-Dimethylstilbene", *Acta Cryst.* **C44**, 505 (1988).

K. TORIUMI, T. KANAO, Y. UMETSU, A. OHYOSHI, M. YAMASHITA, and T. ITO, "Structural Study of Bromo-Bridged One-Dimensional Ni^{II}-Ni^{IV} Mixed-Metal Complexes by Means of EXAFS", *J. Coord. Chem.* **19**, 209 (1988).

K. HORIUCHI, M. MIKURIYA, H. ŌKAWA, and S. KIDA, "Cobalt(III) Complexes of Salen Analog with Thioether Pendant Group. X-Ray Structure Analysis and Thioether Coordination Effects", *Bull. Chem. Soc. Jpn.* **60**, 3575 (1987).

E. KITAURA, Y. NISHIDA, H. ŌKAWA, and S. KIDA, "Structure and Electrochemical Properties of Bis(pyridine)cobalt(III) Complexes of *N,N′*-Ethylenebis(salicylideneimine) Homologues with an Aryl Substituent of Ethylene Backbone. Crystal Structures of $[Co(salpen)(py)_2]PF_6$ and $[Co(salcppn)(py)_2]PF_6$", *J. Chem. Soc. Dalton Trans.*, 3055 (1987).

K. HORIUCHI, M. KOIKAWA, S. BABA, H. ŌKAWA, Y. MAEDA, and S. KIDA, "Cobalt(II) and μ-Oxodiiron(III,IV) Complexes of Salen Analog with Aromatic Thioether Pendant Group, *N,N′*-Disalicylidene-2-methyl-4-(2-methylthiophenyl)-1,2-butanediamine", *Inorg. Chim. Acta* **144**, 99 (1988).

Z.J. ZHONG, H. ŌKAWA, R. AOKI, and S. KIDA, "Synthesis and Properties of One-dimensional Heterometal Assemblies $[Au(TPP)][M(mnt)_2]$ (M=Ni, Pt, Au)", *Inorg. Chim. Acta* **144**, 233 (1988).

M. KOIKAWA, H. ŌKAWA, and S. KIDA, "Manganese(IV) and Manganese(V) Complexes with *N*-(2-Hydroxyphenyl)salicylamides", *J. Chem. Soc. Dalton Trans.*, 641 (1988).

H. ŌKAWA, K. KOGAWA, M. HANDA, N. MATSUMOTO, and S. KIDA, "New Dinucleating Ligand, *N,N′*-Ethylenebis(3-carboxysalicylamine), and Its Dinuclear Copper(II) and Nickel(II) Complexes", *Chem. Lett.*, 1079 (1988).

W. KANDA, H. ŌKAWA, S. KIDA, J. GORAL, and K. NAKAMOTO, "Synthesis and Spectra of Co(Salen) Derivatives Containing Pendant Groups and their Dioxygen Adducts. Pendant Chain Length and Coordinating Ability", *Inorg. Chim. Acta* **146**, 193 (1988).

S. AHRLAND and S. ISHIGURO, "Heats of Solvation of the Mercury(II), Silver(I) and Copper(I) Ions, and of some of Their Halogeno Complexes, in Solvents of Different Coordinating Properties", *Inorg. Chim. Acta* **142**, 277 (1988).

K. OZUTSUMI, S. ISHIGURO, and H. OHTAKI, "An X-Ray Diffraction Study on the Structures of Monochloropentakis(*N,N*-dimethylformamide)copper(II), Trichloromono(N,N-dimethylformamide)- and Tetrachlorocuprate(II) Complexes in *N,N*-Dimethylformamide", *Bull. Chem. Soc. Jpn.* **61**, 715 (1988).

K. OZUTSUMI, S. ISHIGURO, and H. OHTAKI, "Solvation Structure of Copper(II) Ion in *N,N*-Dimethylformamide and *N,N*-Dimethylformamide-Acetonitrile Mixtures Determined by the X-Ray Diffraction Method", *Bull. Chem. Soc. Jpn.* **61**, 945 (1988).

S. ISHIGURO, T. SOTOBAYASHI, K. SATOH, and K. SAITO, "Calorimetric Study of Thiocyanato Complexes of Cobalt(II) Ion in Micellar Solutions of a Nonionic Surfactant", *Inorg. Chem.* **27**, 1152 (1988).

S. ISHIGURO, K. OZUTSUMI, and H. OHTAKI, "Calorimetric and Spectrophotometric Studies of Chloro Complexes of Manganese(II) and Cobalt(II) Ions in *N,N*-Dimethylformamide", *J. Chem. Soc. Faraday Trans. 1*, **84**, 2409 (1988).

H. KUROSAKI, H. ANAN, and E. KIMURA, "Studies on Bleomycin Model Complexes", *Nippon Kagaku Kaishi, Special Articles on "Coordination Chemistry of Biologically Important Substances"*, **No.4**, 691 (1988).

E. KIMURA, M. SHIONOYA, M. OKAMOTO, and H. NADA, "The First Fluorinated Cyclams.", *J. Am. Chem. Soc.* **110**, 3679 (1988).

E. KIMURA, T. KOIKE, H. NADA, and Y. IITAKA, "The First X-ray Crystal Structures of Ni^{II}-Monooxocyclam Complexes. The Effects of the Deprotonated Amide and of an Intramolecular Pendant Pyridine on Cyclam Ligand Field", *Inorg. Chem.* **27**, 1036 (1988).

K. NAKAJIMA, C. SASAKI, M. KOJIMA, T. AOYAMA, S. OHBA, Y. SAITO, and J. FUJITA, "Crystal Structure of a Binuclear *N,N'*-Disalicylidene-(*R,R*)-1,2-cyclohexanediamine-Titanium(IV) Complex and Asymmetric Oxidation of Methyl Phenyl Sulfide with Trityl Hydroperoxide Catalyzed by the Complex", *Chem. Lett.*, **1987**, 2189.

A. NAGASAWA, H.K. TANAKA, M. MIYOSHI, and K. SAITO, "Ligand Isotopic Exchange of *cis*-Bis(acetylacetonato)dioxomolybdenum(VI) in Solution", *Inorg. Chem.* **26**, 4035 (1987).

M. SUZUKI, A. UEHARA, H. OSHIO, K. ENDO, M. YANAGA, S. KIDA, and K. SAITO, "Synthesis and Characterization of Dinuclear Iron(II,II) and Iron(II,III) Complexes with a Dinucleating Ligand, 2,6-Bis[bis(2-pyridylmethyl)aminomethyl]-4-methylphenolate(1–)", *Bull. Chem. Soc. Jpn.* **60**, 3547 (1987).

M. EBIHARA, K. TORIUMI, and K. SAITO, "Syntheses and Properties of Monochalcogenide-Substituted Hexamolybdenum Halide Clusters", *Inorg. Chem.* **27**, 13 (1988).

H. KIDO, and K. SAITO, "Metal Ion Lability Constant Derived from a Linear Free Energy Relationship between Ligand Substitution Rates of *tris*(Acetylacetonato) and *aqua* Complexes of Various Tervalent Metal Ions", *J. Am. Chem. Soc.* **110**, 3187 (1988).

S. FUNAHASHI, K. SENGOKU, T. AMARI, and M. TANAKA, "Dilatometric Studies of Reaction Volumes for the Formation of Metal Complexes in Several Solvents", *J. Solution Chem.* **17**, 109 (1988).

K. ISHIHARA, H. MIURA, S. FUNAHASHI, and M. TANAKA, "Kinetic Study of the Dissociation of Sodium Cryptate(2,2,1)", *Inorg. Chem.* **27**, 1706 (1988).

S. TERO-KUBOTA, K. MIGITA, H. OSHIO, and J. HIGUCHI, "Time-resolved EPR Study of the Excited Triplet States of Zinc Shciff-base Complexes", *Electronic Magnetic Resonance of the Solid State*, ed. by J.A. Weil, (The Canadian Society for Chemistry, Canada 1987) p. 619.

M. HANAYA, S. TERO-KUBOTA, and M. IWAIZUMI, "EPR Studies of the 1,2-Diketone Chelate Paramagnetic Complexes Produced in the Photochemical Reactions of Hexacarbonylbis(η^5-2,4-cyclopentadien-1-yl)dimolybdenum, $[CpMo(Co)_3]_2$, and 1,2-Diketones", *Organometallics* **7**, 1500 (1988).

S. TERO-KUBOTA, K. MIGITA, K. AKIYAMA, and Y. IKEGAMI, "Time-resolved E.S.R. Study of Triplet Ketoamines Generated by Intramolecular Proton Transfer in Free Schiff Bases", *J. Chem. Soc. Chem. Commun.* 1067 (1988).

M. SAITO and H. KASHIWAGI, "*Ab initio* MO Study on Fe Out-of-plane Displacement and Fe-Ligand Vibration in Five-coordinate Fe-porphyrin", *Int. J. Quant. Chem. Symp.* **21**, 661 (1987).

K. OHNO, K. MOROKUMA, F. HIROTA, H. HOSOYA, S. IWATA, Y. OSAMURA, H. KASHIWAGI, S. YAMAMOTO, K. KITAURA, N. KOSUGI, H. NAKATSUJI, S. OBARA, K. TANAKA, M. TOGASHI, and S. YAMABE, "Quantum Chemistry Literature Data Base — Bibliography of *Ab Initio* Calculations for 1986", *J. Mole. Struct. (Theochem)* **136**, 1 (1987).

S. YAMAMOTO, J. TERAOKA, and H. KASHIWAGI, "*Ab initio* RHF and CASSCF studies on Fe-O bond in high-valent iron-oxo-porphyrins", *J. Chem. Phys.* **88**, 303 (1988).

S. YAMAMOTO and H. KASHIWAGI, "CASSCF Study on Iron-Oxo-Porphyrin π Cation Radical: Similarity in Fe-O Electronic Structure between Peroxidase Compounds I and II", *Chem. Phys. Lett.* **145**, 111 (1988).

U. NAGASHIMA and S. YAMAMOTO, "The Ground State Wavefunction of Carbon Monoxide Far from Equilibrium", *Chem. Phys. Lett.* **143**, 299 (1988).

T. OHTA, H. TAKAYA, and R. NOYORI, "BINAP–Ruthenium(II) Dicarboxylate Complexes: New Highly Efficient Catalysts for Asymmetric Olefin Hydrogenations", *Inorg. Chem.* **27**, 566 (1988).

M. KITAMURA, T. OHKUMA, S. INOUE, N. SAYO, H. KUMOBAYASHI, S. AKUTAGAWA, T. OHTA, H. TAKAYA, and R. NOYORI, "Homogeneous Asymmetric Hydrogenation of Functionalized Ketones", *J. Am. Chem. Soc.* **110**, 629 (1988).

M. KITAMURA, I. KASAHARA, K. MANABE, R. NOYORI, and H. TAKAYA, "Kinetic Resolution of Racemic Allylic Alcohols by BINAP–Ruthenium(II) Catalyzed Hydrogenation", *J. Org. Chem.* **53**, 708 (1988).

M. KITAMURA, T. OHKUMA, H. TAKAYA, and R. NOYORI, "A Practical Asymmetric Synthesis of Carnitine", *Tetrahedron Lett.* **29**, 1555 (1988).

M. MIMURO, N. TAMAI, T. YAMAZAKI, and I. YAMAZAKI, "Excitation Energy Transfer in Spinach Chloroplasts. Analysis by the Time-Resolved Fluorescence Spectrum at −196°C in the picosecond Time Range", *FEBS Lett.* **213**, 119 (1987).

I. YAMAZAKI, N. TAMAI, and T. YAMAZAKI, "Picosecond Fluorescence Spectroscoy on Excimer Formation and Excitation Energy Transfer of Pyrene in Langmuir-Blodgett Monolayer Films", *J. Phys. Chem.* **91**, 3572 (1987).

F. TANAKA, N. KANEDA, N. MATAGA, N. TAMAI, I. YAMAZAKI, and K. HAYASHI, "Analyses of Nonexponential Fluorescence Decay Functions of a Single Tryptophan Residue in Erabutoxin b", *J. Phys. Chem.* **91**, 6344 (1987).

I. YAMAZAKI, N. TAMAI, and T. YAMAZAKI, "A Comparative Study on Ultrafast Photonic Energy Transport in Biological Antenna and Artificial Multilayers", *J. Luminescence* **40&41**, 47 (1988).

N. TAMAI, T. YAMAZAKI, and I. YAMAZAKI, "Excitation Energy Relaxation of Rhodamine B in Langmuir-Blodgett Monolayer Films: Picosecond Time-Resolved Fluorescence Studies", *Chem. Phys. Lett.* **147**, 25 (1988).

I. YAMAZAKI, N. TAMAI, T. YAMAZAKI, A. MURAKAMI, M. MIMURO, and Y. FUJITA, "Sequential Excitation Energy Transport in Stacking Multilayers: A Comparative Study between Photosynthetic Antenna and Langmuir-Blodgett Multilayers", *J. Phys. Chem.* **92**, 3553 (1988).

B. WANG, Y. SASAKI, S. IKARI, K. KIMURA, and T. ITO, "Charge Shift along the Metal-Metal Bond in Molybdenum-Tungsten Mixed-metal Complexes, $[M_3(\mu_3\text{-}O)_2(\mu\text{-}CH_3COO)_6(H_2O)_3]^{2+}$ ($M_3 = Mo_2W$ and MoW_2) and $[MoW(O)_2(\mu\text{-}O)_2(\mu\text{-}N,N'\text{-edta})]^{2-}$", *Chem. Lett.* 1955 (1987).

J.K. JESZKA, K. KIMURA, A. TRACZ, H. INOKUCHI, and M. KRYSZEWSKI, "X-Ray Photoelectron Spectroscopy of Tetrathiofulvalene- and Tetrathiotetracene-tetracyanoquinodimethane Charge-Transfer Complexes in Reticulate Doped Polymers", *J. Molec. Electr.* **3**, 157 (1987).

K. KIMURA and S. BANDOW, "Quantum Size Effect Observed in Ultrafine Magnesium Particles", *Phys. Rev.* **B37**, 4473 (1988).

S. BANDOW and K. KIMURA, "Electron Spin Relaxation Time of Ultrafine Zinc Particles Measured by Spin Probe Method", *J. Phys. Soc. Jpn.* **57**, 2807 (1988).

K. KIMURA, "Solid State Properties of Superconductive Fine Particles with Chemically Modified Surface — Particle Contact", *Jpn. J. Appl. Phys. Ser.* **1**, 140 (1988).

T. YAMANAKA, T. HORIGOME, M. SUZUI, K. HAYAKAWA, T. MITANI, and I. YAMAZAKI, "Time-Resolved Spectrophotometric System for Synchrotron Orbital Radiation", *Bunko Kenkyu* (in Japanese) **37**, 277 (1988).

K. AWAGA, T. SUGANO, M. KINOSHITA, T. MATSUO, and H. SUGA, "Thermodynamic Properties of the Mixed Crystals of Galvinoxyl Radical and its Precursory Closed Shell Compound: The Large Entropy Cooperating with the Spin System", *J. Chem. Phys.* **87**, 3062 (1987).

K. AWAGA, T. SUGANO, and M. KINOSHITA, "Ferromagnetic Intermolecular Interaction in the Galvinoxyl Radical: Cooperation of Spin Polarization and Charge-Transfer Interaction", *Chem. Phys. Lett.* **141**, 540 (1987).

T. MITANI, G. SAITO, and H. URAYAMA, "Cooperative Phenomena Associated with Electron and Proton Transfer in Quinhydrone Charge-Transfer Crystal", *Phys. Rev. Lett.* **60**, 2299 (1988).

T. MITANI, T. YAMANAKA, M. SUZUI, T. HORIGOME, K. HAYAKAWA, and I. YAMAZAKI, "Time-Resolved Synchrotron Spectroscopy of Exciton Fluorescence in Anthracene Single Crystals", *J. Lumin.* **39**, 313 (1988).

K. TAKAOKA, Y. KANEKO, H. OKAMOTO, Y. TOKURA, T. KODA, T. MITANI, and G. SAITO, "Infrared Molecular-Vibration Spectra of Tetrathiafulvalene-Chloranil Crystal at Low Temperature and High Pressure", *Phys. Rev.* **B36**, 3884 (1987).

Y. TOKURA, H. OKAMOTO, T. KODA, T. MITANI, G. SAITO, "Nonlinear Electric Transport and Switching Phenomenon in the Mixed-Stack Charge-Transfer Crystal Tetrathiafulvalene-p-Chloranil", *Phys. Rev.* **B38**, 2215 (1988).

Y. TAKAGI and K. YOSHIHARA, "Two-Photon Absorption Sampling Spectroscopy for Fast Transient Luminescence Measurement", 6th Intern. Conf. on Ultrafast Phenomena, Kyoto, 1988, Technical Digest, pp220–221.

H. YONEHARA, T. KASUGA, T. KINOSHITA, and M. HASUMOTO, "The Effect of Field Error of an Undulator Magnet on the Tune", *Jpn. J. Appl. Phys.* **26**, 1939 (1987).

H. YONEHARA, "Study of Stochastic Cooling at the TARN", *J. Sci. of Hiroshima Univ. Ser. A* **52**, 85 (1988).

T. KASUGA, M. HASUMOTO, T. KINOSHITA, and H. YONEHARA, "Longitudinal Active Damaging System for UVSOR Storage Ring", *Jpn. J. Appl. Phys.* **27**, 100 (1988).

K. FUKUI, J. YAMAZAKI, T. SAITO, S. KONDO, and M. WATANABE, "Absorption Spectra of Amorphous and Crystalline SnTe Thin Films in the 2–120 eV Region", *J. Phys. Soc. Jpn.* **56**, 4196 (1987).

T. MURATA, T. MATSUKAWA, and S. NAOE, "XANES and EXAFS Studies on K-Shell Absorption in $K_{1-x}Na_xCl$ Solid Solutions", *Solid State Commun.* **66**, 787 (1988).

Review Articles and Textbooks

I. OHMINE, "Reaction Dynamics in Liquid Phases", *Kagaku* (in Japanese), **2**, Kagakudozin, Kyoto, pp.136 (1988).

H. KANAMORI and E. HIROTA, "Infrared Diode Laser Kinetic Spectroscopy", *The Laser Analytics Letter*, January, 1988.

E. HIROTA, "Carbon Compounds in Current Topics", *Chemistry* (in Japanese) **43**, 546 (1988).

T. KITAGAWA, "Resonance Raman Study on the Role of the Iron-Ligand Bond for Functional Activity of Heme Proteins" *Pure Appl. Chem.* **59**, 1285 (1987).

T. OGURA, A. MAEDA, M. NAKAGAWA, and T. KITAGAWA, "Transient Resonance Raman Spectra of Bacteriorhodopsin and Halorhodopsin" in "*Primary Process of Photobiology*" (T. Kobayashi ed.) p.233 Springer (1987).

T. KITAGAWA, "Photoreduction of Hemeproteins and Iron Porphyrins" *Photomedicine and Photobiology* **9**, 15 (1987).

T. KITAGAWA, "Structure Analysis of Biological Molecules: Raman Spectroscopy" *Cell Engineering* (in Japanese) **7**, 404 (1988).

Y. UDAGAWA, "Structural Study of Heterogeneous Catalyst by EXAFS", *Hyomen* (in Japanese) **26**, 67 (1988).

Y. UDAGAWA, "A Development of EXAFS Apparatus" *Gakujutsu Geppo* (in Japanese) **41**, 611 (1988).

K. TOHJI, "Development of a Laboratory EXAFS System and its Performance — An Application to the Study of Catalyst", *Kagaku to Kogyo* (in Japanese) **41**, 210 (1988).

K. TOHJI, "X-ray Raman Scattering", *J. Cryst. Soc. Jpn.* (in Japanese) **30**, 59 (1988).

K. YOSHIHARA, T. KOBAYASHI, and S. KISHIDA, "Laser Material Processing, Laser Chemistry, and Ultra Fast Phenomena", *The Review of Laser Engineering* (in Japanese) **15**, 563 (1987).

K. YOSHIHARA, "Intramolecular Vibrational Redistribution (IVR) Studied by Ultrafast Spectroscopy", *The Review of Laser Engineering* (in Japanese) **15**, 959 (1987).

T. SAKATA, "Application of Photocatalyst as a Conversion Device of Light into Chemical Energy" *Kogyo Zairyo* (in Japanese) **36**, 50 (1988).

K. HASHIMOTO and T. KAWAI, "Catalytic Reactions Induced by Light Energy — From Application to Electron Transfer Process" *Syokubai* (in Japanese) **30**, 21 (1988).

K. HASHIMOTO, "Organic Synthesis by Photocatalytic Reaction and Electron Transfer between Photoexcited Semiconductor and Adsorbed Molecules" *Kagaku Kogyo* (in Japanese) **39**, 407 (1988).

K. SHOBATAKE, "Lifetime Measurement of Chemical Reaction Intermediates", *Chemistry* (in Japanese) **43**, 60 (1988).

M. SATO, "Characteristic Properties of Oxide Conductors and High Temperature Superconductivity", *Denkikagaku oyobi Kogyobutsurikagaku* (in Japanese) **55**, 733 (1987).

M. SATO, "Survey of the Properties of High Temperature Oxide Superconductors", *Kagaku to Kogyo* (in Japanese) **40**, 1004 (1987).

M. SATO, "Properties of High-T_c Oxides", *Gendai Kagaku* (in Japanese) October issue (1987).

M. SATO, "Magnetic Properties of La based High-T_c Oxides", *Parity* (in Japanese) March issue (1988).

M. SATO, "Studies on Oxide Condutors and High-T_c Oxides", *Superconducting Materials* ed. by S. Nakajima and H. Fukuyama p15 (1988).

M. SERA and M. SATO, "Low Temperature Specific Heat of Bi-Sr-Ca-Cu-O System", *Parity* (in Japanese) June issue (1988).

M.SATO, "Superconductivity of (Ba,K)BiO_3" *Parity* (in Japanese) August issue (1988).

H. KASHIWAGI and M. SAITO, "Existence of Higher Animals Depends on the Electronic Configration of Fe Ion —Ligand Bonds in Metal Complexes from the Viewpoint of Molecular Orbital Theory—" (in Japanese), *Gendaikagaku* **1988–4,** 24 (1988).

H. KASHIWAGI, "Dream in Application of Electron Density Analysis (5) Iron-Porphyrin Complexes" *J. Crystallographic Soc. Japan*, **30**, 165 (1988).

K. SAITO and K. OGINO, "Cobalt(II) Ammine Complexes as Reversible Absorbers of Oxygen", *J. Chem. Education* **65**, 268 (1988).

K. SAITO and Y. SASAKI, "Characteristics of Electron Transfer Reactions of Early Trasition Elements", (Plenary Lecture at 25th International Conference on Coordination Chemistry, 1987) *Pure Appld. Chem.* **60**, 1123 (1988).

K. OKADA, "CaF_2 Window Developed for Ultra-High Vacuum System" in *Bunko Kenkyu* (in Japanese) **5**, 342 (1987).

H. YONEHARA, M. HASUMOTO, T. KASUGA, and T. KINOSHITA, "Tune Shift due to UVSOR Wiggler", Proc. 6th Symp. Accel. Sci. Tech., October 27–29, 1987, Tokyo, p.260.

T. KASUGA, M. HASUMOTO, T. KINOSHITA, and H. YONEHARA, "Single Bunch System for UVSOR", Proc. 6th Symp. Accel. Sci. Tech., October 27–29, 1987, Tokyo, p.195.

T. KASUGA and M. WATANABE, "Status of UVSOR", Proc. 6th Symp. Accel. Sci. Tech., October 27–29, 1987, Tokyo, p.50.

T. KASUGA, H. YONEHARA, T. KINOSHITA, and M. HASUMOTO, "Vacuum System for UVSOR Storage Ring", Proc. IEEE Particle Accel. Conf., March 16–19, 1987, Washington D.C., p.1672.

T. KASUGA, "Effect of Undulator on Stored Beam", Proc 3rd Japan-China Joint Symp. Accel. for Nucl. Sci. and their Application, November 18–20, 1987, Saitama, p.78.

M. WATANABE, "Beam Lines at the UVSOR Facility", *Physica Scripta* **36,** 59 (1987).

S. MORITA, J. FUJITA. K. FUKUI, K. SAKAI, M. WATANABE, E. ISHIGURO, and K. YAMASHITA, "Development of Fusion & Plasma Diagnostics Center— Synchrotro Radiation Experiment (I)— Outline of Calibration Plan on Construction of Beam Line and Primary Monochromator", *Kakuyugokenku* (in Japanese) **58,** 485 (1987).

M. WATANABE, "The Present Status of UVSOR of the Institute for Molecular Science", *Hoshako* (in Japanese) **1**, 41 (1988).

K. KIMURA, "Surface Effect of Ultrafine Particles", *Bull. Jpn. Inst. Metals* (in Japanese) **26**, 1069 (1987).

K. KIMURA, "Ultrafine Particles", *Gakujutsu Gappou* (in Japanese) 41 (1988).

Institute for Molecular Science, Myodaiji, Okazaki 444, Japan